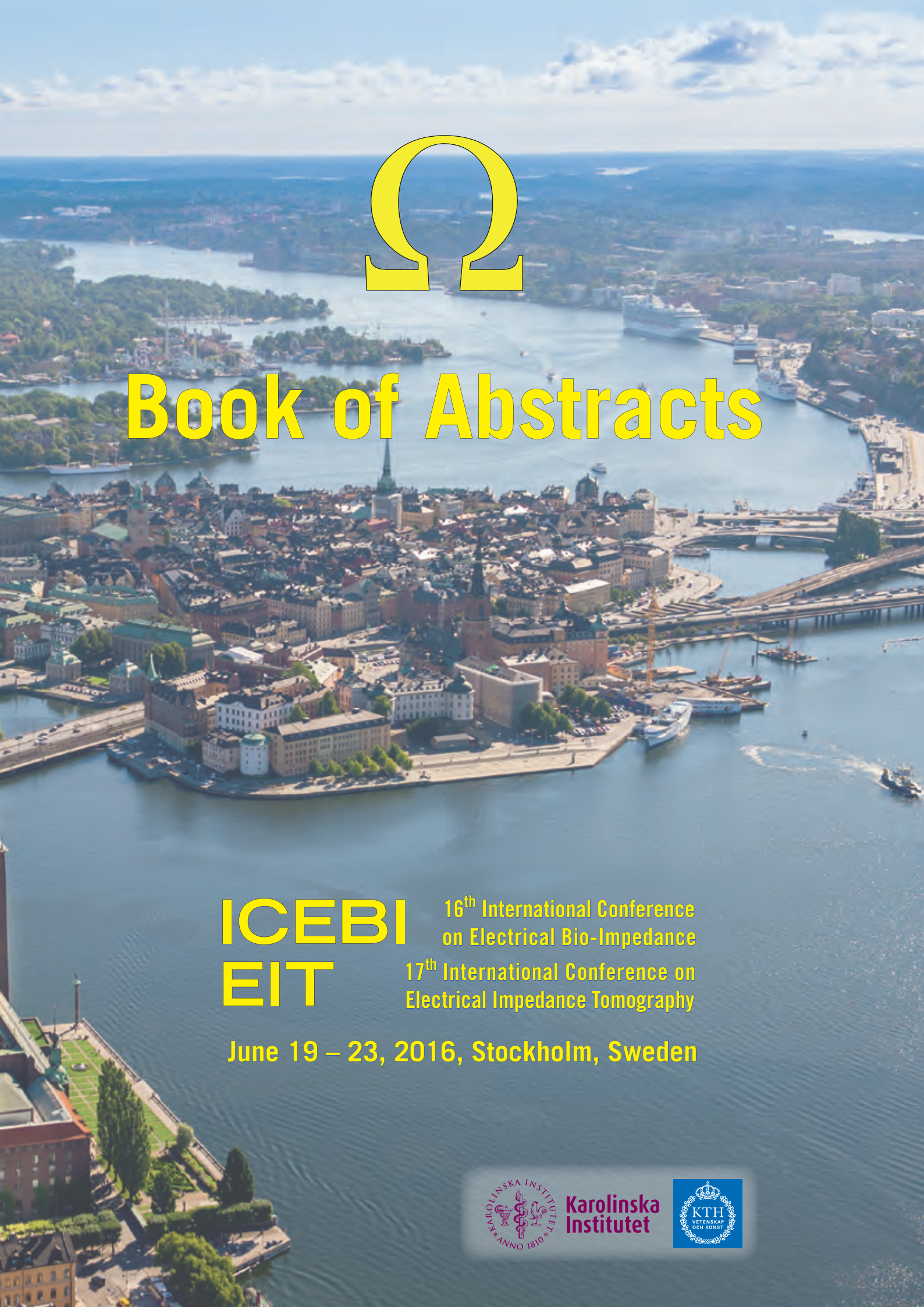

Book of Abstracts

ICEBI
16th International Conference on Electrical Bio-Impedance

EIT
17th International Conference on Electrical Impedance Tomography

June 19 – 23, 2016, Stockholm, Sweden

Karolinska Institutet

KTH VETENSKAP OCH KONST

ICEBI and EIT Stockholm
19–23 June 2016

BOOK OF ABSTRACTS

16th International Conference on Electrical Bio-Impedance Ω **17th Conference on Electrical Impedance Tomography**

The abstracts are published in sequence of their unique 3-digit ID-number, which is also found in the authors index located at the end of this book of abstracts.

ICEBI and EIT Stockholm
19–23 June 2016

Table of Contents

Management Team for ICEBI & EIT in Stockholm 2016 4

International Scientific Advisors Team for ICEBI & EIT in Stockholm 2016 4

Summary of opening address by Keynote speaker Professor Ivar Giaever, Nobel laureate 5

Abstract Index 6

Abstracts 11

Author Index 173

Management Team for ICEBI & EIT in Stockholm 2016

Farhad Abtahi, KTH Royal Institute of Technology

Björn-Erik Erlandsson, KTH Royal Institute of Technology, Deputy Dean

Birgitta Janerot-Sjöberg, Karolinska institutet

Kaj Lindecrantz, KTH Royal Institute of Technology

Mannan Mridha, KTH Royal Institute of Technology

Ingrid Nicander, Karolinska Institutet

Stig Ollmar, Karolinska institutet, Conference Chair

Fernando Seoane, KTH Royal Institute of Technology

Heikki Teriö, Karolinska University Hospital

International Scientific Advisors Team for ICEBI & EIT in Stockholm 2016

Andy Adler	Carleton University, Ottawa	Canada
Richard Bayford	Middlesex University, London	U.K.
Ulrik Birgersson	Karolinska Institutet, Stockholm	Sweden
Brian H Brown	University of Sheffield	U.K.
Kenneth R Foster	University of Pennsylvania	U.S.A.
Eugen Gheorghiu	International Centre of Biodynamics, Bucharest	Romania
Ivar Giaever	Applied Biophysics Inc, Troy, NY	U.S.A.
Alexander Hartov	Thayer School of Engineering, Dartmouth, NH	U.S.A.
David Holder	University College London	U.K.
Alexander Korjenevsky	Institute of Radio-engineering & Electronics, Moscow	Russia
Bill Lionheart	University of Manchester	U.K.
Ørjan G Martinsen	University of Oslo	Norway
Eric McAdams	INSA, Lyon	France
Jan H Meijer	VU Medical Center	Netherlands
Mart Min	Tallinn Technical University	Estonia
Satoru Nebuya	School of Allied Health Sciences, Kanagawa	Japan
Tadeusz Palko	Warsaw University of Technology	Poland
Uwe Pliquett	Institute for Bioprocessing and Analytical Measurement Techniques, Heiligenstadt	Germany
Mingxin Qin	Third Military Medical University, Chongqing	China
Pere J Riu	Universitat Politecnica de Catalunya	Spain
Andrea Robitzki	University of Leipzig	Germany
Saul Rodriguez Duenas	KTH Royal Institute of Technology, Stockholm	Sweden
Ana Rusu	KTH Royal Institute of Technology, Stockholm	Sweden
Hermann Scharfetter	Graz University of Technology	Austria
Ola Stenqvist	University of Gothenburg	Sweden
Leigh Ward	University of Queensland, Brisbane	Australia
Eung Je Woo	Khung Hee University, Seoul	Korea

Summary of opening address by Keynote speaker

Professor Ivar Giaever, Nobel laureate

A COMMERCIAL BIOSENSOR CALLED ECIS

Ivar Giaever and Charles R. Keese
Applied BioPhysics, Inc.
185 Jordan Rd
Troy NY 12180

It is becoming more and more important for scientists or engineers to translate a scientific discovery into a successful business. In this talk I will recollect the problems and tribulations I went through when I started the company Applied BioPhysics, Inc. together with my friend Dr. Charles.R. Keese. The basic principle of the scientific discovery was to culture mammalian cells on small gold electrodes. By monitoring the impedance of the cell-covered electrodes, the morphology and motion of the cells can be inferred in real time. Since these behaviors, such as spreading and locomotion, involve the coordination of many biochemical reactions, they are sensitive to most external parameters including temperature, pH, and a myriad of chemical compounds. This broad response to changes in the environment allows this method to serve as a general biosensor. We have called the method Electrical Cell-substrate Impedance Sensing or ECIS for short. The measurements are easily automated, and the general conditions of the cells can be monitored by a personal computer controlling the necessary instrumentation.

ABSTRACT INDEX

ABSTRACT ID	ABSTRACT TITLE	PAGE NR
105	Time-varying impedance: review of principles and methods	11
108	The ISTI as a measure of SNS function in heart failure	12
109	Arm adipose tissue quotient using segmental bioimpedance	13
110	New coil configuration for unobtrusive vital sign monitoring	14
111	Interfacial impedimetric biosensor: origin of CPE behaviour	15
112	Comparison of lens for early detection of eye agiing	16
114	Fetal monitoring using bio impedance technique	17
116	Measure of bioimpedance to detect tissue inflammation	18
117	Numerical modelling of bioimpedance measure in dentistry	19
118	Detection of glucose by using impedance spectroscopy	20
119	Brachial muscle area estimation for electrical bioimpedance	21
121	Evaluation of magnetic induction system for sleep monitoring	22
122	Rectal impedance parameters in colorectal diseases	23
124	A portable system to measure multi-frequency impedance	24
125	Evaluation of normal fluid status by bioimpedance techniques	25
126	Muscle impedance spectra in duchenne muscular dystrophy	26
127	Interconversion of supine and standing bioimpedance values	27
128	IDH prediction using the PEP and ISTI during haemodialysis	28
129	Bioimpedance probe (BIP) needle in spinal anesthesia	29
130	Bioimpedance for prediction of hypoglycemic trends	30
131	Impedimetric monitoring of neural stem cell differentiation	31
132	Fast and broadband impedance detection	32
133	Investigating the memristive properties of skin	33
134	Non-contact bio-impedance spectroscopy in the food industry	34
135	Quest for the proper B-point in the ICG by echocardiography	35
136	The X-point in the ICG marks aortic valves closure	36
137	Comparing impedance spectroscopy and plasmonic based EIS	37
138	Fat prediction in minced meat with low-cost BIA spectrometer	38
139	Studying the membrane dynamics during cell electropulsation	39
140	Skin bioimpedance and microvascular tone correlations	40
141	Real time in-vivo and in-situ assessment of lung impedance	41
142	Electrical impedance parameters of growing geranium root	42
143	Numerical modelling techniques for bioimpedance and ECG	43
145	Electrical impedance myography quantifies mouse nerve injury	44

ABSTRACT ID	ABSTRACT TITLE	PAGE NR
147	Breathing parameter extraction from localized thoracic bioz	45
148	Cardiac anomalies diagnosis using bioimpedance method	46
149	High frequency sensors in single use culture technology	47
150	Impedance measurements to determine hairy root biomass	48
151	EIS characterisation of hydrodynamics in porous bilayers	49
153	Characterization of graphene oxide coated gold electrodes	50
155	Can impedance cardiography detect pulmonary edema?	51
156	The Russian Bioimpedance Megabase: current state and results	52
157	Bioimpedance - in-vivo vs in-vitro ischemic small intestine	53
158	In-cycle detection of acute myocardial ischemia by fast EIS	54
159	System for local bioimpedance measurements in heart failure	55
160	MIS-phase shift vs US-elastography in breast cancer	56
162	Bioimpedance phase angle: the Russian reference data	57
164	Cardiac and respiration signals recording by an MIT system	58
165	Effects of in vivo muscle injury on muscle impedance in mice	59
166	Bio impedance system for wearable vital sign monitoring	60
167	Real-time microcontroller-based mit phase measurement system	61
168	Mutual capacitance sensors for tissue diagnostics	62
169	Impedance value differences between knees in female athletes	63
170	System for nerve stimulation and bioimpedance measurements	64
171	Comparison between AC & DC exosomatic EDA measuring methods	65
172	Adaptive algorithm for cardiac period normalization in time	66
173	Difference sampling in bio-impedance measurement	67
174	Limitation of signal amplitudes in bioimpedance spectroscopy	68
175	Stable and precise real-time MIT phase measurement system	69
176	Resistive component of meat electrical bioimpedance	70
177	Neural tissue discrimination with machine learning methods	71
178	Chirp signals in impedance spectroscopy	72
179	Using pacemaker leads for bioimpedance and electromyography	73
181	EIT-derived stroke volume is impaired by belt displacement	74
182	Research on heat and cold of resistance by EIS in rose	75
183	Impedimetric sensing of microbial growth in droplets	76
184	Tracing of left ventricular DP/DT using icg and bp signals	77
185	Monitoring of stratum corneum moisture by skin admittance	78

ABSTRACT INDEX

ABSTRACT ID	ABSTRACT TITLE	PAGE NR
186	Parallel leading of ureteral voltaic and ohmic signals	79
187	Evaluation of various wavelets for ICG signals denoising	80
188	Post-stenting arterial healing: an in vitro impedance study	81
189	Floating electrode bioimpedance measurement technique	82
191	An implantable bioimpedance spectrometer	83
192	Microfluidic based impedance analysis of stored whole blood	84
194	Computation of eddy currents inside a human head	85
196	Distinguishing benign from cancerous prostate tissue	86
197	A multi-electrode probe to detect anisotropy of muscles	87
198	Impedimetric analysis of e.Coli biofilms on Meas	88
199	Towards thoracic trauma detection using bioimpedance	89
201	Some errors during impedance measurement	90
202	Universality of low frequency conductance of human hair	91
203	Data mining for biological tissue monitoring	92
204	Sarcopenia and phase angle	93
206	Classification analysis of impedance spectra of tree roots	94
208	Howland current source for wideband bioimpedance application	95
209	Effect of cerebrospinal fluid on mips in ich based on MRI	96
210	A software for monitoring brain edema based on MIPS	97
213	Detection of acute cerebral ischemia in rabbits by MIPSS	98
214	Phase angle in colombian elders diagnosed with sarcopenia	99
215	Modelling with 2.5D approximations	100
219	The simple impedance tool for systolic failure diagnosis	101
220	What does EIT display in case of pneumothorax?	102
221	A robust EIT reconstruction using data correlation	103
222	Investigation into improvements offered by fused-data EIT	104
223	Electrical resistance tomography of conductive thin films	105
224	Heterogeneity of regional ventilation in lung-healthy adults	106
225	Model-based estimation of regional lung perfusion using EIT	107
226	An electronic mesh phantom for planar structure EIT systems	108
227	EIT guided peep versus ards network table and set peep.	109
228	Multiplexing and transient estimates in lung EIT instruments	110
229	Can we predict weaning outcome with EIT?	111
230	A method to calculate overdistension and tidal recruitment	112

ABSTRACT ID	ABSTRACT TITLE	PAGE NR
231	Direct reconstructions from partial-boundary measurements	113
233	Individualized adjustment of mechanical ventilation with EIT	114
235	EIT of evoked and spontaneous activity in peripheral nerve	115
236	Model reduction for fem forward solutions	116
237	Evaluation of EIT images using esophageal electrodes	117
238	An EIT belt design with active electrodes and digital output	118
239	MRI piglet head model for EIT and an IVH simulation	119
240	Bioimpedance imaging to assess abdominal fatness using EIT	120
241	Hypertonic saline injection to detect aorta in porcine EIT	121
242	Pulmonary artery pressure by EIT: experimental evaluation	122
243	Lung aeration in EIT with probability-weighted respiration	123
244	Nerve modelling for imaging fast neural activity using EIT	124
245	Applications of multifrequency EIT to respiratory control	125
248	A nonlinear reconstruction method with a priori data for EIT	126
249	Synthetic bz calculation in MRI based realistic head model	127
251	Alternate algorithm to reconstruct shape in wearable device	128
252	Determination of lung pathology by multi-frequent analysis	129
253	Soft-prior regularization EIT for breast cancer detection	130
255	Effects of simulated air accumulations in the thorax on EIT	131
256	A highly stretchable artificial sensitive skin using EIT	132
257	Using EIT to determine moisture in flood embankment	133
258	A new EIT instrument for lung function monitoring	134
259	Imaging of regional air distributions in porcine lungs	135
260	Feasible method for chest shape estimation used for EIT	136
261	Investigating the safety of 2 k Hz EIT in the rat brain	137
262	A novel active electrode IC for wearable EIT systems	138
263	PYEIT: a python based, open source framework for EIT	139
264	PCA-based characterization in lung EIT	140
265	Fabrication of pressure distribution sensor for EIT imaging	141
267	Liver stiffness measurement by MR-based conductivity imaging	142
268	Multispectral EIT: a manifold approach	143
269	Image fusion of CT/EIT using 3D discrete cosine transform	144
270	EIT diagnosis of pre- and microinvasive cervical cancer	145
271	Optimising the injection protocol for fast neural EIT	146

ABSTRACT INDEX

ABSTRACT ID	ABSTRACT TITLE	PAGE NR
272	Drift – the challenge in brain monitoring with TD-EIT	147
273	Feasibility of parallel EIT simultaneous to EEG in neonates	148
274	A method for imaging epilepsy with EIT and depth electrodes	149
275	Multi-modal home sleep apnea monitor using EIT	150
276	Comparing parallel & sequential EIT in head tanks and nerve	151
277	A noval low cost, portable and multi-frequency EIT system	152
278	Sparse regularization based on spectral graph wavelets	153
279	Determining heart region in EIT images by linear regression	154
280	Rotational EIT setup optimization	155
281	Continuous regional analysis device for neonate lung (CRADL)	156
282	Influence of body movement in EIT bladder volume estimation	157
283	Construction of a robust beagle model for EIT applications	158
285	EIT-based sensing skin for detection of damage in concrete	159
286	Measuring stroke volume with electrical impedance tomography	160
287	Contribution of finite element model of animals to data base	161
288	Weighting functions for image-based validation of EIT	162
289	Multishot SE-EPI sequences for functional MREIT	163
290	Lung ventilation changes during percutaneous tracheostomy	164
291	High speed EIT data acquisition system	165
292	Comparison of electrical and molecular transport properties	166
293	Intraoperative prostate imaging with endoscopic EIT	167
294	EIT monitoring of the liquid-ventilated lung	168
297	Identification of stable breathing periods in EIT recordings	169
299	Depth electrode for neural electrical impedance tomography	170
300	Wireless power transfer for an implantable EIT system	171
301	Impedance & extracellular field potential of cardiomyocytes	172

Abstract Id: 105
Topic: *Signal processing*

TIME-VARYING IMPEDANCE: REVIEW OF PRINCIPLES AND METHODS

Benjamin Sanchez[*1], Seward Rutkove[1], Ebrahim Louarroudi[2]

[1]Department of Neurology, Harvard Medical School, Boston, United States,
[2]Optical Metrology, 3D design and Mechanics Research Group,
University of Antwerp, Antwerp, Belgium

INTRODUCTION Real-life bio-systems are often non-repeatable and satisfy only approximately the linearity and time-invariance assumptions inherent to the concept of frequency response function.

OBJECTIVES Review the existing approaches and recent advances for the impedance study of linear time-variant bio-systems.

METHODS Major inroads into the identification of time-varying impedance have made possible to estimate a linear time-variant model from a single experiment. Starting with generalized Ohm's law, we introduce the principles of identification of the harmonic impedance and analyze its interpretation in the complex plane. We then show that the harmonic impedance can be represented in the complex plane as a evolving impedance vector [1], leading to the so-called circular motion analysis [2]. The two-dimensional representation is then extended to a three-dimensional rotating impedance surface. The new theoretical concepts are illustrated with data originating from phantoms and *in vivo* normal and acutely infarcted myocardium.

RESULTS A detailed review of the applicability of new identification techniques for the impedance measurement of time-variant bio-systems has been performed. The relationship between the various concepts published in the literature is presented. The results show that by using time-variant identification techniques it is possible overcome the limitations of conventional tools based on stepped-sine excitations.

CONCLUSIONS The clinical applications of time-varying impedance identification techniques are vast. The next step will be to extend these findings to electrical impedance tomography.

REFERENCES

1. Sanchez B, Louarroudi E, Pintelon R. Time-invariant measurement of time-varying bioimpedance using vector impedance analysis. Physiol. Meas., 2015,36 (3), 595–620.
2. Sanchez B, Louarroudi E, Rutkove S, Pintelon R. Circular motion impedance analysis of time-varying bioimpedance. Physiol. Meas., 2015. 36(11), 2353–2367.

Abstract Id: 108
Topic: *Clinical applications*

THE ISTI AS A MEASURE OF SNS FUNCTION IN HEART FAILURE

Monica Parry*[1], Melisa Gaspar[2], Rene van Lien[3], Jan H. Meijer[4]

[1]Assistant Professor and Director of Nurse Practitioner Programs, Lawrence S. Bloomberg Faculty of Nursing, [2]BScN (Student), Lawrence S. Bloomberg Faculty of Nursing, University of Toronto, Toronto, Canada, [3]Product Specialist , Heinen & Lowenstein , Rotterdam, [4]Department of Physics and Medical Technology, VU University Medical Centre, Amsterdam, Netherlands

INTRODUCTION Heart failure (HF) is a complex syndrome associated with sympathetic nervous system (SNS) hyperactivity. Impedance cardiography provides data on SNS activity using the pre-ejection period (PEP), typically derived through accurate identification of Q-onset in the electrocardiogram (ECG) and B-point identification in the impedance cardiogram (ICG). In a recent study[1], the Vrije Universiteit Ambulatory Monitoring System (VU-AMS) version 5*fs* detected anticipated SNS changes to postural shift in persons with HF, but 64% of the sample had to be eliminated due to scoring difficulties. Reliability of PEP scoring is sensitive to the selection of correct landmarks, and the tedious manual inspection of Q-onset and B-point detection limits its use in clinical practice settings.

OBJECTIVES The purpose of this pilot study was to evaluate the utility of using the initial systolic time interval (ISTI) to measure PEP in persons with HF.

METHODS In this descriptive study, men and women (n=28) with HF were recruited from an outpatient device clinic at a tertiary care hospital in Ontario, Canada. Participants completed a sit-to-stand posture protocol wearing an ambulatory blood pressure (BP) device and the VU-AMS version 5*fs* impedance cardiography system.

RESULTS Five participants were excluded from the analysis due to poor signal quality and two were excluded due to technical difficulties. The remaining participants (n=21, 75%) were male (n=18, 86%) with a mean age of 71 years (SD=8 years). Most (67%, n=14) had Grade 3 or 4 left ventricular function with a mean ejection fraction of 30% (SD=12). Response to the sit-to-stand posture protocol included a 3% increase in heart rate (p=0.002), a 12% increase in SNS activity (p=0.004), and a 14% decrease in systolic BP (p=0.000).

CONCLUSION When compared to standard PEP scoring practices, ISTI offered more accurate PEP scoring using the R-wave peak on the ECG and the dZ/dt (min) peak (C-point) on the ICG. Given that the information between PEP and ISTI overlap empirically and theoretically, ISTI may be a better marker of SNS activity in persons with HF in clinical practice settings. However, before these technologies can be integrated into clinical practice settings, validation of these results in a larger sample of men and women with HF is warranted.

REFERENCES

1. Parry M, et al. A novel noninvasive device to assess sympathetic nervous system function in patients with heart failure. *Nursing Research.* 2015;64(5) 351–360.

Abstract Id: 109
Topic: *Clinical applications*

ARM ADIPOSE TISSUE QUOTIENT USING SEGMENTAL BIOIMPEDANCE

Ruben Buendia*[1], Tim Essex[2], Leigh Ward[3]

[1]Signals & Systems, Chalmers, Göteborg, Sweden, [2]ImpediMed Ltd, [3]School of Chemistry and Molecular Biosciences, University of Queensland, Brisbane, Australia

INTRODUCTION In [1] a bioimpedance based method was developed for estimating limb adipose tissue quotient. The method was based on segmental single frequency bioimpedance (50 kHz) as well as measurements of the limbs length and circumference. However, at 50 kHz the equivalent electrical circuit of the arm would have a very high capacitive component that confounds the relationship between resistivity and measured resistance of the limbs and, consequently, the relationship between resistance and volume. Furthermore, the database used for calibration and validation of the method was small (n=30).

OBJECTIVE The goal of this study was to develop a method for estimating arm adipose tissue quotient from simple measurements of segmental bioimpedance, height and weight. The method is based on the one proposed in [1], but aimed to overcome its drawbacks.

METHODS Segmental electrical bioimpedance spectroscopic (BIS) measurements of the right arm were performed on 295 subjects. Measurements were fitted to the Cole model in order to obtain R_∞. R_∞ replaced resistance at 50 kHz of the original method. Theoretically, R_∞, the resistance at infinite frequency, is free of capacitive component.

Length and mean cross-sectional area of the arm were obtained from the relationships with height and weight according to the method proposed in [2]. The adipose tissue quotient for the whole arm was determined and compared with that measured by DXA. Regression and Bland-Altman plots were used for comparison of results.

RESULTS The methods were highly correlated (r = 0.79) with a very small bias, 0.02 (5%). However, precision was not high and the methods exhibited wide limits of agreement (2SD) of -0.18 to 0.22, 48% to 58% respectively from the average of all quotients estimations using the mean of both methods.

CONCLUSIONS The possibility of estimating arm fat quotient from a simple measurements of BIS, height and weight was demonstrated. The approach has the advantage of simplicity since only an impedance measurement is required; arm length and circumference being estimated from height and weight based on population-derived algorithms [2]. Although the very small bias demonstrates the method has value for population-based comparisons, the wide LOAs indicate the need for further refinement of the method for it to be suitable for use in individuals.

REFERENCES

1. Biggs, et al. Physiol. Meas. 2001; 22: 365–76.
2. Heymsfield, et al. Nutrition & Metabolism 2008.

Abstract Id: 110
Topic: *Instrumentation*

NEW COIL CONFIGURATION FOR UNOBTRUSIVE VITAL SIGN MONITORING

Hadiseh Mahdavi* [1], Javier Rosell Ferrer[1]

[1]Electronic Engineering, Universitat Politècnica de Catalunya, Barcelona, Spain

INTRODUCTION Although Magnetic Induction (MI) technique is an attractive method for unobtrusive vital sign monitoring –having the advantages of no necessity for direct contact and not blocking by poorly conducting tissues- one major concern in this method is the large background primary magnetic field superimposed to the small secondary field in the receiver coil (RX) which makes it difficult to detect the physiological signal contained only in the secondary field. Considering this problem, a typical MI system design uses a coils configuration in order to cancel out the primary field.

OBJECTIVES This paper demonstrates a new coil configuration for primary field cancellation by applying a new planar gradiometer structure to be used for unobtrusive vital sign monitoring.

METHODS From the three common methods of primary field cancellation, our design is based on subtraction of the signals in a pair of differential coils (gradiometer). This has been used since it's easier to implement and more importantly it cancels the primary field at an earlier stage of MI system. The coils are planar, concentric and implemented in PCB, suitable for being placed under the mattress. The excitation coil (EX) has 8 turn and a central radius of 2.5 cm while the receiver coil has a radius of 10 cm and one turn. The receiver design is based on [1] and is designed to integrate zero flux from the primary field and being sensitive only to the secondary field, so the detected voltage will lead to a minimum background signal. The configuration was validated by using finite element simulations and after implementation on a PCB, was used in experiments for sensitivity studies and evaluation of overall performance of the system.

RESULTS Simulation shows that the primary field was reduced about 100 times applying the new structure, this reduction could not be measured in experiments since without the cancellation method no signal could be detected with the available acquisition system.

CONCLUSION The simulations and experiments show that the new configuration is capable of reducing the induced primary field in the unloaded system while preserving maximum sensitivity to conductivity changes. Moreover the new structure shows lower sensitivity to displacements of object from/over the coils in comparison with the adjacent coil configuration.

IMAGE

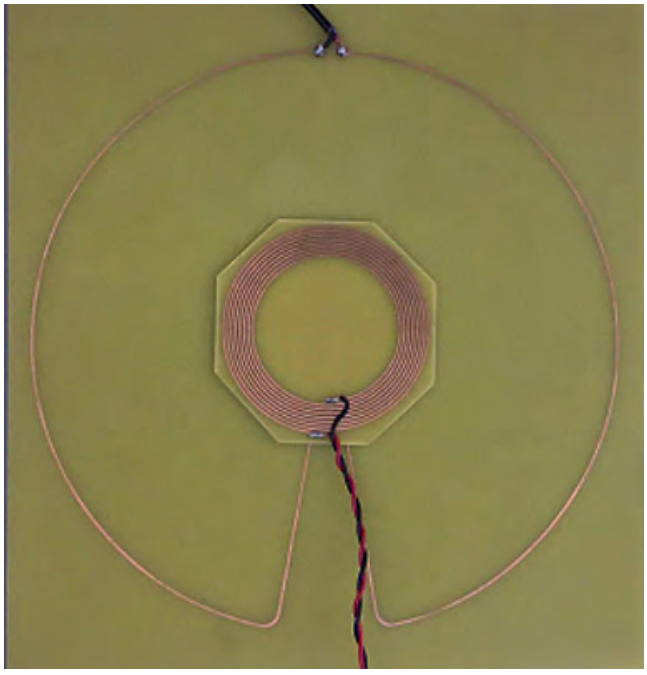

REFERENCES

1. J. Rosell-Ferrer, C.H. Igney, and M. Hamsch, "Planar coil arranement for a magnetic induction impedance measurement apparatus," 2012.

Abstract Id: 111
Topic: *Impedimetric biosensors*

INTERFACIAL IMPEDIMETRIC BIOSENSOR: ORIGIN OF CPE BEHAVIOUR

Terry Chilcott*[1], Chuan Guo[1]

[1]School of Chemical and Biomolecular Engineering, University of Sydney, Sydney, Australia

INTRODUCTION Detection of biomolecules in electrolytes contacting bio-sensitized self-assembling-monolayers (SAMs) is often obscured by electrolyte interfaces in which the ionic flows and forces are defined by the Nernst–Planck-Poisson (NPP) equations. The constant-phase-element (CPE) describes electrical impedances spectra (EIS) of interfaces but is not an NPP solution. In contrast, the Maxwell–Wagner model is a solution and facilitates extraction of impedimetric properties of layers comprising SAMs and associated interfaces [1].

OBJECTIVES Find NPP origins of interfaces and CPE for construction stages of a SAM targeting anti-IgG.

METHODS EIS were acquired of alkyl SAMs terminated with CH_3, COO^-, NHS, IgG and anti-IgG groups in contact with 1-300 mM KCl electrolytes.

RESULTS Modeling yielded conductivities (σ_n) and thicknesses (d_n) consistent with the compositions and structures of the SAMs. The alkyl-Si interface was attributed to a sequence of alkyl thick layers ($d_6 \ldots d_{10}$) proximal to Si, but with conductivities ($\sigma_6 \ldots \sigma_{10}$) increasing with proximity. The sizes of the KCl interfaces ($d_2+d_3+d_4$) and anti-IgG were comparable but orders of magnitude smaller than the Debye length.

CONCLUSIONS CPE behaviors originated in alkyl-Si interfaces. Changes in KCl interfaces were consistent with the electrochemistry of the SAM-termini including detection of targeted anti-IgG.

IMAGE

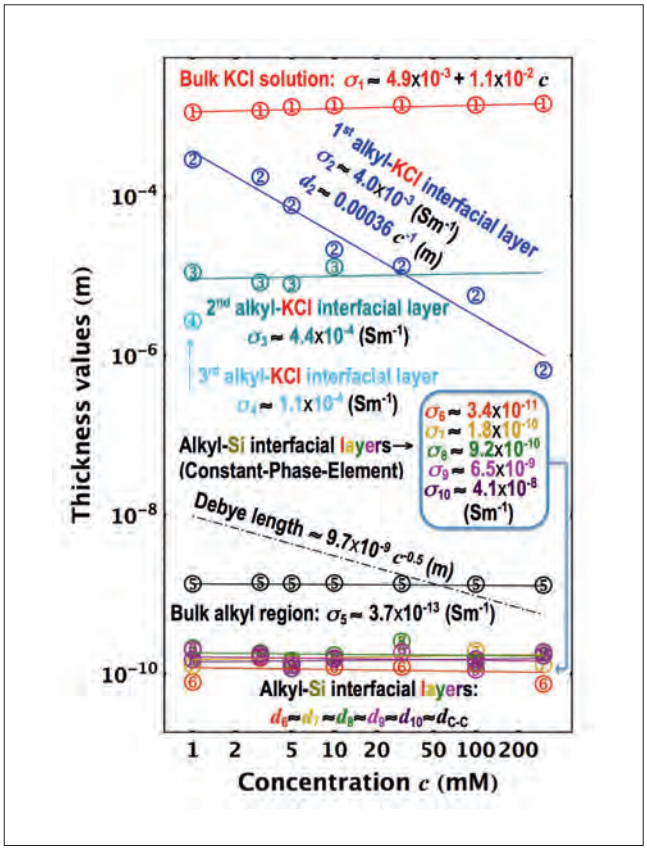

REFERENCES

1. T.C. Chilcott, C. Guo (2013) Electrochimica Acta 98: 274– 287

Abstract Id: 112
Topic: *Clinical applications*

COMPARISON OF LENS FOR EARLY DETECTION OF EYE AGIING

Marie-Valerie Moreno[*1], Antoine Clarion[1], Pierre-Alain Grounauer[2]

[1]BioparHom, Le Bourget du Lac, France, [2]Fabrinal, La Chaux-de-Fonds, Switzerland

INTRODUCTION: Many diseases of the eye are characterized by an increase in hydration. Conversely ageing causes dehydration of the eye (1). This suggests that bioimpedance can be a viable technology for diagnosing some characteristics of the eye, as ageing, with the advantage of being ergonomic, non-invasive and inexpensive.

OBJECTIVE : the purpose of this study is to explore two ocular lens solutions for in vivo measurements for various age of people including elderly.

MATERIALS AND METHODS: we use a multifrequency impedancemeter (Z-Scan, BioparHom©, France) (from 1 khz to 1000 Khz by step of 0,5 khz, 300 µA). We use, two types of non-invasive ocular lens: a total gold electrodes TE and a ring gold electrodes RE (2) (ERG jet, Fabrinal©, Switzerland). 15 people involved in the study, from 6 to 86 years old.

RESULTS: RE shows a higher resistance as expected because of the lower surface of contact with the cornea. The reactances are equivalent. We noted from 0.08 to 0.50 % of variability for RE and from 0.17 to 2.18% of variability for TE. We can suppose that TE is more impacted by the movements of the eyes because of the higher surface contact. Then RE lens seems to be better for assessing electrical data of the eye. We pratice measurements on the population for detecting the effect of ageing on electrical characteristics of the eye.

CONCLUSION: RE lens seems to be valuable for assessing the impact of ageing on electrical data of the eyes. The next step is to do measurements on elderly with glaucoma or DMLA for trying to differentiate ageing and pathology.

REFERENCES

1. Jurgens et al., Electrical impedance tomography of the eye : in vitro measurements of the cornea and the lens, Physiol. Meas 17 (1996) A187–A195.
2. Grounauer et al., The Somnogen Visual Training a New CBT to Fight Insomnia through closed eyes and fNIRS Neuroimaging, Journal of Behavioural and brain science, 4, 477–481, 2014.

Abstract Id: 114
Topic: *Electrical impedance tomography*

FETAL MONITORING USING BIO IMPEDANCE TECHNIQUE

Ramesh Kumar Meena[1], Sarwan Kumar Pahuja[*2], Amit Sengupta[3]

[1]Department of Instrumentation and Control, Dr B. R. Ambedkar National Institute of Technology, Jalandhar, Jalndhar, Punjab, [2]Department of Instrumentation and Control Engneering, National Institute of Technology Jalandhar, Jalandhar, Punjab, [3]Centre for Biomedical Engineering, Indian Institute of Technology Delhi, Delhi, India

INTRODUCTION Presently, the non-invasive techniques are the standard clinical approach because its use is possible during both pregnancy and labor. It helps in monitoring & recording of distributed electric field over a closed object. This paper presents a system for Fetal Monitoring, which system based on bioimpedance principle. This technique also known as electrical impedance tomography. This system consists of the phantom, experimental setup and methods of data acquisition, after that to evaluate its potential from the Phantom. The electrical impedance tomography System offers some benefits over other imaging modalities, such as low cost, no radiation and being non-invasive.

OBJECTIVES The bio-impedance technique is a non- invasive method, such as Electrical Impedance Tomography modality.It helps in monitoring and recording of distributed electric field over a closed object/ phantom. Due to fetal movement and related physiological and morphological parameters of fetus various changes takes place at the surface & these changes provide information about fetal-like fetus temperature, fetal movement, etc.

METHOD EIT imaging technique based on internal conductivity distribution of the body and reconstructing the image from the electrical measurements of electrodes attached to the mother's body. A small amount of AC (mA) having a frequency from 10 KHz to 100 KHz, is inserted through two inputs electrodes and output voltages are measured from the remaining electrodes. In EIT Many methods are used for data aqusition from the the phantom, such as, neighboring method , opposite method, cross, adaptive method.

RESULTS The proposed is validated by conducting an experiment by taking papaya as phantom. Papaya is chosen as it imitates the properties of human's uterus. The phantom papaya is connected with sixteen numbers of electrode. After that measures the voltages points according to the current patterns of EIT methods. Shown in table 1.

CONCLUSION The new technique being proposed in this work is noninvasive, user friendly, economical and for mass health care which can be used by the poor community and the basic health worker.

I (MA) location	Outputs (voltage measurement's in mV) according to electrodes												
1-9 Ref 2	3 .066	4 .123	5 .166	6 .215	7 .266	8 .366	10 .361	11 .261	12 .214	13 .167	14 .130	15 .079	16 .012

Table 1. *Impedance distribution for one current location.*

Abstract Id: 116
Topic: *Clinical applications*

MEASURE OF BIOIMPEDANCE TO DETECT TISSUE INFLAMMATION

Gloria Cosoli[*1], Lorenzo Scalise[1], Enrico Primo Tomasini[1],
Paola Russo[2], Graziano Cerri[2], Gerardo Tricarico[3]

[1]DIISM, [2]DII, Università Politecnica delle Marche, Ancona, [3]INQBA srl, Chiaravalle, Italy

INTRODUCTION Biologic tissues are characterized by specific electrical properties (i.e. electrical conductivity and magnetic permittivity)[1–3]. Tissues inflammation causes an increase of electric conductivity with respect to normal values, due to the presence of liquids (hyperemia and infiltration of the adjacent tissues are typical of the inflammatory process) [4].

OBJECTIVES This work explores the possibility of detecting inflamed tissue areas by means of bioimpedance measurements in the case of oral inflammations, particularly when a dental implant is present. In this way, the therapy could be "personalized" according to the position and the severity of the inflammation detected and also focused on the impaired area, minimizing the involvement of the surrounding tissues.

METHODS In vivo measurements have been made on a patient with dental implants to compare impedance values measured in case of peri-implantitis and healthy data.

RESULTS This preliminary study demonstrates the feasibility of the proposed method. Three measures have been repeated on the inflamed implant, with a resulting modulus of (377±20)Ω (results are expressed as mean±standard deviation), while the absolute impedance measured on the healthy implant is equal to (565±43)Ω.

CONCLUSIONS A bioimpedance measuring system integrated in a therapeutic device could allow the clinician to locate the impaired area and to evaluate the severity of the inflammation. So, the therapy could be adjusted according to the need of the specific clinical case; in fact, therapeutic dose could be selected according to the measured impedance value.

Moreover, bioimpedancemetry would permit the monitoring of the inflammation course.

REFERENCES

1. Gabriel, C., Gabriel, S. & Corthout, E. The dielectric properties of biological tissues: I. Literature survey. *Phys. Med. Biol.* **41,** 2231–2249 (1996).
2. Gabriel, S., Lau, R. W. & Gabriel, C. The dielectric properties of biological tissues: II. Measurements in the frequency range 10 Hz to 20 GHz. *Phys. Med. Biol.* **41,** 2251–2269 (1996).
3. Gabriel, S., Lau, R. W. & Gabriel, C. The dielectric properties of biological tissues: III. Parametric models for the dielectric spectrum of tissues. *Phys. Med. Biol.* **41,** 2271–2293 (1996).
4. Tornuev, Y. V. *et al.* Bioimpedancemetry in the diagnostics of inflammatory process in the mammary gland. *Bull. Exp. Biol. Med.* **156,** 381–383 (2014).

Abstract Id: 117
Topic: *Simulation / modelling*

NUMERICAL MODELLING OF BIOIMPEDANCE MEASURE IN DENTISTRY

Gloria Cosoli[*1], Lorenzo Scalise[1], Paola Russo[2],
Graziano Cerri[2], Gerardo Tricarico[3]

[1]DIISM, [2]DII, Università Politecnica delle Marche, Ancona, [3]INQBA srl, Chiaravalle, Italy

INTRODUCTION In dentistry, oral inflammations are very frequent[1] and can have serious consequences (e.g. peri-implantitis is the main cause of implant failure[2]). Human tissues impedance values vary with their physiological/pathological state[3], so it could be used with diagnostic aims.

OBJECTIVES The authors numerically analyze the bioimpedance measurement by means of 3D Finite Element Method (FEM) of three teeth models, to verify the possibility of distinguishing between healthy and inflamed tissues.

METHODS Various numerical models were considered, both of healthy tooth roots (i.e. canine, incisor and premolar) and of dental implants (i.e. premolar dental implant). Geometric and electrical properties were taken from the literature[4,5], paying particular attention to the inflamed tissue[3]. In order to carry out a parametric study, different-sized inflamed tissue volumes were considered, besides different electrodes shapes and dimensions as well as positioning.

RESULTS Healthy and inflamed tissues impedances were compared and differences of 6÷20% have been found, depending on the considered parameters (e.g. inflammation volume and severity).

CONCLUSIONS Results show that the change due to the inflammatory process is sufficiently pronounced to discriminate between healthy and inflamed tissues, so bioimpedance measurements can be used to locate inflammation; moreover, results from parametric study can aid in the design of a proper bioimpedance meter.

In conclusion, bioimpedancemetry appears to be useful in the diagnostics of inflamed tissues in dentistry.

IMAGE

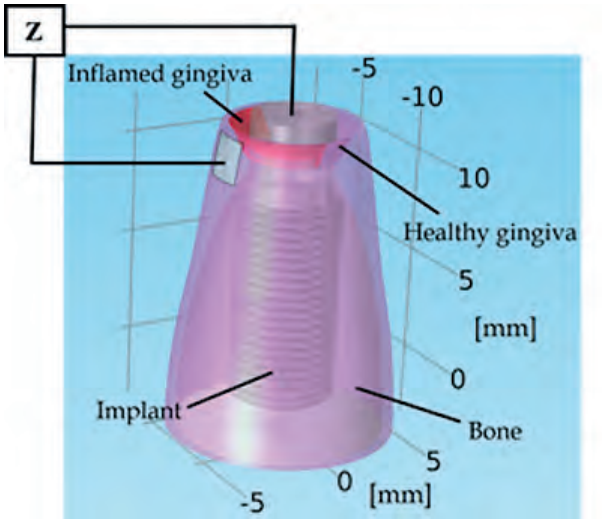

REFERENCES

1. Renvert, S., Roos-Jansåker, A.-M. & Claffey, N. Non-surgical treatment of peri-implant mucositis and peri-implantitis: a literature review. *J. Clin. Periodontol.* **35,** 305–315 (2008).
2. Cao, Z. *et al.* Electromagnetic irradiation may be a new approach to therapy for peri-implantitis. *Med. Hypotheses* **78,** 370–372 (2012).
3. Tornuev, Y. V. *et al.* Bioimpedancemetry in the diagnostics of inflammatory process in the mammary gland. *Bull. Exp. Biol. Med.* **156,** 381–383 (2014).
4. MS, S. J. N. D. *Wheeler's Dental Anatomy, Physiology and Occlusion, 9e*. (Saunders, 2009).
5. Gabriel, S., Lau, R. W. & Gabriel, C. The dielectric properties of biological tissues: II. Measurements in the frequency range 10 Hz to 20 GHz. *Phys. Med. Biol.* **41,** 2251–2269 (1996).

Abstract Id: 118
Topic: *Bioimpedance*

DETECTION OF GLUCOSE BY USING IMPEDANCE SPECTROSCOPY

Pedro Bertemes-Filho[*1], Rodolfo Weinert[1], Thiago Albuquerque[1]

[1]Electrical Engineering, The State University of Santa Catarina, Joinville, Brazil

INTRODUCTION This article is related to non-invasive glucose measurements, which is widely used by people who suffer from diabetes. Diabetes is a group of disease known by high blood glucose. Glucose levels in blood need to be continuously measured in order to keep it under control. Most methods for glucose measurements are invasive, which may causes pain, has a high risk of infection and can lead to finger deformation. Recently, bioelectrical impedance analysis (BIA) bioimpedance has been used as a non-invasive technique. An impedance spectrum is calculated by the ratio between an injecting current and a resulting measured voltage. Electrical properties are then extracted from impedance data by using an equivalent electrical model of the material under study.

OBJECTIVES It develops a bioimpedance system for non-invasive glucose levels measurement and compares with the infrared (NIR) ones. It also investigates a correlation function between glucose level and measured bioimpedance.

METHODS The NIR circuit contains the diode TIL32 and the photodiode SFH206K. The BIA circuit contains both modulus and phase measuring system. Two electrodes inject a current of 1 mAp over a frequency range of 50 to 350 kHz and other two measure the vltage. The phase detector was developed with comparators and Sallen-Key low-pass filters. The electrodes are immersed into saline solutions from *LBS Laboratory*® and glycoside serum from *Baxter*®, which contains 5% of glucose. 10 samples of 10 milliliters (ml) were made by varying the proportion of glycoside serum and physiological saline. The solutions were mixed during 10 minutes to ensure homogenization. Data are sampling at 100 KS/s with a resolution of 16 bits and then recorded to a computer through a USB interface.

RESULTS The BIA system was calibrated and showed a sensibility of 0.1º in phase. NIR results showed that the measured output voltage of the system increases as increasing the glucose concentration at a rate of 1.5 mg/ml/mV. BIA data showed that the measured impedance and the glucose concentration can be interpolated by using an exponential equation with a maximum error of 3,1%.

CONCLUSION The implemented BIA system presented a better sensibility of glucose concentrations compared to the NIR ones. Both NIR and BIA data can be combined in order to perform a more accurate result of glucose levels, which might be useful for a non-invasive blood glucose.

Abstract Id: 119
Topic: *Clinical applications*

BRACHIAL MUSCLE AREA ESTIMATION FOR ELECTRICAL BIOIMPEDANCE

Evelyn Colina-Gallo*[1], Vladimir Cárdenas-Villamizar[2], Carmen Dussán-Luber[3], David Alejandro Miranda-Mercado[4], Carlos Augusto González-Correa[5]

[1]Departamento Acción Física Humana, Universidad de Caldas, [2]Diagnostimed S.A., [3]Departamento de Matemáticas, Universidad de Caldas, Manizales, [4]Departamento de Física, Universidad Industrial de Santander, Bucaramanga, [5]Departamento de Ciencias Básicas, Universidad de Caldas, Manizales, Colombia

INTRODUCTION We are exploring the use of Electrical Bioimpedance for diagnosis of fibromyalgia (FM). Our hypothesis is that biochemical and nanostructural changes associated with FM could alter the electrical resistivity of the muscle.

OBJECTIVES We first tried to answer two questions: What is the muscle cross sectional area (MCSA) in the midpoint of the arm? Given that MCSA, What is the muscle apparent resistivity, subtracting from the total injected current the current passing through dermis, subcutaneous adipose tissue (SAT) and bone?

METHODS From a group of 45 volunteers participating in the study, we took anthropometric measurements and computed tomography images in a subgroup of 23 subjects (10 controls, 13 with FM). With the data obtained, we calculated cross sectional areas for dermis, SAT, bone and muscle, and the amount of the injected current actually passing through each of these compartments at *5 kHz*. We assumed fixed values of resistivity for dermis, fat and bone as *4.5*, *30* and *60 m*, respectively. From this, we calculated the apparent resistivity of brachial muscle.

RESULTS The statistical analysis shows that muscle areas calculated by antrhropometry and TC are comparable (=0.0033, *SD=0.000594*, and *0.00314*, *SD=0.000548*, respectively, with *p=0.3*). Obtained values for muscle apparent resistivity (Table 1) are in the range of reported longitudinal skeletal muscle resistivity (*1.5-3.3 m*).

CONCLUSION Anthropometry could be used alone to calculate the cross sectional areas of dermis, SAT, muscle and bone in order to estimate muscle apparent resistivity in the mid arm. So far, it seems that there is not a statistical significant difference between brachial muscle resistivity of the control group and that of volunteers with FM. Further refinements for this approach are required, which we will try to implement in the next future.

Groups	ρ (Ωm	
	Anthropometry	TC
Total (*n*=23)	1.97 (0.29)	2.06 (0.33)
Controls (*n*=10)	2.03 (0.32)	2.13 (0.38)
With FM (*n*=13)	1.89 (0.24)	1.94 (0.25)

Table 1. *Apparent resistivity (ϱ) calculated using anthropometry (Heymsfield et al 1982) and TC. Values are . In all cases, p > 0.05.*

REFERENCES

1. Heymsfield *et al*. 1982. Am J Clin Nutr 36:680–90.

Abstract Id: 121
Topic: *Instrumentation*

EVALUATION OF MAGNETIC INDUCTION SYSTEM FOR SLEEP MONITORING

Hadiseh Mahdavi* [1], Angel Melchor[1], Javier Rosell Ferrer[1]

[1]Electronic Engineering, Universitat Politècnica de Catalunya, Barcelona, Spain

INTRODUCTION Magnetic induction (MI) method is one of the techniques which could be used in unobtrusive methods for monitoring vital signs. The advantage of MI systems over other methods is that no direct contact is required with the object and the field is not blocked by nonconductive materials like foam or latex mattresses.

OBJECTIVES This paper describes a new magnetic induction system for monitoring vital signs (breathing and heart activity). The hardware and the coils were designed as a low cost sensor for detection of vital signs in bed. Sensitivity of the system to conductivity changes and patient's movements has been studied by simulations and experiments. In addition trials have been performed with volunteers on the bed to compare the performance of the new system with other common methods.

METHODS The system consists of two coils as excitation (EX) and detection (RX) and a phase sensitive detector. The EX is an 8-turn spiral coil with a radius of 2.5 cm and the RX is a one turn coil and a radius of 10 cm, specially designed for cancelling the large background signal from primary field. Coils are planar, coaxial and implemented in PCB in order to be placed under the mattress. The detected signal after amplification (by AD8432) is demodulated (with an AD8302) and later used as an input to BIOPAC-MP36 for comparison with reference signals: photoplethysmogram (PPG) and a pressure sensor. The setup was tested with volunteers over the bed in different postures (supine, prone, and lateral positions) following a protocol, including apnea, normal and deep respiration.

RESULTS Breathing signal is detected easily in both signals (pressure and MI) having equivalent waveforms. For the cardiac activity, the phase of the magnetic system is more sensitive than the magnitude. The study of time signals and frequency spectrums of the three obtained signal (MI, pressure and PPG) shows that they are correlated but the waveforms have different harmonic components. Studying the different postures indicate that the results from supine and prone positions are more reliable and in coherency with the reference signal.

CONCLUSION The differences between the obtained signals from magnetic and pressure sensors indicate that the magnetic sensor detects different contributions of vital signs from those of the pressure sensor which is basically the mechanical and the displacements of the body due to physiological activities.

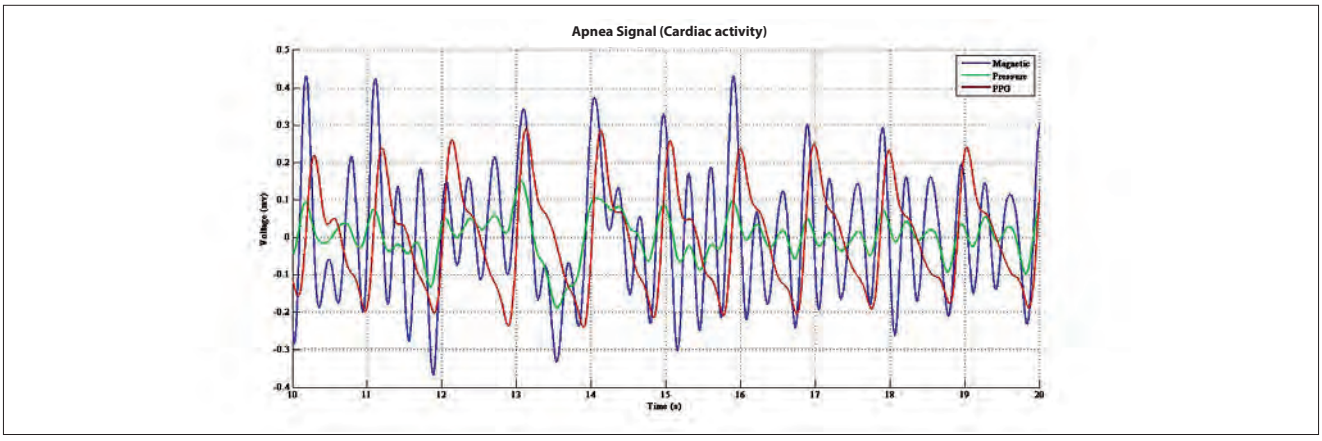

Abstract Id: 122
Topic: *Clinical applications*

RECTAL IMPEDANCE PARAMETERS IN COLORECTAL DISEASES

Edelberto Mulett[*1], Mauricio Osorio[1], Carmen Dussan[2], David Miranda[3], Carlos Gonzalez[4]

[1]Surgical Dept, [2]Mathematics Dept, Universidad de Caldas, Manizales, [3]Physics Dept, Universidad Industrial de Santander, Bucaramanga, [4]Basic Science Dept, Universidad de Caldas, Manizales, Colombia

INTRODUCTION Colorectal cancer (CRC) is the 3rd most common cancer worldwide, and better screening tools are required. We hypothesize that Electrical Impedance Spectroscopy (EIS) readings in the rectum could be used for CRC screening. This hypothesis is based on the evidence that intestinal mucosal permeability increases with CRC, as well as on the theory of field carcinogenesis (FC).

OBJECTIVES To determine the electrical profiles of different colorectal conditions found in a group of adult patients scheduled for total colonoscopy due to different gastrointestinal symptoms.

METHODS Rectal EIS readings were taken in 77 patients who underwent total colonoscopy in a private clinic between 12/2014 and 01/2015. Prior to colonoscopy, EIS readings were taken in four cardinal points on the rectal mucosa of the lower rectum, under direct vision through a plastic anoscope.

RESULTS Endoscopic findings were classified as: 38 normal, 18 polyposis, 8 diverticulosis, 7 with cancer (1 anal, 3 rectal and 3 colonic) and 6 with colitis. From each reading (4 per patient) parameters for the Cole-Cole model were obtained (Table 1): *Ro* the resistivity of extracellular fluid (Ωm); R_i, resistivity at high frequencies (Ωm); τ, mean relaxation time in seconds and α, a heterogeneity parameter. The results suggest that cancer and polyposis could be separated from all other conditions by R_o (p=0.00).

CONCLUSION Initial findings suggest that EIS could be used for separating patients with CRC with readings taken in the rectum, what could be explained by FC. Normal and polyposis show practically the same behavior. Work with much larger samples is needed in order to further develop this hypothesis.

IMAGE

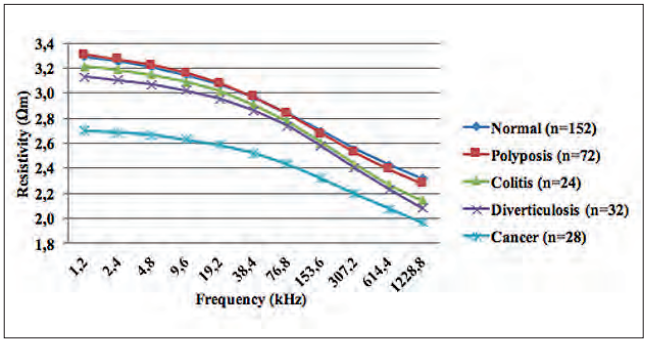

Figure 1. *Means of EIS profiles (4 per patient) of 77 volunteers undergoing total colonoscopy for diverse causes. Values for the curves were obtained using the calculated parameters shown in table 1.*

Diagnosis	Ro (Ωm)	Ri (Ωm)	τ (s)	α
Normal (n=152)	3.41 (0.62)	1.93 (0.57)	46.56 (556.77)	0.46 (0.17)
Polyposis (n=72)	3.43 (0.61)	1.88 (0.63)	1.33 (1.38)	0.45 (0.18)
Colitis (n=24)	3.28 (0.70)	1.82 (0.37)	1.44 (2.47)	0.39 (0.14)
Diverticulosis (n=32)	3.21 (0.70)	1.64 (0.52)	0.70 (0.48)	0.45 (0.15)
Cancer (n=28)	2.75 (0.67)	1.61 (0.65)	0.71 (0.61)	0.39 (0.16)

Table 1. *Means (SD) of the four basic Cole-Cole parameters for impedance readings in the distal rectal mucosa from 77 volunteers undergoing total colonoscopy.*

Abstract Id: 124
Topic: *Instrumentation*

A PORTABLE SYSTEM TO MEASURE MULTI-FREQUENCY IMPEDANCE

Takao Nakamura*[1], Toshimasa Kusuhara[1], Yoshitake Yamamoto[1]

[1]Graduate School of Health Sciences, Okayama University, Okayama, Japan

INTRODUCTION We developed a system to measure the frequency characteristics of bioelectrical impedances that have high time resolution. The frequency characteristics obey the "Cole-Cole circular arc law," characterized by four impedance parameters: Z_0, Z_∞, f_m, and β. Using the developed measuring system, we showed that the movements of throwing motions in baseball were easily distinguished by the impedance parameters[1]. We also developed a portable impedance measuring device by USB mobile phone battery[2].

OBJECTIVES In this paper, we propose a portable system to measure multi-frequency impedance and its parameters for biodynamic analysis and confirm the accuracy of this system.

METHODS The system consists of a portable impedance measuring device that includes five oscillators whose frequencies are 4, 10, 20, 40, and 100 kHz, a portable A/D convertor, and a notebook computer. The five sets of resistance and reactance at each frequency in three set of RC circuits are measured by both this system and LCR meter (4284A, Agilent). We confirm that the accuracy of impedance parameters those are calculated from the five sets of resistance and reactance with a numerical optimization.

RESULTS The errors in Z_0, Z_∞, f_m, and β those were calculated from the five sets of resistance and reactance measured by this system were less than ±0.2%, ±3.5%, ±2.7%, and ±0.5%, respectively.

CONCLUSION The proposed system to measure multi-frequency impedance is sufficiently accurate for estimating bioelectrical impedance parameters. A future study will further develop the analysis method of impedance parameters in biodynamic analysis.

ACKNOWLEDGEMENT This work was supported by JSPS KAKENHI (Grant-in-Aid for Challenging Exploratory Research) Grant Number 26560352.

REFERENCES

1. Nakamura T, Kusuhara T, Yamamoto Y (2013) J Phys Conf Series 434, 12070: 1–4.
2. Nakamura T, Kusuhara T, Yamamoto Y (2015) IUPESM2015 Abstract Book, pp. 424.

Abstract Id: 125
Topic: *Clinical applications*

EVALUATION OF NORMAL FLUID STATUS BY BIOIMPEDANCE TECHNIQUES

Fansan Zhu*[1], Samer Abbas[1], Peter Kotanko[1], Nathan Levin[1]

[1]Renal Research Institute, New York, United States

BACKGROUND Normal fluid status (NFS) can be identified by a hydration marker established in healthy population (HM_H) using bioimpedance techniques. A general population average (HM_G) could be influenced by age and accompanying illness.

OBJECTIVES The aim of this study was 1) to evaluate the effect of age and systolic blood pressure (SBP) on HM_G; 2) to establish average value of HM_H independent of these factors.

METHOD A general population (n=213, males 106, Black 47%) was studied. Whole body and calf bioimpedance were measured with subjects in the supine position (Hydra 4200 device). Body weight, height and SBP were measured. Calf normalized resistivity (CNR), extracellular (ECV) and intracellular (ICV) volumes, ECV/total body water (TBW) were calculated. Subjects were stratified by age; G1: 18 to 35; G2: 36 to 60, G3: 61 to 80 years.

RESULTS Body mass index (BMI), CNR, ICV and ECV/TBW differed significantly between age groups and genders (Table 1). Decreased CNR ($p<0.001$) and increased SBP ($p<0.001$) were associated with age in G2 and G3 but not in G1 ($p=0.55$). CNR in G1 was the same as in 36% of subjects in G2 and 12.5% of subjects in G3. In those subjects in G2 and G3 with CNR levels comparable to G1 subjects, SBP was lower than their peers in each respective age group.

CONCLUSION Average CNR in G1 represents the range of HM_H. CNR is correlated with age in G2 and G3, and these groups were also more susceptible to fluid overload. This relationship can be explained by the link between SBP and age. In about a third of subjects in G2 and G3, CNR was in the range of HM_H, suggesting that increased SBP and associated fluid overload are factors that affect the use of HM in the general population.

KEY WORDS Hydration, Bioimpedance, dialysis.

Table 1

	G1		G2		G3	
	Male (n=37)	**Female(n=34)**	**Male(n=49)**	**Female(n=51)**	**Male(n=20)**	**Female(n=22)**
Age (year)	29.1±4.2	28.6±4	46.6±6.6	47.2±6.6	65.4±7.8	66.7±7.8
BMI (kg/m²)	25.6±5.5	23.0±3.5	27.1±4.3	26.3±4.5	28.1±4.1*	26.3±5.8**
SBP (mmHg)	119.3±12	110.5±11	123.1±17	119.7±19	130.2±19	122.9±24*
CNR Ohm*m³/100*kg)	20.3±2	21.4±2.9	17.4±2.6	18.1±3.1	14.4±2.3**	17.4±2.9**
ECV (L)	18.1±2.3	13.3±1.7	18.4±2.6	14.6±2.1	18.5±1.9	13.8±2.2*
ICV (L)	28.3±5.5	19.2±4.4	26.8±5.3	20.3±4.7	25.0±3.1*	17.6±2.3*
ECV/TBW	0.39±0.04	0.41±0.04	0.41±0.03	0.42±0.05	0.43±0.02**	0.44±0.02*

Abstract Id: 126
Topic: *Clinical applications*

MUSCLE IMPEDANCE SPECTRA IN DUCHENNE MUSCULAR DYSTROPHY

Seward Rutkove[*1], Basil Darras[1]

[1]Neurology, Harvard Medical School, Boston, United States

INTRODUCTION Biomarkers to assess disease progression and therapy efficacy in muscle diseases are greatly needed to speed clinical therapeutic trials (1). The localized application of electrical impedance techniques to muscle, electrical impedance myography (EIM), offers the prospect of providing valuable measures of disease status (2). Since muscle architecture changes with progressive disease (3), we anticipate that impedance alterations would reflect muscle condition and response to a therapeutic intervention.

OBJECTIVES In this study, we compared alterations in the frequency at which the reactance peak occurs between healthy boys and a group of boys with Duchenne muscular dystrophy (DMD). We also evaluated changes across age in both groups since the disease worsens with increasing age.

METHODS A total of 36 boys with DMD and 26 healthy boys aged 2.2-14.6 years were enrolled at Boston Children's Hospital. EIM measurements were performed on multiple muscles using a handheld electrode array connected to a multi-frequency bioimpedance device. Values were averaged across muscles.

RESULTS Mean (±standard deviation) of peak reactance frequency in the group of healthy boys was 481(±184) kHz and was 141(±62) kHz in the DMD boys; this difference was significant (p=2E-13). This provided a specificity and sensitivity of this measure of 94%, and 92% respectively. In the DMD boys, peak frequency positively correlated significantly to age (R=0.43, p=0.008); in contrast, in healthy boys there was a significant negative correlation (R=-0.52, p =0.006).

CONCLUSION The EIM peak reactance frequency readily differentiates healthy boys from those with DMD. Moreover, this measure correlates positively to age in boys with DMD whereas it does so negatively in healthy boys. These results support the concept that EIM peak reactance data reflects the underlying pathological state of the muscle. More importantly, it supports its potential use as a biomarker for future clinical therapeutic trials in DMD and related diseases of muscle.

REFERENCES

1. Govoni A et al. Ongoing therapeutic trials and outcome measures for Duchenne muscular dystrophy. *Cell. Mol. Life Sci.* 2013;70(23):4585–602.
2. Rutkove SB. Electrical Impedance Myography: Background, Current State, and Future Directions. *Muscle Nerve* 2009;40:936–946.
3. Emery AEH. The muscular dystrophies.. *Lancet* 2002;359(9307):687–95.

Abstract Id: 127
Topic: *Clinical applications*

INTERCONVERSION OF SUPINE AND STANDING BIOIMPEDANCE VALUES

Leigh Ward[*1], Wilson Yip[2], Lindsay Plank[3], Sally Poppitt[2]

[1]School of Chemistry and Molecular Biosciences, The University of Queensland, Brisbane, Australia,
[2]Human Nutrition Unit, School of Biological Sciences, University of Auckland,
[3]Faculty of Medical and Health Sciences, University of Auckland, Auckland, New Zealand

INTRODUCTION Bioimpedance analysis is a popular method for the estimating body composition, originally measuring impedance from foot to hand, with the subject supine using skin electrodes. Many population-specific prediction algorithms are available using this protocol. More recent impedance devices measure the subject standing on electrode plates and gripping an electrode handle or bar. Although such devices are programmed with proprietary prediction algorithms, researchers frequently wish to use validated published algorithms specific for their population but obtained using the supine protocol.

OBJECTIVES To determine: the relationship between standing and supine impedance measurements and whether this would allow inter-conversion of measurements between methods.

METHODS Left side body (B), arm (A) and leg (L) impedances were measured (50 kHz) with an ImpediMed SFB7 in 150 healthy Caucasians (82M:68F) after 15 min supine. Current electrodes were located at the base of fingers and toes and sense electrodes midway between the bony prominences at the wrist and ankle. Measurements were repeated with the subject standing on stainless steel (SS) electrode plates: the drive under the ball of the foot; the sense electrode under the heel. Hand electrodes were SS plates in a handle: the drive electrode under the fingers; the sense electrode under the thumb.

RESULTS Impedance values were highly correlated between methods (Pearson r = 0.96, 0.96 & 0.83 for B, A and L respectively) but were significantly different ($P<0.001$ for all, pair t test) and did not lie on the line of identity (concordance r = 0.80, 0.71 & 0.80 for B, A and L respectively). Mean standing impedances were 14.3, 8.8 and 3.6% larger than supine values for B, A and L respectively. Limits of agreement (LOA, supine-standing) were -0.4 to -17.0, -4.4 to -24.3 and 12.7 to -19.9% for B, A and L respectively.

CONCLUSIONS Although methods were highly correlated, the magnitude of the biases and large LOA indicate that inter-conversion of data using regression equations would introduce unacceptably large errors. Larger impedances when standing are due to the increased inter-electrode distance, although offset by decreases in impedance through fluid redistribution to the lower extremities due to gravity.

DISCLOSURES Financial support provided by Fonterra and the New Zealand Ministry for Primary Industries Dairy Primary Growth Partnership Post Farm Gate Programme.

Abstract Id: 128
Topic: *Bioimpedance*

IDH PREDICTION USING THE PEP AND ISTI DURING HAEMODIALYSIS

Ruud van der Stappen[*1], Marc Vervloet[2], Monica Parry[3], Jan Meijer[1]

[1]Department of Physics and Medical Technology, [2]Department of Nephrology and Institute for Cardiovascular Research, VU University Medical Center, Amsterdam, Netherlands, [3]Lawrence S. Bloomberg Faculty of Nursing, University of Toronto, Toronto, Canada

INTRODUCTION The Initial Systolic Time Interval (ISTI) is defined as the time between the R-peak of the electrocardiogram (ECG) and the dZ/dt minimum or C-point of the impedance cardiogram (ICG). The Pre-Ejection Period (PEP) is defined as the time between the R-wave onset or Q-point in the ECG and the 0-crossing before the dZ/dt minimum or B-point in the ICG. Both intervals are measured non-invasively. The PEP is difficult to measure, while the ISTI is easily automated and measured. Both the ISTI and PEP are expected to remain constant during normal function. Intradialytic Hypotension (IDH) is the most common complication of haemodialysis (HD). IDH reduces the efficiency of dialysis and results in subsequent central blood volume depletion, reduced cardiac output and an abrupt drop in blood pressure.

OBJECTIVES The ISTI and PEP were registered for one minute every fifteen minutes during HD sessions of approximately four hours. If the ISTI and PEP increased/decreased proportionally over time during dialysis, the ISTI could be automated and used to give an estimation of the PEP. If IDH could be predicted using either time interval or a combination of the two, timely countermeasures could be taken to prevent pathology.

METHODS ECG and ICG measurements were made in 25 patients of age 59 ± 15 (mean ± SD) undergoing HD. The ICG measurements were made using four electrodes on the left side of the thorax: the two outermost electrodes applied a current through the thorax and the two innermost electrodes measured the voltage difference V(t) over the heart. The impedance Z(t) was then computed. The ECG was computed from the innermost electrodes.

RESULTS The PEP was found to increase by $2.49*10^{-3} \pm 8.69*10^{-3}$ (mean ± SD) seconds per hour HD ($P<0.05$). The ISTI was found to increase by $2.28*10^{-3} \pm 5.24*10^{-3}$ seconds per hour dialysis ($P<0.05$). In patients with IDH (n=2) the PEP increased by $3.22*10^{-3} \pm 7.66*10^{-4}$ ($P<0.10$) and the ISTI increased by $7.02*10^{-3} \pm 1.39*10^{-3}$ ($P<0.10$) seconds per hour HD.

CONCLUSION The ISTI cannot readily be used to estimate the PEP in patients undergoing HD because the PEP and ISTI behave differently amongst different patients. The PEP does not behave differently in patients with an IDH event during HD, showing no promise for IDH prediction. The ISTI increases more in patients with an IDH event and therefore shows promise in predicting IDH events during HD.

IMAGE

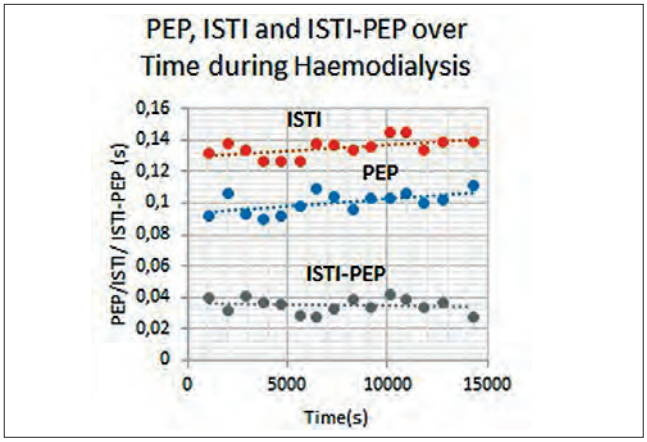

Abstract Id: 129
Topic: *Clinical applications*

BIOIMPEDANCE PROBE (BIP) NEEDLE IN SPINAL ANESTHESIA

Sanna Halonen*[1], Juho Kari[1], Kari Annala[2], Kai Kronström[1], Arvi Yli-Hankala[3]

[1]R&D Department, Injeq Ltd, [2]Anaesthesiology, Tampereen Lääkärikeskus Ltd,
[3]Anaesthesiology, Tampere University Hospital, Tampere, Finland

INTRODUCTION Spinal anesthesia is relatively safe procedure, but some serious complications, even death, occur [1]. Physician is also challenged by anatomic alternations and obesity [2]. A needle guidance, based on for example bioimpedance [3], could increase accuracy and ease the puncture. Here bioimpedance-based tissue-sensing technology is applied for detecting cerebrospinal fluid (CSF).

OBJECTIVES Feasibility of the Bioimpedance Probe (BIP) Needle to detect CSF in lumbar punctures is tested in clinical study. The study provides bioimpedance data for CSF detection model tuning and further development of the needle guidance method.

METHODS BIP Needle consists of a common spinal needle and a removable BIP stylet, which is an insulated electrode wire with special handle. It enables real-time measurement of bioimpedance spectra in bipolar fashion between the electrode wire and needle cannula. In this clinical study, spinal anesthesia punctures were performed with BIP Needle connected to bioimpedance analyzer and tissue classification software (analyzer and needle in the image). When the device detected CSF, it provided a feedback and an experienced anesthesiologist (K.A.) evaluated the performance. Needle location was verified with traditional CSF test. Number of patients in this initial model tuning phase was 10.

RESULTS CSF was detected in all 10 cases. Brief false detections occurred in two cases, but offline analysis showed that model tuning will increase specificity without reducing the sensitivity. Epidural space differentiated from surrounding tissues as fatty tissue, but the variation between individuals was high.

CONCLUSIONS BIP Needle reliable detected CSF in spinal anesthesia in all cases. The recorded data will be utilized for model tuning and the method will be further tested with higher number of patient. BIP Needle has potential to be used as a needle guidance method for spinal anesthesia, and improve accuracy and speed up the procedure.

IMAGE

REFERENCES

1. Pitkänen MT et al. Serious complications associated with spinal and epidural anaesthesia in Finland from 2000 to 2009. Acta Anaesthesiol Scand 57.5 (2013):553–564.
2. Chin KJ et al. Ultrasound imaging facilitates spinal anesthesia in adults with difficult surface anatomic landmarks. Anesthesiology 115.1 (2011):94–101.
3. Kalvøy H et al. Impedance-based tissue discrimination for needle guidance. Physiol Meas 30.2 (2009):129–140.

Abstract Id: 130
Topic: *Clinical applications*

BIOIMPEDANCE FOR PREDICTION OF HYPOGLYCEMIC TRENDS

Christian Tronstad[*1], Ole Elvebakk[1], Ørjan G Martinsen[1,2], Håvard Kalvøy[1], Jan Olav Høgetveit[1,2]

[1]Department of Clinical and Biomedical Engineering, Oslo University Hospital,
[2]Department of Physics, University of Oslo, Oslo, Norway

INTRODUCTION Non-invasive prediction of blood glucose based on bioimpedance has been investigated for more than a decade, but accurate prediction based on bioimpedance alone has never been demonstrated. Correlations have been reported in several papers, but due to inconsistent results, it has been difficult to pinpoint the biophysical explanation for this correlation. So far bioimpedance seems to be a feasible predictor of trends in blood glucose, at best. One particularly important trend is the sharp fall in blood glucose leading to hypoglycemia. The feasibility of bioimpedance as a predictor of trends in blood glucose during hypoglycemic episodes has not been assessed before.

OBJECTIVES Prediction of trends in blood glucose based on bioimpedance could be part of a multisensor system for detection of hypoglycemia. The aim of this part was to assess the performance of prediction in blood glucose trends based on non-invasive bioimpedance measurement.

METHODS 20 type 1 diabetes patients underwent two trials in randomized order, one with normal glucose levels and one where blood glucose was lowered to 2.5 mmol/L before returning to normal values. A constant infusion of insulin was administered based on body weight, and blood sugar was regulated using a variable infusion of glucose. Through two wet-gel electrodes at the proximal side of the underarm, bioimpedance in the frequency range of 1-200 MHz was measured using a vector impedance analyzer (VIA ECHO 2500, AEA Technology, CA, USA) every fifth minutes during the clamp, simultaneously as the blood samples were drawn. The immitance parameters of impedance modulus, phase angle, resistance, reactance, conductance, susceptance and tan delta were inspected for intraindividual correlation to changes in blood glucose. Using k-fold cross-validation with k=10, a prediction model based on partial least squares (PLS) regression was calibrated on the training set, and the performance in trend prediction was evaluated based on correlations in the validation-set.

RESULTS The prediction performance had a mean correlation coefficient on the validation set of 0.65 ± 0.006.

CONCLUSION The performance of trend prediction in blood glucose during hypoglycemia based on bioimpedance measurement is inaccurate, but may provide increased specificity as part of a multisensor system for noninvasive detection of hypoglycemia.

Abstract Id: 131
Topic: *Bioimpedance*

IMPEDIMETRIC MONITORING OF NEURAL STEM CELL DIFFERENTIATION

Heinz-Georg Jahnke* [1], Diana Seidel[1], Andrea Robitzki[1]

[1]Centre for Biotechnology and Biomedicine (BBZ),
Molecular biological-biochemical Processing Technology, Leipzig, Germany

INTRODUCTION According to the needs of assays and screenings, human pluripotent stem cells are a unique source for functional human cell types. Especially human neural stem cell-derived neuronal networks represent the only accessible *in vitro* model that resembles a functional primary human phenotype. However, differentiation and maturation of these cells are a very complex and time-consuming process.

OBJECTIVES In this context, non-invasive label-free techniques to monitor the neuronal differentiation and maturation of human stem cells are highly demanded. Our aim was to demonstrate the successful use of impedance spectroscopy for the sensitive label-free monitoring of the complete differentiation process from progenitor cells to neuronal networks.

METHODS Therefore, we used optimized high-dense microelectrode arrays (MEAs) in combination with high precision impedance analyzers to identify specific impedimetric characteristics for the neuronal differentiation process. Moreover, we performed detailed correlative molecularbiological analyses to validate the identified impedimetric parameters.

RESULTS First, we identified the optimum MEA to analyze the differentiation of reference human neural stem/progenitor cell models by impedance spectroscopy. In this context, we needed to optimize the surface of the MEAs for achieving a long-term stable cell-electrode interface. Afterwards, we identified distinct cell dependent impedimetric parameters that could specifically be associated with the progress and quality of neuronal differentiation. Applying an adapted equivalent circuit model, we were able to understand the identified empiric impedimetric parameters. For validation, we analyzed the expression of progenitor versus mature neural marker and typical structural changes. The correlation analysis revealed a strong predictive power of the identified impedimetric parameters. More strikingly, we could demonstrate the capability of our impedimetric differentiation monitoring system to identify neuronal differentiation accelerating compounds.

CONCLUSION For the first time, we proved that non-invasive impedance spectroscopy can be used for the specific quantitative monitoring of neuronal differentiation processes. Therefore, this technique will be a useful tool for quality control of neuronal differentiation, neurogenic compound identification and moreover, high-content screening demands in the field of safety assessment as well as drug development.

Abstract Id: 132
Topic: *Electrical impedance spectroscopy*

FAST AND BROADBAND IMPEDANCE DETECTION

Uwe Pliquett*[1]

[1]Analysenmesstechnik, Institut für Bioprozess- und Analysenmeßtechnik, Heilbad Heiligenstadt, Germany

INTRODUCTION The selectivity of Impedance detection increases with bandwidth and speed. Especially fast events with characteristic spectra spanning several orders of magnitude in frequency cannot be monitored with slow or narrow bandwidth methods. However, instrumentation for fast and broadband width is usually expensive and requires high computer power.

OBJECTIVES A method is presented, working with simple hardware and low power requirement. The measurement time is as short as the period of the lowest frequency component while the bandwidth extends to 10 MHz. Per frequency decade 10 data points are generated. All hardware is compatible with monolithic integration.

METHODS A step function, either current or voltage, is used for excitation while the answer is generally converted into a current and partially integrated. An ADC converts the integrated signal at predefined times. From the sampled data either an impedance spectrum or the time spectrum can be calculated for further proceeding.

RESULTS The impedance of cell suspensions contacted by microelectrodes was measured with different techniques: step sinus, multi-sinus and step response as described above. While step sinus was used as golden standard, multi-sinus acted as established method in time domain. Both results from multi-sinus and step response showed deviations of less than 3 % in a frequency range between 10 Hz and 10 MHz. Other than sampling the multi-sinus-answer, the jitter at the sample points and ADC-noise is more crucial for assessment of the step answer. While the data volume for the multi-sinus answer reached 2 million points, only 60 points were recorded for the step answer.

CONCLUSION The assessment of the step answer for fast and broad-bandwidth impedance detection with partial integration and adaptive sampling can be as accurate as reference methods but utilizes only a fraction of the resources.

Abstract Id: 133
Topic: *Non-linear phenomena*

INVESTIGATING THE MEMRISTIVE PROPERTIES OF SKIN

Oliver Pabst[*1], Ørjan Grøttem Martinsen[1,2]

[1]Department of Physics, University of Oslo, [2]Department of Clinical and Biomedical Engineering, Oslo University Hospital HF, Oslo, Norway

INTRODUCTION Non-linear electrical properties in skin were already observed in 1983 [1]. These observed properties are specified as memristive properties [2]. The memristor is the fourth passive element which was first described in [3] and "memristive systems" is a more generalized term [4]. The memristive properties of skin enable a new field of research that potentially provides new tools and insights for medical applications.

OBJECTIVES To enable the use of memristive properties of skin for e.g. diagnostics they have to be investigated further. This presentation shall give the results of basic research. Questions that shall be answered are e.g.: Which memristor type is skin (type I or type II) [5]? Under which conditions occur memristive effects?

METHODS The measurements are done with different versions of a custom-built measurement system. It is realized as a two electrode as well as a three electrode system. The desired voltage is applied to the skin and the current through the skin is read at the same time. Different skin sites are measured.

RESULTS For several conditions a pinched hysteresis shaped loop which is characteristic for a memristor [6] could be observed. In Fig. 1 an example is shown. The x-axis represents the applied voltage. The measured voltage which is pictured on the y-axis is proportional to the current through the skin.

CONCLUSION It is shown that skin has memristive properties.

IMAGE

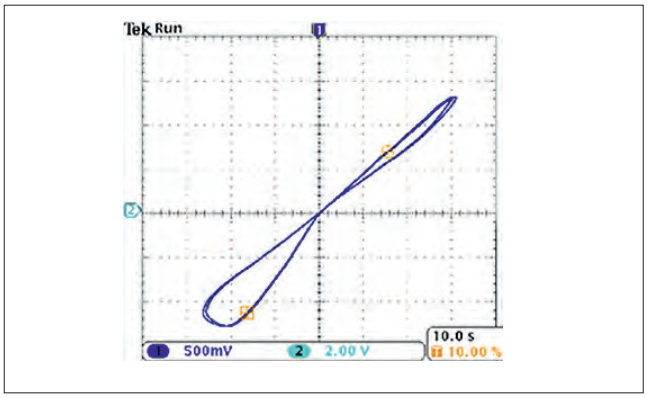

Fig. 1. *Hysteresis loop over 2 periods. Applied sinus voltage with Vpp = 10.5 V and f = 20 mHz. Two electrode system, measured at the left forearm.*

REFERENCES

1. S. Grimnes, "Skin impedance and electro-osmosis in the human epidermis," Medical and Biological Engineering and Computing, vol. 21, no. 6, pp. 739–749, 1983.
2. G. K. Johnsen, C. A. Lütken, Ø. G. Martinsen, and S. Grimnes, "Memristive model of electro-osmosis in skin," Physical Review E, vol. 83, no. 3, p. 031916, 2011.
3. L. Chua, "Memristor-the missing circuit element," Circuit Theory, IEEE Transactions on, vol. 18, no. 5, pp. 507–519, 1971.
4. L. Chua and S. Kang, "Memristive devices and systems," Proceedings of the IEEE, vol. 64, no. 2, pp. 209–223, 1976.
5. D. Biolek, Z. Biolek, and V. Biolkova, "Pinched hysteretic loops of ideal memristors, memcapacitors and meminductors must be'self-crossing'," Electronics letters, vol. 47, no. 25, pp. 1385–1387, 2011.
6. L. Chua, "If it's pinched it's a memristor," in Memristors and Memristive Systems, pp. 17–90, Springer, 2014.

Abstract Id: 134
Topic: *Bioimpedance*

NON-CONTACT BIO-IMPEDANCE SPECTROSCOPY IN THE FOOD INDUSTRY

Michael D O'Toole[*1], Liam A Marsh[1], John L Davidson[1],
Yee Mei Tan[1], David W Armitage[1], Anthony J Peyton[1]

[1]School of Electrical and Electronic Engineering, The University of Manchester, Manchester, United Kingdom

INTRODUCTION Non-contact bio-impedance measurement of food samples over the beta dispersion range can potentially provide a high-throughput, non-destructive means of quality assessment.

OBJECTIVE We investigate the signal-to-noise (SNR) characteristics of a multi-frequency magnetic induction spectroscopy system for non-contact bio-impedance measurement of fruits and vegetable at speeds suitable for, or near to, industrial-scale operation.

METHOD The sensor consists of an arch-shaped gradiometer (160 mm w, 290 mm h, 340 mm l) potted in an aluminium enclosure. Internal walls are screened using graphite paint. Samples pass through the radial centre of the archway on a metal-free conveyor.

An excitation coil in the middle of the gradiometer is driven simultaneously at the following frequencies and currents: 156 kHz (4.97 A), 313 kHz (1.94 A), 625 kHz (0.73 A), 1.25 MHz (0.27 A), and 2.5 MHz (0.08 A). The sample's field is measured by the gradiometer and low-noise amplifier (gain 90 dB, noise 11.9 nV/√Hz). A novel auto-nulling method prevents amplifier saturation. Signals are processed using a NI PXIe-7966R FlexRIO FPGA with NI 5781 baseband transceiver (National Instruments, USA). The system is currently able to process samples every 1.5 seconds with significant scope to increase this speed. Further details are found in [1, 2].

RESULTS A gala apple, white flesh nectarine, salad tomato and baked potato were scanned. The samples showed increasing conductivity with frequency, indicative of the beta-dispersion region, at conductivities between 40–300 mS/m. All samples except potato were in the upper part of the dispersion. The SNR for each sample is shown in figure 1. The lowest SNRs are at the lowest frequency with the lowest conductivity sample, the gala apple, the worse case at 14.7 dB SNR.

CONCLUSION We obtain good SNR for typical fruits down to 156 kHz using a system fast and rugged enough for industrial use. However, this range only covers the top of the beta dispersion. Lower frequencies are desirable as they are more sensitive to cell membrane changes.

IMAGE

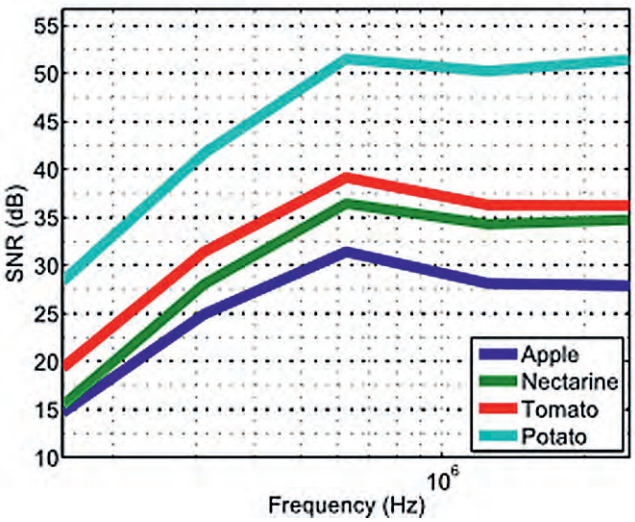

REFERENCES

1. O'Toole et al., Meas. Sci. Technol., 26, 2015.
2. O'Toole et al., IEEE Sens. App. Sym., Croatia, 2015.

Abstract Id: 135
Topic: *Clinical applications*

QUEST FOR THE PROPER B-POINT IN THE ICG BY ECHOCARDIOGRAPHY

Kirsten Broeze[1,2], Richard van der Elzen[1,3], Michael J van Rijssel[4], Maureen A van Eijnatten[*5], Rudolf M Verdaasdonk[1], Ørjan G Martinsen[6], Jan H Meijer[1,6]

[1]Department of Physics and Medical Technology, VU University Medical Center, [2]Faculty of Earth and Life Sciences, [3]Faculty of Sciences, Vrije Universiteit, Amsterdam, [4]Center for Image Sciences, UMC Utrecht, Utrecht, [5]Department of Oral and Maxillofacial Surgery/Pathology, VU University Medical Center, Amsterdam, Netherlands, [6]Department of Physics, University of Oslo, Oslo, Norway

INTRODUCTION In the field of psychophysiology the impedance cardiogram (ICG; thoracic dZ/dt signal) is used to assess the activity of the autonomic nervous system (ANS). The pre-ejection period (PEP) is considered to be a non-invasive measure of the sympathetic activity and is calculated from the time difference between the Q-point in the simultaneously measured electrocardiogram (ECG) and the B-point in the ICG. The B-point is believed to coincide with the moment of the opening of the aortic valves and therefore with the start of the systolic phase of the cardiac cycle. However, in reported studies there is little agreement on the exact position of the B-point in the ICG-signal.

OBJECTIVES The aim of this study was to investigate the synchronicity between the timing of six different, proposed B-point positions and the opening of the aortic valves, simultaneously determined by echocardiography.

METHODS A wide range of heart rates (HR) was induced by an exercise stimulus in sixteen young healthy adults. The differences in timing between each of the possible B-points and the opening of the aortic valves were established at HR of 60 and 120 beats per minute. Also the agreement between the trends of the timing of the B-points and the trend in timing of the opening of the aortic valves with HR was investigated. The differences in slopes with HR were established and tested.

RESULTS None of the proposed B-points were in full agreement with the opening of the aortic valves over the whole range of HR or with the trend in timing with HR. However, the zero-crossing of dZ/dt at the onset of the C-wave and the inflection point in the slope of the down stroke of the C-wave, characterized by the largest minimum in the derivative of the ICG, may be acceptable for indicating the opening of the aortic valves. For both possible B-points the differences in timing with the opening of the aortic valves were small. This last point had a small, but systematic deviation from the moment of opening of the valves, for which should be corrected.

CONCLUSIONS None of the investigated B-points in the ICG corresponded with the moment of opening of the aortic valves over the whole range of HR. Two points may be acceptable as an assessor of this moment. Of these, the zero-crossing of the ICG signal is the most suitable for automated detection.

Abstract Id: 136
Topic: *Clinical applications*

THE X-POINT IN THE ICG MARKS AORTIC VALVES CLOSURE

Kirsten Broeze[1,2], Richard van der Elzen[1,3], Michael J van Rijssel[4], Maureen A van Eijnatten[*5], Rudolf M Verdaasdonk[1], Ørjan G Martinsen[6], Jan H Meijer[1,6]

[1]Department of Physics and Medical Technology, VU University Medical Center, [2]Faculty of Earth and Life Sciences, [3]Faculty of Sciences, Vrije Universiteit, Amsterdam, [4]Center for Image Sciences, UMC Utrecht, Utrecht, [5]Department of Oral and Maxillofacial Surgery/Pathology, VU University Medical Center, Amsterdam, Netherlands, [6]Department of Physics, University of Oslo, Oslo, Norway

INTRODUCTION The left ventricular ejection time (LVET) is defined as the time difference between the opening and the closing of the aortic valves. LVET can be assessed non invasively from the impedance cardiogram (ICG) as the time difference between the moments of the B- and X-points, which represent the opening and closing respectively of the aortic valves in the cardiac cycle. The X-point, a peak in the ICG between the C- and O-wave, is believed to coincide with the moment of the closing of the aortic valves. However, there is uncertainty about the exact position of the X-point in the ICG-signal since more than one peak may occur.

OBJECTIVES The aim of this study was to examine the degrees of synchronicity between the timing of five different proposed X-point candidates and the closing of the aortic valves, simultaneously determined by echocardiography.

METHODS A wide range of individual heart rates (HR) was induced by an exercise stimulus in sixteen young healthy adults. The degrees of agreement were established at heart rates of 60 and 120 beats per minute. Also the agreement between the trends of the timing of the X-point candidates and the trend in timing of the closing of the aortic valves with HR was investigated. The differences in slopes with HR were established and tested.

RESULTS When three peaks are present between the C- and O-wave the middle peak is a good assessor of the closing of the aortic valve. The timing of this peak didn't differ significantly from the moment of closing of the aortic valves both at low and high heart rates. Also the trend with increasing heart rate was not significantly different. However, this peak was not detectable in every heartbeat. When two peaks are present, the second may be acceptable for indicating the closing of the aortic valves, since only at high HR a significant difference in timing was found that was limited.

CONCLUSIONS The moments of three of the five proposed X-point candidates were not in agreement with the moment of closure of the aortic valves over the range of HR and/or the slopes of the trends with HR of the moments of these X-points were significantly different from the slopes of the trends of the moment of closure of the aortic valves. However, the other two proposed X-points can be used as assessors for this moment of closure.

Abstract Id: 137
Topic: *Electrical impedance spectroscopy*

COMPARING IMPEDANCE SPECTROSCOPY AND PLASMONIC BASED EIS

Eugen Gheorghiu*[1]

[1]International Centre of Biodynamics, Bucharest, Romania

INTRODUCTION The quest for impedance assays with increased spatial resolution led to development of a new technique, Plasmonic based Electrical-Impedance-Spectroscopy, P-EIS. This study highlights the theory behind P-EIS, presents a combined EIS and P-EIS experimental set-up, and discusses the results.

OBJECTIVES To reveal advantages and current limitations of P-EIS versus classical EIS.

METHODS P-EIS gathers EIS and Surface Plasmon Resonance,SPR by deploying an electrode exhibiting plasmonic properties in a set-up combining an AC signal generator (as the ones used for EIS) and a SPR module. The basic formalism relating SPR to the surface charge density when applying an AC potential modulation to an electrode (with plasmonic properties) and the interfacial impedance has been recently outlined [1, 2, 3]. However, based on the Drude model and transfer-matrix approach we emphasize the effect of the AC field not only on the oscillation of the SPR-angle but on the entire reflectivity curve.

RESULTS We highlight the actual conditions allowing assessment of the amplitude and phase of the impedance from the P-EIS signal. The main advantage of P-EIS versus the classical EIS analysis is given by the increased spatial resolution of P-EIS without using (arrays) of micro-electrodes or implementing scanning electrochemical microscopy. When performing P-EIS, the whole sensing area is accessible with exquisite spatial resolution which is not limited by the size or distribution of the electrodes (as in the case of EIS) but solely by the (lateral) propagation length of the surface plasmons. Depending on sensor structure and incident light wavelength, this spatial resolution could reach sub-micrometer range.

CONCLUSION P-EIS gathers the capabilities of both EIS and SPR and its outstanding applicative potential spans from biosensing to analysis of living cells. Comparison between classical EIS and P-EIS measurement with emphasis on experimental limitations is also presented in the context of a novel plasmonic EIS microscopy system which is currently developed within ICB.

ACKNOWLEDGMENTS The study was supported by the Romanian National Contract No. 11/2012, ID: PN II-ID-PCCE-2011-2-0075, BIOSCOPE

REFERENCES

1. Lu, J.; Wang, W.; Wang, S.; Shan, X.; Li, J.; Tao, N. *Anal. Chem.* 2012, *84*, 327–333.
2. Foley, K. J.; Shan, X.; Tao, N. J. *Anal. Chem.* 2008, *80*, 5146–5151.
3. Polonschii C., David S., Gáspár S., Gheorghiu M., Rosu-Hamzescu M., Gheorghiu E., *Anal. Chem.* 2014, 86, 8553–8562

Abstract Id: 138
Topic: *Bioimpedance*

FAT PREDICTION IN MINCED MEAT WITH LOW-COST BIA SPECTROMETER

Mart Objartel*[1], Martti Tamm[1], Kadri Kraft[2], Paul Annus[3], Raul Land[3]

[1]Competence Center of Food and Fermentation Technologies, [2] Department of Food Processing,
[3]Thomas Johann Seebeck Department of Electronics, Tallinn University of Technology, Tallinn, Estonia

INTRODUCTION Current classical methods for measuring fat content are based on chemical reactions. They are slow, destructive and will need skilful personnel to carry out. There is a need for instrumental express methods that would allow to measure fat content quickly and with satisfactory accuracy.

It has been shown that bioelectrical impedance can be used to evaluate intra- and extracellular fat content in animal carcasses or parts thereof and also in grinded meat.

OBJECTIVES The aim of this work was to study the applicability of low power and low cost portable impedance spectrometer assessing the correlation between bioimpedance measurements and fat content in meat using neural network (NN) based approach for data analysis.

METHODS Vacuum packaged pork *longissimus dorsi* samples were obtained from local store. Any visible fat was cut from the samples and the lean meat was minced using Braun Multiquick 3 meat mincer G1300.

The minced meat was then divided into approximately 50g pieces and different amounts of rendered pig fat was added to each piece, achieving fat concentration gradient between 2% to 30%

Bioimpedance measurements to obtain impedance (Z, Ω) and phase angle (P, degrees) values on samples were carried out with TMS320f28069-based impedance spectroscopy device with binary excitation.

Gold plated extended 2.54 mm male header (1x4) was used as a tetrapolar electrode.To obtain reference values for fat content in samples, Soxhlet method (SOX) was used with VELP SCIENTIFICA SER 148/6 apparatus.

The data was analysed with MATLAB R2015b Neural Fitting app using a two-layer feed-forward network with sigmoid 10 hidden neurons and linear output neurons. The network was trained with Levenberg-Marquardt backpropagation algorithm. The 54 samples were randomly divided up to: Training 32 samples (60%), Validation 11 samples (20%) and testing 11 samples (20%)

RESULTS Table 1. Regression R Values measure the correlation between outputs and targets. Mean Squared Error (MSE) is the average squared difference between outputs and targets.

	Samples	MSE	R
Training	32	5.14	0.973
Validation	11	23.76	0.89
Testing	11	9.90	0.96

CONCLUSION The preliminary results show that it is possible to train simple NN to predict fat concentration with acceptable accuracy in minced pork meat based on impedance measurements in the range of 1kHz to 349kHz.

IMAGE

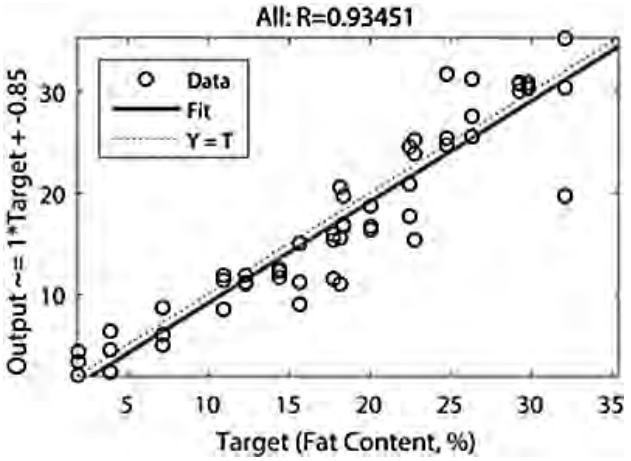

Abstract Id: 139
Topic: *Electrical impedance spectroscopy*

STUDYING THE MEMBRANE DYNAMICS DURING CELL ELECTROPULSATION

Tomas Garcia-Sanchez[*1], Antoine Azan[1], Isabelle Leray[1], Ramon Bragos[2], Lluis M. Mir[1]

[1]Vectorology and Anticancer Therapies, UMR 8203, CNRS, Univ. Paris-Sud, Gustave Roussy, Université Paris-Saclay, 94805 Villejuif, France, [2]Electronic and Biomedical Instrumentation Group, Department of Electronic Engineering, Universitat Politecnica de Catalunya, Barcelona, Spain

INTRODUCTION Cell electropulsation, widely known as cell electroporation, constitutes nowadays an excellent option as a physical method for the incorporation of foreign molecules into the cell cytoplasm, also for extraction of intracellular compounds, with many other applications in vitro and in vivo. The technique, based on the application of high intensity short electric field pulses to biological samples, causes the transient (reversible electroporation) or the definitive (irreversible) permeabilization of cell membrane.

The mechanisms of membrane recovery after electric pulse treatment as well as their dynamics remain still unclear. Electrical measuring methods such as time domain electrical impedance spectroscopy (EIS) represent a suitable option to study the fast events produced during the resealing of cell membrane.

OBJECTIVES The aim of this study is to improve the understanding of the mechanisms of membrane resealing during and after cell electroporation in different experimental conditions by studying the changes in membrane dielectric properties using EIS measurements.

METHODS Measurements were performed in adherent cells by means of a microelectrode structure conceived both for applying the permeabilization pulses and recording impedance signals. To perform the electrical bioimpedance measurements, we used a multisine excitation as the reference signal. In order to reveal the events in the membrane occurring just after pulse application, impedance spectra were recorded with a time resolution of 1 ms in the temporal gap between consecutive pulses (usually on second) of a regular electroporation procedure.

Different experimental conditions were applied to cells during the course of measurements. Namely, variations in the composition of the extracellular medium and different combinations in the number, duration and intensity of the electric field pulses applied.

RESULTS Measurements reveal different dynamic processes in the system that are dependent on the experimental conditions applied. Different time scales are observed ranging from milliseconds to several seconds. Impedance models are used to separate and to interpret the different mechanisms observed.

CONCLUSION Dynamics of membrane recovery during cell electropulsation are a complex mechanism with different time scale events occurring simultaneously. In this sense, we show how EIS is a suitable tool for the real time study of this phenomenon.

Abstract Id: 140
Topic: *Bioimpedance*

SKIN BIOIMPEDANCE AND MICROVASCULAR TONE CORRELATIONS

Sergey Podtaev*[1], Dmitriy Nikolaev[2], Alexander Smirnov[2], Vladimir Samartsev[3], Vasyliy Gavrilov[3], Kirill Tsiberkin[4]

[1]Laboratory of Physical Hydrodynamics, Institute of Continuous Media Mechanics, Perm, [2]Scientific Research Centre "Medas", Moscow, [3]General Surgery Department, Perm State Medical University named after E. A. Vagner, [4]Theoretical Physics Department, Perm State University, Perm, Russian Federation

INTRODUCTION The impedance of the tissues of a living organism is related to their complex structure and the properties of the extracellular medium, e.g. the microcirculation system. Thus, the vascular tone influences the impedance directly. The blood flow in the skin contains information on the endothelium, neurogenic and myogenic activity, which can be found from laser Doppler flowmetry or high-resolution thermometry. The bioimpedance data can also contain similar information.

OBJECTIVES We have studied *in vivo* the influence of temperature on skin impedance during the cold pressor and occlusion tests. Correlations between the vascular tone parameters and the bioimpedance are determined.

METHODS The bioimpedance measurements of human skin are performed using the automatic bioimpedance spectrum analyser ABIS-01 (Scientific Research Centre "Medas", Russia) with the tetra-polar electrode system at frequencies from 2 Hz to 50 kHz.

For high-resolution skin thermometry, we used the "Microtest" monitor (R&D Centre "FM-Diagnostics", Russia), which provides a thermal resolution of 0.005°C. The thermal data processing is based on gapped wavelet analysis. We provide a simultaneous measurement of the impedance spectra and the amplitudes of thermal oscillations in the endothelium, neurogenic and myogenic frequency ranges before, during and after the tests. The characteristic points of Nyquist diagrams are used to compare the impedance and thermometry.

The statistical analysis is based on the Wilcoxon pair test and Spearman's rank correlation coefficient.

RESULTS It was found that there are statistically significant differences in the impedance spectral parameters before, during and after the tests. Moreover, the impedance spectral characteristics and skin temperature variations during the cold pressor test correlate well in the endothelial frequency range. The correlations in the neurogenic and myogenic ranges are weaker. The impedance decreases with increasing amplitude of thermal oscillations, i.e. with increasing blood flow or vasodilation. Vasoconstriction is followed by an increase of impedance.

CONCLUSION It is shown that the microvascular tone of the skin directly influences the electrical properties of tissue. The study provides a simple explanation for the correlation between skin blood flow and bioimpedance parameters.

The study is financially supported by the Russian Scientific Foundation, grant 14-15-00809.

Abstract Id: 141
Topic: *Clinical applications*

REAL TIME IN-VIVO AND IN-SITU ASSESSMENT OF LUNG IMPEDANCE

Nuria Coll[1], Ramon Bragos[1], Ana Maria Muñoz-Fernández[2], Virginia Pajares[2], Alfons Torrego[2], Diego M Castillo[2], Pere J Riu[*1]

[1]Departament d'Enginyeria Electrònica. Centre Recerca Enginyeria Biomèdica, Universitat Politècnica de Catalunya, [2]Servei de Pneumologia, Hospital de la Santa Creu i Sant Pau, Barcelona, Spain

INTRODUCTION Electrical impedance has been used to identify regions with different histological properties in-vivo. Human lungs with different pathologies show specific histological properties so electrical impedance measurements might help to clinical procedures, e.g. as a sampling guide in lung biopsies. In vivo measurements will be affected by ventilation and blood perfusion, and must be safe and fast enough for real medical practice.

OBJECTIVES To determine the feasibility of an impedance measurement methodology applied during actual bronchoscopies in patients with lung diseases, that is able to distinguish histological features.

METHODS A measurement system consisting on a PXI arbitrary waveform generator and a digitizer was used to generate a broadband signal with 25 frequency components from 1 kHz to 1 MHz. A 4-electrode catheter was introduced in several endobronchial localizations though the working canal of a bronchoscope. Applied current and detected voltage are digitized and converted to impedance in a PC. Isolation is provided by an analogue optical system to achieve IEC 60601-1 CF-type safety levels. ECG, ventilation and temperature are also acquired synchronously. The system is thoroughly described elsewhere. In the current setup we acquired 15 s of data, at a rate of 50 impedance spectra per second.

Measurements were obtained from bronchial wall and alveolar regions in 12 patients which underwent bronchoscopy for study, including healthy lungs, emphysema, fibrosis or suspected neoplasia.

RESULTS Healthy lungs show an intense modulation of impedance because of ventilation and perfusion, in the range of 10% to 15% in the absolute value at low frequency and from 20% to 30% at high frequencies. Phase angle is also affected by ventilation at low frequencies and by both ventilation and perfusion at high frequencies. Measurements on the bronchial wall show significantly lower values and modulation indexes than in alveoli. When comparing healthy regions with those affected by fibrosis in the same or different patients, smaller values and modulation indexes are obtained, whereas regions with emphysema are not so clearly distinguished. No side effects were identified during measurements.

CONCLUSIONS The technique seems feasible and able to distinguish different pulmonary tissue features. A systematic measurement protocol must be designed to provide statistical validity to the results obtained so far.

Abstract Id: 142
Topic: *Electrical impedance spectroscopy*

ELECTRICAL IMPEDANCE PARAMETERS OF GROWING GERANIUM ROOT

Eszter Vozary*[1], Anna Takács[2], Viktória Köbli[2], Andrea Tilly-Mándy[2]

[1]Physics and Control, [2]Floriculture and Dendrology, Szent István University, Gödöllő, Hungary

INTRODUCTION The electrical capacitance and the electrical impedance of root and power medium systems are increasingly used in the last time for determination of root development (1,2).

OBJECTIVE The aim of this work to determine electrical impedance parameters that characterize the growth of geranium root.

METHODS Twenty *Pelargonium peltatum* 'Rainbow Rose' cuttings were put into pots filled with Vermiculite irrigated with Hoagland solution. Impedance magnitude and phase angle (in frequency range 30 Hz–30 MHz) were measured with LCR meters HP 4284 A and 4285 A at 1 V at three, four and ten weeks after cutting.

The impedance spectrum of soil was measured between two stainless steel rods of 4 mm diameter and 150 mm length in 50 mm distance. The impedance of root and soil system was measured between a stainless steel electrode in soil 30 mm apart from plant and an aluminium foil on the plant directly over the soil. After open-short correction the difference of root and soil system spectrum and soil spectrum was approached with model,

$$Z=R_0+R_1/(1+(i\omega\tau_1)\Psi_1)+R_2/(1+(i\omega\tau_2)\Psi_2)$$

where R_0, R_1, R_2 are resistances, τ_1, τ_2 are relaxation times, Ψ_1, Ψ_2 are exponents, $\omega=2\pi f$, f is measuring frequency, i is the imaginary unit. The parameters were determined with Solver of Excel and were statistically tested in SPSS 8 program.

RESULTS Good approach of measured spectra with two distributed element in serial connection shows that the root system contains two polarisable compartments in serial way for electric current. Very similar observation was described on willow tree roots (2). The decreasing tendency of R_0, R_1, τ_1 can reflect the increase of length and cross-section in root system.

CONCLUSION The R_1 and τ_1 parameters can be used for characterizing the root development.

REFERENCES

1. Rajkai K, Végh R K, Nacsa T (2005) Electrical capacitance of roots in relation to plant electrodes, measuring frequency and root media. Acta Agronomica Hungarica 53(2) 197–210.
2. Repo T, Laukkanen J, Silvennoinen R (2005) Measurement of the tree root growth using electrical impedance spectroscopy. Silva Fennica 39(2) 159–166.

Weeks after cuttings	R_0 kohm	R_1 kohm	τ_1 µs	Ψ_1	R_2 kohm	τ_2 µs	Ψ_2
3	1,2±0,05 a	69±18,6 a	327±127 a	0,64±0,054 a	7,7±0,59 a	3,0±0,77 a	0,54±0,037 a
4	0,9±0,07 b	47±19,1 ab	151±51,3 b	0,72±0,030 a	8,0±1,66 a	4,5±1,30 a	0,58±0,040 a
10	0,8±0,19 b	36±10,6 b	68±9,1 c	0,73±0,032 a	9,8±3,17 a	3,3±1,08 a	0,62±0,031 a

Table 1. *Parameter values (mean±SD; a,b,c show the significant differences in a column)*

Abstract Id: 143
Topic: *Simulation / modelling*

NUMERICAL MODELLING TECHNIQUES FOR BIOIMPEDANCE AND ECG

Alexander Danilov[*1,2], Alexey Chernyshenko[1], Alexandra Yurova[1,3]

[1]Institute of Numerical Mathematics, Russian Academy of Sciences, Moscow, [2]Moscow Institute of Physics and Technology, Dolgoprudny, [3]Department of Computational Mathematics and Cybernetic, Moscow State University, Moscow, Russian Federation

INTRODUCTION Bioelectrical properties of living tissues are widely used in medical purposes. Both bioelectrical impedance analysis (BIA) and electrocardiography (ECG) are well known diagnose techniques in modern clinics. The numerical modelling of the underlying physical processes may be used to improve these medical techniques. Our research group is working on BIA and ECG modelling with high resolution anatomical human models [1, 2].

OBJECTIVES One can perform sensitivity analysis for specific electrode placements in order to improve BIA techniques. ECG modelling is used to predict the impact of different cardiac abnormalities on the shape of ECG curves.

METHODS Numerical modelling is used to solve the forward problem of electric potential distribution. In order to solve the underlying differential equations one should perform several steps. Image segmentation is used to reconstruct the patient-specific anatomical model. Unstructured tetrahedral mesh is generated and finite element method is used to solve the model equations.

RESULTS Several numerical experiments were performed. The Visible Human Project data were used to perform semi-automatic image segmentation with ITK-SNAP software (itksnap.org). An anatomical human model was reconstructed from segmented image and an unstructured mesh was generated using CGAL Mesh library (www.cgal.org). The differential equations were solved using finite element method with P1 elements using Ani3D library (sf.net/p/ani3d). High sensitivity areas were computed for several BIA schemes (conventional right arm – right leg scheme on Fig.1 left). The body surface electric potential field was computed during heart excitation in order to model forward ECG problem (Fig.1 right).

CONCLUSION The algorithmic pipeline is presented for numerical modelling of BIA and ECG including segmentation, meshing and finite element discretization steps. Several numerical examples of BIA and ECG modelling are presented.

ACKNOWLEDGMENTS The research was supported by Russian Federation President Grant for Government Support of Young Russian Scientists MK–7839.2015.1

IMAGE

REFERENCES

1. A.A. Danilov, V.K. Kramarenko, D.V. Nikolaev, A.S. Yurova. Personalized model adaptation for bioimpedance measurements optimization. Russ. J. Numer. Anal. Math. Modelling, 28:459-470, 2013
2. Yu.V. Vassilevski, A.A. Danilov, T.M. Gamilov, Yu.A. Ivanov, R.A. Pryamonosov, S.S. Simakov. Patient-specific anatomical models in human physiology. Russ. J. Numer. Anal. Math. Modelling, 30:185-201, 2015

Abstract Id: 145
Topic: *Clinical applications*

ELECTRICAL IMPEDANCE MYOGRAPHY QUANTIFIES MOUSE NERVE INJURY

Jia Li[1], Laurent Bogdanik[2], David Arnold[3], Cathleen Lutz[2], Seward Rutkove[*1]

[1]Neurology, Harvard Medical School, Boston, MA, [2]The Jackson Laboratory, Bar Harbor, ME, [3]Neurology, Ohio State University, Columbus, OH, United States

INTRODUCTION Tools to evaluate motor neuron dysfunction are needed for animal models. Most methods are time consuming to apply and require electrical stimulation of a nerve to identify significant changes. Electrical impedance methods applied directly to muscle (i.e., electrical impedance myography, EIM) have the potential of serving that purpose; moreover, they are relatively fast to perform and do not require peripheral nerve stimulation.

OBJECTIVES We studied a simple mouse model of denervation/reinnervation, sciatic nerve crush, to evaluate how basic impedance measures correlate with standard metrics, including compound muscle action potential (CMAP) amplitude and motor unit number estimate (MUNE) as compared to a group of sham-injured mice. Our interest was in determining how effective the three metrics were at discriminating animals that had already mostly recovered from the injury.

METHODS 10 animals underwent sciatic crush and were allowed to recover for a period of approximately 6 weeks. An additional 10 animals underwent a sham procedure in which the skin was opened, but no crush was performed; these were also allowed to recover for 6 weeks. The animals then underwent EIM measurements of the gastrocnemius using a custom-designed 4-electrode array. Measurements were made in both the transverse and longitudinal directions relative to the major muscle fiber direction. The animals also underwent standard electrophysiological assessments of CMAP and MUNE.

RESULTS The sciatic-crushed animals demonstrated a significantly lower mean 50 kHz phase and reactance values than healthy animals (e.g., 50 kHz longitudinal phase of sham 17.4° vs. 15.3° for crush, p=0.035). Differences in MUNE approached significance (p = 0.068), but were non-significant for CMAP (p=0.13). Combining both groups of animals, the EIM 50 kHz phase values correlated significantly to both CMAP and MUNE (r=0.47, p=0.036, and r=0.61, p=0.004, respectively).

CONCLUSION These results support the basic premise that EIM is sensitive to recovering neurogenic injury. This finding is consistent with the results from studies of more severe mouse models, including in amyotrophic lateral sclerosis, in which there is marked motor neuron loss. This measure also correlates with more standard electrophysiologic measures. These findings support the concept that, by assessing muscle, EIM has the potential to play a useful role in pre-clinical and clinical studies of primary nerve injury.

Abstract Id: 147
Topic: *Bioimpedance*

BREATHING PARAMETER EXTRACTION FROM LOCALIZED THORACIC BIOZ

Seulki Lee*[1], Gabriel Squillace[1], Hélène De Cannière[2], Lars Grieten[1, 2, 3]

[1]Wearable Health Solution, Holst Centre / imec, Eindhoven, Netherlands,
[2]Ziekenhuis Oost-Limburg, Genk, [3]Hasselt University, Hasselt, Belgium

INTRODUCTION Thoracic bioimpedance (BioZ) can be used as an indicator of congestion status in congestive heart failure (CHF) patients [1]. Changes in BioZ over days are well correlated with fluid level in patients. It has also been shown that other physiological parameters such as heart rate, respiration rate (RR), blood pressure and oxygen saturation are also correlated with thoracic BioZ [2]. Therefore, combining thoracic BioZ with other parameters might be more effective for congestion status estimation.

OBJECTIVES In this paper, RR and respiration volume (RV) extracted from locally measured thoracic BioZ will be shown. Since BioZ data is obtained from the clinical trial discussed in [1], location of electrodes is already determined for high sensitivity to the fluid level, but not to respiration. This paper will also describe the limitation caused by the localized thoracic measurement.

METHODS Measurements on eight healthy subjects were performed in order to implement and verify the extraction algorithm. Three sessions with various RR, RV, and breathing patterns were administered for each subject, while electrodes are kept in the same configuration as described in [1]. Spirometry was simultaneously performed as a reference. Afterwards, RR and RV analysis using the algorithm is performed on seven CHF patient data.

RESULTS RR and RV analysis on healthy subject data shows that both can be accurately obtained from localized thoracic BioZ when BioZ variation due to breathing is larger than 0.3 ohm. Especially for RV, it is important to have the constant breathing pattern during data collection in order to get the accurate result. In CHF patient data, RR and RV can also be extracted from localized thoracic BioZ. However, for some patients that had difficulties in actual respiration due to other lung problems, RR and RV could not be obtained.

CONCLUSION Localized thoracic BioZ can be used to estimate RR and RV from both healthy subjects and CHF patients when BioZ variation due to breathing is larger than 0.3ohm. Data collection on more patients and correlation analysis between respiration parameters and patient status will be performed as further work.

IMAGE

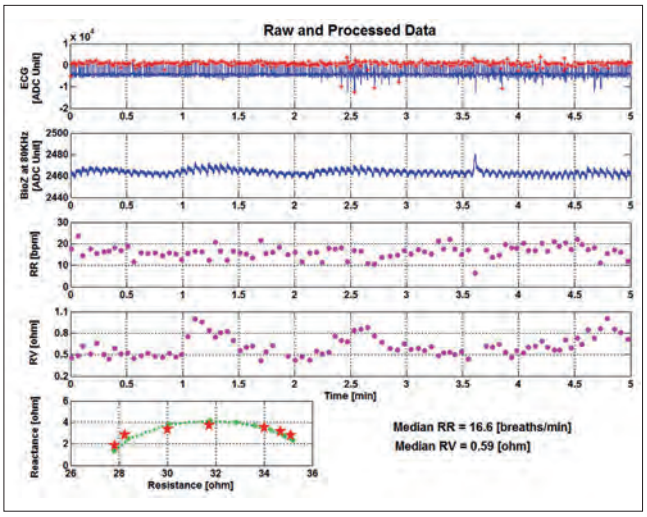

REFERENCES

1. 10.1109/EMBC.2015.7318393
2. 10.1371/journal.pone.0122576

Abstract Id: 148
Topic: *Bioimpedance*

CARDIAC ANOMALIES DIAGNOSIS USING BIOIMPEDANCE METHOD

Ihsen Ben Salah*[1], Kaïs Ouni[1], Ridha Ben Salah[2]

[1]Research Unit Signals and Mechatronic Systems, SMS, UR13ES49, National Engineering School of Carthage, ENICarthage, University of Carthage, Tunis, Tunisia, [2]Prince Sattam Bin Abdulaziz University, Al Kharj, Saudi Arabia

KEYWORDS Bioimpedance, automatic diagnosis, cepstral analysis, artificial intelligence.

INTRODUCTION The majority of the works in the area of diagnosis of cardiovascular anomalies targeted on a temporal signal processing. In this study we aim to design an automatic diagnosis of the cardio-vascular anomalies via a cepstral signal analysis. In this work we describe the signals analysis cepstral approach.

OBJECTIVES The objective of this work is to perform automatic diagnosis by processing the Bioimpedance cardiovascular signal using the cepstral parameters and discriminant analysis method.

METHODS Cepstral method consists on considering that bioimpedance signal y(t) is the response of left ventricle aorta system to a cardiac excitation signal x(t) and the aorta pulsatile response: h(t): $y(t) = x(t) * h(t)$. Let:

$$y_1(t) = FFT^{-1}(Ln|FFT(x(t))| + Ln|FFT(x(t))|) = x_1(t) + h_1(t)$$

$$x_{11}(t) = FFT^{-1}(Exp(FFT(x_1(t))) ; h_{11}(t) = FFT^{-1}(Exp(FFT(h_1(t)))$$

$y_1(t)$, $x_{11}(t)$, $h_{11}(t)$ are respectively the Cepstres C_1, C_2 and C_3 of the Bioimpedance signal. C2 and C3 (Fig.1) are considered as the original signal provided, respectively, by heart and aorta. 140 different signals according to normal cases and different cardiovascular diseases are used in this study. The classification of anonymous individuals is based on the Fischer formula: $d(a,Y_k) = (a - y_k)' . T_{cov} . (a - y_k)$, $d(a,Y_k)$ is the distance between a and class Y_k,, a is the anonymous individual, y_k is the average of Y_k classes, T_{cov} is whole covariance matrix.

RESULTS Our method permits to calculate seven relevant cepstral parameters. The application of the discrimant analysis method has allows us to perform the diagnosis of 30 anonymous cases. The results found in this work indicate that 7 cepstral parameters are sufficient to perform the automatic diagnosis of the cardiovascular system abnormalities with 96.45% of percentage of correctly classified.

CONCLUSION The intelligent method performed in this study permits to confirm the classification of thirty anonymous patients. Quantification results obtained by the bioimpedance signals analysis is confirmed by those obtained with Echo-Doppler method.

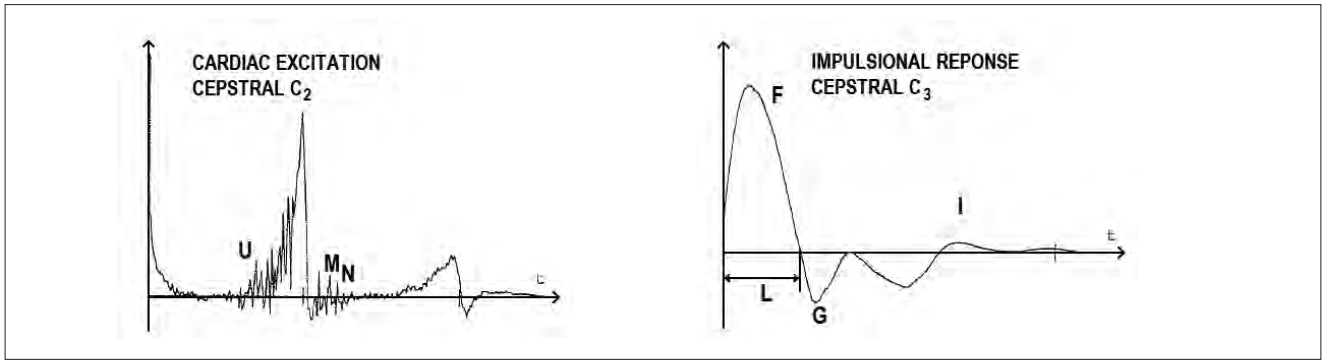

***Fig. 1**. C2, C3 and Cepstral Parameters*

Abstract Id: 149
Topic: *Instrumentation*

HIGH FREQUENCY SENSORS IN SINGLE USE CULTURE TECHNOLOGY

Thomas Nacke*[1], Andreas Barthel[1], Yahor Zaikou[1], Ralf Klukas[2]

[1]Analysenmesstechnik, Institut für Bioprozess- und Analysenmesstechnik e.V., Heilbad Heiligenstadt, [2]IRK Dresden, Mohorn, Germany

INTRODUCTION Contamination-free process measurement is essential for efficient monitoring of fermenters especially for single use bioreactors (SUB). This contribution introduces the use of high-frequency sensors for the contactless measurement of the permittivity and conductivity of fermentation media. The sensor can be installed directly to the outer surface of the fermenter or can be clamped onto tubing.

OBJECTIVES Until now various ex-situ contactless process-monitoring technologies exist that are not yet commercially available for SUB, for instance, optical infrared sensors, ultrasound and High-Frequency (HF) or rather Microwave (MW) Sensors. These ex-situ sensors must be connected to the SUB by means of a special port and associated cabling. MW-Sensors can measure through optically opaque materials und are particularly suited to contactless measurement of conductivity, concentration solid matter or water content.

METHODS Microwave sensors measure the interaction of matter with high frequency electromagnetic electric fields. This technology is particularly well suited for sensor application in non-destructive testing because microwaves can penetrate deep into the material without any direct contact and can even be transmitted through the material. When microorganisms grow in liquid culture media, dead cells are broken down into small uncharged macromolecules. As part of this metabolism, ions are released that lead to a measurable change in the capacitance and electrical conductivity of the medium by using high frequency's dielectric applications.

In Experiment 1 as the central sensor element is a multilayer ceramic chip antenna for the frequency range 400 MHz~500 MHz. Four measurement chambers were built, which were connected to a network analyzer by means of a multiplexer and 50 Ohm coaxial cable. Parallel comparative measurements were performed with a microbiological analyzer BacTrac 100.

RESULTS The comparison with the reference measurements using the SY-LAB microbiological analyzing system (BacTrac 100) shows how the high frequency sensors can monitor the growth of microorganisms in batch culture through measuring the associated change in conductivity of the cell medium.

CONCLUSION This presentation describes high frequency sensors for the contactless monitoring of liquids in cell culture reactors und dosing systems. The contactless nature of these sensors enables the cost-effective production of microwave sensors that can avoid sample contamination.

Abstract Id: 150
Topic: *Impedimetric biosensors*

IMPEDANCE MEASUREMENTS TO DETERMINE HAIRY ROOT BIOMASS

Thomas Nacke[*1], Andreas Barthel[1], Caspar Demuth[2], Varonier Joel[2], Iris Poggendorf[2]

[1]Analysenmesstechnik, Institut für Bioprozess- und Analysenmesstechnik e.V., Heilbad Heiligenstadt, Germany, [2]Life Science und Facility Management, Biotechnology, Zürcher Hochschule für Angewandte Wissenschaften, Wädenswil, Switzerland

INTRODUCTION In this paper, we describe applications of dielectric spectroscopy to monitor hairy roots in suspensions. Hairy root are plant organ cultures that are genetically stable without plant hormones in the medium. Transformed hairy roots have the potential to produce a variety of small and large molecules not found in the whole plant or in untransformed roots. They are often used for the production secondary metabolites that are valuable as pharmaceuticals, cosmetics or food additives. In this work, transformed tobacco roots (SR1-pGES) that produce geraniol were cultured.

OBJECTIVES For a quantitative approach to control the cultivation of hairy roots, a number of relevant biological state variables such as viability and biomass must be known. Therefore, reliable on-line instrumentation is required. Dielectric permittivity of cell suspensions is an indication of viable biomass concentration.

METHODS The root mass was cultured on petri dishes and then biomass was weighed on a laboratory scale and finally transferred to SyLab tubes) for the impedance measurements. The measurements were performed between 1 kHz and 10 MHz on a self-built impedance analyser system, which consists of an USB Handyscope (HS5, 500 MS/s 14 bit dual channel high resolution oscilloscope with function generator, TiePie engineering) together with an specially designed front-end from iba for a precise measurement of the current flow and voltage drop in a wide frequency range.

RESULTS The results showed a linear correlation between calculated normalized capacitance and the fresh root biomass. Further experiments were done with roots grown directly in the SyLab tubes. Again, the calculated capacitances correlated well with the root biomass.

CONCLUSIONS A first step for an automatic technique of determining the hairy roots biomass and growth rate has been developed. Further experiments will be done with roots grown directly in the SyLab tubes. In a next step, contactless measurement of the biomass will be carried out in petri dishes and the scale up in (mist-) bioreactors. For these experiments, a high frequency setup will be used, allowing online monitoring of the cultivation without the risk of contamination.

Abstract Id: 151
Topic: *Electrical impedance spectroscopy*

EIS CHARACTERISATION OF HYDRODYNAMICS IN POROUS BILAYERS

Terry Chilcott*[1], Hadeel Obeedallah[1], Alice Antony[2], Greg Leslie[2]

[1]School of Chemical and Bimolecular Engineering, University of Sydney,
[2]UNESCO Centre for Membrane Science and Technology, University of New South Wales, Sydney, Australia

INTRODUCTION Studies of bio-entities in bilayers on SiO_2 report confusing interpretations attributed to differences in the lipid leaflets. These differences can be attributed to osmotic pressures arising from ionic partitioning between the solutions in contact with these leaflets [1] that drive water through pores which momentarily form to assist incorporation of bio-entities. Inductive manifestations in electrical impedance spectra (EIS) have been attributed to electrophoretic effects of anisotropic water fluxes through membranes [2].

OBJECTIVES To detect inductive manifestations in bilayers, observed in synthetic membranes [3]

METHODS EIS were acquired during the self-assembly of bilayers on SiO_2.

RESULTS Modeling of the EIS yielded inductive parameters and Maxwell-Wagner layers comprising SiO_2, prroximal & distal laeflets of bilayers and solution interfaces.

CONCLUSIONS Modelling of EIS characterized anisotropic fluxes through pores in bilayers.

IMAGE

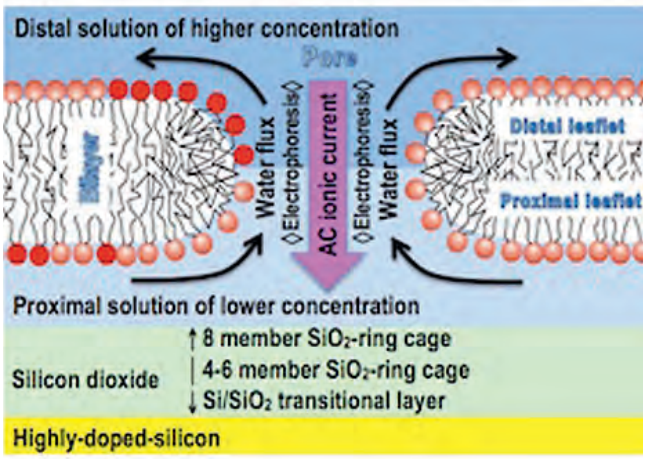

REFERENCES

1. T.C. Chilcott, C. Guo (2013) Electrochimica Acta 98: 274–287.
2. T.C. Chilcott (2013) J. Membr. Sci. 438: 65–76.
3. T.C. Chilcott, J. Cen, J.Kavanagh (2015) J. Membr. Sci. 477: 25–40.

Abstract Id: 153
Topic: *Electrodes*

CHARACTERIZATION OF GRAPHENE OXIDE COATED GOLD ELECTRODES

Yekta Ülgen*[1]

[1]Institute of Biomedical Engineering, Bogazici University, Istanbul, Turkey

INTRODUCTION Graphene oxide is oxygenated form of the graphene and has also been utilized in biomedical research such as a bio-sensing tool [2, 3]. Impedance spectroscopy, commonly used in physiological assessment of biological cells, blood cells viability and diagnostics is also utilized with graphene and its derivatives for biomedical applications [3].

OBJECTIVE In this study, the effects of graphene oxide coating on gold electrode impedance is examined by using two-electrode impedance measurement system.

METHODS Gold electrodes (Fig.1) are produced by standard lithography procedures, consisting of application of triprime on the soda lime glass surface, and then coated with graphene oxide using self-assembly method. [1-3] The impedance of redox solution in the wells are measured through gold electrodes and graphene oxide coated electrodes at 10 mV AC excitation signal, from 20 kHz to 1 MHz, by using the HP 4284A LCR Meter.

RESULTS AND CONCLUSION From the Nyquist diagram, it is seen that the electrode contribution diminishes at high frequencies and the impedance values mostly represent the impedance of redox solution. Since the redox solution is identical in both measurements, the impedance values in the low frequency range represent the electrodes.

The results from 8 specimens show that and that graphene oxide reduces by a factor of almost 50% the impedance of the gold electrodes.

IMAGE

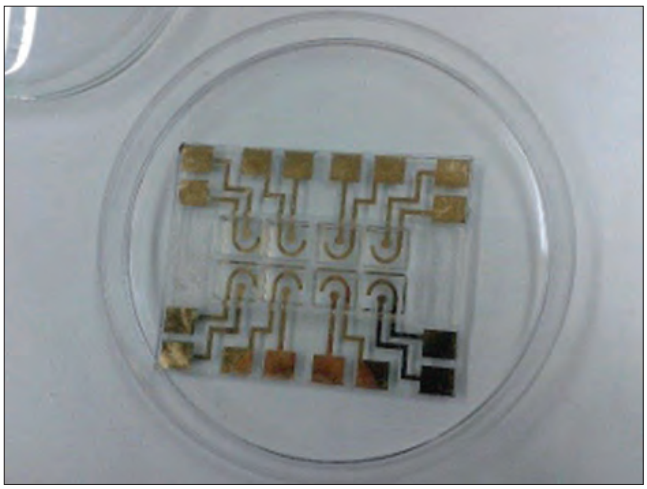

REFERENCES

1. K. S. Kim, Y. M. Um, J.-R. Jang, W.-S. Choe, and P. J. Yoo, *ACS Appl. Mater. Interfaces*, vol. 5, no. 9, pp. 3591–8, 2013.
2. Z. Wang, J. Zhang, P. Chen, X. Zhou, Y. Yang, S. Wu, L. Niu, Y. Han, L. Wang, F. Boey, Q. Zhang, B. Liedberg, and H. Zhang, *Biosens. Bioelectron.*, vol. 26, no. 9, pp. 3881–3886, 2011.
3. R. Lanche, V. Pachauri, D. Koppenhöfer, P. Wagner and S. Ingebrandt, *Phys. Status Solidi*, vol. 211, no. 6, pp. 1404–1409, 2014.

Abstract Id: 155
Topic: *Clinical applications*

CAN IMPEDANCE CARDIOGRAPHY DETECT PULMONARY EDEMA?

Robert P Patterson* [1]

[1]Institute for Engineering in Medicine, University of Minnesota, Minneapolis, United States

INTRODUCTION Impedance cardiography was develop in the 60's to measure cardiac output, but many researchers have reported using the change of the base impedance(Zo) of the thorax as a measure of pulmonary edema. This study aims to evaluate this measurement using a high resolution impedance model of the thorax.

OBJECTIVES To determine if changes in lung resistivity can cause significant changes to thoracic impedance Zo.

METHODS A finite difference model of the thorax with 3.8 million elements, created from MRI images, was used to calculate the thoracic Zo as it is modified by changes in lung tissue resistivity. In the model current and voltage pick up electrodes were place on the neck and lower thorax in the position normally used in impedance cardiography. The modelling started with a normal lung resistivity of 1400 ohm-cm and decreased in value with 200 ohm-cm steps until reaching 400 ohm-cm. Separately for comparison, skeletal muscle resistivity was changed starting at 225 ohm-cm and decreased in value with 5 ohm-cm steps until reaching 200 ohm-cm.

RESULTS For a lung resistivity decrease of 200, 400, 600, 800 and 1000 ohm-cm, the decrease of thoracic impedance was -0.18, -0.41, - 0.7, -1.1, and -1.76 ohms, respectively. In comparison a skeletal muscle resistivity decrease of 5, 10, 15, 20, and 25 ohm-cm resulted in the decrease of thoracic impedance of -0.29, -0.6, -0.9, -1.21, -1.53 ohms, respectively.

CONCLUSION Investigators have typically reported Zo decreases of 2 to 5 ohms in patients with heart failure and pulmonary edema. The observed small fractional impedance changes resulting from large lung resistivity changes could not explain the values seen in the clinical data. Tidal breathing typically causes an impedance change of 0.1 to 0.3 ohms and the cardiac signal is approximately 0.1 ohms. The small changes added by possible lung resistivity changes could not be reliably detected. The much larger impedance change typically seen in patients most likely can be explained by fluid accumulation in other tissues such as muscle. Note the high sensitivity of muscle resistivity to Zo changes. Therefore, isolated pulmonary edema cannot be reliably detected by impedance cardiography.

Abstract Id: 156
Topic: *Bioimpedance*

THE RUSSIAN BIOIMPEDANCE MEGABASE: CURRENT STATE AND RESULTS

Sergey Rudnev[*1,2], Dmitry Nikolaev[3], Konstantin Korostylev[1], Svetlana Shchelykalina[1,4], Olga Starunova[1], Tatiana Eryukova[1], Vladimir Kolesnikov[1], Vladimir Starodubov[1]

[1]Federal Research Institute for Health Organization and Informatics of Ministry of Health of the Russian Federation, [2]Institute of Numerical Mathematics of the Russian Academy of Sciences, [3]Medas Ltd, [4]Pirogov Russian National Research Medical University, Moscow, Russian Federation

INTRODUCTION Despite known limitations, bioelectrical impedance analysis (BIA) remains the most widely used technique of body composition assessment both in the community and at the bedside. BIA data from various health surveys, such as KNHANES, KSCDC, NHANES and UK Biobank, are utilized to provide population specific references and diagnostic cut-points for obesity, malnutrition, physical disability, metabolic syndrome risk, and other conditions. In Russia, mass data of the population screening are collected by the national network of Health Centres (HCs) since 2009 using a number of methods, including BIA.

OBJECTIVES Our aim was to process BIA data from HCs in order to generate BIA database for the purposes of epidemiological monitoring.

METHODS BIA data were obtained from HCs both directly (in 2012 and 2015) and indirectly – from the federal database of HCs. To provide comparable results, only data from the same type of BIA meters, ABC-01 'Medas' (Medas Ltd, Moscow), were considered. These were presented by 320 Health Centres from 62 out of 85 regions of Russia. The measurements were made using conventional tetrapolar whole body scheme with ECG (Schiller or FIAB) electrodes placed on ankle and wrist. The initial number of measurements was 2.35 mln. Additional selection criteria were used in order to remove technical errors, frauds, and repeated measurements of the same patient. The centile reference tables for BIA parameters were obtained using GAMLSS program in R. Standardized prevalences of diseases and risks were estimated according to existing criteria using demographic pyramid of Russia.

RESULTS After application of the selection criteria, cross-sectional BIA database was formed containing the results of 1.64 mln measurements. The database features large sample size, a wide range of age groups surveyed, and fairly good coverage of regions. The smoothed centile reference data for directly assessed and estimated BIA variables in males (n=549026) and females (n=1087684) were obtained (e.g., see Fig 1). As an example, the standardized prevalence of obesity in our males according to WHO criteria was 11% in children and 18% in adults.

CONCLUSION The obtained database can be used for the assessment of physical status, body composition, prevalence of malnutrition and epidemiological risks.

ACKNOWLEDGEMENT This work is supported by the Russian Science Foundation grant no 14-15-01085.

IMAGE

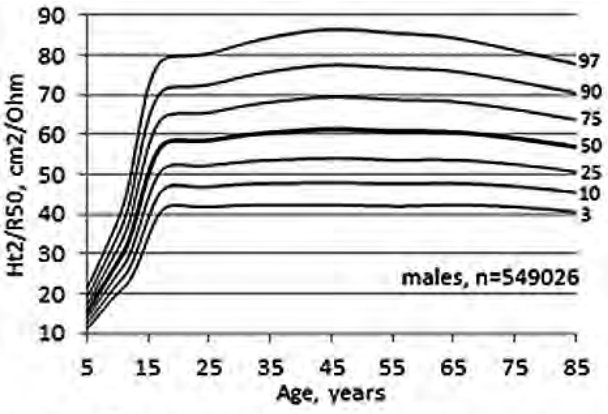

Fig. 1. The resistance index reference centile curves for Russian males

Abstract Id: 157
Topic: *Bioimpedance*

BIOIMPEDANCE - IN-VIVO VS IN-VITRO ISCHEMIC SMALL INTESTINE

Runar Strand-Amundsen[*1,2], Christian Tronstad[1], Ørjan G. Martinsen[2], Jan Olav Høgetveit[3], Tom Erik Ruud[4], Tor Inge Tønnessen[5,6]

[1]Department of Clinical Engineering, Oslo University Hospital, [2]Department of Physics, University of Oslo, [3]Department of Clinical Engineering, , Oslo University Hospital, [4]Department of Surgery, Baerum Hospital, [5]Department of Emergencies and Critical Care, Oslo University Hospital, [6]Institute of Clinical Medicine, University of Oslo, Oslo, Norway

INTRODUCTION The small intestine is a multi-layered structure, with several distinct tissue types. Ischemia related changes occur at different times in the different intestinal layers. When a piece of the small intestine is removed and are subject to ischemia in-vitro, many of the same pathological changes occur as in-vivo, but there is no immune response, and no edema due to intramural circulation. Bioimpedance has been used to investigate changes in electrical parameters during ischemia in various tissues. Some researches use in-vitro models while others use in-vivo models.

OBJECTIVES The objective of this study is to assess the difference in ischemia related time development of electrical parameters in in-vivo versus in-vitro small intestine

METHODS Measurements were performed using a two-electrode setup, with a Solartron 1260/1294 impedance gain-phase analyser. Electrodes were placed on the surface of the ischemic jejunum, applying a constant voltage, and measuring the resulting electrical admittance. The in-vivo measurements were conducted on (n = 7) pigs. After induction of anaesthesia, an ischemic model with warm, full mesenteric occlusion on 30 cm of the jejunum was implemented. Measurements were taken from 0-6 hours of ischemia. The in-vitro measurements have so far been conducted on 4 samples from 2 pigs. After induction of anaesthesia, two 30 cm pieces of the jejunum are resected. The pieces are stored at 37 degrees Celsius and measurements taken from 0-12 hours of ischemia.

RESULTS In the in-vitro measurements the low frequency resistance increases drastically early on and remains high for approximately 6 hours, before the impedance drops drastically when the cell membranes are destroyed after the cells have died. In the in-vitro intestine there is no circulation, and thus no edema, bleeding, immune response or effects from the surrounding tissues, and therefore the reduction in extracellular volume dominates the low frequency impedance for many hours. In the in-vivo measurements, the immune response and intramural circulation give rise to extracellular edema, which conteracts much of the effects we see in-vitro with a decrease in the extracellular volume. In both in-vivo and in-vitro we se a gradual increase in capacitance, indicating increased intracellular volume.

CONCLUSION The changes in ischemia related time development of electrical parameters in in-vivo versus in-vitro small intestine differs significantly.

Abstract Id: 158
Topic: *Clinical applications*

IN-CYCLE DETECTION OF ACUTE MYOCARDIAL ISCHEMIA BY FAST EIS

Ramon Bragos*[1], Gerard Amorós-Figueras[2], Esther Jorge[2], Benjamín Sánchez[1,3], Tomás García-Sánchez[1,4], Juan Cinca[2], Javier Rosell-Ferrer[1]

[1]Electronic and Biomedical Instrumentation Group, Department of Electronic Engineering, Universitat Politècnica de Catalunya, [2]Department of Cardiology, Hospital de la Santa Creu i Sant Pau,Universitat Autonoma de Barcelona, Barcelona, Spain, [3]Department of Neurology, Division of Neuromuscular Diseases, Beth Israel Deaconess Medical Center, Harvard Medical School, Boston, United States, [4]Vectorology and Anticancer Therapies, UMR 8203, CNRS, Univ. Paris-Sud, Gustave Roussy, Université Paris-Saclay, Villejuif, France

INTRODUCTION Previous publications have shown the ability of electrical impedance spectroscopy (EIS) as a tool for myocardial state characterization in normal and acute myocardial ischemic conditions. The spectra were usually obtained using stepped sine sweep, then showing only the slow changes induced during the ischemic process. In the recent years, several tools for fast impedance acquisition have been developed, and their ability to characterize the in-cycle impedance spectrum have also been published.

OBJECTIVES The aim of this work is to show the results of the combination of both methods: multisine-based fast impedance spectroscopy applied to the in-situ and in-vivo characterization of myocardial acute ischemia using EIS measurements into the cardiac cycle.

METHODS Measurements were performed using the already described set-up based on an arbitrary-waveform multifrequency impedance analyzer built over a PXI system from National Instruments and a custom front-end. Myocardial impedance was measured continuously during the cardiac cycle using 26 different simultaneous excitation frequencies (1 kHz–1 MHz) in 7 anesthetized open chest pigs. Animals were submitted to 30 minutes regional ischemia by acute left anterior descending coronary artery occlusion. The electrocardiogram, left ventricular (LV) pressure, LV dP/dt and aortic blood flow were recorded simultaneously.

RESULTS The measurements confirmed the already known average changes in the impedance spectrum along the ischemia time course (magnitude rise at low frequencies and negative phase increase around 300 kHz and also below 10 kHz) but also showed changes in the in-cycle impedance shape at different frequencies. While the relative amplitude changes of impedance-time waveforms are not relevant, the shapes become more rounded along the ischemia and the delays respect to the pressure wave also change, allowing the determination of several estimators of the tissue state and providing tools to interpret the physiological changes that occur during ischemia.

CONCLUSION The structural and mechanical myocardial dysfunction induced by acute coronary occlusion can be recognized by specific changes in the systolic-diastolic myocardial resistivity curve. Indicators of evolving acute myocardial ischemia can be deduced from multifrequency impedance values, their shapes and their delays in relation to physiological variables.

Abstract Id: 159
Topic: *Instrumentation*

SYSTEM FOR LOCAL BIOIMPEDANCE MEASUREMENTS IN HEART FAILURE

Javier Rosell-Ferrer[*1], Jordi Rubió-Pons[1], Antonio López-Marín[1], Samuel Borreguero[2], Antonio Ordoñez[3], Ana Maria Campos-Pareja[3], Encarnación Gutierrez-Carretero[4]

[1]Department of Electronic Engineering, Universitat Politècnica de Catalunya, Barcelona, [2]Talemnology, [3]Instituto de Biomedicina de Sevilla IBIS, [4]Instituto de Biomedicina, Area del Corazón, H.U. Virgen del Rocio, Universidad de Sevilla, Sevilla, Spain

INTRODUCTION There are no simple and reliable methods to accurately assess a patient's fluid status. Signs and symptoms of fluid retention are unreliable and may not be obvious until late stages. Previous publications have shown the ability of impedance spectroscopy as a tool for the accurate assessment of hydration status, especially in renal failure, but also in heart failure (HF). In HF, most of the research is in chest systems combining ECG and bioimpedance.

OBJECTIVES The aim of the system under development is to give a prompt warning of fluid decompensation in HF patients at home.

METHODS The system is based on an AD5933 for impedance measurements with a custom front-end a microprocessor and a Bluetooth communication module. The control of the system is done with a smart phone. Localized impedance measurements are obtained in the lower limb with a 4-electrode method using commercial available electrodes for ECG, with an inter-electrode distance of 6 cm and 3.5 cm between injectors and voltage detectors. Measurement frequencies are: 5, 10, 20, 50, 100 and 200 kHz. The system has a dynamic range up to 300 Ω, with a resolution of 0.1 Ω. The obtained impedances were fitted to a Cole model as a preliminary evaluation in order to define the best estimators for HF decompensation.

RESULTS We measured voluntaries to evaluate the repeatability and the effect of body position in the measured impedance and HF patients with different degrees of fluid accumulation. Measurements in healthy voluntaries showed values between 35–45 Ω for the real part and 4 to 7 Ω for the imaginary part. We used the head-down tilt technique to produce fluid changes during the experiments. The measurements confirmed the high sensibility of local bioimpedance to changes in the hydration of the underlying tissues, but also the errors, especially at high and low frequencies, produced by electrode-skin impedances. In patients, we obtained a strong reduction on both parts real and imaginary, being the worst case a real part of 9.7 Ω with and imaginary part of 1.7 Ω (at 50 kHz).

CONCLUSION A battery powered wireless system has been constructed to measure local bioimpedance spectrums in the lower leg. Experiments in voluntaries confirmed the high sensibility of the system. Measurements in HF patients has much lower impedance values than in voluntaries. The obtained results must be correlated with other methods to define the best estimators for an earlier warning of HF decompensation.

Abstract Id: 160
Topic: *Clinical applications*

MIS-PHASE SHIFT VS US-ELASTOGRAPHY IN BREAST CANCER

Alejandro Corzo*[1], María C. Uscanga[2], Juan L. Ortíz[3], José A. González[3], Lucila M. Lozano[4], Honorina Martínez[4], Carla I. Guerrero[5], César A. González[4,6]

[1]Universidad del Ejército y Fuerza Aérea/ Esc. Mil. Gds. Snd., SEDENA, [2]Centro de Diagnóstico Oportuno de Cáncer de Mama, Hospital Militar de Especialidades de la Mujer y Neonatología/SEDENA, Mexico, [3]Centro de Diagnóstico Oportuno de Cáncer de Mama, Hospital Militar de Especialidades de la Mujer y Neonatología/ SEDENA, [4]Universidad del Ejército y Fuerza Aérea/Esc. Mil. Gds. Snd., SEDENA, [5]Instituo Politecnico Nacional/ Escuela Superior de Medicina, [6]Instituto Politécnico Nacional/Escuela Superior de Medicina, México, Mexico

INTRODUCTION Impedance measurements based on Magnetic Induction Spectroscopy (MIS) for Breast Cancer (BC) detection has been proposed in some studies. Elastography has been recognized as a B-mode ultrasound (US) post-processing technique that enables the assessment of tissue stiffness or Strain Ratio (SR) to detect malignant breast lesions. MIS and SR allow evaluate electrical and mechanical properties of tissue respectively, thus; in BC condition MIS and SR reflect changes in tissue conductivity and stiffness respectively, that might be associated.

OBJECTIVE Evaluating and comparing the use of a non-invasive technique based on MIS for detection of patho-physiological conditions in breast tissue associated to its volumetric electrical conductivity changes through Inductive Phase Shift ($\Delta\Theta$) with tissue stiffness changes given by US-SR for the differentiation of BC.

METHODS Female volunteer patients separated in two experimental groups (Control; n=28 and BC; n=20) were measured by an experimental inductive spectrometer designed to estimate volumetric ($\Delta\Theta$) in human breast tissue at four frequencies: 0.01, 0.1, 1 and 10 MHz, and compare with US-SR findings. All patients were examined with both conventional US and elastography by experienced radiologists. $\Delta\Theta$ and US-SR data were homogenized in every patient with respect its contra-lateral breast measurement in such a way that the effect of age, corporal mass index even hormonal cycle phase factors were neutralized. The histopathology result obtained from ultrasound-guided core biopsy or operation excisions were used as reference standard. A parametric t-student test was used for comparing mean values of $\Delta\Theta$ and US-SR data in Control *vs* BC groups. The study was developed in the Center of Breast Cancer Timely Diagnosis-Military Specialist Hospital for Women and Neonatology of the Mexican Army and was approved by the "Research" and "Bioethics" Committees of the Institution.

RESULTS Increments in volumetric inductive phase shift measurements at 0.1MHz as well as in levels of elastic stiffness were evident in BC with respect to control conditions ($p<0.05$).

CONCLUSION Inductive phase shift increments at frequencies in the Beta dielectric dispersion region could be associated to changes in the cell structure and elastic stiffness estimated by US-SR and has the potential to detect pathological conditions in breast tissue associated to cancer. Further complementary studies are warranted to confirm the observations.

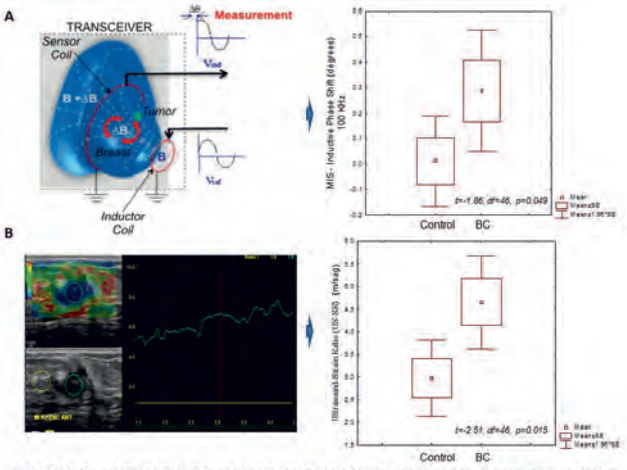

Fig. 1. **A**) Inductive Phase Shift ($\Delta\Theta$) and **B**) Ultrasound-Strain Ratio (US-SR) measurements in BC *vs* Control.

Abstract Id: 162
Topic: *Bioimpedance*

BIOIMPEDANCE PHASE ANGLE: THE RUSSIAN REFERENCE DATA

Svetlana Shchelykalina[*1,2], Dmitry Nikolaev[1,3], Sergey Rudnev[1,4], Vladimir Kolesnikov[1], Olga Starunova[1], Aleksandr Smirnov[3]

[1]Federal Research Institute for Health Organization and Informatics of Ministry of Health of the Russian Federation, [2]Pirogov Russian National Research Medical University, [3]MEDAS Ltd., [4]Institute of Numerical Mathematics of the Russian Academy of Sciences, Moscow, Russian Federation

INTRODUCTION The bioelectrical impedance analysis (BIA) phase angle (ϕ), which is directly calculated from measured reactance and resistance, is considered to be a valuable indicator of health. It is used for the assessment of malnutrition and serves as a prognostic indicator in cancer, liver cirrhosis, HIV/AIDS, hemodialysis and critical illness. A number of population references for ϕ were reported. The data show significant intragroup and intergroup differences depending on age, sex, body mass index (BMI) and patients' conditions. The use of BIA by the national network of Health Centres which was established in 2009 led to the appearance of the Russian bioimpedance database.

OBJECTIVES Our aim was to construct population reference data for the bioimpedance ϕ in Russians depending on age, sex, and BMI.

METHODS Cross-sectional data of BIA measurements of 549026 male and 1088754 female subjects aged 5-85 years were obtained with the same type of BIA meters (ABC-01 'Medas', SRC Medas, Moscow) at frequency 50 kHz in supine position using conventional tetrapolar electrodes placement. Percentile reference tables of ϕ for BMI were constructed using GAMLSS package in R.

RESULTS The surface plots for the median values of ϕ in Russians are shown in Fig 1. Depending on BMI, these values were between 5.5°–6.2° in 13-years old adolescent boys and girls, within the intervals 6.9°–7.5° and 6.2°–6.7° in middle-aged men and women, and within the intervals 6.1°–6.5° and 5.8°–6.2° in 65-years-old men and women, respectively.

In our adults, BMI values less than 18 kg/m^2 were rare. The same applied to our children with BMI values more than 30 kg/m^2. So, for these BMI intervals, we were unable to present ϕ medians for the full age range of the study group.

The obtained median values of ϕ were similar to Swiss and greater than the German reference values in both sexes (within 0.5°–1.0°). As compared to US reference data, our median ϕ values were lower in men and similar in women. More work should be done to explain these differences, including a comparison of the equipment and electrodes used, and measurement conditions.

CONCLUSION The Russian population reference data will be used as a basis for ϕ classification in ambulatory and clinical settings.

ACKNOWLEDGEMENT This work is supported by the Russian Science Foundation grant no 14-15-01085.

IMAGE

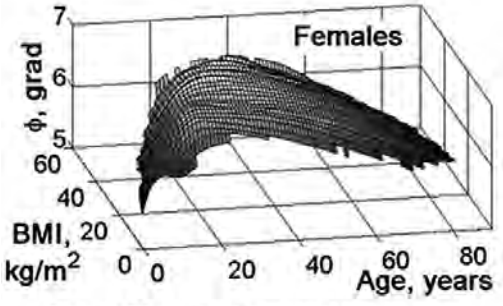

Fig. 1 The median ϕ values in our study group: age and BMI dependence

Abstract Id: 164
Topic: *Bioimpedance*

CARDIAC AND RESPIRATION SIGNALS RECORDING BY AN MIT SYSTEM

George Panayi[1], Ralf Patz[*2], Stuart Watson[3], Sotos Voskarides[1]

[1]Department of Electrical Engineering, Computer Engineering and Informatics, Cyprus University of Technology, Limassol, Cyprus, [2]Fachbereich Informatik und Elektrotechnik, University of Applied Sciences, Kiel, Germany, [3]Department of Medical Physics, Salford Royal NHS Foundation Trust, Salford, United Kingdom

INTRODUCTION Magnetic Induction Tomography (MIT) is a technique that employs alternating magnetic fields to apply an excitation current within a sample for imaging its passive electromagnetic properties. In comparison to Electrical Impedance Tomography, MIT has the advantages of operating through air gaps or electrically insulating materials and not requiring contact with the object.

OBJECTIVES The development of an MIT system aiming at the fully contactless concurrent recording of the human cardiac and respiration rates at rest and after strenuous activity.

METHODS The system comprised a single-channel coil array, a signal processing and measurement unit incorporating an FPGA and a host computer. It operated at 10 MHz and for the measurements a recording rate of 20 Hz was used. Three measurement protocols were examined: normal breathing, post-strenuous recovery and breathing pattern. Four volunteers participated in the measurements. In normal breathing the volunteers breathed normally for 2 minutes. In post-strenuous activity the volunteers increased their heart rate above 100 beats per minute (bpm) and remained in the coil array until recovery. In breathing pattern the volunteers performed a breathing sequence (normal breath, no breath, normal breath, very deep breath, normal breath) for 2 minutes. A 3-lead ECG device recorded the volunteers' ECG concurrently to the measurement. The digital post-processing of the measurements was performed in MATLAB using frequency (FFT) and time-frequency (STFT) analysis.

RESULTS The system recorded successfully and concurrently the volunteers' respiration and cardiac signals. The recording rate of 20 Hz proved sufficient to record tachycardia. For normal breathing the cardiac and respiration rates could be determined using FFT analysis and STFT. For post-strenuous activity the MIT signal was irregular and the cardiac signal could not be discriminated using FFT analysis however it was discriminated using STFT. The system recorded the breathing sequence and distinguished between the breathing patterns however during the very deep breathing the cardiac signal could not be discriminated by the FFT or the STFT.

CONCLUSIONS The system can concurrently record the cardiac and the respiration signal and can discriminate between the normal cardiac rate and tachycardia. However further work is required to better discriminate the cardiac and the respiration signals.

Abstract Id: 165
Topic: *Clinical applications*

EFFECTS OF IN VIVO MUSCLE INJURY ON MUSCLE IMPEDANCE IN MICE

Benjamin Sanchez[*1], Shama R Iyer[2], Jia Li[1], Richard M Lovering[2], Seward Rutkove[1]

[1]Department of Neurology, Harvard Medical School, Boston,
[2]Department of Orthopaedics, University of Maryland School of Medicine, Baltimore, United States

INTRODUCTION Duchenne muscular dystrophy (DMD) [1] is a genetic disorder characterized by progressive muscle degeneration and weakness, and ultimately premature death. DMD, the most common and severe muscular dystrophy, is caused by the absence of dystrophin. Muscle weakness and fragility (i.e., increased susceptibility to damage) are hallmarks of DMD and the 6-minute walk test is one of the only meaningful clinical endpoints available to clinicians.

OBJECTIVES We used a novel *in vivo* injury model to induce quadriceps injury in healthy and dystrophic mice, to test our hypothesis that electrical impedance myography (EIM) reflects the overall contractile response of muscle to injury, relating EIM response to *in vivo* functional deficits in both healthy and dystrophic muscles.

METHODS We measured 10 wild type (WT) and 10 dystrophic (*mdx*) mice from C57BL/10ScSnJ strain (male, 2 month old, body weight 27.4±2.7 g and 27.8±2.1 g, respectively). With the animal anaesthetized, the thigh was stabilized and the ankle was secured on to a lever arm. The axis of the knee was aligned with the axis of a stepper motor and a torque sensor. The femoral nerve was stimulated subcutaneously and injury resulted from 15 forced lengthening contractions superimposed on to maximal quadriceps contractions through a 60º arc of motion. Quadriceps impedance was measured before and after injury. *In vivo* functional recovery was assessed 24 h after injury. The opposite thigh served as a control. Statistical significance $p<0.05$ was assessed using Mann-Whitney two-tailed t-test.

RESULTS Injury resulted in a significant loss of maximal isometric torque in *mdx* (68±14.3%) and WT (22±15.7%) muscles. The change in resistance (10 kHz) in WT and *mdx* mice after injury was, respectively, 25.6±4.3% ($p<0.01$) and 25.5±4.2% ($p<0.05$); after 24h, however, *mdx* showed a greater change in resistance (57.1±8.5%, $p<0.001$) compared to WT (45.1±5.4%, $p<0.01$).

CONCLUSIONS The data suggest that EIM can be used as a biomarker to determine contractile alterations in skeletal muscle associated with injury and/or disease. To the best of our knowledge, this is the first use of impedance after an *in vivo* injury. The impact of these findings will be of value for testing the success of novel therapies for muscular dystrophy disease.

REFERENCES

1. Sanchez B et al. Evaluation ofelectrical impedance as a biomarker of myostatin inhibition in wild type and muscular dystrophy mice. PLoS One, 2015, 10(10):e0140521.

Abstract Id: 166
Topic: *Bioimpedance*

BIO IMPEDANCE SYSTEM FOR WEARABLE VITAL SIGN MONITORING

Gabriel Squillace*[1], Seulki Lee[1], Victor van Acht[1], Marianne Vandecasteele[1]

[1]Wearable Health Solutions, Holst Center, Eindhoven, Netherlands

INTRODUCTION Wearable bio-impedance (BioZ) systems bring clinical value by enabling long-term continuous monitoring of patients. We have shown that localized BioZ can indicate congestion levels of heart failure patients using imec's wearable BioZ monitor [1,2]. Combining BioZ and vital sign monitoring into wearables can bring additional benefits since symptoms are a combination of cardio-respiratory complications such as palpitations, fatigue, dyspnea and reduced physical activity[3].

OBJECTIVES Design a wearable vital sign monitoring platform to measure BioZ, electrocardiogram (ECG), electrode-tissue impedance (ETI), 3-axis accelerometer and air pressure with embedded signal processing and Bluetooth.

METHODS The solution proposed is based on a SoC called MUSEIC [4]. It provides low power circuits for BioZ, ECG, ETI and auxiliary channels. Different from existing solutions, MUSEIC supports low-noise and highly configurable BioZ measurement. Single or multi-frequency mode, sine or square wave current, four current amplitudes, and different frequency profiles can be chosen for BioZ measurement at a sampling rate of 1 kHz. 3-channel ECG with ETI and other sensors, such as microphone, which can also be sampled at 512 Hz and 1 kHz, respectively.

RESULTS The result is a fully integrated system (W:30mmW x L:74mm x H12mm) including a 3.7 V 500 mAh battery. It consumes 35 mW on average, resulting in 52 hours of continuous recording. A recording with the proposed platform is shown in the figure below, displaying ECG, single (80 kHz) and multi-frequency BioZ, and 3-axis accelerometer data. The data is transmitted in real time to a smartphone and to a cloud server via Bluetooth.

CONCLUSION A platform proposed is suitable for various wearable and continuous vital sign monitoring applications thanks to its outperforming sensors and small form factor. Data collection and analysis in several applications is part of the future work.

IMAGE

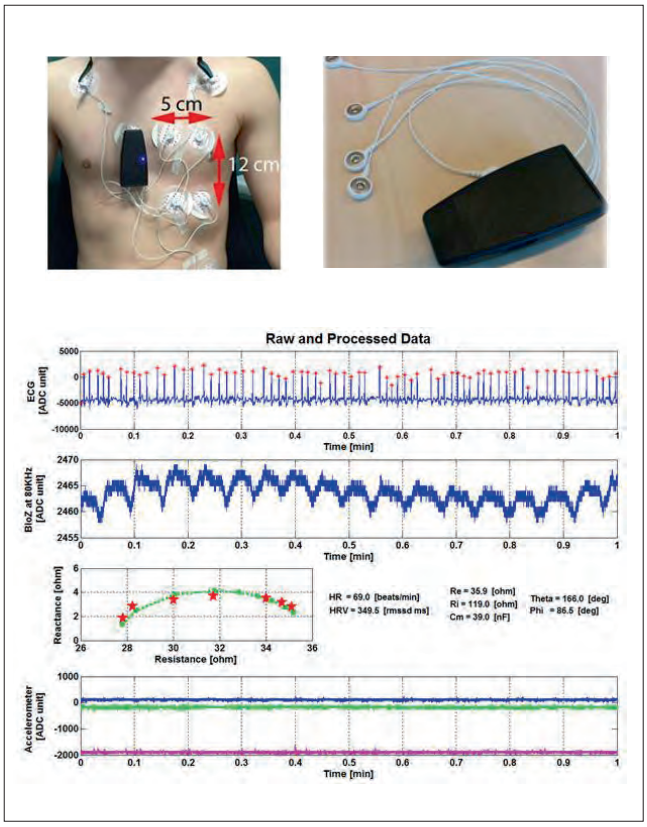

REFERENCES

1. J. Phys.: Conf. Ser. 434 012013.
2. 10.1109/EMBC.2015.7318393.
3. ESC Guidelines for the diagnosis and treatment of acute and chronic heart failure.
4. 10.1109/JSSC.2014.2359962.

Abstract Id: 167
Topic: *Instrumentation*

REAL-TIME MICROCONTROLLER-BASED MIT PHASE MEASUREMENT SYSTEM

Ralf Patz*[1], Juri Koch[1], Victor Golev[1], George Panayi[2]

[1]Faculty of Computer Science and Electrical Engineering, University of Applied Sciences, Kiel, Germany, [2]Department of Electrical Engineering, Computer Engineering and Informatics, Cyprus University of Technology, Limassol, Cyprus

INTRODUCTION Magnetic Induction Tomography (MIT) is a technique for contactless mapping of a sample's passive electromagnetic properties. An alternating primary magnetic field induces eddy currents in the sample which in turn produce a secondary alternating magnetic field containing the information. The electrical conductivity of the sample can be determined by measuring the phase difference between the signals of the primary and the secondary magnetic fields.

OBJECTIVES The development of a real-time low-cost microcontroller-based zero-crossing phase measurement system and characterization in a single channel MIT scanner.

METHODS A phase measurement system based on a dsPIC (Microchip) was developed for a single channel MIT scanner system operating at 10MHz. The system consists of an analogue down-conversion board using the active mixers AD835, an XOR gate, a dsPIC33F and a PC.

The system operates as follows: Two input signals (primary and secondary) are down-converted from 10 MHz to 10 kHz, filtered (low-pass), amplified, squared and fed to the XOR gate which produces a pulse whose width represents the phase difference. A gated timer in the dsPIC counts the width of each XOR pulse at a rate of 40 MHz and the result is send (USB) to the computer for real time phase calculation in Matlab.

The system was characterized for phase precision and drift on its own and in a single channel MIT scanner. The phase precision was calculated from the standard deviation of 16 phase measurements (measurement time 50ms), and the phase drift from the average of 16 phase measurements every minute over a period of 6 hours. The system was tested with five 500ml saline solutions (<2S/m).

RESULTS The phase measurement system achieved a phase precision of 2 millidegrees and a phase drift of 10 millidegrees. A dependency from the room temperature during the drift measurements was observed. The use of thermal insulation and temperature control reduced the phase drift to 3.1 millidegrees. Connected to a single channel MIT scanner the phase precision was reduced to 5 millidegrees and the phase drift to 12 millidegrees. The correlation between the saline solutions and the phase was 0.9999.

CONCLUSIONS The system provides a low cost option for a single channel MIT system. The results showed the need for active temperature control in order to reduce the phase drift. The phase precision and drift of the complete MIT scanner system was 5 millidegrees and 12 millidegrees, respectively.

Abstract Id: 168
Topic: *Bioimpedance*

MUTUAL CAPACITANCE SENSORS FOR TISSUE DIAGNOSTICS

Amin Mansoorifar[1], Ahmet Sabuncu[*1], Ali Beskok[1]

[1]Mechanical Engineering , Southern Methodist University, Dallas, United States

INTRODUCTION MCSs make use of the fact that the capacitance between two electrodes can be altered by a third conducting object, which decreases the charge hold between electrodes. Therefore, the mutual capacitance between electrodes decreases depending on the electrical properties of the object. Among other capacitive touch technologies, MCSs are widely used in industry, and especially, in mobile phone screens. Although the MCS technology is commercially available, application of the technology for tissue diagnostics has not yet been explored.

OBJECTIVE The objective of this work is to explore the applicability of the MCS technology for tissue diagnostics.

METHODS We used MCSs that are composed of vertical and horizontal strips of gold electrodes separated by a thin dielectric layer (glass and polydimethylsiloxane). In the experiments, while one electrode is in contact with the sample, the other electrode is beneath the dielectric layer. Impedance measurements were conducted between 1 kHz and 10 MHz to probe samples at an intersection of vertical and horizontal electrodes. Standard dielectric liquids, KCl solutions (23, 84, 1500, and 12,880 µS/cm), and vegetable tissues were measured using the MCS. The capacitance spectrum was also simulated using a commercial finite element model solver (COMSOL Multiphysics).

RESULTS Capacitance spectra of the vegetables are shown in Figure 1. The results indicate two dispersions in all vegetable tissues. While the characteristic frequencies of the dispersions observed for red potato and carrot were similar, sweet potato exhibit different dispersion frequencies. Numerical simulation results indicated a good fit between experiments with liquids and simulations. Furthermore, systematic numerical simulations with varying electrode width indicated that larger electrode widths have greater penetration depths into the tissues. Thinner dielectric layers with greater permittivity increase the sensitivity of the measurement.

CONCLUSIONS The preliminary experiments and simulations indicated applicability of MCSs for tissue bioimpedance measurements. Numerical simulations tools developed here were to be useful with comparison to experiments for predicting sensor response. Specifically, electrodes with larger width have higher electric field penetration depth into the samples. We are currently working on MCS measurements of human tissue samples.

IMAGE

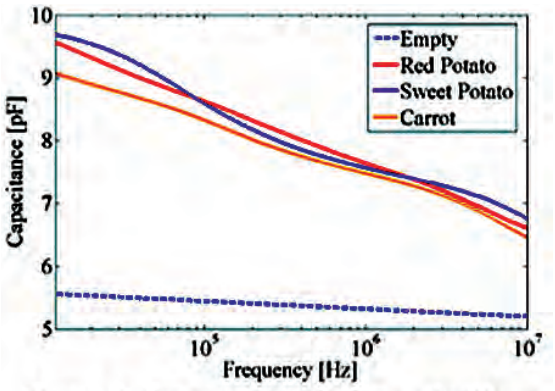

Figure 1. Capacitance spectrum of different vegetables tissues.

Abstract Id: 169
Topic: *Clinical applications*

IMPEDANCE VALUE DIFFERENCES BETWEEN KNEES IN FEMALE ATHLETES

Marco Balleza Ordaz*[1], Marysol García Pérez[1],
Miguel Vargas Luna[1], María Raquel Huerta Franco[2]

[1]Medical Physics, [2]Department of Sciences Applied to Work, University of Guanajuato, León, Mexico

INTRODUCTION The medical trials used to diagnostic knee pathologies are the x-ray and MRI techniques. The x-ray reveals injuries in hard tissues (bones), while MRI evidences the injuries in soft tissues (meniscus and tendons). These medical trials are expensive in most cases. Our research group propose the electrical bio-impedance (EBI) technique as an option to assess the knee condition.

OBJECTIVE The main objective of this research is to compare the impedance parameters between knees with and without meniscal injury in female athletes.

MATERIALS AND METHODS

a) Volunteers. In this study participated six sports-women (Age: 19.5±0.8 years, BMI: 20.4±3 kg/m^2). All volunteers were assessed for meniscal problems, comparing right and left knees by a sports medical professional staff. All volunteers had a good physical condition according to the parameters of the American College of Sports Medicine. Body composition was also measured.
b) Procedure. The bio impedance parameters where obtained by a BIOPAC System (MP150), which injects an electrical current of 1 mA at different frequencies (12.5 kHz, 25 kHz, 50 kHz, 100 kHz). In order to monitor the knee condition by bio-impedance, four electrodes in each knee were placed. All volunteers were asked to fully extend each leg in periods of 5 seconds to perform the test at 30 seconds.
c) Signal processing. All data were analyzed by using Matlab software. The impedance data was analyzed and compared at different impedance frequencies. Subsequently, these results were correlated with the clinical findings performed for all the volunteers.
d) Statistical analysis. The comparison of impedance parameters between knees with and without meniscal injures were made using a t-test for independent groups.

RESULTS All the volunteers have showed meniscal injure in the right knee; however there were not statistical differences when we compare the length of the lower pelvic limb the mean and standard deviation (X±SD), were: 91.9±7.4 vs. 91.8±7.0, for right and left limbs (t=0.02, p=0.98). The mean and standard deviation of the bio impedance parameters were as follows: 48.9±10.7 vs. 71.5±19.1. When we compare with a t-test we found significant differences between knees with and without injure (t=-3.58, p=0.002).

CONCLUSIONS In this study we demonstrated that the impedance technique could be a good option to monitor the knee condition.

Abstract Id: 170
Topic: *Instrumentation*

SYSTEM FOR NERVE STIMULATION AND BIOIMPEDANCE MEASUREMENTS

Dejan Krizaj[1], Robert Brajkovič[*1], Janez Rozman[2],
Pedro Bertemes Filho[3], Robert Frangež[4], Monika Žužek[4]

[1]Lab for bioelectromagnetics, University of Ljubljana, [2]Centre for Implantable Technology and Sensors, ITIS d.o.o, Ljubljana, Slovenia, [3]Departamento de Eng. Elétrica, Universidade do Estado de Santa Catarina, Joinville, Brazil, [4]Veterinary faculty, University of Ljubljana, Ljubljana, Slovenia

INTRODUCTION Electrical bio-impedance spectroscopy (EBS) and electrical nerve stimulation (ENS) enable monitoring of bio-impedance of biological tissues and excitation of nerve tissues with electrical signals. Accurate constant current excitation is necessary in both EBS and ENS systems, where electrical pulses are used for excitation of nerve tissues. Characteristics of pulses will determine their ability to stimulate a nerve and quality of stimulation will be affected by the polarity and electrode type, the electrode-nerve distance and by interactions at the electrode-tissue interface.

OBJECTIVES Design and development of a flexible combined system that is capable of stimulation and monitoring of the bioimpedance of the nerve tissue at the same time.

METHODS The device design is based on usage of a DAQ device RedPitaya with an addition of a customized front-end circuitry. The system consists of processing and measuring part and the measurement setup. The latter is a specially designed and constructed silicone connection chamber with platinum electrodes for selective nerve stimulation and bioimpedance measurements. The chamber enables in vitro and in vivo measurements only for research purposes and its electrodes can be changed. Specific excitation waveforms were used in conjunction with the current source for effective nerve stimulation. Immediately after stimulation, response of the nerve tissue to sinusoidal current excitation of several frequencies was recorded and bioimpedance values were determined. Experiment 'in vivo" was carried out on an isolated sciatic nerve of a rat.

RESULTS Response to the excitation current pulse depends on the current intensity, characteristics and duration of stimulation. The response also varies with the electrode size, its geometry and electrode positioning. Bioimpedance spectroscopy after current pulse stimulating was performed in the frequency range from 1Hz to 500 kHz with 2-point and 4-point method. The difference indicates the presence of reactions at the electrode-nerve tissue interface.

CONCLUSION The developed combined stimulation/bioimpedance measurement system is very flexible and as such very useful for research and analysis of different types of nerve stimulating applications and optimizations of stimulation electrodes.

Abstract Id: 171
Topic: *Bioimpedance*

COMPARISON BETWEEN AC & DC EXOSOMATIC EDA MEASURING METHODS

Oliver Pabst[*1], Christian Tronstad[2], Ørjan Grøttem Martinsen[1,2], Sverrre Grimnes[1,2]

[1]Department of Physics, University of Oslo, [2]Department of Clinical and Biomedical Engineering, Oslo University Hospital HF, Oslo, Norway

INTRODUCTION Electrodermal activity (EDA) measurements have been used for research and clinical applications for many years. Using a direct current (DC) excitation signal for EDA measurements is still the standard due to its use in history. The main advantage of using an alternating current (AC) signal instead, is the possibility to measure Skin Conductance (SC) and Skin Potential (SP) simultaneously at the same electrode [1]. The Society for Psychophysiological Research now starts to accept this method. However, more research is required before the society will recommend the use of the AC method as a standard [2].

OBJECTIVES A direct comparison between AC and DC conductance measurements should be done. Therefore the EDA of several test subjects is recorded by using the AC and the DC method at the same time. The results of both methods are compared by evaluating EDA parameters. These parameters are amplitude, rise and recovery time of the responses, the ratio between peak time and duration of the responses and conductance levels.

METHODS An custom-built measuring system enables applying of an AC and a DC voltage at the same time and same skin site. This is done by superposition of both signals. Due to its common use the measuring system is realized as a bipolar system. The test sessions consist of active phases (in which the test subjects were ask to solve mathematical tasks) and relaxation periods in between.

RESULTS The measurements are done on 28 test subjects. In Fig. 1 an example plot from the test sessions is given.

CONCLUSION A first view on Fig. 1 gives already the assumption that the results of both methods are quite similar. This is affirmed by statistical analysis over all responses of all test subjects.

IMAGE

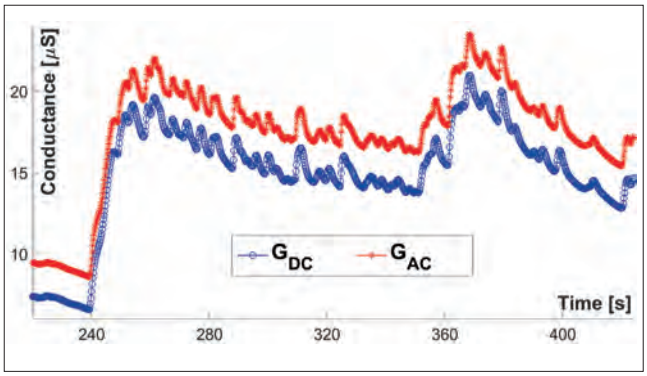

***Fig. 1**. Example plot of one test session. AC and DC conductance measurements are done simultaneously. The applied DC voltage is 500 mV and the applied AC voltage is a sinus voltage with an amplitude of 500 mV and f = 20 Hz. The measurements are done on the palmar skin site.*

REFERENCES

1. S. Grimnes, A. Jabbari, Ø. G. Martinsen, and C. Tronstad, "Electrodermal activity by dc potential and ac conductance measured simultaneously at the same skin site," Skin Research and Technology, vol. 17, no. 1, pp. 26–34, 2011.
2. W. Boucsein, D. C. Fowles, S. Grimnes, G. Ben-Shakhar, W. T. Roth, M. E. Dawson, and D. L. Filion, "Publication recommendations for electrodermal measurements," Psychophysiology, vol. 49, pp. 1017–1034, 2012.

Abstract Id: 172
Topic: *Signal processing*

ADAPTIVE ALGORITHM FOR CARDIAC PERIOD NORMALIZATION IN TIME

Andrei Krivoshei[*1,2], Hasso Uuetoa[3], Mart Min[1], Paul Annus[2], Tiina Uuetoa[4], Jürgen Lamp[2]

[1]TJS Department of Electronics, Tallinn University of Technology, [2]ELIKO Competence Center, Tallinn, Estonia,
[3]Sahlgrenska University Hospital, Gothenburg, Sweden, [4]East-Tallinn Central Hospital, Tallinn, Estonia

The paper presents an adaptive algorithm for the cardiac Electrical Bio-Impedance (EBI) period normalization in time domain. The problem of the proposed period normalization is arisen from [1,2], where the possibility of the central aortic pressure (CAP) waveform estimation from the radially measured EBI signal is described and investigated. During the mentioned researches some questions about comparability of the signal periods are appeared. Firstly, how two signal periods with different durations can be compared. Especially the cardiac EBI periods, taking into account that such periods waveforms are stretched (or squeezed) non-linearly with reference to theirs durations. Secondly, how to normalize such periods to provide correct ensemble processing, e.g. ensemble averaging, principal component analysis (PCA) and etc.

The proposed paper is trying to solve these problems. In the paper all periods in the signal are normalized in time domain with reference to the first period in this signal, at the current stage. The periods starting points are selected at the beginnings of the respective systolic processes. For the normalization the vector of time instances of the reference period is transformed into the orthogonal Legendre polynomial coefficients up to third order. Such a transformation is used to reduce dimensionality of the adaptation procedure. The coefficients values are used as initial parameters in the adaptive algorithm. Thus, in the proposed method the time vector of the period, which to be normalized, is scaled to minimize the sum of the root square errors between the selected and the reference periods waveforms. In turns, the selected period waveform is recalculated by interpolating the original waveform and the new time instances vector, which is updated (scaled) and inversly transformed from the Legendre basis coefficients.

IMAGE

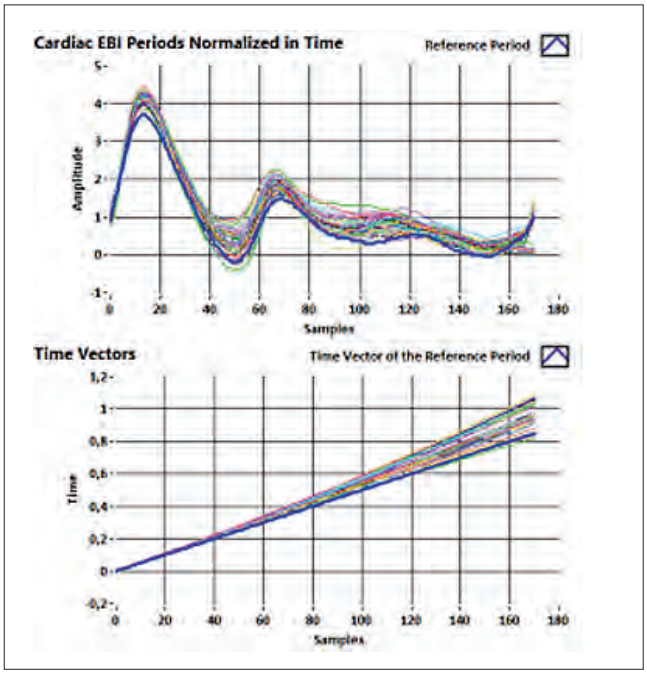

REFERENCES

1. Krivoshei, A., Uuetoa, H., Min, M., Lamp, J., Annus, P. and Uuetoa, T., "Estimating the Transfer Function Between the CAP and Radial EBI Cardiac Periods: Use of PCA for Dominating Spectral Features Analysis," International Journal of Bioelectromagnetism, 17 (1), 31–35, 2015.
2. Krivoshei, A., Min, M., Uuetoa, H., Lamp, J., and Annus, P., "Electrical Bio-Impedance based non-invasive method for the central aortic blood pressure waveform estimation," Proc. 14th Bienn. Balt. Electron. Conf. BEC2014, pp. 181–184, Oct. 2014.

Abstract Id: 173
Topic: *Instrumentation*

DIFFERENCE SAMPLING IN BIO-IMPEDANCE MEASUREMENT

Paul Annus[*1,2], Marek Rist[1,2], Marko Reidla[2], Mart Min[1]

[1]Thomas Johann Seebeck Department of Electronics, Tallinn University of Technology, [2]Eliko, Tallinn, Estonia

INTRODUCTION Information contained in bio-impedance is typically twofold: long term variations and spectral content of the so called base impedance, and short term fluctuations on top of it, which can be related to certain biological processes of interest. In case of bioimpedance based plethysmography determination of changing tissue volumes in the body is of interest. Direct digitalization of the response signals form live subject poses several challenges.

OBJECTIVES Two volumes of general interest are the cardiac stroke volume and the respiratory minute volume. Both of these cause changes in measured bioimpedance values over the thorax area. Second of them is relatively easier to detect, since the variations are large (typically over 1%) compared to the base impedance. Cardiac stroke however causes much smaller changes (typically below 0, 1%) in thorax area bioimpedance readings. If direct conversion with typical 16 bit analog to digital converter (ADC) is considered, then less than 6 bits are left for digitalization of the important information. Several solutions have been proposed, such as direct carrier compensation, and multistage conversion. Proposed solution is believed to be simpler yet powerful.

METHODS It has been known that clever synchronous quadrature sampling will considerably simplify related signal processing. In its simplest form samples related to real and imaginary parts are simply summed. Generally it still requires relatively fast converters with many bits, if good signal to noise ratio is required for detecting tiny biological modulation on top of the large base impedance. Undersampling, while lessening speed requirements, has a cost of increased noise level.

Detachment of sampling and conversion stages is proposed in current paper. It is enough to digitize the difference of two samples, taken at 90° and 270° relative to the excitation waveform, to calculate real part of the bioimpedance. For imaginary part 0° and 180° samples are required. As an example fast Sample-and-Hold (SH) circuits DS1843 from Maxim Integrated can be used for achieving desired result.

RESULTS AND CONCLUSION Impact of the large base value of the bioimpedance can be eliminated by placing simple SH circuits in front of the ADC, and more bits are left for direct digitalization of the biological modulation on top of the bioimpedance signal. Introduced principle can easily be adapted for construction of task oriented application specific integrated circuits (ASIC).

IMAGE

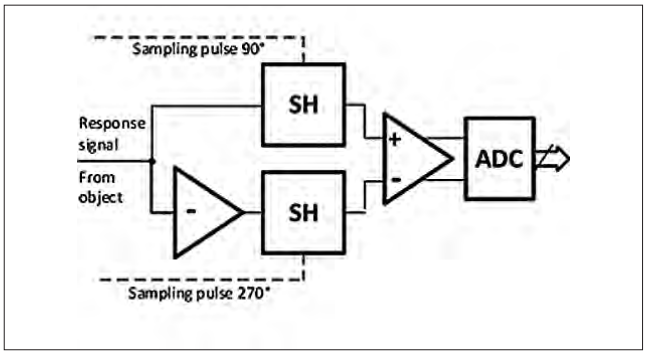

Abstract Id: 174
Topic: *Electrical impedance spectroscopy*

LIMITATION OF SIGNAL AMPLITUDES IN BIOIMPEDANCE SPECTROSCOPY

Jaan Ojarand[*1], Marek Rist[1,1,2], Mart Min[2]

[1]Eliko Competence Centre, [2]Thomas Johann Seebeck Department of Electronics,
Tallinn University of Technology, Tallinn, Estonia

KEYWORDS impedance spectroscopy; signal-to-noise ratio; optimal excitation; amplitude limitation.

INTRODUCTION Amplitudes of the excitation signals are strictly limited in electrical bioimpedance measurements and the signal-to-noise ratio (SNR) becomes low. Though the optimization of signal waveforms minimizes their amplitudes [1], it does not take noise into account. Amplification of the noisy low-level signals causes overloading of measurement channels – nonlinearities appear and distortions of measurement signals take place. Well defined limiting of noisy signals is required to minimize the corruption of measurement results.

OBJECTIVES The appropriate limiting depends on the signal-to-noise ratio. Fast operating limiter with adjustable limitation levels has to be designed. The errors are to be analyzed for different SNR values.

METHODS The computer aided simulation with subsequent experimentation has been chosen for the research. An experimental electrical circuit of the limiter on the bases of operational amplifiers with limiting components in the feedback loops is designed for testing the simulation results.

RESULTS An example of a limited noisy waveform is illustrated in Fig.1a. SNR of the 4-component multisine signal with 0.1 mA amplitudes is -6 dB. The limiting level was set to ± 3.5V. Magnitude spectrum of ten consecutive measurements is shown in Fig.1b.

CONCLUSION The proposed limitation of noisy signals enables to cover near to full-scale amplitude range without significant degradation of results if the noise level reaches to or even exceeds the signal value.

IMAGE

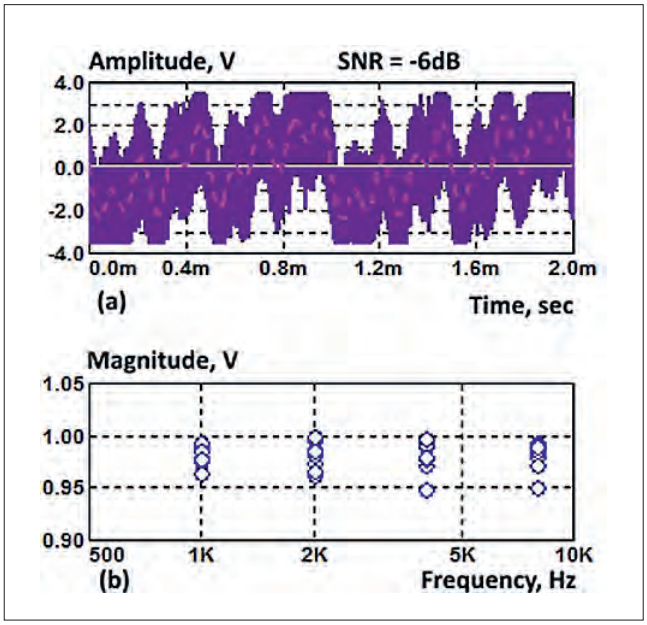

Figure 1. *Diagrams of the limited signal waveform (a) and its magnitude spectrum (b).*

REFERENCES

1. Pintelon R and Schoukens J 2012 *System Identification: A Frequency Domain Approach*, 2nd ed. (New Jersey: Wiley).

Abstract Id: 175
Topic: *Electrical impedance tomography*

STABLE AND PRECISE REAL-TIME MIT PHASE MEASUREMENT SYSTEM

Ralf Patz* [1], Thorsten Brandt[1], Johannes Holthusen[1]

[1]Faculty of Computer Science and Electrical Engineering, University of Applied Sciences, Kiel, Germany

INTRODUCTION Magnetic Induction Tomography (MIT) is a contactless and non-invasive method for mapping of passive electromagnetic properties of tissue. The electrical conductivity of a sample can be measured using the phase difference between a primary field and a perturbed secondary signal. For biological tissues a phase precision of <1m° and a low phase drift is required. This abstract reports a FPGA-based MIT system that achieves both objectives.

OBJECTIVES The development and characterization of a phase-stable MIT measurement system with a sub-millidegree phase precision.

METHODS The system comprises of a Xilinx System-on-Chip (SoC) mounted on a Red Pitaya system board. The SoC contains a FPGA matrix and a dual-core ARM CortexTM-A9 processor. Two 125 MSps DACs and ADCs are connected for signal generation and capture. One DAC is used to generate the primary signal (10MHz) using an internal FPGA Direct-Digital-Synthesis (DDS) block. This signal is fed back to the two ADC channels. A digital Phase-Sensitive-Detection (PSD) was implemented in the FPGA followed by a decimating Cascaded Integrator-Comb (CIC) filter. The signal rate is reduced to 59.6 Hz and the signal is passed to the ARM core for further processing. The phase difference between the two signals is calculated and transmitted via the LAN interface to a PC.

RESULTS The system was characterized for phase precision and drift. The phase precision was measured by calculating the standard deviation of 16 phase measurements (measurement time 17 ms). At the maximum signal amplitude a phase precision of 142 microdegrees was achieved, which degraded to 22.6 millidegrees when the signal input was attenuated by 60 dB. The 1 millidegrees threshold was reached with an attenuation of 24 dB. The phase precision was measured over a frequency range of 0.5 to 50 MHz and showed that the best phase precision is achieved between 5 and 10 MHz.

The phase difference was measured every minute for a period of 11 hours to obtain the phase drift. The system needs a warm up period of 60 minutes after which it exhibits a phase drift of 2.6 millidegrees.

CONCLUSION The system showed a high phase precision of 142 microdegrees combined with a low drift after an initial warm up period (2.6 millidegrees). The measurement rate was 59.6 Hz with a time constant of 17 ms, making the system suitable for real-time measurements. Further work includes the characterization of the measurement system in a MIT scanner

Abstract Id: 176
Topic: *Bioimpedance*

RESISTIVE COMPONENT OF MEAT ELECTRICAL BIOIMPEDANCE

Gianni Battacone[1], Alberto concu[*2], Giuseppe Pulina[1], Marco Acciaro[3], Carla Manca[3], Daniele Concu[2], Filippo Tocco[2], Andrea Fois[2]

[1]Department of Agricultural Science, University of Sassari, Sassari, [2]2C Technologies Srl, Academic Spinoff, University of Cagliari , Cagliari, [3]Department of Animal Production, Agris Sardegna Agency, Sassari, Italy

INTRODUCTION Measurement of the meat electrical bio-impedance (Z_M) consents to evaluate cells integrity. When a constant electrical current (CC) at high frequency is injected into tissues it virtually nullifies the capacitive reactance of the slaughtered muscle cell and Z_M only depends on the equivalent resistance due to the intracellular (Ri) and extracellular (Re) fluids [$Z_{M=}$(Ri+Re)/(Ri·Re)].

OBJECTIVES The aim of the study was to develop a portable Z_M device able to inject a CC (1 mA) with a fixed frequency of 100 KHz into slaughtered muscles. In this way it would be simple to measure the meat ripening on the basis of the Z_M fall because of Ri decreases and Re increases progressively after slaughter.

METHODS Z_M device was connected with a serial-over-USB to a PC for running a dedicated software developed to oversee the operations of the device. The software communicated with the microcontroller using a command and control proprietary binary protocol. In a slaughtered calf (about 16 months aged), Z_M was assessed by both the right and left side portions of the longissimus dorsi muscle (LDM) placed between the 7th and 12th thoracic vertebra. Measurements were obtained in the 2nd and in the 7th day post-slaughter. Right LDM was kept between 2°C and 5°C; left LDM was frozen at -18°C until to 6th day, then it was thawed at 5°C. For several times at each test session, two copies of copper wires (0.5 mm diameter), positioned along the muscle fibres, were applied to inject the CC and detect the Z_M, respectively.

RESULTS At 2nd day post-slaughter both sides of LDM showed similar values of Z_M (right=133±3Ω, left=129±4Ω). Differently at 7th day the Z_M of right LDM was 115±5 Ω and the left one was 63±6 Ω.

CONCLUSION The evident drop of Z_M in the left slaughtered LDM could depend on muscle structure damages i.e. breaking down of Z line, disruption of continuity of fibres, upon formation of ice crystals. Thus our Z_M device could be used to check the degree of ripening in slaughtered meat and also to check if the meat was undergone to processes of freezing and thawing.

KEYWORDS meat bioimpedance; portable device; frozen meat

Abstract Id: 177
Topic: *Clinical applications*

NEURAL TISSUE DISCRIMINATION WITH MACHINE LEARNING METHODS

Håvard Kalvøy* [1], Axel R. Sauter[2], Christian Tronstad[1], Ørjan G. Martinsen[1, 3]

[1]Department of Clinical and Biomedical Engineering, [2]Division of Emergencies and Critical Care, Department of Anaesthesiology, Oslo University Hospital, [3]Department of Physics, University of Oslo, Oslo, Norway

INTRODUCTION Electrical impedance data from multi frequency measurements have been used to detect intraneural needle placement, aiming to reduce nerve damage in Regional Anaesthesia (Kalvøy & Sauter 2015). For optimization of the method and clinical implementation, we are gathering and analysing in-vivo data obtained in pigs and human volunteers. One of these experiments are here analysed with two different classification methods.

OBJETIVES The objective of this study was to compare two methods: Support-Vector Machines (SVM) and Artificial Neural Networks (ANN), for classification of bioimpedance data and their ability to discriminate intraneural placements from other tissue types.

METHODS Impedance measurement at 31 frequencies between 1 kHz and 1 MHz (logarithmically distributed) was done with ISX-3v2-mini (Sciospec, DE). The BNC-ports were used in a 3-electrode setup, with Stimuplex A needles (BBraun, DE) as measurement electrodes and BlueSensor Q ECG-electrodes (Ambu, DK) as reference and current-carrying electrodes. Tissue data was collected from muscle, fat, subcutaneous fat, artery, vein, sciatic nerve and axillary nerve, in eight pigs (30-37 kg). Each tissue type was measured in five consecutive needle positions on left and right side. Due to missing data the resultant dataset contained 549 impedance sweeps. All 31 frequencies in each dataset were represented by modulus, phase angle, and a calculated delta parameter that was obtained by calculating the difference in phase angle between two consecutive measurement frequencies. Sciatic and axillary nerve was considered as intraneural placements, and the analysis was preformed to discriminate these from all the other tissue types. Classification models for the impedance variables were developed using SVM and ANN, and the classification performance was evaluated based on 10 runs with random permutations of k-Fold cross-validation (k=10).

RESULTS SVM and ANN were similar in performance based on the average area under the curve of a ROC plot (0.82 vs 0.80 respectively), but the SVM had less variation between runs (0.005 std) than the ANN (0.036 std).

CONCLUSION Both methods were able to discriminate the intraneural placements from the other placements. SVM seems preferential in classification model development for these measurements.

REFERENCES

1. Kalvøy H and Sauter AR, Detection of intraneural needle-placement with multiple frequency bioimpedance monitoring: a novel method. J. Clin. Monit. Comput, Apr 23. 2015.

Abstract Id: 178
Topic: *Electrical impedance spectroscopy*

CHIRP SIGNALS IN IMPEDANCE SPECTROSCOPY

Mart Min*[1], Olev Märtens[1], Raul Land[1]

[1]Thomas Johann Seebeck Department of Electronics, Tallinn University of Technology, Tallinn, Estonia

INTRODUCTION Impedance spectroscopy of living time-variant systems (beating heart, breathing lungs, pulsating blood) require broadband measurement during the exactly defined short time intervals. Synthesis of excitations and in-time processing of the responses are equally important. Scalability of chirp signals in time and frequency domain [1] makes them attractive for adaptive spectroscopy.

OBJECTIVES Spectroscopy of time-variant bioimpedances is required for performing the detailed impedance cardiography and plethysmography. The objectives are: 1) to find the signal waveforms, which enable adaption to the variations of impedance spectra in time domain, 2) provide accurate real-time signal processing of the response signals in frequency domain.

METHODS The synthesis of chirp signals with broad but adjustable frequency spectrum and controllable duration is taken under study for their implementation as the scalable signals for performing the impedance spectroscopy adaptive to the rate of bioimpedance variations. Chirplet transform of the response signal operates as a matched filter enabling the highest signal-to-noise ratio. Mathematical considerations and computer simulations were used for obtaining the results together with physical experimentations.

RESULTS We have demonstrated that the impedance spectrum of the time-variant bioimpedance can be measured successfully by the aid of spectroscopic device operating with the windowed chirp signals.

CONCLUSIONS The chirp waveform is appropriate not only for generation of excitation signals, but is effective also for the processing of response signals using the chirplet transform or a simple convolution within a relatively short time-domain window by in-phase and quadrature reference chirps [2], see Fig. 1.

IMAGE

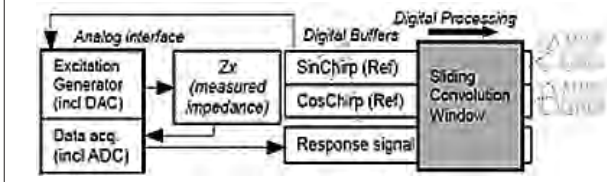

***Fig. 1**. Data acquisition and signal processing in chirp based impedance spectroscopy.*

REFERENCES

1. Paavle T, Min M and Parve T 2012 *Aspects of Using Chirp Excitation for Estimation of Bioimpedance Spectrum*, in: Fourier Transform – Signal Processing, Dr Salih Salih (Ed.), (Rieka, Croatia, InTech) http://www.intechopen.com/books/fourier-transform-signal-processing/aspects-ofusing-chirp-excitation-for-estimation-of-bioimpedance-spectrum.
2. Märtens O, Min M, Land R, Annus P, Saar T and Reidla M 2014 *Method and Device for Frequency Response Measurement.* US Patent 8,854,030.

Abstract Id: 179
Topic: *Electrical impedance spectroscopy*

USING PACEMAKER LEADS FOR BIOIMPEDANCE AND ELECTROMYOGRAPHY

Fred-Johan Pettersen[*1,2,3], Ørjan Grøttem Martinsen[1,2], Jan Olav Høgetveit[1,2], Morten Flattum[4], Håvard Kalvøy[1], Hans Henrik Odland[3,5]

[1]Department of Clinical and Biomedical Engineering, Oslo University Hospital HF, [2]Department of Physics, University of Oslo, [3]Center for Cardiological Innovation , [4]Department of Cardiology, [5]Womens and Childrens division, Oslo University Hospital HF, Oslo, Norway

INTRODUCTION As electrical bioimpedance is used in an increasing number of applications, it is also natural that electrical bioimpedance is used together with other types of instrumentation and equipment. A natural question will then be how are the instruments and equipment affecting each other and? We have investigated one particular setting: The use of pacemaker leads for bioimpedance and electromyography (EMG) measurements in heart while simultaneously using the leads for pacing. We have limited the task by looking at configurations that we believe is of particular interest.

OBJECTIVES Determine how sharing of a pace lead between an active pacemaker and bioimpedance measurement tool affect measurements in hearts.

METHODS In vivo measurements of impedance were done simultaneously with pacing using three bi-polar electrodes in the heart and two skin electrodes. Impedance was measured 190 times/s at five logarithmically distributed frequencies from 20 kHz to 750 kHz.

Bioimpedance were measured using a Sciospec ISX-3v2 mini with two 4-electrode configurations and one 3-electrode configuration, and pacing were done using an external pacemaker programing unit. A selection of pace voltage, rate, and locations were used. Pacemaker settings were partly directed by patient conditions. All pacing were done bi-polar.

To investigate non-physiological effects, some measurements were duplicated in vitro.

RESULTS We found that:
a) The impedance measurements were highly distorted for up to 35 ms by the pacemaker pulse.
b) The impedance measurements did not cause myocardial capture or other effects.
c) Bioimpedance waveform morphology was affected by pace set-up.

And for some configurations of bioimpedance measurement:
d) Myocardial capture can be detected.
e) The external pacemaker experienced interference with EMG, but pacing was not affected.
f) The EMG measurements within the heart had high-frequency interference, which can be removed by a low-pass filter.

CONCLUSION Pacing on electrodes used for electrical bioimpedance and EMG can be done provided the instruments can handle the pace voltages. There are limitations that may be in conflict with what we desire, in particular this is the interference from the pacemaker on bioimpedance and EMG signals. The interference from the bioimpedance measurements is acceptable. Finally, the information in the measurements indicates that the combination of equipment can be useful for further research and for implementation into medical equipment.

Abstract Id: 181
Topic: *Electrical impedance tomography*

EIT-DERIVED STROKE VOLUME IS IMPAIRED BY BELT DISPLACEMENT

Fabian Braun[*1,2], Martin Proença[1,2], Josep Solà[1], Mathieu Lemay[1], Jean-Philippe Thiran[2,3]

[1]Systems Division, Centre Suisse d'Electronique et de Microtechnique (CSEM), Neuchâtel, [2]Signal Processing Laboratory (LTS5), Ecole Polytechnique Fédérale de Lausanne (EPFL), [3]Department of Radiology, University Hospital Center (CHUV) and University of Lausanne (UNIL), Lausanne, Switzerland

INTRODUCTION Until today, the non-invasive measurement of stroke volume (SV) remains a challenge [1]. A potential candidate to solve this problem is EIT, which allows for a continuous monitoring of cardiac blood volume variations derived from intra-thoracic impedance changes. While recent work has shown good potential of EIT to measure SV via EIT [2, 3], the sensitivity of this approach to the shift - or displacement – of the EIT electrodes remains unknown.

OBJECTIVES To investigate the influence of longitudinal (up/down) and rotational (left/right) electrode shifts on EIT-based SV estimation by means of simulations on a human thorax model.

METHODS A previously reported haemodynamic 3D impedance model of the human thorax [4] was extended with a realistic heart [5] and pulmonary [6] model. By altering the ventricular volumes, 11 different SVs (46 to 106 ml) were simulated. Five EIT belts with 16 electrodes were placed on equidistantly spaced transversal planes at the level of the heart. Besides, rotational and longitudinal electrode shifts were introduced for the belt located in the middle.

The cardiac conductivity change $\Delta\sigma_C$ and the calibrated EIT-based SV estimates SV_{EIT} were determined for all the simulated EIT images [3]. They were compared to the reference values SV_{Ref} by means of correlation and absolute or relative errors.

RESULTS For all ordinary belt placements, a strong correlation ($R>0.99$) between $\Delta\sigma_C$ and SV_{Ref} and low errors between SV_{Ref} and SV_{EIT} (<2.6 ml) were observed. The errors caused by belt shifts are listed in the table below.

CONCLUSION While ordinary belt placements show a good performance, our simulations reveal that belt shifts can induce significant errors, which severely impair the estimation of absolute SV values. These findings call into question the intra-subject repeatability and the inter-subject comparability of SV values obtained with the current setup. Future work should concentrate on finding an improved setup less sensitive to electrode displacements.

REFERENCES

1. Critchley LAH (2013). *InTech.*
2. Pikkemaat R, et al. (2014). *Anesth Analg,* 119(1).
3. Proença M, et al. (2015). *Physiol Meas*, 36(6).
4. Braun F, et al. (2015). *Physiol Meas*, 36(6).
5. Braun F, et al. (2015). In *EIT2015.*
6. Proença M, et al. (2016). *IEEE T BIO-MED ENG* (submitted).

	Shift Direction									
	Down		Up		Left			Right		
Shift (cm)	1.8	3.5	1.8	3.5	1.3	2.7	4.0	1.3	2.7	4.0
Abs. Error (ml)	7±2	12±4	-10±5	-21±10	4±4	11±10	20±16	-1±3	1±5	5±8
Rel. Error (%)	10±4	17±5	-14±7	-30±13	6±6	16±14	28±23	-1±5	2±7	7±11

Abstract Id: 182
Topic: *Electrical impedance spectroscopy*

RESEARCH ON HEAT AND COLD OF RESISTANCE BY EIS IN ROSE

Ruihang CUI[1], Shaoran FAN[1], Meiling JIAO[2], Yu MENG[3], Gang ZHANG[*4]

[1]College of Horticulture, Agricultural University of Hebei, Baoding , Hebei, [2]College of Horticulture, Agricultural University of Hebei, Baoding , Hebei, [3]College of Landscape and Travel, Agricultural University of Hebei, Baoding , Hebei, [4]College of Horticulture, Agricultural University of Hebei, Baoding, Hebei, China

The temperature is maximum restraining factor for planting roses in northern China. Therefore, the cold resistance and heat resistance are very important to study in roses. The one-year-old stems in 2-years-old grandiflora roses 'MagiaNera' were used to determine the heat resistance from April to August 2014 and the cold resistance from September 2014 to the next January of 2015 by means of the methods of electrolyte leakage (EL) and electrical impedance spectroscopy (EIS). And the changes of EIS parameters in high temperature and low temperature stresses were studied in detail. Results showed that, the spectra of different periods were all single arc, during the heat stress study period, the spectrum had a slight expansion trend, and in the late cold acclimation the spectrum enlarged substantially. The changes of some of the EIS parameters and heating as well as freezing temperatures could be well fitted by Logistic equation, and there was no obvious difference with the results of EL method. The mathematical models to estimate the semi-lethal temperature of the sample with EIS parameters were obtained. The semi-lethal temperature under high temperatures stress could be estimated by specific resistance *r*, with the regression equation $y = -0.5529x^2 + 9.4672x + 11.813$ (R^2=0.72 , *r*=0.85), and the best parameter for freezing temperatures stress was distribution coefficient of relaxation time*y*, with the regression equation $y = -126.67x^2 + 190.23x - 79.364$ (R^2=0.94 , *r*=0.97). The semi-lethal temperature range of the 'MagiaNera' was -15.92°C~47.31°C.

Abstract Id: 183
Topic: *Electrodes*

IMPEDIMETRIC SENSING OF MICROBIAL GROWTH IN DROPLETS

Brian P. Cahill*[1], Karippai Nobu[1], Stefan Wiedemeier[1], Yingjia Li[1], Andreas Barthel[1], Thomas Nacke[1], Gunter Gastrock[1]

[1]Institut für Bioprozess- und Analysenmesstechnik, Heilbad Heiligenstadt, Germany

INTRODUCTION When bacteria grow, non-polar molecules are metabolized to ions and acids and the medium conductivity increases. Sensing the medium conductivity allows the bacterial growth to be measured [1]. Cahill et al. presented the contactless conductivity measurement of microfluidic droplets [2].

OBJECTIVES This work describes how the contactless conductivity measurement of droplets can facilitate the high-throughput detection of microbial growth using impedance spectroscopy. This enables a low-cost high-throughput microfluidic device for applications in biotechnology.

METHODS *Escherichia Coli* (*E. Coli*) K12 was chosen for these experiments because of its rapid doubling time. During preliminary culture the *E. Coli* was grown overnight to its maximum growth. This cultured bacterium is separated from the medium using centrifugation and washed twice using LB medium and suspended in the culture medium of interest. A segmented flow of culture medium and perfluorinated oil, Novec 7500, was generated. The droplets had a length of circa 3 mm in 0.5 mm Teflon tubing. A polycarbonate chip with 0.5 mm channel diameter incorporating two metal electrodes allowed impedimetric sensing of droplets. The electrodes and chip were coated with a thin hydrophobic layer to prevent wetting problems due to biofoulling. Impedance spectra were acquired using a high-speed USB oscilloscope and amplifier in the frequency range from 10 kHz to 10 MHz in less than 20 ms per spectrum.

RESULTS By pumping droplets through the impedance chip at half an hour intervals it was possible to follow the dependence of the metabolic process taking place in the droplet on medium composition, temperature and initial bacterial concentration. The bacterial growth kinetics followed a sigmoid curve: (i) initially a lag phase is observed, (ii) rapid bacterial growth is observed (exponential phase) and (iii) the stationary phase is reached and the signal change reduces considerably.

CONCLUSION The sensor enables the impedimetric analysis of bacterial growth kinetics in droplet-based bioreactors. Reduced droplet volumes lead to more rapid bacterial culture of droplets that initially contain a single or a few bacteria. This sensor opens up electrical sensing for high-throughput toxicity testing.

IMAGE

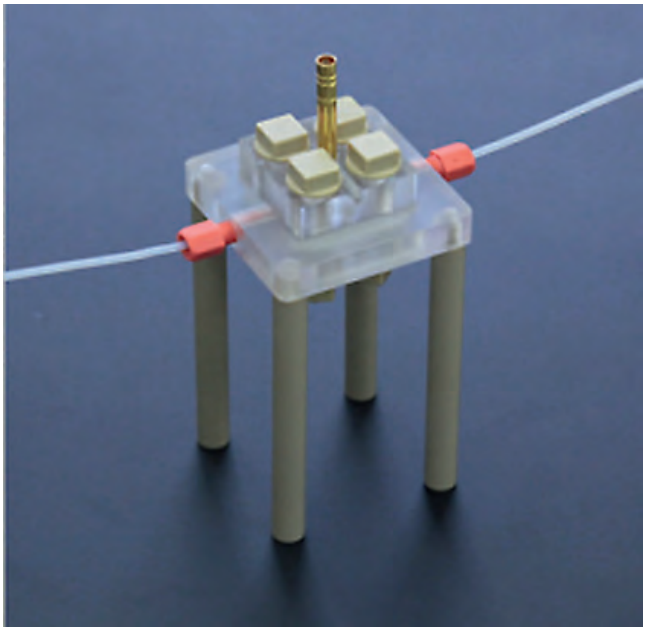

REFERENCES

1. T. Nacke, A. Barthel, M. Meister, B.P. Cahill, 2013, Chemie Ingenieur Technik 85 179–185.
2. B.P. Cahill, R. Land, T. Nacke, M. Min, D. Beckmann, 2011, Sensors and Actuators B: Chemical 159, 286–293.

Abstract Id: 184
Topic: *Clinical applications*

TRACING OF LEFT VENTRICULAR DP/DT USING ICG AND BP SIGNALS

Vladimir Ermishkin[*1], Elena Lukoshkova[1], Vladimir Lakomkin[1], Alexander Abramov[1], Olga Tarasova[2,3], Gregory Kheimets[1], Alexander Pevzner[1], Anatoly Rogoza[1], Olga Vinogradova[2], Valeri Kapelko[1]

[1]Russian Cardiology Scientific & Production Complex, [2]Institute of Biomedical Problems of the Russian Academy of Sciences, [3]M.V. Lomonosov Moscow State University, Moscow, Russian Federation

INTRODUCTION Impedance cardiogram (ICG) provides a suitable method for noninvasive monitoring of changes in left ventricular (LV) contractility. Pre-ejection period (PEP) can be a valuable index to follow up the sympathetic responses during functional tests. However, PEP is sensitive not only to neurogenic influences but also to mechanical factors, such as ventricular filling or diastolic blood pressure (DBP).
A more perfect index, the mean rate of pressure rise (RPR), can be evaluated as RPR = (DBP-P_0)/(PEP-T), where P_0 and T are pressure and time corrections to approximate the pressure rise in LV during its isovolumic contraction more closely. In several clinical studies, RPR was offered as a noninvasive analog of invasive index $dP/dt|_{max}$ and used for cardiologic risk stratification, while no reference was found about tracing of individual RPR responses during tests.

OBJECTIVES In rats, we checked a consistency between RPR estimates and the direct LV pressure measurements of $dP/dt|_{max}$. Our other aim was to calculate the trends of RPR changes in syncope patients during functional tests and compare them to the concurrent responses of PEP or other indices.

METHODS In rats under urethane anesthesia, ECG and thoracic ICG, LV pressure with a Millar catheter gauge and arterial BP with a solution-filled catheter were synchronously recorded. Responses of RPR and LV $dP/dt|_{max}$ to some cardiotropic or vasoactive drug infusions were studied. In studies with syncope patients, ECG, ICG and continuous BP were recorded with a computerized complex Task Force Monitor (TFM, Graz, Austria). RPR was calculated from the exported beat-by-beat data of PEP_R (from the peak R of ECG to a B-point in dZ/dt) and DBP, taking P_0 = 5 mm Hg and T=0.

RESULTS In rats, RPR (with T and P_0 matched individually) closely correlated with LV $dP/dt|_{max}$ measured directly in LV, r = (0.92-0.99). In patients, RPR calculated from the TFM data demonstrated more reasonable changes compared to PEP during the tests in which DBP markedly increased (handgrip) or decreased (active standing, presyncope phase of tilt, Valsalva maneuver).

CONCLUSION RPR most closely reflects the shifts in the invasive index $dP/dt|_{max}$ and surpasses PEP and other ICG-based parameters in evaluation of changes in LV contractility. It is especially useful for noninvasive tracing of contractility responses during functional testing of patients with impaired autonomic regulation.

Abstract Id: 185
Topic: *Bioimpedance*

MONITORING OF STRATUM CORNEUM MOISTURE BY SKIN ADMITTANCE

Toshimasa Kusuhara*[1], Takao Nakamura[1], Kiyoko Shirai[1], Yoshitake Yamamoto[1]

[1]Graduate School of Health Sciences, Okayama University, Okayama, Japan

INTRODUCTION We can obtain a lot of information related to health from the skin on outermost layer of the human body. The stratum corneum moisture is one of these information. If we lost the stratum corneum moisture, skin disappeared original suppleness, and pathological changes occur. Evaluating methods of the stratum corneum moisture are very important.

OBJECTIVES In this study, we confirm availability of the admittance method in monitoring temporal changes of moisturized effect. We measured the stratum corneum moisture of forearm's skin by the admittance method (AM) and the corneometer (CM). And the skin was protected by 2 types protective solution to occur moisturized effect.

METHODS AM was measured by LCR meter (4284A, Agilent) with a concentric circular electrode in 100 kHz. The stratum corneum moisture was measured by CM (CM825, Courage +Khazaka). [Experiment 1] Subjects were 4 healthy persons. Their forearms were measured 6 times every 1 hour. [Experiment 2] It was the same as in Experiment 1, but the skin was coated by a moisturizer and a sunscreen.

RESULTS [Experiment 1] Coefficient of variation (CV) of AM was 0.657, CV of CM was 0.257. However, since a range of values of AM was also greater than CM, we have performed logarithmic compression to be the same as CM. As a result, CV of AM became 0.250 about the same as CM. [Experiment 2] We performed the aforementioned logarithmic compression on the obtained AM. And time series data of AM and CM were normalized by the each initial value. In a moisturizer, AM increased when the skin was coated. However, this moisturizing effect was gradually reduced. CM did not show the clear moisturizing effects like AM. In a sunscreen, AM increased when the skin was coated, and this moisturizing effect was continued. CM did not show the clear moisturizing effects like AM.

The reason of these differences between AM and CM was a difference of the measuring region. AM detected the stratum corneum moisture of a surface layer. on the other hand, CM detected the stratum corneum moisture of a deep layer.

CONCLUSION The skin admittance could detect the stratum corneum moisture of a surface layer. Therefore, AM is more useful than CM in monitoring the temporal change of the moisturizing effect by coating.

Abstract Id: 186
Topic: *Clinical applications*

PARALLEL LEADING OF URETERAL VOLTAIC AND OHMIC SIGNALS

Irina Mudraya*[1], Sergey Revenko[2], Vladimir Kirpatovsky[3], Andrey Nesterov[2], Irina Kabanova[3]

[1]experimental, Institute of Urology, [2]Institute of Experimental Cardiology, [3]Insitute of Urology, Moscow, Russian Federation

INTRODUCTION Excitation-contraction coupling in ureter is an important indicator of functional integrity of the urinary system.

OBJECTIVES Acute assessment of ureteral electrical and mechanical activity in animals by simultaneous recording of voltaic and impedance (ohmic) signals *in situ*.

METHODS In experiments on narcotized rabbits, the ureter was isolated and electrically insulated by a Parafilm strip. Two *ring*-shaped ureteral electrodes placed at the distance of 0.4 cm were connected to a rheograph delivering the probe current of 2 mA at 100 kHz and to a biopotential amplifier. The subcutaneous reference electrode was placed in a hindleg. The voltaic and ohmic signals were digitized at 160 Hz and fed to a PC. All devices and software were from Biola (Moscow).

RESULTS The ureteral voltaic and ohmic impulses (the latter viewed as indirect indicator of mechanical activity) were recorded at rest and during dilation of ureter with infused physiological saline. At rest, the amplitudes of these signals were 150–250 μV and 30–40 Ohm with the baseline impedance of 350–450 Ohm. The repetition rate of virtually coinciding voltaic and ohmic signals ranged 0.05–0.06 Hz. Dilation of ureter increased the repetition rates of both signals to 0.08 Hz and disturbed their synchronicity. At this, the amplitude of ohmic signals decreased by about 10-fold, while there was only a decreasing trend (by 7%) in the amplitude of voltaic signals. In overdilated ureter, only arrhythmic voltaic pulses were observed without ohmic signals.

CONCLUSIONS The advanced method yields parallel data on electrical and mechanical activity of the ureter. Correlation of voltaic and ohmic signals can be used to assess the strength of excitation-contraction coupling in ureter. This method can assess the disturbances in contractile and electrical performance of the ureter. Similar approaches can be tested to analyze the work of other smooth muscle organs.

Abstract Id: 187
Topic: *Signal processing*

EVALUATION OF VARIOUS WAVELETS FOR ICG SIGNALS DENOISING

Souhir Chabchoub[*1], Sofienne Mansouri[1], Ridha Ben Salah[2]

[1]University of Tunis El-Manar, ISTMT, Laboratory of Biophysics and Medical Technologies, Tunis, Tunisia, [2]Prince Sattam Bin Abdelaziz University, KSA, Saudi Arabia

INTRODUCTION The determination of the hemodynamic parameters from the Impedance cardiography signal (ICG) signal, like the stroke volume and the cardiac output, requires the detection of the characteristic points. However, in practice, the ICG signal is generally affected by several kinds of artifacts such as the respiration and motion artifacts. These artifacts may cause errors in the detection of the characteristic points and the computation of hemodynamic parameters. Thus, the analysis of the ICG signal became inaccurate and more difficult.

OBJECTIVE In this paper, we proposed a wavelet denoising method to eliminate the artifact from ICG signal.

METHODS First, a total of 30 subjects were enrolled in this study. There were 15 males and 15 females aged between 21 and 50 years. Second, to denoise the ICG signal, a comparison is carried out between different discrete wavelet transform functions (DWT) by varying their order. The Daubechies (db), Symlet (Sym) and Coiflet (Coif) wavelet functions are tested and evaluated. Thus, the suitable wavelet method is selected. The performance of the best wavelet method is evaluated by the signal to noise ratio (SNR) and the root mean square error (RMSE).

RESULTS The results show that the Daubechies wavelet function (db8) has the highest SNRo and the lowest RMSE value regardless of the level of SNRi input (**Image**). Thus, the performance of Daubechies wavelet eighth-order (db8) is better compared to other wavelet functions.

CONCLUSION We concluded that the Daubechies wavelet function (db8) is the most efficient denoising method and it can filter the ICG signal with the minimum degradation of the signal.

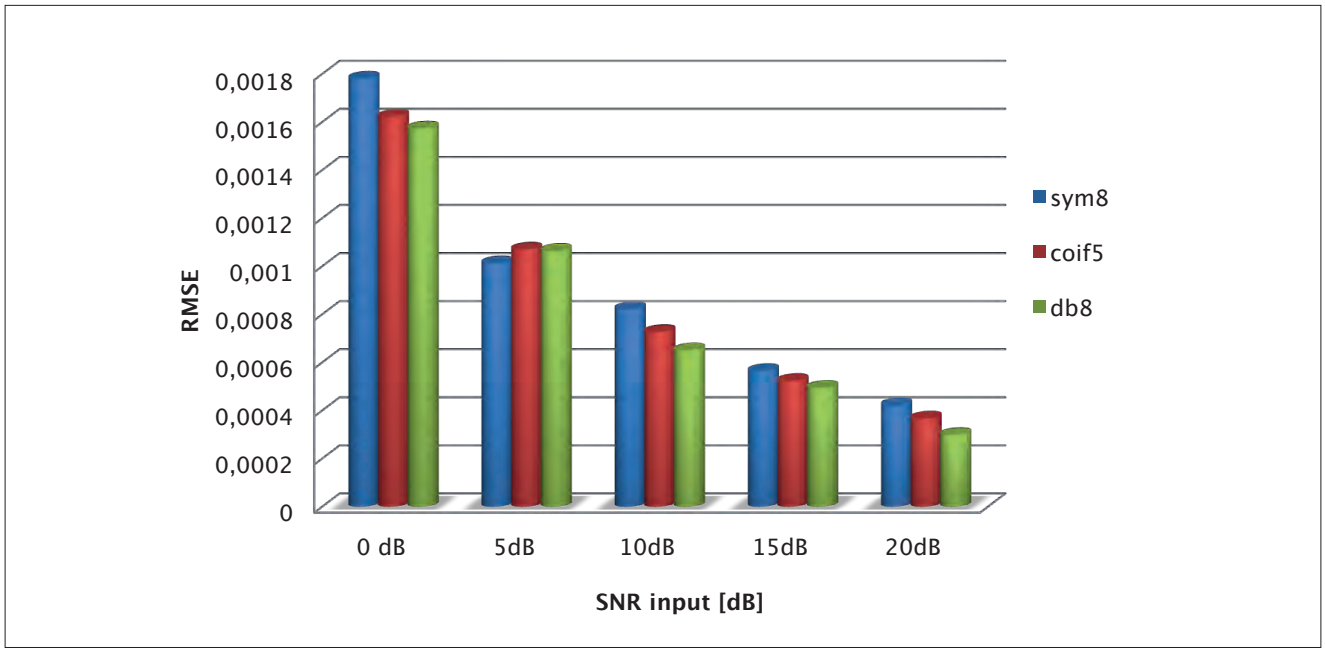

Abstract Id: 188
Topic: *Clinical applications*

POST-STENTING ARTERIAL HEALING: AN IN VITRO IMPEDANCE STUDY

Ian Holland[*1], Christopher McCormick[1], Patricia Connolly[1]

[1]Department of Biomedical Engineering, University of Strathclyde, Glasgow, United Kingdom

INTRODUCTION The permanent implantation of a stent into a coronary artery is a common method for ameliorating vessel narrowing arising from atherosclerosis. Following the procedure, preferable arterial wall healing is characterised by regrowth of an Endothelial Cell (EC) monolayer over the exposed stent surface, reducing the risk of thrombosis. However restenosis, predominantly comprising the proliferation of Smooth Muscle Cells (SMCs) can cause vessel narrowing. Previous research has suggested that the stent itself could be used as an electrode to analyse the critical post stenting recovery phase, informing clinicians without the need for invasive imaging [1].

OBJECTIVES The study had three aims. Firstly to develop an in vitro platform technology that can provide non-invasive near real time cell characterisation on stent comparable populations. Secondly to investigate impedance changes in two models of clinically relevant scenarios: re-endothelialisation and restenosis. Finally the potential for in vivo applications was assessed.

METHODS Tissue culture dish surfaces were modified to include platinum black coated gold electrodes. Primary porcine ECs and SMCs were seeded onto electrodes and grown to confluence whilst a bespoke automated system performed impedance spectroscopy measurements (1 kHz to 1 MHz) at 130 minute intervals. Light and time-lapse microscopy was used to assess cell coverage. After incubation cells were fixed and imaged using fluorescence microscopy.

RESULTS The system developed provided impedance data alongside time lapse imaging. Rises in total impedance correlated with cell coverage observed through microscopy. Analysis of real impedance data revealed distinct profiles for ECs and SMCs. See image of real impedance profiles normalised from initial seeding time, profiles representative of 5 EC (A) and 3 SMC (B) experiments. A post confluence decline in real impedance was seen at lower frequencies for ECs, potentially due to cell junction formation. End point staining affirmed cell type and attainment of confluency.

CONCLUSION The study demonstrated that confluent populations of SMCs and ECs give rise to distinct impedance signatures demonstrating the feasibility for monitoring restenosis after coronary stenting. Further work will aim to investigate a novel co-culture model comprising both cell types.

IMAGE

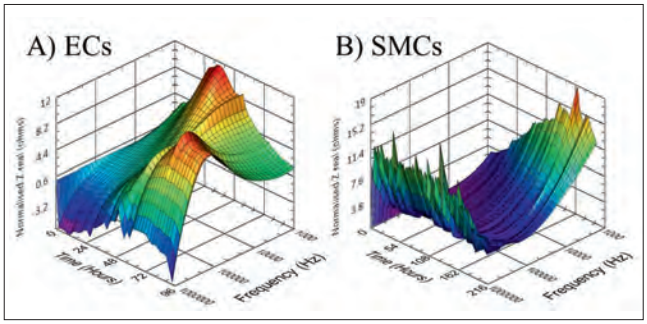

REFERENCES

1. L. Shedden, The Intelligent Stent, EngD. thesis, University of Strathclyde, Dept of Bioengineering, Glasgow, 2008.

Abstract Id: 189
Topic: *Bioimpedance*

FLOATING ELECTRODE BIOIMPEDANCE MEASUREMENT TECHNIQUE

Dejan Križaj[*1], Robert Brajkovič[1], Pedro Bertemes-Filho[2], Fabricio Noveletto[3]

[1]Faculty of Electrical Engineering, University of Ljubljana, Ljubljana, Slovenia, [2]Electrical Engineering, [3]Elecrical Engineering, Universidade do Estado de Santa Catarina, Joinville, Brazil

INTRODUCTION Bioimpedance has been used for diagnosis, monitoring, tissue characterization and body composition over the last 40 years. Of particular interest of usage of the bioimpedance method is determination of electrical properties of a specific area of the analyzed structure. For this purpose we investigate a method of floating electrode measurement, where the conductive floating electrode is placed on top of the structure above the Object Of Interest (OOI) with different conductivity than the surrounding material. The floating electrode is not in any physical contact with the circuitry but influences the current flow density. Its influence can be measured and related to the underlying electrical properties of the OOI.

OBJECTIVE To investigate the floating electrode measuring technique using bioimpedance measurements. It also investigates the sensitivity of the technique using measured data.

METHOD It was a modeling by finite element method using COMSOL. The volume is composed of two materials with different specific resistivity. The four electrode technique is used. The current density distribution is calculated and displayed with and without the object of interest placed underneath the floating electrode. A phantom was made by a plastic reservoir of 20x13x40 cm filled with saline solution. Five EMG electrodes of 10 mm diameter without gel were placed 30 mm apart on the bottom of the reservoir. The OOI was a rubber ball of 25 mm diameter placed at three different depths (0, 10 and 20 cm). Impedance was measured in the frequency of 1 to 100 kHz and then sensitivity upon frequency is calculated.

RESULTS Simulations showed that when the floating conductive electrode is placed on top of the structure above the OOI, it attains a certain potential and influences the current distribution inside the structure. As expected larger differences are achieved in case the specific conductivity of the circular object is smaller than the surroundings. The measurements showed a decrease in impedance when the floating electrode is used, especially at higher frequencies. On the other hand, the sensitivity is higher when using the floating electrode at higher frequencies (< 100 kHz), specially close to the electrode.

CONCLUSION Performed simulations and measurements indicate that bioimpedance measurement method with a floating conductive electrode might serve as a valuable tool for determination of local influences on total measured impedance.

Abstract Id: 191
Topic: *Embedded systems*

AN IMPLANTABLE BIOIMPEDANCE SPECTROMETER

Saul Rodriguez* [1], Stig Ollmar[2], Ana Rusu[1]

[1]KTH Royal Institute of Technology, [2]Karolinska Institute, Stockholm, Sweden

INTRODUCTION Measuring bioimpedance of internal organs is a challenging task that poses many technical problems. Non-invasive methods, such as measurements on the skin, are plagued with artifacts that make enormously difficult to correctly characterize internal tissues. Furthermore, a rigorous electrical characterization of internal organs tissues under different physiological conditions needs the analysis of complex impedances at many frequency points over several decades. Accordingly, there is a need of a miniature bioimpedance sensor suitable for implantation.

OBJECTIVES To meet this need, this research targets an implantable bioimpedance sensor which performs 4-terminal impedance spectroscopy of animal and human living tissues from 2 kHz to 2 MHz (11 points logarithmically spaced). The implantable device has the shape of a coin of approximately 13 mm diameter (Figure), and it is powered by an external reader. Therefore, it does not require batteries to operate, so it can in principle be used indefinitely. The reader is connected via Bluetooth to an Android device which shows the measured impedances.

METHODS The main challenge in this research is to fully integrate a 4-terminal impedance sensor, energy harvester, communication circuits, digital controller, and electrodes inside a biocompatible package. An Application Specific Integrated Circuit (ASIC) which includes most of the required electronics was designed and fabricated (Figure). The active area of the chip occupies 1.22 mm x 1.2 mm and consumes only 165 uA from a 1.8 V power supply, which makes it perfectly suitable for implantable applications.

RESULTS The ASIC has been mounted on a printed-circuit-board (PCB) prototype and connected to 4-terminal gold electrodes, a coil inductor, and an 8-bit PIC microcontroller. This prototype has been validated by performing electrical characterization, electrochemical tests (measuring impedance of saline solution), and ex-vivo tests.

CONCLUSIONS A batteryless bioimpedance ASIC for implantable spectroscopy has been implemented and successfully tested on freshly excised organs of sheep. The on-going efforts focus on the implementation of a fully integrated spectrometer for in-vivo testing.

IMAGE

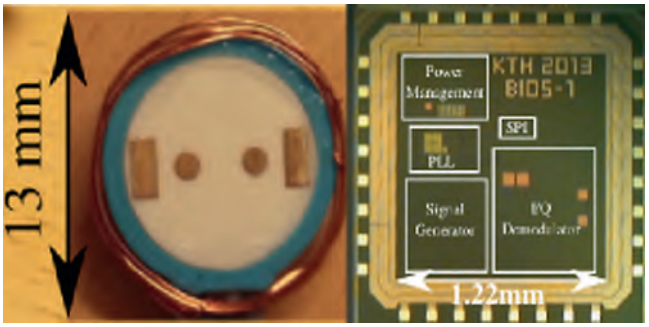

Abstract Id: 192
Topic: *Electrical impedance spectroscopy*

MICROFLUIDIC BASED IMPEDANCE ANALYSIS OF STORED WHOLE BLOOD

Osman Melih Can[*1], Fatma Gülden Şimşek[1], Mehmet Yumak[1], Yekta Ülgen[1]

[1]Institute of Biomedical Engineering, Bogazici University, Istanbul, Turkey

INTRODUCTION Red Blood Cells (RBCs) undergo chemical and morphological changes called storage lesions during storage for transfusion purposes. Especially, erythrocytes lose their flexible biconcave shapes and swell to form stiff spheroechniocytes. Measuring quality of stored blood is highly interested in transfusion medicine recently. Blood is electrically anisotropic because of the influence of the orientation of the erythrocytes. There are two well defined states of orientation: random and parallel orientation. Random orientation is attained in stationary condition; parallel orientation in flowing [1]. Therefore, it is hypothesized that impedimetric differences of stored and normal blood under various flow rates in a microfluidic channel will show us the levels of chemical and morphological changes of the stored blood.

OBJECTIVES The aim of the study is to use microfluidic system to investigate storage lesions of red blood cells by measuring the Cole Cole parameters of RBC suspension with the change of flow rate. Main goal of this study is to present an alternative microfluidic based technique for measuring quality of the stored blood in quality control laboratories in blood banks.

METHODS 12 RBC concentrates were obtained from Turkish Red Crescent North Marmara Regional Blood Bank in Istanbul. On the first, 42nd and 70th days of the storage 5 ml of sample was drawn from blood bags. Collected RBC suspensions were analyzed in microfluidic system without further centrifugation. The microfluidic device consists of glass, which has two lithographically produced gold electrodes on, and polydimethylsilioxane (PDMS) covering the glass. SU-8 was used to create 100-micron channel for samples to flow. Flow rate of the RBC suspensions was controlled by syringe pump. Impedance values of the samples were measured at frequency range between 4 Hz to 1 MHz for three different flow rates. Cole Cole parameters were recorded for three different flow rates and storage durations.

RESULTS This paper presents the Cole Cole parameter changes of stored versus normal blood at different flow rates as an indicator for the level of storage lesions.

CONCLUSION Microfludics based electrical impedance spectroscopy can be a promising diagnostic tool in transfusion medicine for measuring quality of banked blood.

REFERENCES

1. Fujii M, K. Nakajima, K. Sakamoto, and H. Kanai. 1999. "Orientation and Deformation of Erythrocytes in Flowing Blood," Annals of New York Academy of Science, 873, 245–261.

Abstract Id: 194
Topic: *Electrical impedance tomography*

COMPUTATION OF EDDY CURRENTS INSIDE A HUMAN HEAD

Mingyang Lu*[1], Wuliang YIN[1], Anthony Peyton[1], Michael O'Toole*[1]

[1]School of Electrical and Electronic Engineering, The University of Manchester, Manchester, United Kingdom

INTRODUCTION A custom FEM solver based on edge-elements has been developed using the weakly coupling theory. This solver is more efficient than typical commercial solvers since it reduces the vector eddy current equation to a scalar one. Eddy current in bio tissues can be computed with this solver. An example for eddy currents distribution in a realistic human head is shown. With this solver, there is no need to mesh the excitation coil and the object only need to be meshed once.

OBJECTIVES An efficient finite element solver is developed, which can easily simulate the eddy currents induced by an excitation coil in any sectional views for normal and pathological conditions (such as internal and peripheral strokes), and the change in coil impedance due to the presence of the pathological conditions can also be obtained.

METHODS The FEM formulation is based on the Rayleigh-Ritz-Galerkin method. The head model is excited by a coil of 62.5 mm in radius with a current (1 A), positioned right on its top with a distance of 147mm to the head centre. A receiver coil is symmetric with the exciting coil about the head centre.

RESULTS Sectional views in x-axis, y-axis, as well as z-axis can be easily obtained for the distribution of eddy currents in all tissue types with various dielectric properties. The bio-impedance about the head with altering coils position can also be obtained.

CONCLUSION: simulation of realistic head eddy current is possible.

IMAGE

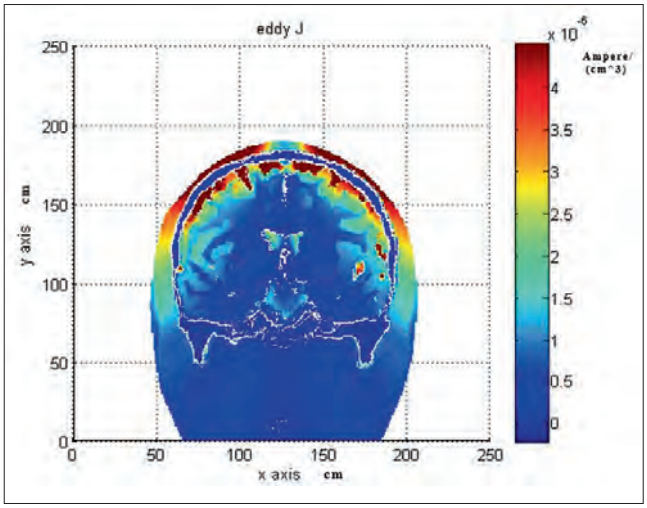

Abstract Id: 196
Topic: *Electrical impedance spectroscopy*

DISTINGUISHING BENIGN FROM CANCEROUS PROSTATE TISSUE

Aditya Mahara*[1], Shadab Khan[1], Ethan Murphy[1], Ryan Halter[1]

[1]Thayer School of Engineering, Dartmouth College, Hanover, United States

INTRODUCTION A 17-electrode intraoperative-capable probe and Dartmouth EIT system is used to collect ex-vivo prostate data from 18 patients that includes 104 benign probed measurements and 12 cancer measurements. Results show that there is statistical differences in resistance and reactance between benign and cancerous measurements at 6 discrete frequencies from 5 kHz-400 kHz.

METHODS A radially configured intraoperative 17-electrode microendoscopic probe was used to evaluate ex-vivo human prostate samples. The electrode distribution is such that a central 1mm diameter gold plated electrode is surrounded by two rings of eight 1mm electrodes radially spaced at 1.75mm and 3mm from the central electrode, respectively.[1] Impedance measurements are recorded at 6 discrete frequencies (5 kHz –400 kHz) using a Dartmouth EIT system.[2] Following a RALP procedure, the prostate is sectioned into 3–5 mm thick slices and impedance spectra are recorded. A pathologist provides the pathological state of each probed region. Regions of 100% cancer or 100% benign tissues were selected for analysis. Impedance data recorded from a 0.1 S/m saline solution is used to calibrate all ex-vivo impedance spectra to minimize channel-to-channel variations.

RESULTS Average resistance and reactance for 6 discrete frequencies were computed. Each average value is calculated using data from all patients and 8 tetrapolar impedances – done separately for the inner and outer rings. The difference in resistance and reactance for inner and outer rings were both statistically significant at a 5% significance level. As shown in Fig. 1- 1. Both inner and outer ring impedances are higher for cancerous tissue than they are for benign tissues for all 6 discrete frequencies; 2. As expected, impedance values decrease with increasing frequency; 3. The outside ring has lower impedance in general compared to the inner ring.

CONCLUSION The spectroscopic data obtained from 18 patients demonstrate statistically significant distinction between cancerous prostatic tissues and benign regions. Moving forward, ex vivo dataset will be explored further along with conducting an in vivo study. The ultimate goal will be to provide surgeons real-time information regarding the pathological state of the probed region.

IMAGE

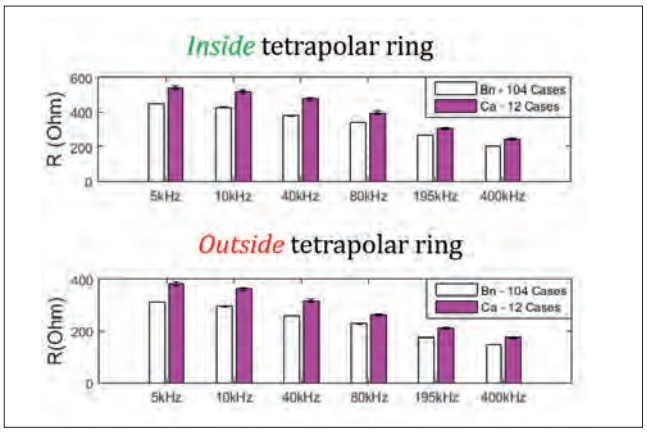

REFERENCES

1. Mahara A, et.al. *IEEE Trans. on Medical Imaging,* 2015.
2. Khan S, et.al. *IEEE Trans. on Medical Imaging,* 2015.

Abstract Id: 197
Topic: *Clinical applications*

A MULTI-ELECTRODE PROBE TO DETECT ANISOTROPY OF MUSCLES

Yohan Dassonville*[1], Christine Barthod[1], Michelle Passard[1], Marie-Valérie Moreno[2]

[1]Univ. Savoie Mont Blanc, SYMME, Annecy, [2]Bioparhom Scop, La Motte Servolex, France

INTRODUCTION Electrical anisotropy of human muscle with non-invasive impedance measurements has been highlighted by Epstein [1]. The use of such information may be very interesting either to quantify the evolution of diseases that affects the muscles like myopathy, or to follow the muscle regeneration of athletes following to muscle tear or contracture [2][3].

OBJECTIVES Usual impedance measurement is realized using disposable electrodes. However, the placement and the repositioning of these electrodes to measure several places take time. Moreover, diagnostic are often unreliable because of bad angular resolution and poor reproducibility. It is important to get all the features of evolution of the anisotropy reflecting a physiological change. This paper introduces a compact multi-electrode probe (Figure 1) in order to detect electrical anisotropy of muscles with several tetrapolar measurement modes. This probe will include impedance measurement module with wireless communication.

METHODS The measurement protocol is realized thanks to the use of multiplexers that allow to choose an electrode pair in the outer ring for current injection (frequency range: 5 to 1000 kHz) and another one in the inner ring for pickup measurement and to realize the perpendicular test without changing the probe position. The choice of the electrodes has been done to ensure a good electrical contact with the skin.

RESULTS In order to validate our probe, dry measurements were carried out on five healthy subjects on the right biceps and were repeated five times per person. Ten frequencies, three currents and four angles were implemented in a first approach so as to validate the probe. The electrical anisotropy of the muscle is successfully measured with a standard deviation intra person lower than ± 2 W on R and X. Thereafter the number of subjects will be expanded to twenty.

CONCLUSION The integration of different parts in a single probe provides portability and better handling. A finer angular resolution will allow more accurate measurement of anisotropy.

IMAGE

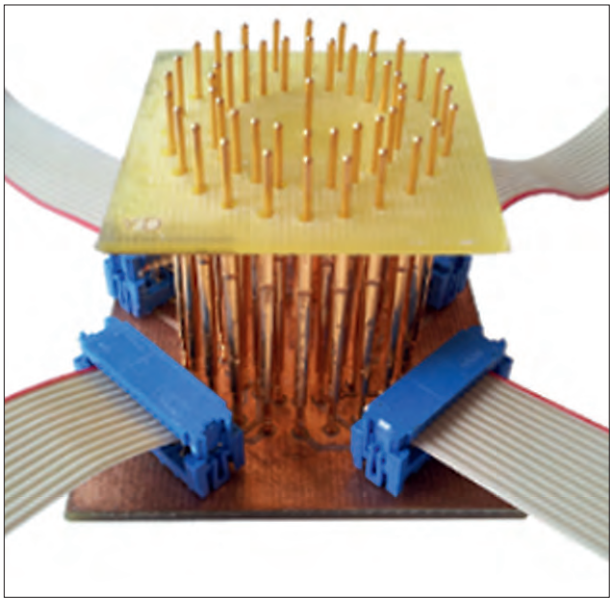

REFERENCES

1. B. R. Epstein et al., "Anisotropy in the dielectrc properties of skeletal muscle," *Med. Biol. Eng. Comput.*, vol. 21, no. January, pp. 51–55, 1983.
2. S. B. Rutkove et al., "Localized bioimpedance analysis in the evaluation of neuromuscular disease," *Muscle Nerve*, vol. 25, no. 3, pp. 390–397, 2002.
3. L. Nescolarde, et al., "Localized bioimpedance to assess muscle injury.," *Physiol. Meas.*, vol. 34, pp. 237–45, 2013.

Abstract Id: 198
Topic: *Impedimetric biosensors*

IMPEDIMETRIC ANALYSIS OF E.COLI BIOFILMS ON MEAS

Erkuden Goikoetxea[*1,2], Ami De Weert[1], Jos Vanderleyden[1], Hans Steenackers[1], Dries Braeken[2]

[1]Centre of Microbial and Plant Genetics, Department of Microbial and Molecular Systems, Katholieke Universiteit Leuven, Leuven, [2]Life Science Technologies, imec, Heverlee, Belgium

INTRODUCTION Bacteria embed themselves in a hydrated extracellular polymeric substance (EPS), forming a biofilm layer which makes them up to one thousand times more tolerant to disinfection. There is little information available about the biophysical properties of biofilms, and their relation to e.g. antibiotic resistance, 3D structure, etc. Next to conventional biomass staining assays, CFU counts and colony morphology studies, impedimetric sensors are an emerging technology to monitor biofilms. However, only information on the biofilm growth cycle has been reported, and not on the biofilm structure itself.

OBJECTIVES By comparing wild type (wt) and ΔcsgD mutant of E. *Coli* TG1, we examined how a specific gene coding for EPS production influences the biofilm structure.

METHODS Impedance measurements were performed with Autolab on a commercial MEA. The amplitude of the AC input voltage was 10 mV_{p-p} and the measured frequencies ranged from 1 to 100 kHz. Confocal laser scanning microscopy was used to image the biofilms. *E.coli* cells expressed GFP and ConA was used to stain the EPS. The biofilms were formed from an initial inoculum of $3x10^8$cells/ml in TSB 1/20 for 24 h.

RESULTS From the |Z| plot (Figure 1A) we observed that both biofilms increase the impedance as they block the current path. Bare electrodes are modeled by an RC series circuit where the cutoff frequency, f_c, $(1/2\prod RC)$ is approximately 400 Hz. Therefore, the effect of both biofilms can be interpreted as a shift of the f_c towards lower frequencies due to their high resistance. For the wt, f_c was found to be at 20 Hz and for the mutant 10 Hz. Interestingly, the mutant displays higher resistance than the wt. Less current could thus flow through the mutant biofilm, which resulted in dominating capacitive behavior in both |Z| and phase plots. On the one hand, the EPS in the wt biofilm is highly hydrated; water and ions are by far the largest components, which reside in pores and nutrient transport channels. On the other hand, the mutant lacks these structures, through which current could pass easier.

CONCLUSION We present an impedance assay for bacterial biofilm detection based on MEAs. We detected mature biofilm growth through a shifted cutoff frequency. Moreover we could differentiate between *E.coli* TG1 wt and its ΔcsgD mutant, which lacks the typical structure of biofilms.

IMAGE

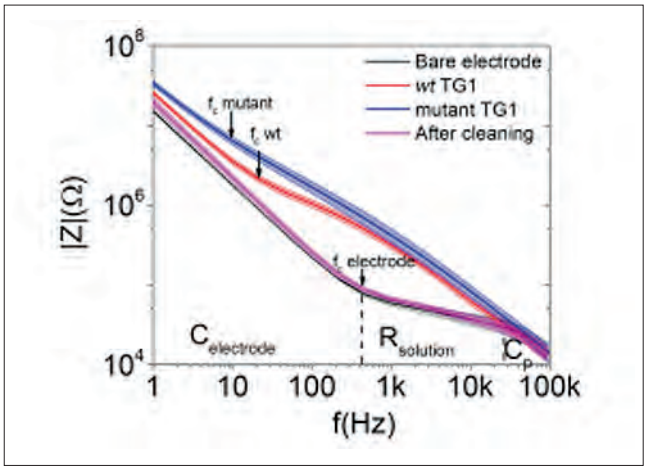

Abstract Id: 199
Topic: *Clinical applications*

TOWARDS THORACIC TRAUMA DETECTION USING BIOIMPEDANCE

Ruben Buendia*[1], Hans Granhed[2], Bengt-Arne Sjöqvist [1],
Per Örtenwall[2], Stefan Candefjord[1], Eva-Corina Caragounis[2]

[1]Signals and Systems, Chalmers University of Technology,
[2]Trauma ward, Sahlgrenska University Hospital, Gothenburg, Sweden

INTRODUCTION Thoracic trauma is the most common type of injury as consequence of motor vehicle vcashes. Bioimpedance measurements offer a novel opportunity to non-invasively monitor trauma healing as well as detecting hidden trauma. Bioimpedance is a non-invasive, harmless, non-expensive, rapid and easy to use technology; therefore it is ideal for the pre-hospital environment. Resistance (R) is inversely proportional to extracellular fluid and Reactance (X) indicate cell membrane mass and function. Furthermore healthy membranes cause a phase difference in the transit of voltage and current; thus, the greater the Phase angle (PA), the healthier the membranes, and decreases in PA reflect impaired membrane function [1]. This way, thoracic trauma patients are expected to present decreased R as damage tissue lets intracellular fluid escaping from the cells. X and PA are as well expected to decrease due to cell membranes damage.

OBJECTIVE Testing the feasibility of bioimpedance for thoracic trauma detection.

METHODS Single frequency EBI measurements at 50 kHz were performed using Akern BIA 101 and Akern electrodes. Electrodes were symmetrically placed on both sides of the thorax following configuration of the *Cheetah Nicom* device. Thoracic EBI measurements values are greatly affected by size and shape of the thorax, also by small differences in electrodes position. For that reason the ratios between right and left sides were considered. This greatly minimize individual differences and measurements inaccuracies. Thus, R, X and PA ratios between right and left sides were considered. By the time being 12 healthy controls and 5 thoracic trauma patients were measured by the same researcher.

RESULTS Healthy controls values were R=1.01±0.07, X=1.05±0.08 and 1.03±0.04. Patients' results and characteristics are in the following table; all patients had broken ribs.

Patients	1	2	3	4	5
R	0.93	0.83	0.99	0.70	1.11
X	1.04	0.78	1.15	0.78	1.08
PA	1.11	0.94	1.15	1.14	0.95
Sex	M	M	M	W	M
Side of injury	left	right	left	right	Right
Injury Severity Score	9	4	9	9	10
Pneumothorax	N	N	Y	N	N
Hemothorax	Y	N	N	Y	Y

As expected, PA was the most stable parameter. Most values of patients' measurements were outside of one mean±std of the controls distribution, -all in case of the PA. PA ratio of all patients differ as expected from healthy controls except for patient 4.

CONCLUSION EBI might have the potential to detect thoracic trauma. However more subjects are needed to support this hypothesis.

REFERENCES

1. HC Lukaski EJCN 2013 67, S2–S9.

Abstract Id: 201
Topic: *Electrical impedance spectroscopy*

SOME ERRORS DURING IMPEDANCE MEASUREMENT

Paul Annus[*1,2], Raul Land[3], Mart Min[1]

[1]Thomas Johann Seebeck Department of Electronics, Tallinn University of Technology, [2]Eliko,
[3]Thomas Johann Seebeck Department of Electronics, Tallinn University of Technology, Tallinn, Estonia

INTRODUCTION Concepts of resonance and impedance have been around for more than hundred years and are generally considered as well developed and mature. Nevertheless recent editorial of Journal of Electrical Bioimpedance (JEB) states "Impedance surprises", and does it quite rightfully though. Care must be exercised when measuring electrical bioimpedance as a very complex phenomenon, but even measurement of simplest structures, such as resistors, capacitors and coils might give "surprising" results. In order to examine electrical bioimpedance of the human head an experiment was conducted. Inductive coupling was chosen with a simple four turn coil around the head. Coil impedance spectrum was measured with Wayne Kerr 6500P precision impedance meter and strange behavior of the phase curve was observed at closer inspection. Instead of the phase jump from +90° to the -90° at resonant frequency, the phase rose near resonant frequency sharply to 180° and then jumped to -180°. The instrument was switched to show the real part of the impedance, and indeed it was negative. Many experiments were conducted thereafter, and similar behavior was often detected with different wirewound objects, with and without biological objects nearby.

OBJECTIVES Negative real part on the electrical impedance indicates energy source inside measurable object, which was out of the question. Coupling with some outside objects however seemed plausible. Two of them seemed possible: inductive and capacitive. Objective was to find reasonable explanation how such measurement results can appear.

METHODS Different coupling options were modelled, and resulting impedance curves from model were compared to real measurement results. Unfortunately the most tempting option was rejected at first, due to modelling errors. Different circuits were also analyzed in order to find closed form formula to explain the measurement results.

RESULTS It was confirmed that if capacitive coupling to the ground is introduced then computerized model, formulas, and measurement results coincide very well.

CONCLUSION Even when measuring impedance of the simplest possible structures it is possible to get highly erroneous results. In real measurement situations, when more complex objects, such as biological structures, are examined the results, even if not so obviously wrong as showing negative real part of the impedance, can and typically will suffer from unwanted side effects.

IMAGE

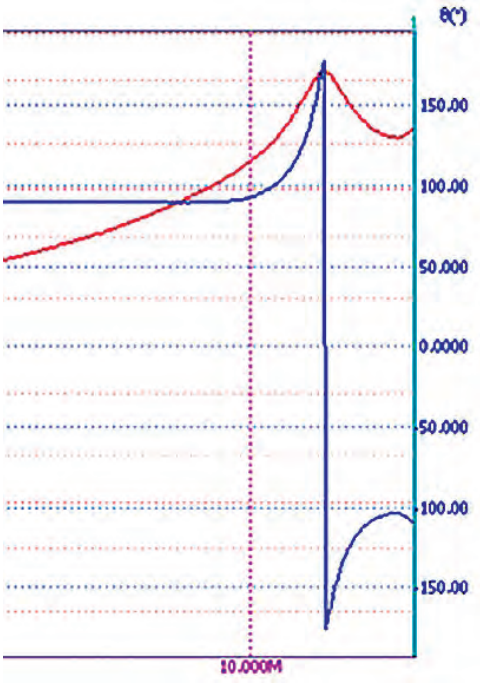

Abstract Id: 202
Topic: *Bioimpedance*

UNIVERSALITY OF LOW FREQUENCY CONDUCTANCE OF HUMAN HAIR

Ørjan Grøttem Martinsen[*1,2], Sisay Mebre Abie[1], Joakim Bergli[1], Yuri Galperin[1]

[1]Department of Physics, University of Oslo, [2]Department of Clinical and Biomedical Engineering, Oslo University Hospital, Oslo, Norway

INTRODUCTION Many disordered solids show a remarkable universality in the frequency dependence of the AC conductivity. This has been demonstrated for a range of different materials such as glasses, amorphous conductors, and electron conducting polymers. Typically, the curves showing the conductance as a function of frequency for different temperatures fall on a common master curve when conductance and frequency are scaled appropriately.

OBJECTIVE The objective of this study was to investigate the possible existence of scaling properties in the AC conductance of human hair by using electrical impedance spectroscopy measurements and scaling the measurement results.

METHODS The electrical impedance of bundles of hair was measured at 0.1 Hz to 1 MHz and 2 V rms, using a Solartron 1260/1294 impedance analyzer and a two-electrode system inside a CTS series C type climatic chamber. Temperatures from 10 to 80 degrees Celsius and humidities from 40 to 95 % were used. The curves showing the conductance as a function of frequency were normalized (each measured value divided by the DC conductance) and the frequency was normalized with regard to both DC conductance and temperature or relative humidity (multiplying with the temperature or dividing by the relative humidity).

RESULTS The impedance of the hair was found to vary with both temperature and relative humidity. Scaling the results with regard to temperature or relative humidity made the results fall into a single master curve, hence confirming the existence of universality in the low frequency conductance of human hair.

CONCLUSION Hairs show a clear sign of the existence of universality of AC conductance. The cause of this universality is still unclear.

Abstract Id: 203
Topic: *Electrical impedance spectroscopy*

DATA MINING FOR BIOLOGICAL TISSUE MONITORING

Mahdi Guermazi*[1], Nabil derbel[2], Olfa Kanoun[1]

[1]Chair for Measurement and Sensor Technology, Chemnitz University of Technology , Chemnitz, Germany,
[2]CEM Lab, National School of Engineers of Sfax (ENIS), Sfax, Tunisia

As basis for developing an in-vitro measurement method for monitoring the freshness of meat, an appropriate method for feature extraction was proposed .

There are different possibilities for selecting features which serve as basis for classification. The proposed method consist on the use model parameters together with characteristic points in the impedance spectrum as features for the classification procedure. The information's gated from the measured impedance for different beef muscles in different periods will be tested using the PCA method.

Before dealing with PCA computing, the inputs and test data of the three cases, model parameters (MP), characteristics points (CP) and model parameters + characteristics points (MP + CP) are defined. The test data have exactly the same dimension then the inputs data.

The first two components for the feature composed by model parameters, for the characteristic points and for the model parameters + characteristic points explain more than 90% of the variances. In order to verify which feature should we use for classification, a simple idea is used consisting on the principle of superposition of the test data in the corresponding region of inputs data after KNN calculation. The method of KNN (k-nearest neighbors algorithm) was used to give a complete two dimensional presentation presented in a geometrical plot of the data.

The result of the superposition of model parameters test data on the KNN partition, 1 erroneous output that corresponds to SM-B-F, the percent of accuracy is 91 %. The accuracy for the characteristic points is 66% with 4 erroneous outputs that corresponds to the muscles, SM-B-C, SM-B-F, SM-V-C and LD-V-F. For the feature composed by the characteristics points and model parameters we get 12 correct outputs that corresponds to 100% of accuracy. Feature extraction based on the use of model parameters show a good results but with adding the characteristic points we get the best results that will be used for the diagnosis of the meat and for the classification.

IMAGE:

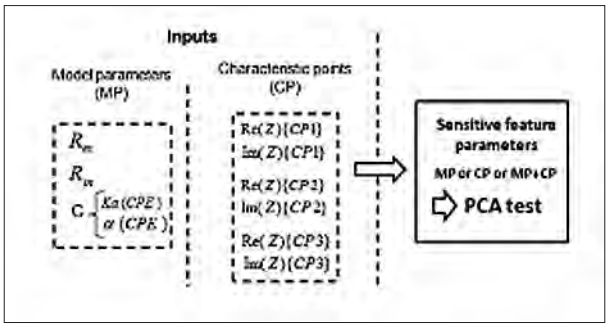

REFERENCES:

1. M. O'Farrell, E. Lewis, C. Flanagan, W. Lyons, N. Jackman: "Comparison of k-NN and neural network methods in the classification of spectra data from an optical fiber-based sensor system used for quality control in the food industry'', Sensors and Actuators B: Chemical, Vol. 111–112, pp. 354–362, 2005.

Abstract Id: 204
Topic: *Clinical applications*

SARCOPENIA AND PHASE ANGLE

Clara Helena Gonzalez-Correa[*1,2,3], Ana Milena López-Salazar[4,5], David Ricardo González-González[4,5]

[1]Basic Sciences, [2]Research Group on Bioelectrical Impedance, [3]Research Group on Nutrition, Metabolism and Food Safety, [4]Clinic, [5]Research group on Gerontology and Geriatrics, Universidad de caldas, Manizales, Colombia

INTRODUCTION Nowadays old adults live longer. Therefore, it is important to have tools to assist them correctly and perform interventions to prevent and diagnose chronic diseases that increase in parallel, such as sarcopenia. Sarcopenia has three main components: decreased skeletal muscle mass (SM), function and strength. Skeletal muscle mass is the main feature of sarcopenia definition in the elderly. Its loss has been associated to functional impairments that have impact on health costs both for the patient and the society. Although the most common technique to evaluate SM is dual x ray absorptiometry (DEXA), which performs appendicular lean mass for SM estimates, this tool is not always available because is costly and cumbersome. Bioelectrical impedance analysis is a more accessible alternative that has demonstrated good agreement with DEXA. Some authors found that phase angle; one of BIA parameters, is related to SM and muscle strength independently of age and other factors.

OBJECTIVE to evaluate the relationship between diagnoses of sarcopenia and phase angle in elderly patients.

METHODS A representative sample (n=210) of the population aged 65–75 years living in Manizales-Colombia, was evaluated. Clinical history as self report, handgrip strength, anthropometric measurements, skeletal muscle mass by bioelectrical impedance analysis and the Short Performance Physical Battery were performed.

RESULTS There were 124 women and 86 men, mean age 69,2 ± 3,1 years. General BMI was 25,3 ± 3,6 (kg/ m^2). The overall SPPB was 9,9 ± 1,7 points. The skeletal muscle mass index was 7,3 ± 0,9 for females and 9,9 ± 1,0 kg/ m^2 for males. The mean and SD of grip strength of dominant hand was 21.2 ± 5.3 kg/f in females and 35.6 ± 6.6 kg/f in males. The mean value of phase angle was 6,4 ± 0,7 for normal males (n= 77) and 6,6 ± 0,7 for sarcopenic males (n= 9) p = 0,71 (α= 0,05) . The mean value for normal females was 6,1±0,8 (n= 113) and 5,3± 0,5 for sarcopenic females (n= 11) p= 0,002. (α= 0,05)

CONCLUSION This study showed that phase angle may be an indirect measure of sarcopenia for females but not for males.

KEYWORDS Phase angle, sarcopenia, elderly population.

Abstract Id: 206
Topic: *Electrical impedance spectroscopy*

CLASSIFICATION ANALYSIS OF IMPEDANCE SPECTRA OF TREE ROOTS

Tapani Repo[*1], Anna Korhonen[1], Tarja Lehto[2], Raimo Silvennoinen[3]

[1]Joensuu unit, Natural Resources Institute Finland (Luke), [2]School of Forest Sciences,
[3]Department of Physics and Mathematics, University of Eastern Finland, Joensuu, Finland

Trees sense their environment and adjust their cellular metabolism to adapt to prevailing conditions to cope with harsh winter conditions. However, the tolerance limit for low temperatures may be exceeded occasionally, whereupon damage may occur, first at the cellular level and then appearing with delay in growth and survival of plants. Roots hidden in the soil are typically the most sensitive organs to freezing in winter. Risk to be damaged is especially high in the boreal tree seedling nurseries if the seedlings are stored outside with missing insulating snow cover. However, there are no good methods for detection of root injuries.

We developed a novel method for detection of freezing injuries in root systems. The method is based on the electrical impedance spectra (βdispersion range) of root systems. These have typically a large variation in the absolute scale and therefore we used classification analysis (CLAss-Featuring Information Compression, CLAFIC). The CLAFIC-method is based on a subspace method with two variants where the longest projection vector defines the sample class. In the classification, the spectra are first normalized (Euclidian). Then the spectra of the frost exposed samples are compared with the spectra of the non-exposed samples, the latter forming a training group in the analysis. In this way we could detect if the root system was damaged or not.

REFERENCES

1. Repo T, Korhonen A, Lehto T and Silvennoinen R. 2015. Assessment of frost damage in mycorrhizal and non-mycorrhizal roots of Scots pine seedlings by using classification analysis of their electrical impedance spectra. Trees, DOI 10.1007/s00468-015-1171-x
2. Repo, T., Korhonen, A., Laukkanen, M., Lehto, T. and Silvennoinen, R. 2014. Detecting mycorrhizal colonisation in Scots pine roots using electrical impedance spectra. Biosystems Engineering 121: 139–149. http://dx.doi.org/10.1016/j.biosystemseng.2014.02.014

Abstract Id: 208
Topic: *Bioimpedance*

HOWLAND CURRENT SOURCE FOR WIDEBAND BIOIMPEDANCE APPLICATION

Pedro Bertemes-Filho[*1], Volney Vincence[1]

[1]Electrical Engineering, Universidade do Estado de Santa Catarina, Joinville , Brazil

INTRODUCTION An impedance spectrum is calculated by the ratio between an injecting current and a resulting measured voltage and then electrical properties are extracted from the material under study. Precise measurements requires precise current source and measuring circuit. Current sources are considered as an essential block in order to deliver controlled current to a wide range of working loads and large bandwidth. To comply with such requirements the output impedance of the current source must be much larger than the load impedance at any frequency of operation. However, stray capacitances from cables and circuitry reduce the output impedance, specially at higher frequencies.

OBJECTIVES it is to propose a new modified Howland current source (MHCS) for a wide frequency range applications in electrical bioimpedance. It also investigate the performance of the proposed MHCS when using multiplexer in the circuitry.

METHODS Pspice simutations were performed in the frequency range of 1 Hz to 100 MHz. It was implemented a mirrored modified Howland current source. The output current of 1.5 mApp is multiplexed by the analog multiplexer (mux) ADG528 and then injected into a resistive load of 1000 Ohms. The error of the output current is measured and feedbacked into the input of the circuit.

RESULTS The flat response of the circuit is in the frequency of 100 Hz to 1 MHz, without mux and error feedback. The mux decrease signifcantly the output impedance but is increase when the error feedback circuit is switched on. The new current source showed a gain of one decade in the frequency response at lower and higher frequencies, when compared to the standard circuit.

CONCLUSION A new Howland current source was implemented and simulated. Impedance tomography may benefit from this type of circuit for a wider applications.

Abstract Id: 209
Topic: *Signal processing*

EFFECT OF CEREBROSPINAL FLUID ON MIPS IN ICH BASED ON MRI

Mingxin Qin*[1], Qingguang Yan[1]

[1]College of Biomedical Engineering, Third Military Medical University, Chongqing, China

INTRODUCTION Intracranial hemorrhage (ICH) has extremely high mortality and morbidity rates. At present, the non-invasive detection of ICH mainly depends on computed tomography (CT) and magnetic resonance imaging (MRI) scanning. However, these imaging methods cannot monitor the development of ICH. The magnetic inductive phase shift (MIPS), which is proportional to the conductivity of the measured object, is a non-contact and non-invasive technique.

METHODS The current study aims to use this technique to measure the amount of bleeding and monitor the development of ICH. First, the average brain conductivity change in ICH growth was theoretically analyzed. Second, the MIPS measurement system, which included a double-end exciting coil setup and a phase difference measurement system, was designed. Third, a four-layer spherical numerical model that simulated ICH was built. The change in MIPS was calculated with the increase in bleeding volume. Fourth, an internal capsule hemorrhage model was established on a rabbit by injecting autologous blood. In this procedure, 3 mL blood was injected at a constant speed of 3 mL/1 h, and MIPS was calculated synchronously using the measurement system. Lastly, another eight rabbits underwent MRI Sampling Perfection with Application optimised Contrastusing different flip-angle Evolution(SPACE) sequence scanning synchronously with the blood injection process but without MIPS measurement. The volume reduction of the cerebrospinal fluid (CSF) was measured.

RESULTS The animal results of MIPS measurement group are consistent with the simulation results and the theoretical analysis. MIPS initially declined and then increased with increasing blood injection volume, which indicated the existence of a turning point. The results of the MRI scanned group indicates that the average CSF reduction in the eight rabbits after blood injection is approximately equal to the average injection volume that corresponds to the turning point of the MIPS group.

CONCLUSION Thus, we conclude that CSF is already exhausted and the compensatory stage has already ended when the MIPS turning point occurs. The MIPS method can detect ICH growth and blood level increase in a regular manner. The turning point in MIPS changes may have clinical significance. Moreover, it is expected to provide an early warning for ICH growth.

Abstract Id: 210
Topic: *Bioimpedance*

A SOFTWARE FOR MONITORING BRAIN EDEMA BASED ON MIPS

Mingxin Qin*[1], Gen Li[2]

[1]College of Biomedical Engineering, Third Military Medical University,
[2]Bioengineering College, Chongqing University, Chongqing, China

INTRODUCTION The main reason of brain injury is the traumatic brain edema(TBE); therefore, it plays a very key role for observing the state of the illness, guiding treatment, judging operation opportunity and doing prognosis evaluation to build a real-time continuous monitoring. It is badly in need of equipment that can be used for TBE patients to achieve real-time and continuous monitoring for a long time at present.

OBJECTIVE MIPS is a new method based on testing the the disease tissue conductivity and the dielectric coefficient, to detect the brain diseases. In this paper, we design a software based on MIPS, which can monitoring TBE in real-time and continuously.

METHOD The raise of brain water content causes the fall of brain conductivity. On the basis of MIPS principle, the MIPS value will change signicantly due to the fall of brain conductivity. It is resonalbe to monitoring brain edema by MIPS changing. Previous MIPS detection system in our reaserch group needs to set the measured parameters before researching and record MIPS data artificially, and it cannot observe the variation trend of MIPS data in real time. So, it can not realize the real-time continuous monitoring for a long time. In this paper, by writing computer program we realize the automatic operation of previous system and design a interface to show the real-tme change trend of MIPS. The software can help previous system satisfy the practical needs of the real time and continuous monitoring for TBE. To verify the feasibility of this software, 10 New Zealand rabbits are chosen to built freezing TBE model and to monitor for 24 hours by this software.

RESULT The experiment result shows that the MIPS of experiment group decrease significantly , and the MIPS of the control group do not have an obvious change. The TBE datas in 24 hours from 15 rabbits (10 rabbits are for experiment group, and others is for control group) are collected. The MIPS average change of 10 rabbits in experiment group during 24 hours is about 10±3.7719°, and that of 5 rabbits in control group is about 0.1537±2.1141°.

CONCLUSION Combining with MIPS and computer programming technology, we design a software that can monitor TBE in real time and continuously. The experiment result shows that this easy controlling software indeed has the ability to monitor TBE with highly sensitivity. This a primary research, our research group will continue to optimize the software to ensure MIPS can be used for monitoring TBE on clinic.

Abstract Id: 213
Topic: *Electrical impedance spectroscopy*

DETECTION OF ACUTE CEREBRAL ISCHEMIA IN RABBITS BY MIPSS

Mingxin Qin*[1], Wei Zhuang[1]

[1]College of Biomedical Engineering, Third Military Medical University, Chongqing, China

INTRODUCTION Acute cerebral ischemia is one of an important clinical disease that is usually detected and studied with MRI, CT and PET. Magnetic inductive phase shift is a new method for detection of cerebral ischemia, detection system based on this method is non-contact, miniaturized and low-cost which can be used as a substitute for large medical equipment in poor areas.

OBJECTIVES In order to detect acute cerebral ischemia more efficiently and obtain more useful information in a broad band, we established a magnetic induction phase shift spectroscopy (MIPSS) detection system.

METHODS Twenty five rabbits were studied by using coaxially paralleled dual-coils within 1 MHz–200 MHz frequency range in linear scanning mode, and all subjects were measured for 1 hour. Established rabbit acute cerebral ischemia model according to the bilateral carotid artery occlusion method, the rabbits were divided into control group (no ligation group), experimental group (unilateral ligation group and bilateral ligation group). Characteristic frequency (CF) with the highest detection sensitivity was selected for further analysis and processing.

RESULTS The results showed that the average phase shift of transmission parameter S_{21} detected under CF of no ligation group was -0.095 °±0.016°, unilaterally ligation group was -3.927°±0.523°, and bilateral ligation group was -8.723°±1.183° within 1 hour measuring time. The average phase shift of reflection parameter S_{11} measured under CF of no ligation group was 0.164 °±0.049 °, unilaterally ligation group was 4.679°±0.899°, and bilateral ligation group was 10.158°±1.726° with in 1 hour measuring time. MIPSS could distinguish several states and different severity of cerebral ischemia in rabbits with a statistical significance of $p<0.05$.

CONCLUSION The results suggest that the MIPSS detection method has the potential for clinical diagnosis and real-time monitoring of acute cerebral ischemia, and can effectively distinguish different severity of cerebral ischemia.

Abstract Id: 214
Topic: *Clinical applications*

PHASE ANGLE IN COLOMBIAN ELDERS DIAGNOSED WITH SARCOPENIA

Pablo Castano[*1], Clara Gonzalez [2], Felipe Marulanda [1]

[1]Ciencias clínicas , [2]Ciencias básicas , Universidad de Caldas , Manizales , Colombia

INTRODUCTION The phase angle is an electrical impedance parameter related to cell integrity which correlates with the functional and nutritional status and has been used as prognostic biomarker in various pathological conditions. Its normal value in healthy individuals is between 5 and 7 degrees and decreases with age. Some studies have concluded that the phase angle is linearly associated with the force of the hand grip and the rate of skeletal muscle mass, which makes this measure an inexpensive marker that identifies elders at risk of sarcopenia.

OBJECTIVES To establish the association between the phase angles with muscle strength and muscle mass in elders diagnosed with sarcopenia.

METHODS 15 individuals aged more than 65 years were diagnosed with sarcopenia. A phase angle less than 5 degrees was regarded as abnormal. Muscle strength was measured on the dominant hand, muscle mass was measured by DEXA and physical performance was assessed by SPPB. Pearson's coefficient was calculated to establish the strength of the association between phase angle and measurements of maximum hand grip strength and skeletal muscle mass index obtained by DEXA. Cohen's kappa index was calculated to establish the level of agreement between a phase angle decreased and the final diagnosis of sarcopenia using DEXA.

RESULTS The association between the phase angle and maximum grip strength was good when the Pearson correlation coefficient was calculated (r=0.64, p = 0.0098 95% CI 0.1941-0.8688). The association between the phase angle and skeletal muscle mass was lower but acceptable, (0. 6 p = 0.0191 CI 0.1199-0.8489 95%). The strength of correlation between phase angle decreased and the final diagnosis of sarcopenia was bad when Cohen's kappa (k less than 0.4) was calculated. None of the patients had a phase angle lower than 5 degrees. The average was 7.63 degrees.

CONCLUSION There is an acceptable degree of association between phase angle and muscle strength and muscle mass, which makes this parameter a useful screening tool to identify elderly who may have sarcopenia. However, the final diagnosis of sarcopenia requires other criteria as proposed by various scientific societies in the world.

Abstract Id: 215
Topic: *Electrical impedance tomography*

MODELLING WITH 2.5D APPROXIMATIONS

Alistair Boyle* [1], Andy Adler[1]

[1]Carleton University, Ottawa, Canada

INTRODUCTION In EIT, the 2.5D approximation is a method of reducing a 3D forward modelling problem to a 2D problem. We show that (a) the 2D modelling errors can be important, particularly for half-space like configurations (breast and prostate imaging, for example), and (b) that due to stimulus pattern sensitivity, the finite limit in the z-direction was only relevant out to a dipole spacing beyond the electrodes, at which point truncation errors were negligible. Presented in this work, is a new 2.5D forward solver appropriate for use with the new EIDORS iterative Gauss-Newton solver. We show efficient implementations of adjoint and FEM system matrix-derivative methods.

OBJECTIVES We aim to identify what model parameters lead to measurement error when a 2D model is incorrectly selected for a 3D problem. We propose the 2.5D forward solver as a suitable solution for some scenarios.

METHODS Many 2D and 3D half-space models were generated. Electrodes were placed uniformly along the top surface in a colinear array. The model generation was parametrized for: number of electrodes, boundary distance, mesh density, electrode diameter, and electrode contact impedance. An analytic model was also constructed. Convergence was observed or the parameter was determined to not contribute significantly to measurement error.

A 2.5D forward solver was constructed which utilized the 2D model geometry, but constructed a Fourier Transform in the z-direction. The forward problem was then solved as multiple two-dimensional forward problems and numerically integrated to construct the inverse Fourier Transform.

RESULTS Both the 2D & 3D models solutions converged with boundaries x * 3 d, y * 2 d, and (for 3D) z * 2 d, for array length d, where the electrode array in the x-direction. 2D measurements always had significant errors with respect to the 3D solutions. Other parameters did not contribute significantly to forward modelling errors.

The 2.5D forward solver was found to give correct results. Further algebraic manipulations should lead to computational efficiencies.

CONCLUSION Two-dimensional modelling errors can contribute to significant reconstruction errors. The 2.5D forward solver is an important tool for EIT and can contribute to better quality reconstructions.

IMAGE

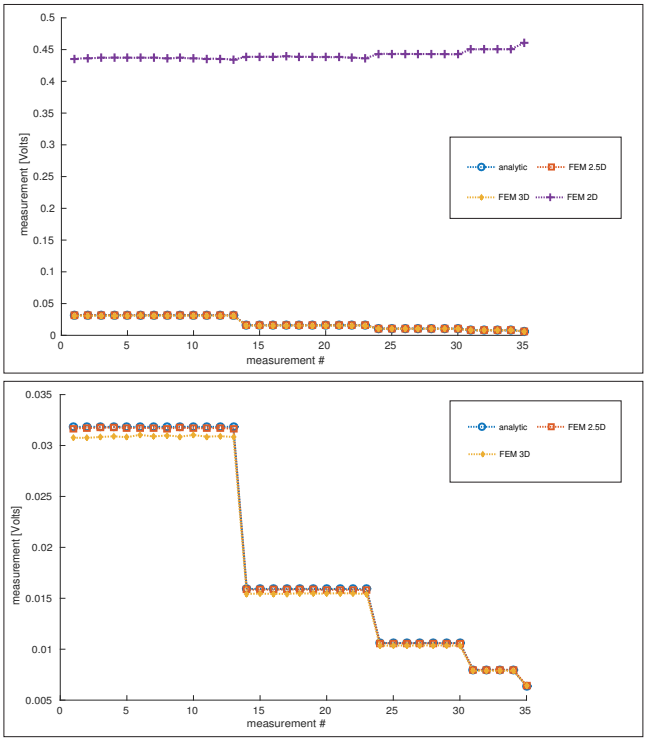

REFERENCES

1. A. Dey and H. F. Morrison (1979). "Resistivity modeling [...]" GEOPHYSICS, 44(4), 753–780.
2. Xu, S.-z., Duan, B.-c. and Zhang, D.-h. (2000), Selection of the wavenumbers *k* [...], Geophysical Prospecting, 48: 789–796.

Abstract Id: 219
Topic: *Clinical applications*

THE SIMPLE IMPEDANCE TOOL FOR SYSTOLIC FAILURE DIAGNOSIS

Tadeusz Palko[*1], Kazimierz Peczalski[1]

[1]Institute of Metrology & Biomedical Engineering, Warsaw University of Technology, Warsaw, Poland

INTRODUCTION The Echocardiography guided diagnostic methods are currently prominent in systolic failure symptoms assessment. The diagnosis can be gained by CT, MRI or radionuclear methods based on scanning principle as for instance SPECT.

The systolic failure symptoms can be generated by two basic defects: a. the ineffective work of ventricles of the heart caused by poor condition of muscles of the heart (cardiomyopathy) or impaired geometry of systole by for instance myocardial infarction , b. the mechanical dyssynchrony (MD) of the heart (right to left ventricle contraction delay>40 ms.). Both defects can be observed in some patients.

OBJECTIVES The preliminary Impedance Cardiography (IC) screening of patients for further highly specialized and expensive diagnosis can speed up and optimize systolic failure origin assessment.

METHODS The two channels IC device was designed and used for clinical studies. The impedance signal related flow in the right pulmonary artery was measured by two pairs of leads (current pair and voltage signal pair) located to the right of the sternum in the second intercostals area. The distance between inner voltage signal electrodes was in the range of 6-8 cm depending on the patient. The flow in upper aorta was measured also by two pairs of leads located longitudinally to the sternum (higher in first intercostals area and second on the level of xiphisternum). In this case the distance between signal electrodes was in range of 12–18 cm. The current tetrapolar impedance method reducing of influence of contact impedance were applied for both channels. The pulmonary circulation channel frequency of AC generator was 63 kHz and the systemic circulation channel was 95 kHz. The AC current of 1 mA was applied for both channels. Different frequencies of AC were applied for each channel in order to avoid interference between two generators signals.

RESULTS Authors applied two channel impedance cardiography (IC) for the assessment of: a. MD for selection of systolic heart failure patients for the Cardiac Resynchronization Treatment, b. ventricular septal defect, c. atrial septal defect, d. stenosis of aorta, e. stenosis of pulmonary artery.

CONCLUSIONS

1. The aortic and partial pulmonary (only right pulmonary artery) flow can be measured at the same time

2. The systolic failure patients can be preliminary selected for MD and non MD group for further diagnosis and treatment

Abstract Id: 220
Topic: *Electrical impedance tomography*

WHAT DOES EIT DISPLAY IN CASE OF PNEUMOTHORAX?

Guenter Hahn[*1], Barbara Cambiaghi[1], Anita Just[1], Joerg Dittmar[1], Tomaso Mauri[2], Nils Kunze-Szikszay[1], Onnen Moerer[1]

[1]Department of Anesthesiology , University Medical Center Göttingen, Goettingen, Germany, [2]Department of Anesthesiology, Intensive Care and Emergency Medicine IRCCS Ca' Granda Foundation, Hospital Maggiore Policlinico di Milano, Milan, Italy

INTRODUCTION EIT has the potential to become a valuable tool to detect a Pneumothorax (PTX) in high-risk intensive care patients due to the ability of EIT to monitor the lung status continuously at the bedside. Although several reports [1-3] have proven the detectability of PTX by EIT, the course of a spontaneous PTX in all phases has not been analysed yet.

OBJECTIVES By using EIT, we accidentally monitored a spontaneous PTX in a pig model from its very early signs, during transition to final manifestation and pleural drainage. Our objective of a detailed analysis was to get a deeper insight into possible pattern of development of PTX, especially in the early phase.

METHODS A deeply anaesthetized pig (65kg) being part of a larger study related to ventilator induced lung injury (VILI) was monitored by a Pulmovista 500$^{\grave{O}}$ (Draeger Medical, Luebeck, FRG) collecting tomographic series with an acquisition rate of 50 Hz. The ventilatory component and the spikes of the local time courses were separated by principal component analysis.

RESULTS We observed off-line a spike-like pattern of impedance changes already at normal ventilatory pressure and without any clinical signs of PTX. Spike levels were: 0.154 ± 0.059 (right) and 0.048 ± 0.050 (left). Application of a mean plateau pressure of 42 cmH_2O for inducing VILI resulted in a marked increase of end-expiratory impedance on the right side of the thorax. End-expiratory levels (mean ± SD, change referred to initial condition) were 0.320 ± 0.057 (right) and 0.193 ± 0.147 (left) confirming a full manifestation of PTX.

CONCLUSION The predominant spikes in the time course at the side of the affected lung are considered to be a very early sign of a leaking lung tissue and an evolving PTX.

REFERENCES

1. Costa E L, Chaves C N, Gomes S, Beraldo M A, Volpe M S, Tucci M R, Schettino I A, Bohm S H, Carvalho C R, Tanaka H, Lima R G and Amato M B 2008 Real-time detection of pneumothorax using electrical impedance tomography *Critical care medicine* **36** 1230-8.
2. Miedema M, Frerichs I, de Jongh F H, van Veenendaal M B and van Kaam A H 2010 Pneumothorax in a Preterm Infant Monitored by Electrical Impedance Tomography: A Case Report *Neonatology* **99** 10-3.
3. Preis C, Luepschen H, Leonhardt S and Gommers D 2009 Experimental case report: development of a pneumothorax monitored by electrical impedance tomography *Clin Physiol Funct Imaging* **29** 159-62.

Abstract Id: 221
Topic: *Electrical impedance tomography*

A ROBUST EIT RECONSTRUCTION USING DATA CORRELATION

Kyounghun Lee*[1], Jin Keun Seo[1]

[1]Computational Science and Engineering, Yonsei university, Seoul, Republic of Korea

INTRODUCTION Electrical impedance tomography (EIT) for lung imaging has been suffered from dealing with the forward modeling error caused by the thorax movements during ventilation. The inherent ill-posed nature of EIT combined with the boundary geometry uncertainties produces serious boundary artifacts when using conventional image reconstruction methods. This work proposes a new reconstruction method that effectively deals with the boundary geometry uncertainties.

OBJECTIVE Provide a robust lung EIT method which effectively deals with the boundary uncertainties caused thorax movements.

METHOD We use correlations between the columns of the sensitivity matrix and the EIT-data to reduce the forward modeling errors caused by the boundary movements. The correlations allow to compute directly a weighted average of conductivity change without solving the linearized EIT system, and are capable of extracting the factors of the EIT-data related to the boundary artifacts.

RESULT We performed human experiments to test the performance of the proposed method from the data using 16-channel and 32-channel EIT systems. The below figures are the comparison for performance between a conventional method(left) and the proposed method(right). As shown the images below, the proposed method provides more clear image for visualization of lung without artifacts.

CONCLUSION The proposed method effectively deals with the boundary uncertainties due to thorax movements, by using correlations between the columns of the sensitivity matrix and the EIT-data.

IMAGE

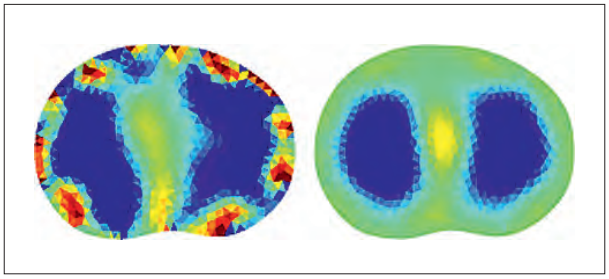

Abstract Id: 222
Topic: *Electrical impedance tomography*

INVESTIGATION INTO IMPROVEMENTS OFFERED BY FUSED-DATA EIT

Ethan Murphy* [1], Aditya Mahara[1], Ryan Halter[1]

[1]Thayer School of Engineering, Dartmouth College, Hanover, NH, United States

INTRODUCTION In recent years there have been several studies that have fused multiple sets of standard electrical impedance tomography (EIT) data to form an improved fused-data EIT (FD-EIT) image, e.g. [1]-[3]. In this study, two methods to perform FD-EIT are evaluated. Accurate absolute reconstructions of saline-tank experiments were produced using rotational EIT (i.e. the electrodes were rotated about a fixed domain); this appears to be a novel contribution that also highlights FD-EITs improvements to resolution. SVD and error analysis further illustrate the improvements and limitations of FD-EIT.

OBJECTIVES The objective was to implement FD-EIT for absolute reconstruction and to provide methods to more clearly demonstrate the improvements and limitations of FD-EIT.

METHODS An inverse approach was developed using standard Gauss-Newton algorithm with Laplace-smoothing regularization, a dual-mesh method, and an encoding of all electrodes from all rotations into a single finite element mesh. Two inversion approaches were evaluated: Inversion then data fusion (I/DF) and data fusion then inversion (DF/I). Improvements were analyzed via a set of experiments designed to illustrate the minimum distinguishable separation between two inclusions. SVD analysis was performed on combined Jacobians, a stacked matrix consisting of the combined Jacobians and the regularization matrix, and via Picard's condition.

RESULTS DF/I significantly outperformed the I/DF technique. Absolute reconstructions using DF/I for 1, 2, 4, and 8 rotations reveal that FD-EIT improved the distinguishable distance between inclusions by 1–1.5 cm when the inclusions were 2–4 cm from the tank center (Fig. 1). SVD analysis revealed up to 3.1x more stable singular vectors for DF/I, which also indicates improved resolution. Error analysis suggested a clear method to determine minimum rotational step sizes.

CONCLUSION FD-EIT significantly improved upon standard EIT in terms of qualitative and quantitative metrics. The ability to perform absolute reconstructions using FD-EIT represents an important step towards FD-EIT's use in medical applications

IMAGE

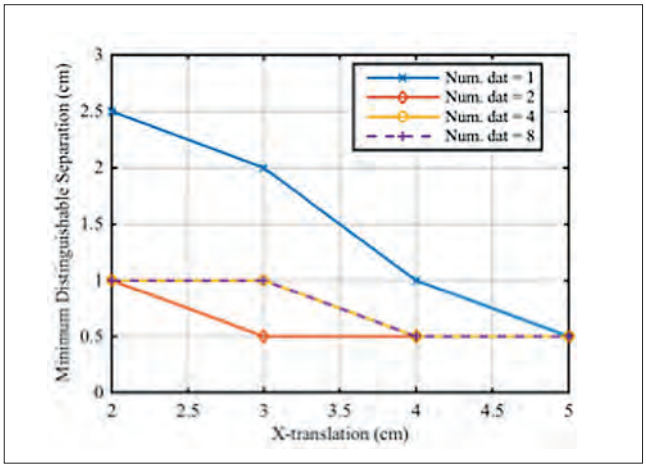

REFERENCES

1. SC Murphy and T York, *Meas. Sci. Technol.*, vol. 17, pp. 3042–3052, 2006.
2. CN Huang, et al., *Meas. Sci. Technol.*, vol. 18, no. 9, pp. 2958–2966, 2007.
3. X Zhang, et al., *Physiol. Meas.*, vol. 36, no. 6, pp. 1311–1335, 2015.

Abstract Id: 223
Topic: *Electrical impedance tomography*

ELECTRICAL RESISTANCE TOMOGRAPHY OF CONDUCTIVE THIN FILMS

Alessandro Cultrera*[1], Luca Callegaro[1]

[1]INRIM - Istituto Nazionale di Ricerca Metrologica, Turin, Italy

INTRODUCTION Electrical Resistance Tomography can be applied to conductive thin films in order to recover maps of local conductivity [1]. Local properties on relatively large area and homogeneity of thin films can be successfully addressed. These aspects are crucial for thin film and intergated device technologies.

OBJECTIVES The aim of this contribution is to highlight the effectiveness of ERT on thin films and material technology as a novel approach.

METHODS ERT is tested on commercial thin films (nominal sheet conductance 143 mS.sq) in order to have a standard reference material. Samples of the cm scale are both uniform and defect-induced by laser scribing (low conductivity inclusions) rather than metal deposition (high conductivity inclusions). Electrical connections at the samples' boundary are made with a needle-probe system.

Measurements are performed by means of a switching system provided of a dc current surce and a voltmeter. Absolute reconstruction methods are employed within a finite element environment (EIDORS) using a cicrular 2D mesh with point-electrodes. Optimal regularisation parameters are selected by L-curve method

Other consolidated techniques are applied to the same samples to validate the results.

RESULTS In table are reported the results for a uniform sample. As a crosscheck, the sample was investigated via four-point probe and van der Pauw techniques. Sheet conductance values agree by a large amount.

Sheet conductance (mS.sq) of uniform conductive films

ERT	four-point probe	van der Pauw
138±7	136±15	140±6

In figure (a) is reported the L-curve corresponding to the experimental data of a 16 electrode measurement on a sample with an high conductivity inclusion. In figure (b) the corresponding map is reported.

Spatial resolution was tested by increasing the number of electrodes from 8 to 16 in some samples with both type of inclusion described above. Features comparable to the inter-electrode distance can be resolved. An interesting aspect that emerges in this application is the substantial equivalence of different stimulation-measurement patterns.

Conclusion ERT revealed as an effective technique to test the properties and quality of thin films and 2D materials.

IMAGE

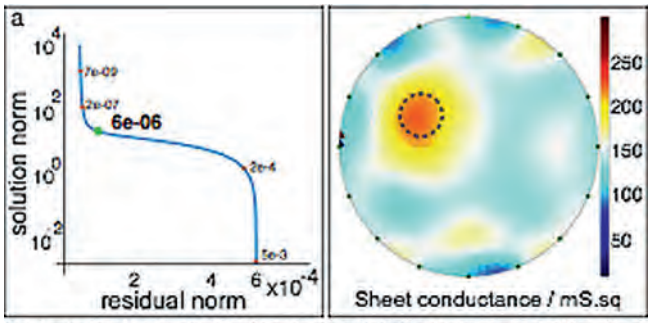

(a) L-curve for a 16 electrode measurement on a sample with a highly conductive inclusion. Bold indicates the optimal regularisation paramenter. (b) Reconstructed sheet conductance map. The outline over the colour map inidates the real inclusion.

REFERENCES

1. A. Cultrera and L. Callegaro, "Electrical Resistance Tomography on thin films: sharp conductive profiles," in *Research and Technologies for Society and Industry Leveraging a better tomorrow (RTSI), 2015 IEEE 1st International Forum on, Turin (Italy)*, 2015, pp. 297–301.

Abstract Id: 224
Topic: *Electrical impedance tomography*

HETEROGENEITY OF REGIONAL VENTILATION IN LUNG-HEALTHY ADULTS

Barbara Vogt* [1], Kathinka Ehlers [1], Victoria Hennig[1], Zhanqi Zhao[2], Norbert Weiler [1], Inéz Frerichs[1]

[1]Dept. of Anaesthesiology and Intensive Care Medicine, University Medical Centre Schleswig-Holstein, Campus Kiel, Kiel, [2]Institute of Technical Medicine, Furtwangen University, Villingen-Schweningen, Germany

INTRODUCTION Electrical impedance tomography (EIT) could potentially be used to monitor regional lung ventilation in patients with chronic lung diseases. However, little is known about the regional lung function in lung-healthy subjects which, however, is a prerequisite for reliable identification of regional ventilation deterioration in patients with lung diseases.

OBJECTIVES The aim of our study was to assess the regional lung function in allegedly lung-healthy adults using electrical impedance tomography (EIT). In addition, we checked whether the regional lung function was influenced by the history of tobacco consumption.

METHODS We examined 177 allegedly lung-healthy adults in three groups: 63 non-smokers (48±19 yr, mean age± SD), 68 ex-smokers (55±16) and 45 currents smokers (47±15) during forced expiration manoeuvre using EIT (Goe-MF II EIT, CareFusion, Höchberg, Germany) at 33 images/s. In each image pixel, we identified the beginning and the end of the forced expiration and determined the following parameters: forced vital capacity (FVC), forced expired volume in 1 s (FEV_1), FEV_1/FVC, the times needed to expire 50%, 75% and 90% of the pixel vital capacities (t_{50}, t_{75}, t_{90}).Then we generated histograms of pixel FEV_1/FVC, t_{50}, t_{75} and t_{90} frequency distributions and calculated their mean values in all subjects. For further characterization of ventilation heterogeneity, we determined the coefficients of variation (CV) of pixel FEV_1/FVC, t_{50}, t_{75}, and t_{90}.

RESULTS The frequency distributions of pixel FEV_1/FVC and the corresponding CV values distinguished significantly the non-smokers from the other two groups ($p<0.0001$). A significant effect of smoking was also identified in the frequency distributions of pixel t_{50}, t_{75} and t_{90} and by the respectively corresponding median (t_{50} $p=0.0003$; t_{75} $p<0.0001$; t_{90} $p<0.0001$). The corresponding CV distinguished between non-smokers and the other two groups ($p<0.0001$).

CONCLUSION In our study, we created a large data base of EIT data characterizing regional lung function in a reference population of lung-healthy adults. A set of EIT-derived measures was used to characterize the ventilation distribution in the lungs. Using these measures, we were able to clearly distinguish non-smokers from ex-smokers and current smokers.

We acknowledge the support by the European Union (WELCOME project, grant 611223).

Abstract Id: 225
Topic: *Electrical impedance tomography*

MODEL-BASED ESTIMATION OF REGIONAL LUNG PERFUSION USING EIT

Benjamin Hentze*[1], Thomas Muders[2], Henning Luepschen[2], Christian Putensen[2], Steffen Leonhardt[1], Marian Walter[1]

[1]Philips Chair for Medical Information Technology, RWTH Aachen University, Aachen,
[2]Department of Anaesthesiology and Intensive Care Medicine, University of Bonn, Bonn, Germany

INTRODUCTION EIT with contrast agents seems to be a promising method for hemodynamic monitoring at the patient's bedside [1,2,3].

OBJECTIVES The aim of this work is to create a model [4] to describe contrast agent flow through the cardio-pulmonary system after injection into a central venous catheter (CVC). Subsequently functional images of regional lung perfusion are derived from the model parameters.

METHODS EIT image series from previous porcine animal experiments were used [5]. The images were recorded during apnea after the injection of a 10% saline bolus into a CVC using the EEK2 (Draeger Medical GmbH, Germany) at 40 Hz. First, a temporal low-pass filter was applied to the images. Every image pixel was corrected for linear apnea drift. From regions of interest (ROI) for heart and lung three "most informative" pixels were selected by the time of their global impedance minima (see Fig. 1, top right): For right heart (RH) the earliest, for left heart (LH) the latest and for lung (L) the median time was chosen. Second, a three-sectioned model was designed (see Fig. 1, top left). Each section comprises an intravascular and an extravascular compartment. Exchange of contrast agent takes place via flow and diffusion. Ideal mixing is assumed in the compartments. Three EIT pixels are formed by linear combination of the contrast agent concentrations in the compartments using a "pixel mapping" matrix (3x3). Last, the model was non-linearly fit to the three "most informative" pixels using a trust-region approach. An "image mapping" matrix (1024x3) was calculated by linearly fitting the resulting model to the entire EIT image series using a least mean squares method.

RESULTS The model showed its ability to accurately approximate the recorded EIT image series (see Fig. 1, bottom). Furthermore functional images of regional lung perfusion were derived from the model parameters.

CONCLUSIONS Functional imaging in EIT can greatly benefit from models describing the processes underlying image formation. In order to develop and validate the designed model, extensive data has to be collected under various hemodynamic conditions in further experiments.

IMAGE

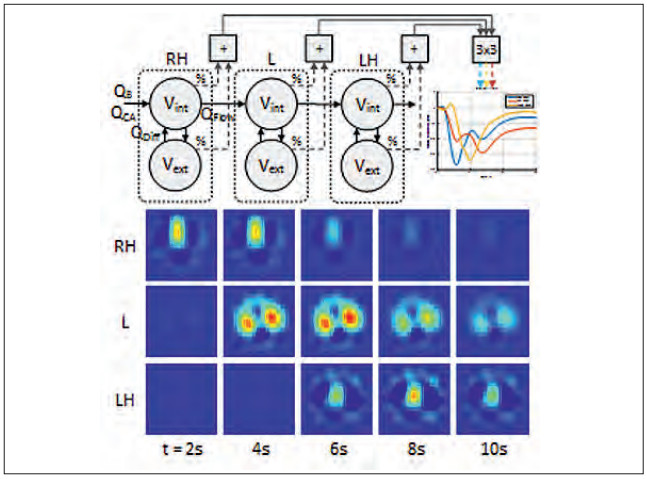

REFERENCES

1. Leonhardt S, et al. Intensive Care Medicine 38(12): 1917-1929, 2012
2. Nguyen D T, et al. Physiological Measurement 36(6):1297-1309, 2015
3. Borges J B, et al. Journal of Applied Physiology 112(1):225-236, 2012
4. Tanaka H, et al. Clinics 63(3):363-370, 2008
5. Luepschen H. Ph.D. thesis, RWTH Aachen University, Germany, 2012

Abstract Id: 226
Topic: *Electrical impedance tomography*

AN ELECTRONIC MESH PHANTOM FOR PLANAR STRUCTURE EIT SYSTEMS

Ali Zarafshani[1], Tabassum Qureshi[1], Thomas Bach[2], Chris Chatwin[1], Manuchehr Soleimani[*3]

[1]Bioelectrical Research Group, Engineering and Design, University of Sussex, [2]Sensatech Research, Brighton, [3]Engineering Tomography Laboratory, Electronics & Electrical Engineering, University of Bath, Bath, United Kingdom

Evaluation of planar EIT systems used in clinical studies can be based on a realistic E-phantom. This paper describes a mesh phantom based on an 85 electrode planar mesh structure. The design presents a dynamic mesh phantom to assess the performance of the planar topology to simulate *in vivo* conditions. The phantom is especially designed for the Sussex EIT system to validate system measurements.

INTRODUCTION There are two phantom types to assess an EIT system: physical and electronic phantoms. The physical phantom that is used for EIT systems typically is composed of a conductive saline solution with objects embedded in this medium. The medium and object have different impedances, which permit the EIT system to detect changes of impedance. Physical phantoms have common problems of: short life, inflexibility, instability and uncontrollable physical characteristics. The E-phantom is used to assess the system characteristics of the EIT system. These results can then be used to improve the performance of the system. The advantages of an E-phantom compared with a physical phantom are: improved quality, reproducibility, predictability and stability of signals.

METHODS Most of the research in the design of E-phantoms have focused on its application to the ring topology found in some EIT systems [1-3]. An E-phantom is designed to assess and validate the function of the Sussex EIT system. In order to design a mesh phantom for a planar electrode array with a homogeneous conductivity distribution, a FEM method has been applied. It uses discretization over the entire domain of the continuous conductive medium Ω [4]. In order to assess the performance of the EIT system, the Sussex EIT board and E-phantom are directly connected to the 85 electrodes as shown in Figure 1.

RESULTS The average SNR of 82.28 dB with a max and min value of 91.06 dB and 76.42 dB was achieved. An average modelling accuracy of 99.47 % was achieved.

CONCLUSIONS The purpose of the phantom is intended for system validation and performance testing during all phases of the clinical trials: pre-trial, during trial and future clinical derivatives.

IMAGE

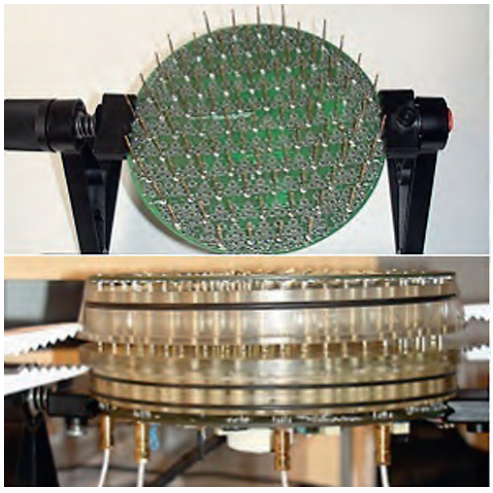

REFERENCES

1. H. Griffiths, *Physiol. Meas.* 16:A29, 1995.
2. H. Griffiths, *Clin. Phys. Physiol. Meas.*9:15, 1988.
3. H. Gagnon, *IEEE Tran.Biomed. Eng.* 57:2257-66, 2010.
4. P. P. Silvester and R. L. Ferrari, *Finite Elements for Electrical Engineers.* Cambridge university press, 1996.
5. A. Surowiec, *IEEE Tran.Biomed. Eng.*35:257-63, 1988.

Abstract Id: 227
Topic: *Electrical impedance tomography*

EIT GUIDED PEEP VERSUS ARDS NETWORK TABLE AND SET PEEP.

Serge Heines*[1], Ulrich Strauch[1], Dennis Bergmans[1]

[1]Intensive Care, Maastricht University Medical Centre+, Maastricht, Netherlands

INTRODUCTION In patients with ARDS, PEEP is often set according to the PEEP/FiO_2-table introduced by the ARDS network study. Through the years individualized methods for PEEP titration such as electrical impedance tomography (EIT) have been proposed for ARDS patients. EIT is used for PEEP titration to minimise alveolar derecruitment and overdistension.[1]

OBJECTIVES We hypothesize that EIT guided optimal PEEP differs from both the optimal PEEP according to the ARDSnet table and the optimal PEEP according to the physician (PH).

METHODS EIT guided PEEP settings were analysed in 29 ARDS patients (6 mild, 17 moderate, 6 severe). The optimal EIT guided PEEP settings defined as the best compromise between alveolar overdistension and collapse, were compared to the PEEP set by the PH and the optimal PEEP according to the ARDSnet table. A PEEP difference greater than or equal to 4 cmH_2O is defined as a clinical relevant difference.

RESULTS In 38% of the cases EIT guided PEEP was equal to the ARDSnet table and in 34% to the PH PEEP. In 21% of the cases the PH PEEP was equal to the ARDSnet table. There is no significant difference in mean value between ARDSnet, PH and EIT guided PEEP. The individual differences are shown in figure 1. A PEEP difference greater than or equal to 4 cmH_2O occurs in 29% of the cases (ARDSnet vs. PH 34%, ARDSnet vs. EIT 21%, PH vs. EIT 31%).

CONCLUSION Optimal PEEP settings by PH differs considerably from EIT or ARDSnet table guided PEEP. A PEEP/FiO_2 table is a standardized approach and probably not suitable for the individual patient. Measuring proxy parameters like oxygenation, best compliance, stress index or pressure volume curves may be misleading because they are all based on global parameters which do not exclude regional overdistension, collapse or atelectrauma, especially in patients with ARDS. But are frequently used in clinical practice by PH. As regional overdistension and alveolar collapse can be visualized using EIT[2], this technique can be helpful in a patient tailored lung protective ventilation strategy.

IMAGE

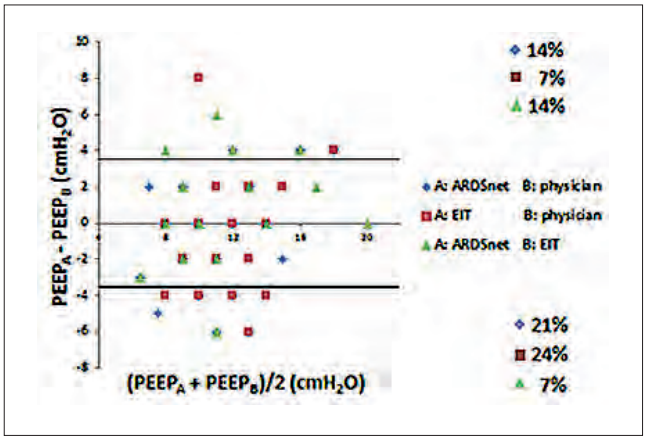

***Figure 1**: Bland Altman plot of differences in PEEP between ARDSnet and PH (diamond), EIT and PH (square), ARDSnet and EIT (triangle). Percentages of cases with a differences in PEEP equal or more than 4 cmH2O.*

REFERENCES

1. Long Y, et al., Chin Med J (Engl) 2015; **128**(11): 1421-7
2. Costa EL, et al., Intensive Care Med 2009; **35**(6): 1132-7

Abstract Id: 228
Topic: *Electrical impedance tomography*

MULTIPLEXING AND TRANSIENT ESTIMATES IN LUNG EIT INSTRUMENTS

Michael Crabb[*1], Peter Green[2], Paul Wright[2], William Lionheart[1]

[1]School of Mathematics, [2]School of Electrical and Electronic Engineering,
University of Manchester, Manchester, United Kingdom

INTRODUCTION EIT instruments must provide estimates of the transimpedance relationships between groups of electrodes within a larger ensemble. In this paper we consider the impact of multiplexing, used to address these groups, on measurement performance.

OBJECTIVES When an electrode passes from a current excitation to passive state, a transient is observed in the voltage signal. Typically, any transient following multiplexing is dealt with using some combination of pre-measurement settling time and gain reduction, to avoid saturation. Settling time is particularly costly in high frame-rate systems, where a significant proportion of signal energy is also discarded. We present an algorithm based on [1] that allows transimpedance estimation from data including substantial transient or saturation effects.

METHODS We assume the electrode-skin interface can be modelled as a capacitor and resistor in parallel, which implies a signal that is the addition of an exponential decay and sinusoidal component of interest. Three parameters are estimated in the proposed algorithm: the exponential decay time constant, and both the exponential decay and sinusoidal component of interest amplitudes. We compare this to a classical method, in which initial cycles are neglected and a Fourier Transform is applied to extract the sinusoidal component of interest.

RESULTS The accuracy and precision of transimpedance estimation achievable using the proposed algorithm is compared to the classical approaches of settling and gain reduction, using both synthetic and human test data. We observe that the proposed algorithm can generate better estimate of the signal amplitude then a classical method (in which the first cycle of sampled data is neglected).

CONCLUSION The proposed algorithm provide good estimates to transimpedance even when large transients are present in the signal, when classical methods would provide poor amplitude estimates. Time constant estimation is useful to conductivity reconstruction in its own right, since we can infer impedance characteristics of the electrode from it. We wish to extend these algorithms to real time multiplexing systems.

REFERENCES

1. Karjalainen M. *et al.*, 2002 Estimation of model decay parameters from noisy response measurements *J. Audio Eng. Soc.* **11** 867–878.

Abstract Id: 229
Topic: *Electrical impedance tomography*

CAN WE PREDICT WEANING OUTCOME WITH EIT?

Zhanqi Zhao*[1], Mei - Yun Chang[2], Knut Möller[1]

[1]Institute of Technical Medicine, Furtwangen University, Villingen-Schwenningen, Germany,
[2]Department of Internal Medicine, Far Eastern Memorial Hospital, Taipei, Taiwan

INTRODUCTION Prolonged mechanical ventilation (PMV) promotes diaphragmatic weakness due to both atrophy and contractile dysfunction. PMV and weaning failure are indicators of poor prognosis.

OBJECTIVES We examined if EIT could be used to monitor the weaning process and if possible, to predict the outcome of weaning at the beginning of spontaneous breathing trial.

METHODS Regional intratidal gas distribution (ITGD) index was calculated for the tidal volume distribution during inspiration [1]

$$ITGD_k = SUM_{ROI}(I_{j,k} - I_{j,0}) / SUM_{Lung}(I_{i,k} - I_{i,0}) * 100\%$$

where ROI, region of interest, represents the dependent regions or non-dependent regions. Pixel j and i are pixels that belong to ROI and the defined lung regions, respectively. Time point 0 depicts the beginning of inspiration. We slightly modified the original method proposed in [1] where inspiration was divided into 8 iso-volume parts. In the present study, inspiration time is divided into 8 equal parts (time point k).

A total of 15 patients with PMV was evaluated. The ventilation mode was switched from volume assist-control mandatory ventilation to continuous positive airway pressure plus 100% automatic tube compensation (ATC) for one hour and subsequently to 70% ATC for another hour.

RESULTS Four different scenarios of regional ITGD were found. In scenario No. 1, the lower the support level is, the higher the percentage of ventilation distribution in dorsal regions will be. In scenario No. 2, the ventilation distribution in dorsal regions are so dominant, that only around one fifth or less volume is distributed to the ventral regions during ATC. Not like the previous 2 scenario, in No. 3, ventilation is mainly distributed in ventral regions at all phases. Scenario No. 4 is similar to No. 1 but a decrease in ventilation (instead of increase) in dorsal regions is observed with lower support level (70% ATC). Scenario No. 1 was found in 8 out of 15 patients. Scenarios No. 2, 3 and 4 were found in 1, 5 and 1 out of 15 patients, respectively. Totally 4 patients failed spontaneous breathing trial (2 patients with Scenario No. 1 and 2 with Scenario No. 3).

CONCLUSION EIT has the potential to monitor the weaning process and to predict the outcome of spontaneous breathing trial.

REFERENCES

1. Lowhagen K, Lundin S, Stenqvist O. Regional intratidal gas distribution in acute lung injury and acute respiratory distress syndrome—assessed by electric impedance tomography. Minerva Anestesiol 2010;76(12):1024–1035.

Abstract Id: 230
Topic: *Electrical impedance tomography*

A METHOD TO CALCULATE OVERDISTENSION AND TIDAL RECRUITMENT

Zhanqi Zhao*[1], Knut Möller[1]

[1]Institute of Technical Medicine, Furtwangen University, Villingen-Schwenningen, Germany

INTRODUCTION Improper settings of the ventilator may lead to high transpulmonary pressures, alveolar overdistention, cyclic recruitment/derecruitment and biotrauma, which induce or aggravate lung injury.

OBJECTIVES The aim of the study was to introduce an EIT-based method to classify lungs into normally ventilated, overinflated, tidally recruited/derecruited and recruited regions.

METHODS EIT images at end-inspiration ($I_{I,P}$) and end-expiration ($I_{E,P}$) were identified, where P denoted arbitrary positive end-expiratory pressure (PEEP) levels. We defined tidal image $I_{TV,P} = I_{I,P} - I_{E,P}$. Assuming Z_k were pixels in images with impedance value of Z ($k \in K$, $K=\{1, 2, \ldots, 1024\}$). Lung regions at end-expiration included pixels $m \in M$ where $Z_{m,E} \geq 25\% \times \max(Z_{k,E})$. Lung regions for tidal breathing included pixel $n \in N$ where $Z_{n,TV} \geq 20\% \times \max(Z_{k,TV})$. Regions *o* are considered to be overinflated, if they belong to lung regions at end-expiration but are not or minimally ventilated during tidal breathing ($o \in O$, $O=M-N$). Regions *t* are considered to undergo cyclic alveolar collapse and reopening if they are ventilated during tidal breathing but collapsed at end-expiration ($t \in T$, $T=N-M$). Regions *r* are considered to be recruited compared to reference PEEP step P1, if they belong to lung regions at end-expiration at current PEEP step but not at P1 ($r \in R$, $R=M_{Pn}-M_{P1}$, $n \neq 1$).

RESULTS We tested our novel method in 2 patients with acute respiratory distress syndrome. The results coincided with observation of lung mechanics and blood gases.

CONCLUSION The method gives intuitive information of overdistension and recruitment for intensivists. To our knowledge, it is the first method that directly assesses tidal recruitment/derecruitment quantitatively at the bedside.

A limitation of the method is that threshold values have to be preset for lung regions identification. We have little information about the optimal threshold for proposed method. We have tested other threshold combinations and found that changes of threshold would alter the number of pixels in regions, but fortunately the trends along with PEEP stayed, which are important for decision making.

Abstract Id: 231
Topic: *Electrical impedance tomography*

DIRECT RECONSTRUCTIONS FROM PARTIAL-BOUNDARY MEASUREMENTS

Andreas Hauptmann[*1], Matteo Santacesaria[2], Samuli Siltanen[1]

[1]Department of Mathematics and Statistics, University of Helsinki, Helsinki, Finland,
[2]Department of Mathematics, Politecnico di Milano, Milano, Italy

INTRODUCTION The mathematical background of partial-boundary measurements in electrical impedance tomography is discussed and it is explained how to extend the theory of direct inversion by the D-bar method to partial-boundary data. The D-bar method is so far the only regularization method for the full non-linear problem, as shown in [2], and is additionally capable of real-time reconstructions [1].

OBJECTIVES The measurements are modelled by a partial-boundary Neumann-to-Dirichlet map (ND-map) that can be represented by single layer potentials. Furthermore, the error of partial-boundary to full-boundary data is analyzed for two specific choices of boundary data. It is shown that the error in ND-maps depends linearly on the measurement domain. The result extends further to the reconstruction error.

METHODS An extrapolation approach of the measured data is proposed to represent the partial-boundary ND-map with respect to an orthonormal basis of boundary functions. To obtain a fast reconstruction algorithm, an approximate scattering transform, needed to solve the D-bar equation, is directly computed from the ND-map.

RESULTS Numerical verification of the convergence result is presented for simulated data. Reconstructions are computed from simulated and real measurement data.

CONCLUSION It is shown that one can obtain stable direct reconstructions from partial-boundary data by the D-bar algorithm. Furthermore, the reconstruction error to full-boundary data depends linearly on the measurement domain and can be verified numerically.

REFERENCES

1. M. Dodd and J. L. Mueller, *A real-time d-bar algorithm for 2-d electrical impedance tomography data*, Inverse problems and imaging, 8 (2014), pp. 1013–1031.
2. K. Knudsen, M. Lassas, J. Mueller, and S. Siltanen, Regularized D-bar method for the inverse conductivity problem, Inverse Problems and Imaging, 3 (2009), pp. 599–624.

Abstract Id: 233
Topic: *Electrical impedance tomography*

INDIVIDUALIZED ADJUSTMENT OF MECHANICAL VENTILATION WITH EIT

Tobias Becher[*1], Valerie Buchholz[1], Timo Meinel[1],
Dirk Schädler[1], Norbert Weiler[1], Inez Frerichs[1]

[1]Anesthesiology and Intensive Care Medicine, University Medical Center Schleswig-Holstein, Kiel, Germany

INTRODUCTION Prevention of ventilator-induced lung injury (VILI) is a major clinical challenge. EIT can detect causes of VILI like alveolar cycling and overdistension [1,2]. We developed an EIT-based algorithm for individualized adjustment of positive end-expiratory pressure (PEEP) and tidal volume (V_T) with the aim of reducing alveolar cycling and overdistension and inducing lung recruitment.

OBJECTIVES To apply the EIT-based algorithm in patients with acute respiratory distress syndrome (ARDS) and to assess its feasibility for individualized adjustment of ventilator settings.

METHODS We conduct a pilot clinical study in patients requiring mechanical ventilation for early ARDS. EIT measurements are performed using the PulmoVista 500 device (Dräger, Lübeck, Germany). Patients are initially ventilated according to the ARDS network algorithm [3] using a low PEEP strategy and V_T of 6 ml / kg predicted body weight (phase ARDSNet). The patients are then ventilated according to the EIT-based algorithm during a four-hour period (phase EIT). During the phase EIT, measurement maneuvers for overdistension and alveolar cycling are performed every 30 minutes and PEEP and V_T are adjusted according to the EIT results. After the four-hour period, the resulting V_T, PEEP, PaO_2 / FiO_2 ratio, respiratory system compliance (C_{rs}), driving pressure (ΔP [4]), standard deviation of regional ventilation delay (SDRVD40) [2] and other parameters are assessed and compared to the values measured at the end of the phase ARDSNet. All results are presented as mean values ± standard deviation.

RESULTS To date, 8 patients (4 male, 4 female, age 62±17 years, height 171±7 cm) were included. V_T and PEEP changed from 398±54 (ARDSNet) to 388±117 ml (EIT) and from 8.6±1.1 to 14.3±2.6 mbar, respectively. PaO_2/FiO_2 ratio improved from 159±31 to 233±56 mmHg, C_{rs} from 37±7 to 40±13 ml/mbar and ΔP decreased from 10.8±1.6 to 9.8±1.5 mbar. SDRVD40 decreased from 11.2±4.1 (ARDSNet) to 8.6±2.5 % (EIT).

CONCLUSIONS Our preliminary results indicate that adjustment of mechanical ventilation according to the EIT-based algorithm is feasible and leads to individualized ventilator settings that could be useful in reducing alveolar cycling and overdistension and in inducing lung recruitment.

REFERENCES

1. Zick G, et al. PLoS One. 2013;8(8):e72675.
2. Muders T, et al. Crit Care Med. 2012;40(3):903–11.
3. Brower RG, et al. N Engl J Med. 2004;351(4): 327–36.
4. Amato MB, et al. N Engl J Med. 2015;372(8): 747–55.

Abstract Id: 235
Topic: *Electrical impedance tomography*

EIT OF EVOKED AND SPONTANEOUS ACTIVITY IN PERIPHERAL NERVE

Kirill Aristovich[*1], Camille Blochet[1], James Avery[1], Matteo Donega[2], David Holder[1]

[1]Medical Physics and Biomedical Engineering, University College London, London,
[2]Bioelectronics R&D , GlaxoSmithKline, Stevenage, United Kingdom

INTRODUCTION EIT could potentially be used for imaging neural activity over milliseconds with high spatial resolution without penetrating the nervous tissue [1]. Here we present and validate with neurotracing methods (Cholera Toxin Subunit B) the images of fascicular neural activity measured during evoked stimulation in *in-vivo* rat experiments. We also assess the feasibility of imaging spontaneous traffic activity in the composite nerve.

OBJECTIVES 1) Validation of EIT images of evoked activity with independent neurotracing techniques. 2) The feasibility of imaging spontaneous phasic activity in peripheral nerves.

METHODS 30-channel, platinized stainless steel-on-silicone rubber EIT array was placed around the sciatic (validation) or vagus (feasibility) nerve in anaesthetized rats. For the validation study the distal peroneal and tibial branches were electrically stimulated with square pulses. EIT data were acquired during consecutive injections of alternating current, with amplitude 5–75 μA and frequency 3–15 kHz, through a pair of electrodes at a time with simultaneous voltage recordings on the remaining electrodes (30 sec. per injection). CTB conjugated with AlexaFluor 488 (Tibial) and 555 (Peroneal) was injected in corresponding branches, followed by histological fluorescent imaging of the sciatic nerve in the location of the electrode. During the feasibility study current was injected for 1 minute per pair to allow back-averaging with electrocardiogram (ECG) and respiration pattern (RP).

Acquired data were demodulated with 4 kHz bandwidth, averaged (stimulation), or back-averaged (ECG and RP). Cross-sectional images of activity during first 200 ms following the stimulation onset were reconstructed with 0.5 ms resolution [1].

RESULTS AND CONCLUSION Spatially distinguishable sciatic nerve evoked activity with centre-to-centre separation distance of 0.57 +/- 0.04 mm (mean +/- S.E.) was obtained for tibial and peroneal branches and compared to histological findings (n=12, N=3, Figure 1). ECG- and RP-correlated (C=0.9, P<0.05, n=8, N=4) impedance changes during phasic activity were obtained however SNR was not sufficient for imaging. Work in progress is 1) proper statistical cross-validation, and 2) SNR improvement to allow spontaneous phasic activity imaging.

IMAGE

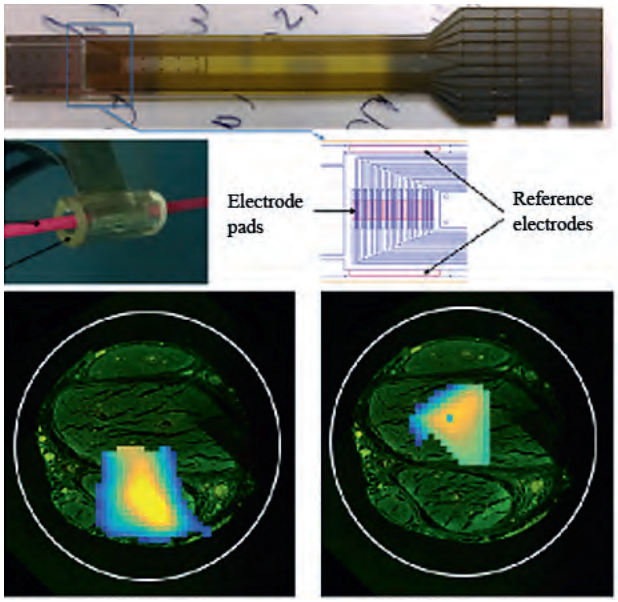

REFERENCES

1. Aristovich, Packham et. al."Imaging fast electrical activity in the brain with electrical impedance tomography", Neuroimage, vol. 124, no. Pt A, pp. 204–13, Jan. 2016.

Abstract Id: 236
Topic: *Electrical impedance tomography*

MODEL REDUCTION FOR FEM FORWARD SOLUTIONS

Andy Adler*[1], William Lionheart[2]

[1]Systems and Computer Engineering, Carleton University, Ottawa, Canada,
[2]School of Mathematics, University of Manchester, Manchester, United Kingdom

INTRODUCTION EIT estimates the internal conductivity distribution from body surface electrodes via the solution of an inverse problem. For iterative solvers, the solution time is typically dominated by the time to solve the FEM at each iteration. There is thus a strong incentive to develop techniques to reduce the solution time. Related techniques have been pursued by several groups (i.e. [1])

To obtain accurate forward solutions, it is typically necessary to model a large region far away from the electrodes. This is most severe in geophysical or endoscopic EIT; but it is also true of traditional EIT applications where, for example, the chest and abdomen extend above and below the electrode plane(s). In extended regions, we simply need to model the effect of the extended region on the ROI. This effect can be thought of in two ways: 1) the extended region can be represented by its Dirichlet to Neumann map, or 2) a resistor model representation of the FEM, the extended region can be replaced by an equivalent resistor mesh

OBJECTIVE To implement the model reduction scheme and verify its accuracy and improved calculation time.

METHODS Consider an FEM with regions (R = ROI, E = Extended). With appropriate reordering of the FEM node numbering, unconnected FEM system matrix, S, is block diagonal blocks [R,E]. The connectivity matrix has three regions: 1) nodes connected only to R (represented as [A ; 0]), 2) nodes on the boundary of R and E (and connected to both, represented as [B ; C]), and 3) nodes connected only to E ([0 ; D]). The connectivity matrix C = [A B 0; 0 D C], and the connected FEM system matrix is C'*S*C.

The 2×2 block matrix inverse, the inverse of [A|B;C|D] has a block inv(A - B*inv(D)*C) in the A position. Thus the equivalent connected system matrix for its effect on nodes in R is

[A'RA , A'RB ; B'RA , B'RB + C'EC - DEC'*inv(D'ED)*C'ED]

The term, C'EC - DEC'*inv(D'ED)*C'ED, models the effect of the extended region. It depends only on connectivity matrices and the system matrix E and can thus be precalculated.

RESULTS Software was implemented to verify these calculations. The calculation of the exended region term is approximately the time for the full model calculations. At each subsequent step, the model calculation is approximately the same as for the ROI model alone.

DISCUSSION Model reduction techniques allow more rapid forward calculations.

REFERENCES

1. Calvetti et al, Inv Prob and Imaging 9:749–76, 2015.

Abstract Id: 237
Topic: *Electrical impedance tomography*

EVALUATION OF EIT IMAGES USING ESOPHAGEAL ELECTRODES

Andy Adler[1], Stephanie Eng[*1], Martin Grambone[2]

[1]Systems and Computer Engineering, Carleton University, Ottawa, Canada,
[2]Berner Fachhochschule, Biel, Switzerland

INTRODUCTION EIT is most sensitive near its electrodes. Placing an internal electrode should improve EIT performance in the image center. The least invasive location for this internal electrode is the esophagus. Two simulation studies of the use of an esophageal electrode have been performed [1] and [2], and showed the predicted improvements. These studies were limited by considering only simulations and a single stimulation and measurement pattern.

OBJECTIVE To evaluate the benefit of an internal electrode, as a function of its position, stimulation and measurement pattern, using simulation and tank measurements.

METHODS We investigated using a single esophageal electrode using a finite element simulation and a tank phantom. In both cases, the geometry was that of a cylindrical tank with a single transverse plane of electrodes. Images were compared to a reference configuration of 32 electrodes on the medium surface in a single plane. The experimental configuration was to place one of the electrodes from the tank surface into the tank medium. A non-conductive ball was displaced from the edge to the medium center. EIT data were acquired using several different "skip" values. The electrode was in the medium center and 50% of the radius toward the edge.

RESULTS Images were reconstructed using a GREIT and a GN algorithm. Measures of resolution, noise performance and image amplitude were made. Results show an overall improved performance near the center electrode on all measures. Results for tank data (not shown) show similar trends, although image artefacts need to be carefully managed in the reconstruction.

DISCUSSION Internal electrodes can improve EIT image quality. Our results match previous simulation work [1,2] as well as approaches using boreholes used in geophysical EIT. Interestingly, in [3] a similar approach is proposed, but called "Esophageal" Impedance Tomography. For invivo use, however, several issues need to be considered. First, electrical safety is of key concern, since the electrode is close to the heart. We recommend the esophageal electrode be only used for measurement and not current stimulation. Next, image reconstruction is very sensitive to the electrode location. In practice the esophageal electrode can move, and the imaging must compensate.

REFERENCES

1. JN Tehrani et al Comput Math Methods Med. 2012:585786.
2. TF Schuessler et al Proc IEEE EMBS, 559–560, September 1995.
3. Z Lin at al Gastroenterology 146:S342–S343, 2014

Abstract Id: 238
Topic: *Electrical impedance tomography*

AN EIT BELT DESIGN WITH ACTIVE ELECTRODES AND DIGITAL OUTPUT

Ioan Jivet[*1], Alin Brandusecu[2]

[1]Applied Electronics Department, University Polithnica Timisoara,
[2]Applied Electronics, Univesity Politehnica Timisoara, Timisoara, Romania

INTRODUCTION The reported reference design is based on the commercially available AEF4300 IC. The ASIC was designed specifically for bio-impedance with multiple ports for both impressed current and voltage measurement. The main objectives of the work reported in the paper, is a generic design of an EIT belt with maximally active electrodes, using commercially available components.

METHODS Experiments used the AFE4300 in tetra-polar arrangement and the obstacles of using such a solution in EIT have been determined.

The major short-coming, is the low values of voltages measured. This is due to the fixed to 0.35 mA impressed current of the AFE4300. The IC was designed for a larger total impedance, thus only a part of ADC full scale is spanned by measurements in an EIT arrangement.

The ADC sampling frequency is also limited to 860 sps, but since the nodes can do measurements simultaneously, the estimated 50 impedance image frames/s is acceptable for most clinical applications. In the design each electrode pair is fit with a differential buffer amplifier and an AFE4300. Several other versions with a decreased number of AEF4300 are presented. The penalty for less IC's used is a reduction in the impedance image frame rate.

RESULTS The AFE4300 Eval Kit was used with a tetra-polar electrode arrangement on a human torso. The measured voltage values, signal to noise ration and estimated impedance image frame rate, have been determined. The measured voltages where found small but quantifiable. Further experiments have been conducted with a prototype differential amplifier, added in the voltage measurement chain for each electrode pair with a gain of 10–50. The solution was found to fix the scale problem.

Heart rate and respiration rate can also be determined, using a specific configuration of the weight module on a selected electrode pair.

The current consumption for a design with 16 electrode, is estimated at less then 20 mA. This feature makes it possible to use the design in a wearable wireless belt.

CONCLUSION A reference design of an EIT belt using the AFE4300 with supplemental amplifying buffers shows promising for practical implementation. The reduced values for some functional parameter of the proposed design, when compared with recently developed EIT belts found in the literature, is balanced by its SPI only digital interface, low total cost and feasibility of making it wireless wearable.

KEYWORDS EIT ASIC belt, active electrodes.

Abstract Id: 239
Topic: *Electrical impedance tomography*

MRI PIGLET HEAD MODEL FOR EIT AND AN IVH SIMULATION

Mariano Fernandez-Corazza[1], Rosalind Sadleir[*2], Sergei Turovets[3,4], Don Tucker[4,5]

[1]LEICI - Instituto de Electrónica, Control y Procesamiento de Señales, National University of La Plata, La Plata, Argentina, [2]School of Biological and Health Systems, Arizona State University, Tempe, [3]NeuroInformatics Center, University of Oregon, [4]Electrical Geodesics Inc, [5]Department of Psychology, University of Oregon, Eugene, United States

INTRODUCTION One application of EIT is the detection and monitoring of acute strokes, such as intraventricular hemorrhages (IVH) in premature neonates [1]. Experiments with piglets provide a test bench for validation. Geometrically realistic head models would improve the sensitivity in the EIT and concurrent EEG approach. Most image processing tools are optimized for humans and require extra efforts when applied to animal models. A scalable piglet head model can be useful for EIT researchers.

OBJECTIVES Develop a detailed finite element (FE) piglet head model available for the scientific community, and use it in a preliminary EIT sensitivity study of IVH grade II and III.

METHODS An MR MR T1- weighted image of a male neonate piglet was obtained (0.19 x 0.19 x 1 mm) using a 3T Philips scanner at the University of Florida. We semi-automatically segmented slice by slice as: scalp (0.4 S/m), skull (0.03 S/m), brain (0.5 S/m), eyeballs (1.5 S/m), and ventricles (1.79 S/m) using *MIPAV*. The interface surfaces were extracted using *iso2mesh*, in a process involving several rescaling, smoothing, remeshing, and repairing steps. A 1–2mm thin CSF layer was added artificially. 16 electrodes were located from pictures semi-automatically using *electrodewizard* [2], and modeled as bilayer cylinders of metal (500 S/m) and conductive gel (1.5 S/m). An inhomogeneous tetrahedral mesh was generated from the surfaces using *iso2mesh*.

We simulated 0.05 to 1 ml of injected blood (0.67 S/m) in 20 steps, first filling the ventricles (IVH grade II) and then the brain tissue (grade III). The EIT forward problem was solved using the FE method [3] for each step, with 1mA of applied current.

RESULTS We built a geometrically realistic 6-layer tetrahedral mesh of 1.6 million of elements (Fig 1a) and computed the stretch factor (SF) quality metric, resulting in 0.13% of all elements with a SF < 0.05. We found a maximum difference of 100 µV at the most sensitive electrode for IVH grade II phase and -60 µV for grade III (Fig 1b).

CONCLUSION The model is available at the UO NIC site: http://nic.uoregon.edu/projects.php. We expect this model becomes useful for scientists in need of a high quality piglet electrical head model. Our results support the use of EIT to detect hemorrhagic stroke, particularly IVH grade II and III, and they will be contrasted with real data in future works.

IMAGE

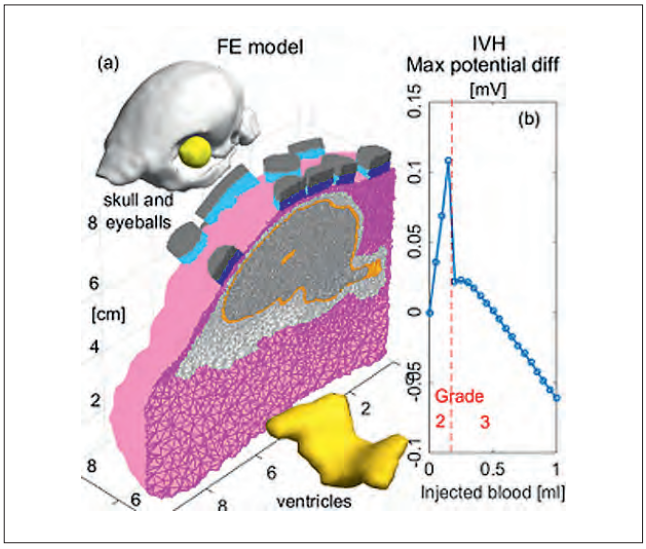

REFERENCES

1. doi:10.1109/IEMBS.2009.5334510.
2. ing.unlp.edu.ar/leici/ElectrodeWizzard/.
3. doi:10.1016/j.bspc.2013.08.003.

Abstract Id: 240
Topic: *Electrical impedance tomography*

BIOIMPEDANCE IMAGING TO ASSESS ABDOMINAL FATNESS USING EIT

Hyeuknam Kwon[*1], Seungri Lee[1], Jin Keun Seo[1]

[1]Computational Science & Engineering, Yonsei University, Seoul, Republic of Korea

INTRODUCTION This paper presents a static electrical impedance tomography (EIT) technique to evaluate abdominal obesity by estimating subcutaneous fat and visceral fat. EIT has fundamental drawbacks in the absolute admittivity imaging, because it is very sensitive to the forward modeling errors due to the boundary geometry errors and the absence of reference data. To probe abdominal fat with reducing effects of boundary geometry error, we develop a local reconstruction method which allows to identify the border between subcutaneous fat and muscle by using special current injection patterns to make reference-like data.

OBJECTIVES We develop the local reconstruction method of finding the border between subcutaneous fat and muscle using special current injection patterns.

METHODS We found a linear relation between the reference-like data and a measured data corresponding to the special current injection patterns. This relation allows to eliminate the influence of the subcutaneous fat from the measured data under the assumptions regarding on subcutaneous fat. To find the border between subcutaneous fat and muscle, the local reconstruction method is suggested by taking advantages of the data of removed the influence of subcutaneous fat.

RESULTS The performance of the proposed method were demonstrated with numerical simulations, phantom and human experiments. As shown in the figure of numerical simulation result, the border between subcutaneous fat and muscle can be found in the local region corresponding to the special current injection patterns.

CONCLUSION The proposed local reconstruction method can find border between subcutaneous fat and muscle.

Abstract Id: 241
Topic: *Electrical impedance tomography*

HYPERTONIC SALINE INJECTION TO DETECT AORTA IN PORCINE EIT

Florian Thuerk*[1], Andreas Waldmann[2], Karin H. Wodack[3], Michael F. Grässler[3], Sarah Nishimoto[3], Constantin J. Trepte[3], Daniel Reuter[3], Stephan H. Böhm[2], Stefan Kampusch[1], Eugenijus Kaniusas[1]

[1]Institute of Electrodynamics, Microwave and Circuit Engineering, Vienna University of Technology, Vienna, Austria, [2]Swisstom AG, Landquart, Switzerland, [3]Department of Anesthesiology, Center of Anesthesiology and Intensive Care Medicine, University Medical Center Hamburg-Eppendorf, Hamburg, Germany

INTRODUCTION Automated assessment of hemodynamically functional structures, such as the aorta, by electrical impedance tomography (EIT) is still a major challenge. While physiological parameters like the pulse arrival time (PAT) or local conductivity characteristics [1] seem to be suitable for this task, a reliable identification of the aorta is necessary first. We propose here methods in the time and space domain to detect aortic EIT-pixels in response to an injection of a hypertonic saline bolus into the aortic arch.

METHODS A hypertonic saline bolus (10ml, 20% NaCl) was injected into the aortic arch of 6 anesthetized pigs (Ethics approval No.53/11) during ceased ventilation and applied EIT (Swisstom BB^2) at T9/10. EIT images were reconstructed using GREIT [2], utilizing individual thorax contours from segmented computed tomography (CT) images. The resulting time-dependent image $\mathbf{X}(t)$ in $\mathbb{R}^{64x64}$ was low-pass filtered (f<0.8Hz) and analyzed in each pixel x_{ij} after the bolus injection. The aortic peak in $\mathbf{X}(t)$ and its prominence was calculated from local maximum and neighboring minima of x_{ij}, respectively (Fig. 1b). The spatial maximum of the resulting time-independent matrix was defined as aortic pixel p_A (Fig. 1a).

RESULTS AND CONCLUSIONS Sharp profiles around p_A were observed in all pigs and were closely located to the anatomical aorta (with distance of 5±3 px from the true aorta location). A complete overlap of p_A and aorta from CT can be hardly expected because of limitations in EIT reconstruction. In addition, estimated PAT at p_A was in the range of 102±14ms in contrast to p_H and p_L (Fig. 1c).

The present work evaluates temporal conductivity modulation in EIT after injection of a hypertonic bolus with the final goal to assess hemodynamics and position of aortic region.

IMAGE

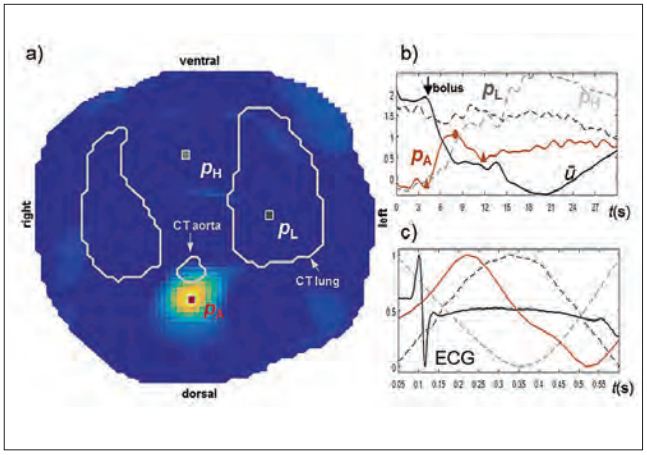

Figure 1: *a) Detection of aortic pixel p_A in EIT with anatomical contours from CT. b) Selected pixels x_{ij} and the average voltage $\bar{u}$. c) Averaged cardiac components and ECG.*

REFERENCES

1. Solà, Josep, et al. "Non-invasive monitoring of central blood pressure by electrical impedance tomography: first experimental evidence." Medical & biological engineering & computing 49.4 (2011): 409–415.
2. Adler, Andy, et al. "GREIT: a unified approach to 2D linear EIT reconstruction of lung images." Physiological measurement 30.6 (2009): S35.

Abstract Id: 242
Topic: *Electrical impedance tomography*

PULMONARY ARTERY PRESSURE BY EIT: EXPERIMENTAL EVALUATION

Martin Proença[1, 2], Fabian Braun[* 1, 2], Josep Solà[1], Andy Adler[3], Mathieu Lemay[1], Jean-Philippe Thiran[2, 4], Stefano Rimoldi[5]

[1]Systems Division, Centre Suisse d'Electronique et de Microtechnique (CSEM), Neuchâtel, [2]Signal Processing Laboratory (LTS5), Ecole Polytechnique Fédérale de Lausanne (EPFL), Lausanne, Switzerland, [3]Systems and Computer Engineering, Carleton University, Ottawa, Canada, [4]Department of Radiology, University Hospital Center (CHUV) and University of Lausanne (UNIL), Lausanne, [5]Department of Cardiology and Clinical Research, Inselspital Bern, University Hospital, Bern, Switzerland

INTRODUCTION Current solutions for the follow-up of patients with pulmonary hypertension are invasive and seldom compatible with unsupervised continuous monitoring [1]. We have recently shown, via simulations in a model of the human thorax, the feasibility of tracking changes in pulmonary artery pressure (PAP) in a non-invasive, unsupervised and continuous manner by electrical impedance tomography (EIT) [2].

OBJECTIVES The purpose of the current study was to confirm the viability and evaluate the performance of our approach in real experimental EIT data.

METHODS EIT recordings were acquired on three healthy subjects. During the protocol, the subjects were breathing nitrogen-enriched air via a mask attached to an altitude simulator, thus undergoing hypoxia-induced PAP variations. A timing parameter physiologically related to the PAP was automatically extracted from the EIT data. Reference systolic PAP values were measured by Doppler echocardiography.

RESULTS Strong correlation scores (see table below) were found between our PAP-related EIT parameter and the reference PAP.

Subject 1	Subject 2	Subject 3
$r = -0.995$ $p < 0.001$ $N = 6$	$r = -0.975$ $p < 0.001$ $N = 7$	$r = -0.861$ $p = 0.028$ $N = 6$

CONCLUSION Our findings are the first experimental evidence of the possibility of tracking changes in PAP by means of EIT. Nevertheless, our study is limited in terms of number of subjects and number of measurements per subject. If confirmed in larger datasets, these findings could open the way for a new generation of non-invasive, unsupervised and continuous PAP monitoring systems for patients with pulmonary hypertension.

REFERENCES

1. M. D. McGoon and G. C. Kane, Pulmonary hypertension: diagnosis and management, Mayo Clin. Proc., vol. 84, no. 2, pp. 191–207, 2009.
2. M. Proença et al., Non-invasive pulmonary artery pressure monitoring by electrical impedance tomography, IEEE T. Bio.-Med. Eng., *submitted*.

Abstract Id: 243
Topic: *Electrical impedance tomography*

LUNG AERATION IN EIT WITH PROBABILITY-WEIGHTED RESPIRATION

Eugenijus Kaniusas*[1], Florian Thürk[1], Stefan Kampusch[1],
Alice Wielandner[2], Helmut Prosch[2], Frederic Toemboel[3], Stefan Böhme[3]

[1]Institute of Electrodynamics, Microwave and Circuit Engineering, Vienna University of Technology,
[2]Department of Biomedical Imaging and Image-guided therapy, [3]Department of Anesthesia,
Pain Management and General Intensive Care Medicine, Medical University of Vienna, Vienna, Austria

INTRODUCTION Ventilation distribution in lungs is of primary importance. The transition from spontaneous to artificial ventilation alters regional aeration [1]. Assessment of these alterations is required for an optimal setting of ventilators. 3-D geometrical center of ventilation [1] and clustering algorithms [2] in EIT can be used to estimate the regional ventilation.

We propose a simple and low-power 2-D method to assess regional lung ventilation with preserved dorsal-to-ventral resolution while deriving the gravity center of ventilation and its spatial prominence.

METHODS Three pigs (20-30kg) were studied in healthy (H) and after lung lavage (L) (ethics approval ETK_01082015), with ventilator in pressure controlled mode at the rate of 6/min. EIT measurements (PioneerSet, Swisstom) were performed at the mid-sternal level for different PEEP levels of 0, 5, 10, 15 mbar.

The time-dependent EIT x_{ij} (t) (64x64px and 12 breathing cycles) was low-pass filtered (at 0.5Hz) to emphasize respiration. Probability distributions p of the respiratory deflections Δx_{ij}^{n} for nth cycle along the lateral position j were assessed. Gravity center Δx_i^c of ventilation was estimated as a function of the dorsal-ventral position i:

$$\Delta x_i^c = \Sigma\Sigma \Delta x_{ij}^{n} \cdot p(\Delta x_{ij}^{n}).$$

A novel triangular index $p(\Delta x_i^c)/\Sigma p(\Delta x_{ij}^{n}) = p(\Delta x_i^c)$ of p was estimated, which describes the spatial distribution of Δx_{ij}^{n} at ith level. Low and high $p(\Delta x_i^c)$ indicate variable and constant Δx_{ij}^{n}, respectively.

RESULTS AND CONCLUSIONS Shifts of Δx_i^c and $p(\Delta x_i^c)$ along i are shown in Fig. 1. The shift of the gravity center of Δx_i^c (Fig. 1) related to PEEP 0 in H was 0.3%, 4.9% and 6.5% towards dorsal side at PEEP 5, 10, and 15 in H. In L, the associated shifts were -3%, 0%, 4.6% and 9.8% at PEEP 0, 5, 10 and 15.

A low SNR method is proposed to assess redistribution of air in response to PEEP along the dorsal-ventral axis and to develop a trade-off between lung over-distention and re-opening in real-time. Validation with CT as the ground truth follows.

This study has been funded by the Vienna Science and Technology Fund (WWTF) through project LS 14069.

IMAGE

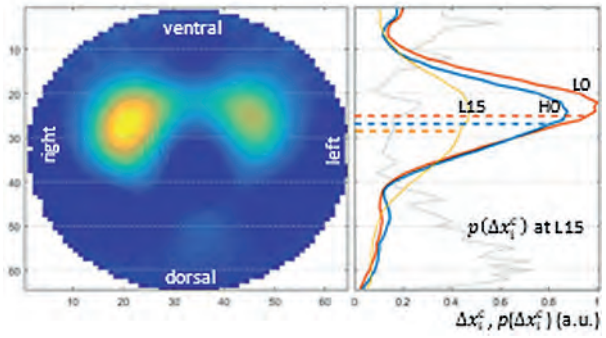

REFERENCES

1. I. Frerichs et al. "Monitoring perioperative changes in distribution of pulmonary ventilation by functional electrical impedance tomography." Acta Anaesthesiol Scand. 42(6) 721–726 (1998).
2. P. Horler et al. "Unsupervised vector quantization for robust lung state estimation of an EIT image sequence." IEEE 27th Inter. Symp. Computer-Based Med. Syst., 493-494 (2014).

Abstract Id: 244
Topic: *Electrical impedance tomography*

NERVE MODELLING FOR IMAGING FAST NEURAL ACTIVITY USING EIT

Ilya Tarotin[*1], Kirill Aristovich[1], David Holder[1]

[1]Medical Physics and Bioengineering, University College London, London, United Kingdom

INTRODUCTION EIT can be used to image fast changes in the brain and nerve [1]. To image fascicle traffic in nerve, frequency and amplitude of EIT current should be accurately chosen in order to obtain the largest possible impedance response and not to induce action potentials. Thus, simulation studies are required and a biophysical model of the nerve needs to be developed.

OBJECTIVES This study aimed to develop a preliminary 3D nerve model consisting of 100 randomly distributed interacting excitable fibres and find the safe amplitude of EIT current for various frequencies that does not induce action potentials.

METHODS 100 interacting unmyelinated 1D fibres were randomly distributed inside a cylinder (fig.1a). Each axon contained ion channels simulated with Hodgkin-Huxley equations. Model of action potential propagation along each axon was coupled with extracellular space simulated by Maxwell equations:

$$-\nabla(\sigma_e(\nabla V_e))=j_{m,}$$

where σ_e, V_e are external medium conductivity and electric potential, j_m is membrane current. AC of various frequency and amplitude was applied through cylindrical electrodes (fig.1a).

RESULTS FEM model of the 100-fibres nerve was developed; propagating action potentials were induced by external electrodes. Simulated intracellular and extracellular action potentials (fig.1b and c) were identical with those recorded *in-vivo* [2]. Safe EIT current levels were found: 500 Hz AC safe level is 0.1 mA/cm^2, 1 kHz – 0.4 mA/cm^2, 1.5 kHz – 0.6 mA/cm^2, 2 kHz – 0.8 mA/cm^2.

CONCLUSION A developed FEM 3D model of the nerve was used to find safe current levels for EIT imaging of fast neural activity. Research in progress includes development of a full FEM 3D model of autonomic nerve consisting of >1000 myelinated and unmyelinated fibres of different calibres simulated with the models used in [3] and [4]. This would allow optimal parameters for EIT imaging of nervous fascicle traffic to be obtained, including above-found safe EIT current level for the new model; the frequency of applied EIT current leading to the highest impedance response; and the relationship between nerve conductance and diameter.

IMAGE

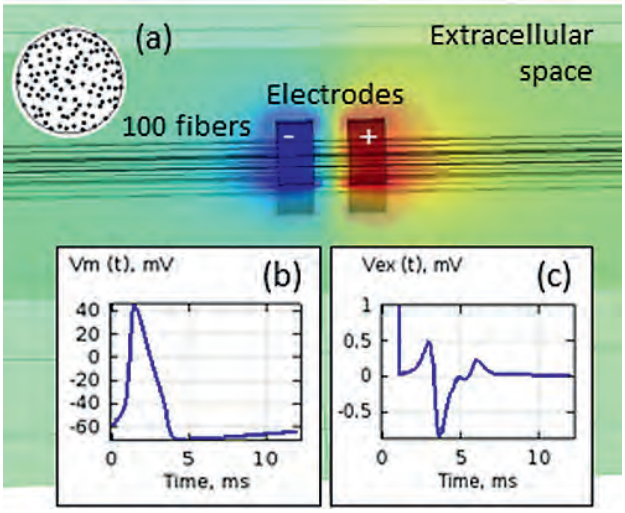

REFERENCES

1. Aristovich KY et al. *NeuroImage* 124 (2016): 204–213.
2. Hodgkin AL, Huxley AF. *J. Physiol* 117.4 (1952): 500.
3. Bostock H et al. *J. Physiol* 441 (1991): 537.
4. Tigerholm J et al. *J. Neurophysiol* 111.9 (2014): 1721–1735.

Abstract Id: 245
Topic: *Electrical impedance tomography*

APPLICATIONS OF MULTIFREQUENCY EIT TO RESPIRATORY CONTROL

Henry Tregidgo*[1], William Lionheart[1]

[1]Mathematics, University of Manchester, Manchester, United Kingdom

INTRODUCTION Methods have been proposed for the recovery of ventilation parameters and procedural generation of pressure controls for mechanical ventilation with the use of respiratory monitoring through EIT, via the high conductivity contrast of air in a region to determine ventilation profiles [1].

However, through the use of multi-frequency EIT it is possible to reconstruct the full complex admittance, which could be combined with the permittivity contrast [2] and dispersion relations of blood [3] to differentiate between concentrations of blood and other fluids within the body.

OBJECTIVES Assuming that regional blood content can be determined from multi-frequency EIT by the reconstruction of local permittivity, it becomes necessary to define strategies using this information to improve patient outcomes. The objectives of this work are to define realisable benefits of performing multifrequency EIT as well as incorporate permittivity derived blood content into practical models of respiration.

METHODS This work examines ODE models for respiration proposed for the recovery of regional respiratory parameters and definition of control profiles for mechanical ventilation. The extension of these models to include blood content variables involves refinements to parameter recovery as well as the use of perfusion estimates to weight control target states towards balanced ventilation perfusion ratios.

RESULTS The result of expanding the models stated above is a strategy for improving respiratory monitoring and control using not only regional air flow and parameters but also the distribution of blood in the lungs.

CONCLUSION The advantages of differentiating not only between air, liquid and lung tissue but also different fluids within the thorax are a strong incentive for the further development of multi-frequency EIT systems and reconstruction algorithms.

REFERENCES

1. Tregidgo HF, Crabb MG, Lionheart WRB. In *Proc. 16th Int. Conf. Biomedical Applications of EIT,* Switzerland 2015.
2. Nopp P, Harris N, Zhao TX, et al. *Medical and Biological Engineering and Computing* 35(6): 695–702, 1997.
3. Ülgen Y, Sezdi MA. Physiological quality assessment of stored whole blood by means of electrical measurements. *Medical & biological engineering & computing*. 2007 Jul 1;45(7):653–60.

Abstract Id: 248
Topic: *Electrical impedance tomography*

A NONLINEAR RECONSTRUCTION METHOD WITH A PRIORI DATA FOR EIT

Sarah Hamilton* [1]

[1]Mathematics, Statistics, and Computer Science, Marquette University, Milwaukee, United States

INTRODUCTION EIT imaging recovers the internal conductivity and permittivity distributions of an object from electrical measurements taken at the surface of an object. The reconstruction task is a severely ill-posed nonlinear inverse problem that is highly sensitive to measurement noise and modeling errors. Over the past decade, D-bar methods have shown great promise in producing noise-robust implementable real-time imaging algorithms by employing a low-pass filter in a nonlinear Fourier domain. Unfortunately, the low-pass filtering can lead to a loss of sharp edges in both conductivity and permittivity reconstructions. Patients suffering from serious respiratory illnesses often undergo at least one CT scan (e.g., diagnosis, monitoring), yet repeated CT scans lead to undesirable exposure to radiation. Each CT scan contains spatial information known with high certainty such as approximate heart and lung sizes and locations. Including this information into EIT reconstruction methods could significantly sharpen and improve EIT images of conductivity and permittivity distributions in the plane of electrodes.

OBJECTIVES The main objective of the work is to create a fast non-iterative nonlinear noise-robust reconstruction method for conductivity and permittivity imaging that includes spatial a priori information.

METHODS Recently, [1] showed that incorporating such spatial prior data can greatly improve the spatial sharpness of a conductivity image. Their method directly imbeds the a priori information into a nonlinear solution method based on well-established D-bar methods [5]. In this work, the approach is extended to develop a nonlinear reconstruction algorithm for admittivity (conductivity & permittivity) EIT imaging on non-circular domains based on [2-4].

RESULTS The method was tested on simulated noisy EIT voltage data for patients suffering lung pathologies (pneumothorax, pleural effusion). No pathology was assumed in the spatial prior, yet the true pathology is clearly visible in the new reconstructions demonstrating the effectiveness of the proposed method. Furthermore, the approach stands up well to noise as can be seen in the included figure.

CONCLUSION The new a priori method for admittivity imaging is noise-robust and flexible to various priors. Using basic location information from a CT scan can greatly improve EIT images and reveal new pathologies potentially cutting back on unnecessary exposure to radiation.

IMAGE

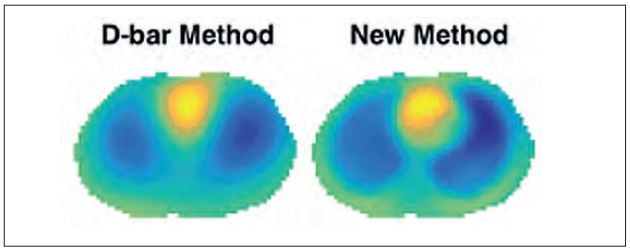

Abstract Id: 249
Topic: *Electrical impedance tomography*

SYNTHETIC BZ CALCULATION IN MRI BASED REALISTIC HEAD MODEL

Aprinda Indahlastari[1], Munish Chauhan[1], Rosalind Jane Sadleir[*1]

[1]SBHSE, Arizona State University, Tempe, United States

INTRODUCTION Finite element (FE) modeling is a popular tool to model current flow distributions in the human head caused by transcranial direct current stimulation (tDCS). However, to the best of our knowledge, none of the existing tDCS FE models have reported direct comparisons to experimental measures.

OBJECTIVES Here we present a roadmap to calculate magnetic flux density (B_z) from realistic FE models of tDCS so that they can be compared against in-vivo human MREIT B_z measurements. Calculated B_z values can then be used to reconstruct conductivity volumes.

METHODS MRI derived head models were segmented into eleven tissue types and assigned literature referenced conductivities. Two pairs of electrodes mimicking tDCS treatment configurations were placed as a FP-OZ, T7-T8 montage with anodes at FP and T7. We ran a forward model on the segmented head to solve for current density. Synthetic B_z in a specified 2D plane was then calculated from the current density by using the Biot-Savart law [1]. An isotropic conductivity volume was then reconstructed using CoReHA [2] based on the synthetic B_z values calculated from both montages.

RESULTS Figure 1 shows segmented head conductivity (A), reconstructed conductivity volume (B), voltage (C,D) and synthetic B_z (E,F) distributions in FP-OZ (C,E) and T7-T8 (D,F) montage. B_z distributions agree with the RHL corresponding to their respective voltage distributions.

CONCLUSION Synthetic B_z from FE simulation in this study will be validated against B_z measured in MREIT-based current density imaging. Conductivity reconstruction process can be applied to MREIT B_z data and compared to simulated conductivity. Finally, synthetic B_z calculation can be used to solve projected current density as another approach to reconstruct conductivity volumes.

IMAGE

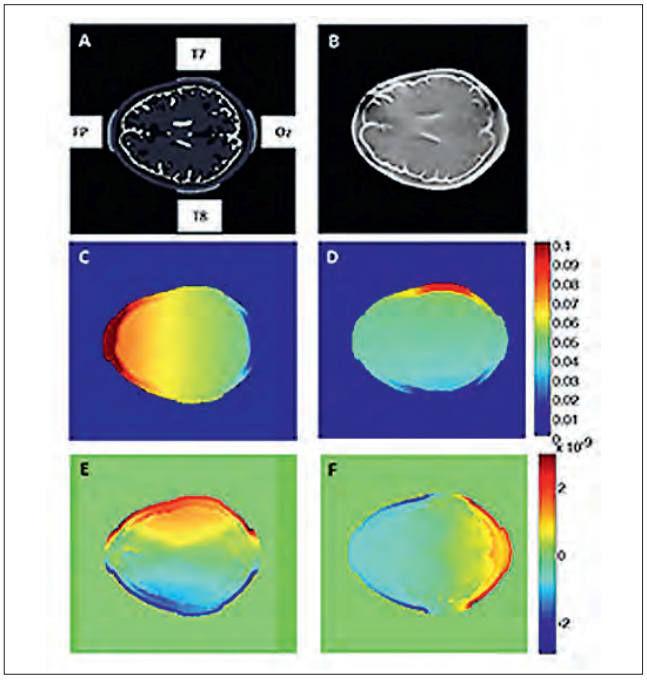

REFERENCES

1. E. J. Woo and J. K. Seo, "MREIT for high-resolution conductivity imaging," Physiol meas, vol. 29, no. 10, pp. 1–26, 2008.
2. Jeon, K., et al. "CoReHA: conductivity reconstructor using harmonic algorithms for MREIT", J Biomed Eng, vol 30, pp:279–287, 2009.

Abstract Id: 251
Topic: *Electrical impedance tomography*

ALTERNATE ALGORITHM TO RECONSTRUCT SHAPE IN WEARABLE DEVICE

Andrew Tizzard[1], Andreas Demosthenous[2], Richard Bayford[*1]

[1]School of Science & Technology, Middlesex University,
[2]Electronic and Electrical Engineering, University College London, London, United Kingdom

INTRODUCTION This group has previously presented work [1] on the development of technology for acquiring patient-specific thorax boundary hape using flexible bend sensors. The bend sensors measure curvature to estimate points for B-spline interpolation. The estimation method was based on a previously developed algorithm [2].

OBJECTIVES Evaluate a modified approach that establishes end point gradient. A B-spline is interpolated through the gradients and then integrated to reconstruct the final curve.

METHODS Previous results [1] were compared with the new *derivative* (D) algorithm. A section through a neonate shape was used to simulate each algorithm and positional errors evaluated. A point outside the original is a positive error and inside negative. This was carried out using 8, 12 & 16 bend sensors in 2 ways: uni-directionally (U) around the curve and bi-directionally (B) by reconstructing each half and averaging the endpoint [1].

RESULTS All errors except from the SB 16-sensor reconstruction were Gaussian as determined from a normality test. For each of the 8, 12 and 16 sensor reconstructions, variances were equal. One-way ANOVA with Tukey's post-hoc analysis was carried out on each.

DISCUSSION Errors appear to be reduced on all D results except U 12-sensor test. However, for 8 and 12 sensor tests ANOVA infers no significant difference. For 16 sensors there are significant error improvements. The D algorithm has the particular advantage that B-spline interpolation can be carried out a lower degree than the S algorithm improving the robustness of the reconstruction.

CONCLUSIONS For higher resolution reconstruction (16 sensors) results show that the D algorithm reduces positional errors compared to the S algorithm.

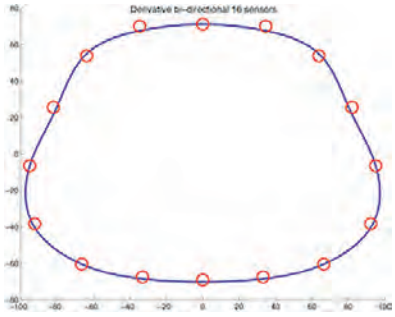

REFERENCES

1. Khor, J M, Tizzard, A, Demosthenous, A and Bayford, R 2014 Wearable sensors for patient-specific boundary shape estimation to improve the forward model for electrical impedance tomography (EIT) of neonatal lung function *Physiol. Meas.* **35** 1149–61.
2. Starck, J R, Murray, G, Lawford, P V and Hose, D R 1999 An inexpensive sensor for measuring surface geometry *Med. Eng. Phys.* **21** 725-9.

No Sensors	8				12				16			
Direction	U		B		U		B		U		B	
Method	S	D	S	D	S	D	S	D	S	D	S	D
Mean error (mm)	-2.56	-0.78	-2.69	-1.37	-0.05	0.25	-1.04	0.02	-1.83	0.28	-2.36	0.30
SD	5.39	5.49	5.91	7.23	2.06	3.11	1.75	2.10	2.44	1.60	2.07	1.20
Error improvement	1.78		1.32		-0.20		1.01		1.56		2.06	
Pairwise *p* (adjusted)	0.924		0.967		0.988		1.000		0.010		0.001	
Tukey group	A	A	A	A	A	A	A	A	B	B	A	A
ANOVA *p*	0.887				0.506				<0.0005			

Abstract Id: 252
Topic: *Electrical impedance tomography*

DETERMINATION OF LUNG PATHOLOGY BY MULTI-FREQUENT ANALYSIS

Nadine Hochhausen[*1,2], Jakob Orschulik[2], Susana Santos[2], Steffen Leonhardt[2], Michael Czaplik[1]

[1]Department of Anaesthesiology, University Hospital RWTH Aachen,
[2]Chair for Medical Information Technology, RWTH Aachen University, Aachen, Germany

INTRODUCTION Electrical Impedance Tomography (EIT) is an innovative technique that is capable of visualizing ventilation and changes in regional impedance distribution (1). Additionally, there are scientific evidences demonstrating that lung edema or atelectasis might be detected by measuring changes in thoracic impedance, using bioimpedance spectroscopy (BIS) (2). Therefore, multi-frequency EIT may be a proper candidate to combine both, advantages of EIT and BIS.

OBJECTIVE The aim of this study using lung segments from pig cadavers is to examine if multi-frequent impedance measurement is capable to differ between water and blood content in lung lobes.

METHODS In this study, we inserted either water or blood post-mortem into healthy lung lobes after anatomical partioning. Lung lobes were taken from euthanized pigs after an unrelated animal trial that was performed in general anaesthesia followed by a spontaneous breathing period. Bioimpedance measurements were conducted in a self-made measurement chamber with a Precision LCR Meter (Agilent E4980A, Agilent Technologies)) using a frequency range between 1 kHz and 1 MHz, before and after inserting water or porcine blood. Real and imaginary parts of the complex impedance Z were measured at 1 kHz, 10 kHz, 100 kHz and 1 MHz. Different indices, named α and β, were created to compare the slope of the curve (impedance over frequency). The α index is given by the equation $\alpha = (Z(1\,MHz)-Z(10\,kHz))/(Z(10\,kHz)-Z(1\,kHz))$, the β index is given by the equation $\beta=(Z(100\,kHz)-Z(10\,kHz))/(Z(10\,kHz)-Z(1\,kHz))$, for the real and the imaginary part of the complex impedance Re(Z) and Im(Z): α_{Re}. α_{Im}, β_{Re} and β_{Im}. Statistical analysis was calculated using the Mann-Whitney - U- test, comparing air-filled, blood-filled and water-filled lung segments.

RESULTS For blood as compared to air, α_{Im} and β_{Im} indices differed ($p=0.048$ and $p=0.028$); for water as compared to air α_{Re} and β_{Re} did ($p<0.001$ both). Moreover, between blood- and water-filled lung segments, significant difference in β_{Re} occurred ($p=0.002$).

CONCLUSIONS In an experimental setting, a differentiation between intrapulmonal blood or water is possible by multi- frequency impedance analysis, regarding real and imaginary part of different indices. EIT using several discrete frequencies therefore should be able to detect specific lung pathologies.

REFERENCES

1. Orschulik et al. Proceeding of RGC 2014, St. Petersburg, Russia.
2. Santos et al. Lecture Notes on Impedance Spectroscopy, 2014

Abstract Id: 253
Topic: *Electrical impedance tomography*

SOFT-PRIOR REGULARIZATION EIT FOR BREAST CANCER DETECTION

Ethan Murphy*[1], Aditya Mahara[1], Ryan Halter[1]

[1]Thayer School of Engineering, Dartmouth College, Hanover, United States

INTRODUCTION There has been numerous efforts to develop EIT for breast cancer detection. Unfortunately, reconstruction in EIT is ill-posed, resulting in diffuse, low-resolution images difficult to interpret for diagnostic purposes. One approach to overcoming this problem is to co-register EIT with a higher resolution method such as mammography [1], MRI [2], or ultrasound [3]. Incorporating this high-resolution data into the inversion process via soft-prior regularization can improve image quality and diagnostic potential. Comparisons of several inverse techniques are performed. This work appears to be the first reported implementation of these soft-prior techniques using absolute reconstructions on measured tank data (Fig. 1a).

OBJECTIVES The objective was to determine an EIT reconstruction method that is capable of detecting breast cancer.

METHODS The inverse approach uses the standard Gauss-Newton algorithm and compares Laplace-smoothing regularization without prior information to two different soft-prior regularization methods: Type-A and Type-B. Type-A completely separates different regions, and Type-B uses US data to weight regularization penalties across boundaries. Simulated weights are used as a surrogate measure of US data in this study. We consider including (I) the mammary gland or (II) the mammary gland and tumor boundaries into the soft-prior schemes. Absolute images from tank data (16 electrodes, 10 cm radius) with a mammary gland (9 cm radius) and tumor (2 cm diameter) located at 2, 3, and 4 cm from the boundary are produced. Reconstructions are qualitatively analyzed.

RESULTS Reconstructions using Type A-II regularization appear to clearly detect the tumor and to significantly outperform the other methods (Fig. 1b). The standard EIT algorithm is unable to detect the tumor at any of the three positions.

CONCLUSION Type A-II Soft-prior regularization appears to perform well on this phantom data in detecting the tumor, and thus provides good rationale for developing a bi-modal EIT system incorporating this soft-prior scheme.

IMAGE

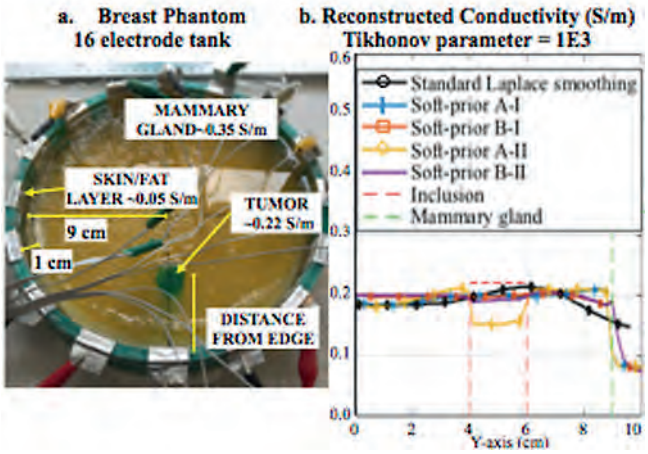

REFERENCES

1. G Boverman, et al., *IEEE Trans. Med. Imaging*, vol. 27, no. 10, pp. 1439–1448, 2008.
2. PM Meaney, et al., *Med. Physics*, vol. 40, no. 10, 103101, 2013.
3. G Steiner, et al., *Physiol. Meas.*, vol. 29, no. 6, pp. S63–S75, 2008.

Abstract Id: 255
Topic: *Electrical impedance tomography*

EFFECTS OF SIMULATED AIR ACCUMULATIONS IN THE THORAX ON EIT

Anita Just*[1], Jörg Dittmar[1], Michael Quintel[1], Günter Hahn[1]

[1]Department of Anesthesiology, University Medical Center, Göttingen, Germany

INTRODUCTION EIT is a promising technique for ventilation monitoring of intensive care patients. Especially, it can detect ventilation induced lung problems as well as oedema, hemothorax, barotrauma or pneumothorax. However, the interpretation of EIT results can be challenging in some cases due to the fact, that assumptions made in image reconstruction may be invalid in case of these patients. E.g. the assumption of only small impedance changes isn't valid anymore under these conditions.

OBJECTIVES In order to investigate the effects of air accumulation in the thorax on the EIT image reconstruction synthetic data sets of a 3D human thorax model were calculated which can be used to reconstruct images of impedance changes and absolute resistivities of the lungs.

METHODS A simplified 3D model of human thorax was created from CT scans of a patient with healthy lungs using Simpleware 6.0 (Simpleware Ltd., Exeter, UK). Here, only the thorax and the lung were considered. The 3D FE mesh of thorax and lungs were imported into COMSOL Multiphysics 5.0 (COMSOL AB, Stockholm). The resistivity of the thorax was set to 5 m and that of the lung considered to be homogeneous varied between 3 and 20 m (lungs fully deflated/inflated). Successively, parts of the lungs then were replaced by air filled regions with high resistivity. 16 electrodes were attached to the thorax in a plane and simulations were done assuming adjacent patterns. From the simulated data sets of voltage differences, images of impedance changes and resistivity distributions were reconstructed.

RESULTS Results show a clear increase of reconstructed thorax impedance with increasing amount of air beneath the lungs. The 3D spatial distribution of air influences the reconstructed resistivities outside the air filled regions. Also an influence of this accumulation of air on impedance changes reflecting ventilation in the lung region is possible. The detectability of small amounts of air reaching the pleural cavity in the early phase of a developing pneumothorax was simulated.

CONCLUSION Accumulation of air in the thorax can be detected by EIT. The influence of the 3D spatial distribution of air has to be taken into account if results of EIT on patients are to be interpreted quantitatively. The value of EIT as a possible tool for the detection of a developing pneumothorax in its early phase, e.g. in ventilation of high risk patients is worth to be further investigated by simulation and frequent monitoring of patients.

Abstract Id: 256
Topic: *Electrical impedance tomography*

A HIGHLY STRETCHABLE ARTIFICIAL SENSITIVE SKIN USING EIT

Stefania Russo*[1], Alessandro Tognetti[2], Nicola Carbonaro[2], Samia Nefti-Meziani[1]

[1]Autonomous System and Robotics Research Centre, University of Salford, Manchester, United Kingdom,
[2]Research Centre E. Piaggio, University of Pisa, Pisa, Italy

INTRODUCTION Current sensing technologies are very challenging to implement over 3D surfaces and present wires within the active sensing area, limiting their overall deformation and creating fragility. These critical limitations hinder their integration for artificial skin purposes, while a soft and low-cost solution is needed, especially on high-deformable areas.

OBJECTIVES This project aims to develop a wearable and portable pressure sensitive sensor for replacing the current industrial touch screens; in fact, they present high costs and the problem of hand occupation, and so reduced productivity. By developing an artificial sensitive skin, this new interface can facilitate and speed up the control process in an industrial environment.

METHODS As a proof of concept, we demonstrate how the first prototype of an Electrical Impedance Tomography (EIT) based pressure sensor can detect surface contacts and show their locations. The sensor is stretchable and it can be used as a wearable system as it is capable of covering curved or flat shapes.

The chosen material was a Medtex 130 conductive knit fabric, silver-plated highly conductive nylon, light-weight, low cost, and with homogeneous conductivity.

The material was cut in a circular shape with a diameter of 10 cm and 8 stainless steel circular button electrodes were pierced into the sample with a 3.5 cm gap in between. The single layer sample was then placed on a soft foam support to decrease the sensitivity to stretching in the vertical axis when pressure is applied. For the future portability of the system we have developed an experimental set-up with a constant current generator supplied by 5 V which is able to inject a constant current of 16 mA.

RESULTS A 250 gr load (2.5N) of 3 cm diameter was placed at the centre of the sensor. Differential voltage readings were acquired and sent to EIDORS software for the image reconstruction. As shown in Figure, the sensor was able to recognise the applied load through a change in the internal conductivity. The reconstructed image presents a blurred area near the area of pressure due to a high response to stretching.

CONCLUSION A first prototype of a wearable pressure sensitive sensor has been developed. Future studies will focus on the development of a conductive material with decreased electrical response to stretching and the study of different algorithms for improving its resolution.

IMAGE

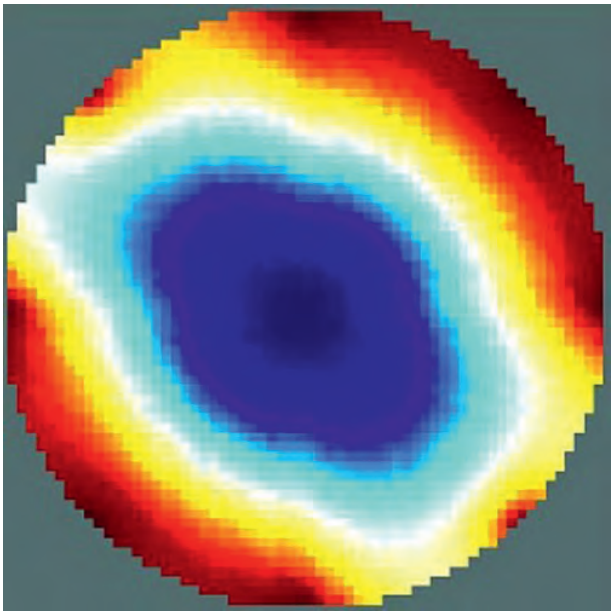

Abstract Id: 257
Topic: *Electrical impedance tomography*

USING EIT TO DETERMINE MOISTURE IN FLOOD EMBANKMENT

Tomasz Rymarczyk[*1], Przemysław Adamkiewicz[1], Jan Sikora[2]

[1]Research & Development, Netrix S.A., [2]Institute of Electronics and Information Technology, Lublin University of Technology, Lublin, Poland

INTRODUCTION This paper presents the new method examining the flood embankment dampness by electrical impedance tomography. Numerical methods of the shape and the topology optimization were based on the topological derivative, the shape derivative, the level set function and Gauss-Newton method [1,3]. Discussed techniques can be applied to the solution of inverse problems in electrical impedance tomography [2].

OBJECTIVES There were implemented algorithms to identify unknown conductivities (dampness). The purpose of the presented methods are obtaining the image reconstruction by the proposed solution. Electrical impedance tomography was used to determine the moisture of the test flood blank on a specially built model. Numerical methods of the shape and the topology optimization were based on the level set representation and the shape differentiation.

METHODS Numerical methods were based on the topological and shape derivative. These methods have been applied very successfully in many areas of the scientific modelling. The approach was based on the shape sensitivity including the boundary design of the elastic interface. The structure is represented by an implicit function. The zero level set defines the change of the shape.

RESULTS A simulation of the line measurement model was done to examine the EIT reconstruction algorithm. Figure shows the image reconstruction. The area around red lines determines dampness (the different value of the conductivity).

CONCLUSION New nondestructive methods of the monitoring flood embankment model were tested. They are iterative algorithms where repeatedly the shape boundary evolves smoothly and the searched object is detected. The combination of the proposed algorithms and the line measurement was effective in the simulation and the laboratory experiment.

IMAGE

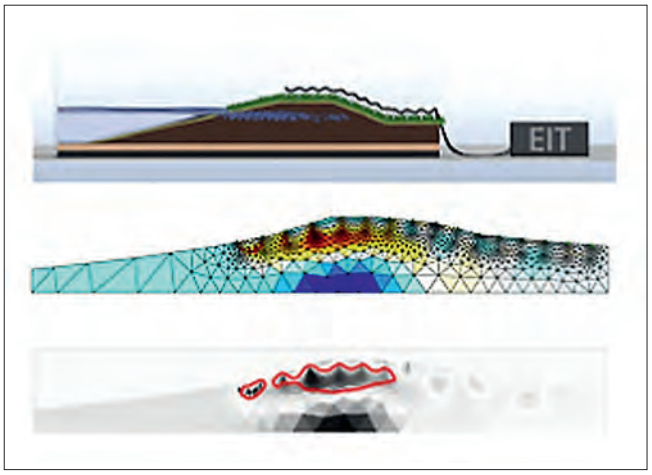

REFERENCES

1. S. Osher, J.A. Sethian, Fronts Propagating with Curvature Dependent Speed: Algorithms Based on Hamilton-Jacobi Formulations. J. Comput. Phys. 79 (1988), 12–49.
2. T. Rymarczyk, Using electrical impedance tomography to monitoring flood banks, International Journal of Applied Electromagnetics and Mechanics 45 (2014), 489–494.
3. J. Sokolowski, A. Zochowski, On the topological derivative in shape optimization, SIAM Journal on Control and Optimization, vol. 37 (1999), 1251–1272.

Abstract Id: 258
Topic: *Electrical impedance tomography*

A NEW EIT INSTRUMENT FOR LUNG FUNCTION MONITORING

Paul Wright[*1], Peter Green[1], Michael Crabb[2],
Taweechai Ouypornkochagorn[3], Hugh McCann[3], William Lionheart[2]

[1]School of Electrical & Electronic Engineering, [2]School of Mathematics, The University of Manchester, Manchester, [3]School of Engineering, The University of Edinburgh, Edinburgh, United Kingdom

INTRODUCTION We report on the current status of a new EIT instrument, being developed for lung function monitoring in critical care settings. This instrument has some architectural similarities with our previous functional EIT system (fEITER) but includes additional features, intended to enhance its utility as a research tool. These include increased flexibility in the choice of current injection strategy, amplitude and frequency, and a programmable front-end gain and attenuation stage, similar to those found in high-end ultrasound systems and oscilloscopes. The instrument's architecture is intended to maximize the accuracy and precision of the recorded transimpedance data.

OBJECTIVES To assess the instrument noise performance achievable within a flexible EIT architecture and compare it to physiological noise within the measurement.

METHODS We evaluate the noise performance of the new architecture on resistor phantoms and in human trials, using data collected from a 6-channel proof-of-concept system. We compare these results to data obtained from our fEITER instrument and to published performance data for similar EIT instruments.

RESULTS We show that instrument noise in a flexible EIT architecture, operating at frame rates appropriate to lung monitoring, can be reduced to around 1 microvolt rms. We show that, in many cases, this is less than the level of physiological noise associated with vascular activity.

CONCLUSION Modern electronics have made it possible to reduce instrument noise within, even high frame rate and fully flexible, EIT systems below the level of physiological noise present. There is now considerable scope for the separate quantification of vascular, respiratory and myogenic contributions within EIT signals.

Abstract Id: 259
Topic: *Electrical impedance tomography*

IMAGING OF REGIONAL AIR DISTRIBUTIONS IN PORCINE LUNGS

Hun Wi[*1], Guek Young Jang[1], Chi Ryang Chung[2],
Tong In Oh[1], Gee Young Suh[2,3], Eung Je Woo[1]

[1]Department of Biomedical Engineering, Kyung Hee University, [2]Department of Critical Care Medicine, Samsung Medical Canter, [3]Devision of Pulmonary and Critical Care Medicine, Department of Medicine, Samsung Medical Center, Sungkyunkwan University School of Medicine, Seoul, Republic of Korea

INTRODUCTION About 50 million patients are mechanically ventilated and many of them suffer from ventilator induced lung injury[1]. Lung protective ventilation is highly desirable to save patients' lives. There exist unmet clinical needs for real-time monitoring of regional lung ventilation. Electrical impedance tomography (EIT) has been suggested as a non-invasive real-time bedside imaging technique that can quantitatively visualize air distributions in lungs[2].

OBJECTIVE We verified the performance of our custom-designed 16-channel parallel EIT system, KHU Mark2.5 [3], for ventilation monitoring. We present results of *in vivo* experiments of porcine lungs to visualize distributions of aeration and compliance during ventilation with positive end expiratory pressure (PEEP).

METHODS We prepared four pigs (average weight of 29.5 kg and chest circumferences of 64 cm). We ventilated the animal with a mechanical ventilator (Hamilton-G5, Hamilton Medical, Switzerland). The pig was monitored using a patient monitor (IntelliVue MP50, Philips, Nederland). The ventilator provided values of airway pressure and tidal volume. Initial ventilator setup included (1) TV(tidal volume) of 10 ml/kg, (2) RR(respiration rate) of 20 breaths/min and (3) PEEP of 0 cmH_2O. We varied the setting with TV of 180 to 450 ml, RR of 10 to 20 bpm and PEEP of 0 to 30 cmH_20. We acquired EIT images from each pig at various settings. We used a time-difference image reconstruction algorithm based on the sensitivity matrix using a model with subject-specific boundary shape and electrode positions.

RESULTS Figure shows EIT images at 9 PEEP values. Incremental functional residual capacity images show the incremental baseline air distribution at each PEEP. TV images clearly indicate changes in aeration during tidal ventilation. Compliance images indicate that compliance decreased as we increased PEEP. All images visualized shapes of lungs with a significantly less amount of geometrical errors compared with the cases using a circular model.

CONCLUSION We could reconstruct real-time lung aeration images of pigs. Analyzing the images with ventilator settings such as RR, airway pressure, TV and PEEP, we could successfully quantify regional distributions of aeration and compliance.

IMAGE

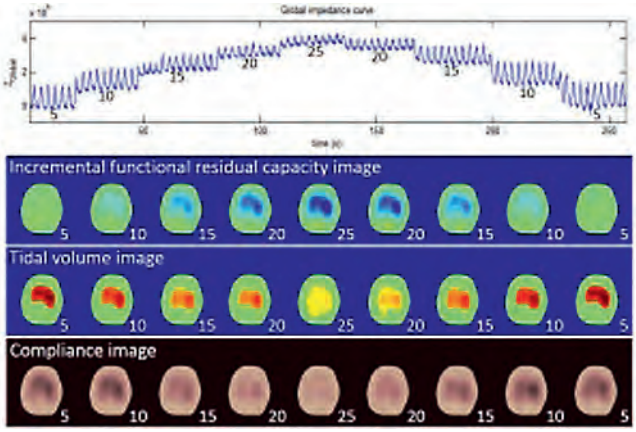

REFERENCES

1. Amato et al., New England Journal of Medicine, vol. 338, pp. 347–54, 1998.
2. Adler et al., Physiol. Meas., vol. 33(5), pp. 679–694, 2012.
3. H. Wi et al., IEEE Trans. on BioCAS , vol. 8, pp. 119–128, 2014.

Abstract Id: 260
Topic: *Electrical impedance tomography*

FEASIBLE METHOD FOR CHEST SHAPE ESTIMATION USED FOR EIT

Satoru Nebuya[*1], So Hifumi[1], Hiroshi Kumagai[1], Brian Brown[2]

[1]Graduate School of Medical Sciences, Kitasato University, Kanagawa, Japan,
[2]Department of Cardiovascular Science, University of Sheffield, Sheffield, United Kingdom

INTRODUCTION Electrical Impedance Tomography (EIT) is a medical imaging technique for reconstructing distribution of tissue resistivity by applying weak current into a body and by measuring body surface voltages. Evaluating lung function is a typical application of EIT and the measurement accuracy has known to be affected by errors in a chest shape of subject by means of previous studies.

OBJECTIVES We proposed a novel estimating method of a chest shape using curvature sensors that could be integrated into a wearable EIT device and evaluated measurement accuracy in shape estimation.

METHODS The developed EIT belt included 16 curvature sensors for chest shape estimation and 16 electrodes for EIT measurement. Chest shape was estimated using curvature data and chest circumference with the proposed algorithm. To estimate chest shape, X-Y coordination of each curvature sensors with equally spaced was predicted by rotational transfer and spline interpolation was used. Measurement accuracy was evaluated by applying the proposed method to an ellipse shape with 20cm in X-axis and 10cm in Y-axis, the same ellipse with 20 % random noise and two CT images of thorax. To evaluate accuracy of estimated shape, we defined eccentricity '*e*' that was aspect ratio of estimated shape and compared it between actual and estimated shapes respectively.

RESULTS Error in eccentricity '*e*' was approximately 3% in ellipse shape without noise, 7% in ellipse shape with noise and 7% in two CT images respectively. The result was considered that our proposed method was useful to estimate shape for accurate EIT measurement using a wearable EIT.

CONCLUSION We conclude that we proposed a shape estimating method with curvature sensors and showed accuracy of shape estimation. But further improvement was needed to achieve more accurate chest shape estimation.

Abstract Id: 261
Topic: *Electrical impedance tomography*

INVESTIGATING THE SAFETY OF 2 KHZ EIT IN THE RAT BRAIN

Sana Hannan*[1], Mayo Faulkner[1], David Holder[1]

[1]Medical Physics, University College London, London, United Kingdom

INTRODUCTION EIT of fast neural activity can be undertaken with a resolution of 200 µm and 1 ms through electrode arrays placed on the cortex to image epileptic seizures and evoked potentials. A carrier frequency of ~2 kHz allows this temporal resolution to be achieved whilst avoiding EEG artefacts [1]. Prolonged cortical stimulation may cause neural injury through excitotoxicity and electrochemical reactions at the tissue-electrode interface [2]. Although the current density threshold for this damage is 250 A/m^2 for 50 Hz DC cortical stimulation [2], the safety of current levels used in our fast neural cortical studies (~50 µA, 177 A/m^2, 2 kHz) is yet to be assessed.

OBJECTIVES The present study investigated whether current levels used in these EIT studies induce histologically detectable neuronal damage in the rat cerebral cortex.

METHODS 2 kHz current was applied continuously for 1 hour between 0.6 mm-diameter source electrodes, in a 60-electrode epicortical array placed on one hemisphere in adult Sprague-Dawley rats anaesthetised with isoflurane, and a 15 mm-diameter sink electrode in the mouth. 3 stimulation protocols were tested: (a) single 1 mA injection (positive control); (b) 10, 25, 50, 75 and 100 µA injections in parallel through 5 electrodes, for which modelling showed no significant overlap between current propagation; or (c) single 100 µA injection (based on results from (b)). Following termination of stimulation, brains were fixed in formalin and histologically processed with Haematoxylin and Eosin (H&E) and Nissl stains.

RESULTS Histological analysis revealed no evidence of neuronal damage with currents up to 100 µA, equating to a 354 A/m^2 current density (Fig. 1A; n=13 sites, 5 rats), compared to 1 mA injection (Fig. 1B; n=3 sites, 3 rats).

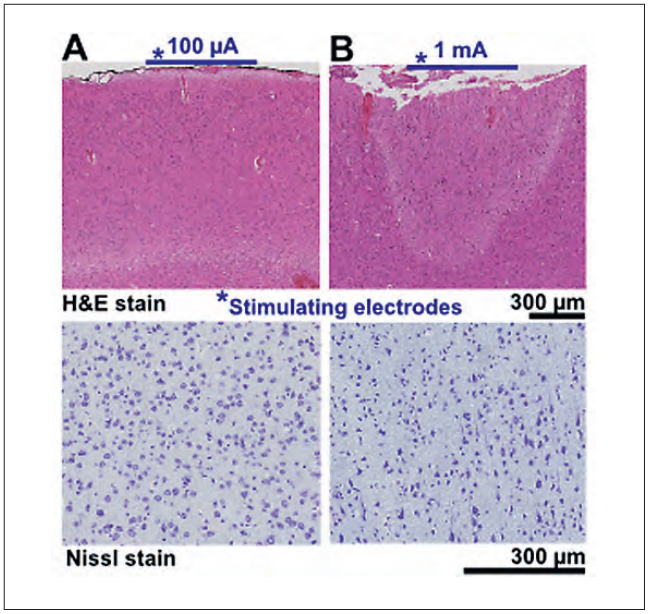

Fig. 1. *(A) Normal neuronal morphology following 100 µA application. (B) 1 mA application expectedly caused a conical ischaemic focus and severe neuronal damage marked by a shrunken, hyperchromic appearance.*

CONCLUSION The safety of continuous 2 kHz cortical stimulation with current densities up to 354 A/m^2 was validated. Since EIT protocols generally entail intermittent current injections, the probability of inducing neural injury at any electrode site can be expected to be even lower. Further work is required to assess the effects of such current applications in EIT over longer periods.

REFERENCES

1. Aristovich KY et al. *NeuroImage* **124**: 204–213, 2016.
2. McCreery DB et al. *IEEE Trans Biomed Eng* **37**: 996–1001, 1990.

Abstract Id: 262
Topic: *Electrical impedance tomography*

A NOVEL ACTIVE ELECTRODE IC FOR WEARABLE EIT SYSTEMS

Yu Wu* [1], Peter Langlois[1], Richard Bayford[2], Andreas Demosthenous[1]

[1]University College London, [2]Middlesex University London, London, United Kingdom

INTRODUCTION Each year fifteen million babies are born prematurely and many suffer from respiratory failure due to immaturity of the lung and lack of breathing control. Although respiratory support, especially mechanical ventilation, can improve their survival, it also causes severe injury to the vulnerable lung resulting in severe and chronic pulmonary morbidity lasting in to adulthood. Thus a lung aeration monitoring device for continuous non-invasive bedside monitoring of infants lung function is urgently needed.

OBJECTIVE This paper presents an active electrode IC for use in the wearable EIT device for neonate lung. The IC includes a high performance current driver, a low-noise voltage buffer and two boundary shape-information sense buffers.

METHODS AND RESULTS The IC is designed in 0.35-µm CMOS technology for operation from ±9V power supplies. The current driver can provide an output current up to 6 mA_{p-p}, and has an output impedance over 1.7 MΩ at 500 kHz. The voltage amplifier has an input-referred noise of 23 nV/√Hz at 10 kHz. Used as a unity gain buffer, the amplifier provides an output voltage swing of 14 V for signal frequencies up to 500 kHz and is able to drive large capacitive loads. The targeted wearable EIT system requires patient-specific boundary shape estimation to improve the forward model for image reconstruction. This can be facilitated by using shape sensors (e.g., stretch and bend resistors) in the wearable EIT system [1]. For this reason, shape sensor buffers are provided on chip. Figure 1 shows the layout of the active electrode IC which occupies an active area of 5 mm^2. Table I summarizes its post-layout simulated performance.

CONCLUSION An active electrode IC has been presented. It comprises a high performance current driver, a voltage amplifier and two sensor buffers. Post-layout simulations have confirmed its correct operation. The IC has been recently fabricated and is currently being tested. Measured results and comparison with other work will be presented at the conference.
Acknowledgement: This work has received funding from the European Union's Horizon 2020 research and innovation programme 2014-2018 under grant agreement no. 668259 (Project: CRADL).

IMAGE

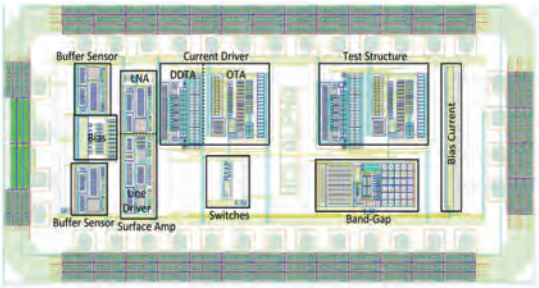

Figure 1: Layout of the active electrode IC.

Specification	Current Driver	Voltage Buffer
Bandwidth	500 kHz	1 MHz
Phase	-3.4°	-4°
Gm/Gain	1.99 mA/V	1 V/V
Output impedance	1.7MΩ @ 500 kHz	30 mΩ
Input-referred noise	-------	23 nV/√Hz

Table I. Post-layout performance summary of the IC.

REFERENCES

1. J. M. Khor, A. Tizzard, A. Demosthenous, and R. Bayford, "Wearable sensors for patient-specific boundary shape estimation to improve the forward model for electrical impedance tomography (EIT) of neonatal lung function," Physiol. Meas., vol. 35, no. 6, pp. 1149–1161, 2012.

Abstract Id: 263
Topic: *Electrical impedance tomography*

PYEIT: A PYTHON BASED, OPEN SOURCE FRAMEWORK FOR EIT

Benyuan Liu*[1], Bin Yang[1], Canhua Xu[1], Junying Xia[1], Xiuzhen Dong[1], Feng Fu[1]

[1]Department of Biomedical Engineering, Fourth Military Medical University, Xi'an, China

INTRODUCTION Nowadays, the EIDORS toolkit is widely used for developing and evaluating EIT algorithms. However, EIDORS is based on MATLAB, which is basically a functional language and has weak Object Oriented Programming (OOP) capability. In clinical applications, most software are build using C++. The algorithms developed in MATLAB need to be translated to C++ which consumes lots of work. Therefore, MATLAB may not be suited for rapid-prototyping of EIT systems.

OBJECTIVES We present a python-based, open-source EIT package called pyEIT. It is a multi-platform software released under the Apache License v2.0, see http://github.com/liubenyuan/pyEIT. In this paper, we focus on illustrating basic design principles of pyEIT by using some intuitive examples in forward computing and inverse solving of EIT.

METHODS The codes are purely written in Python. It relies on NumPy for vectorized operations on multi-dimensional arrays, SciPy for linear algebra and Matplotlib for visualization. pyEIT is organized with easy-to-use in mind.

1. forward computing. We use Finite Element Method (FEM) for forward computing. A typical 2D-EIT problem can be simulated as,

```
# Setup EIT scan conditions, 16 electrodes, adjacent mode
elDist, step = 1, 1
exMtx = eit_scan_lines(16, elDist)
fwd = forward(mesh, elPos)
f0 = fwd.solve(exMtx, step=step, perm=perm0)
f1 = fwd.solve(exMtx, step=step, perm=perm1)
```

2. inverse solvers. We implement some typical EIT reconstruction algorithms such as Filtered Back Projection (FBP), sensitivity based method (denoted by JAC) and GREIT. An example demonstrates the inverse solving process is (take GREIT for example),

```
eit = greit.GREIT(mesh, elPos, exMtx=exMtx, step=step, parser='std')
ds = eit.solve(f1.v, f0.v, normalize=True)
```

3. visualization. The EIT images can be visualized using tripcolor or imshow using Matplotlib,

```
ax1.tripcolor (no2xy[:, 0], no2xy[:, 1], el2no, np.real (ds_jac))
ax2.imshow(np.real(ds_greit), interpolation ='nearest')
```

RESULTS The figure demonstrates some EIT images reconstructed using FBP, JAC and GREIT.

CONCLUSION We present in this paper an open-source, Python based platform for evaluating and implementing EIT reconstruction algorithms. It is OOP-based and is purely written in Python with easy-to-use in mind. The python-based implementation can be extended with GPU accelerated capability by using open source packages such as pyCuda or cuMat, which we believe may have great value for large-scale 3D EIT computing.

IMAGE

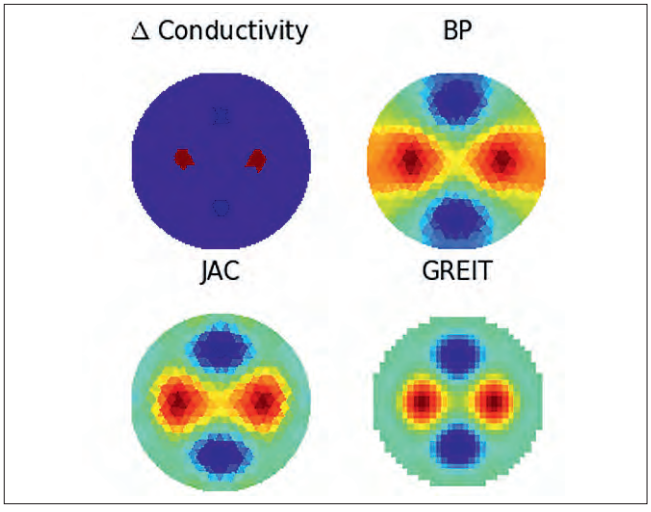

Abstract Id: 264
Topic: *Electrical impedance tomography*

PCA-BASED CHARACTERIZATION IN LUNG EIT

Liangdong Zhou*[1], Jin Keun Seo[1]

[1]Computational Science & Engineering, Yonsei University, Seoul, Republic of Korea

INTRODUCTION Electrical impedance tomography (EIT) is considered as a promising diagnostic tool to monitor lung conditions continuously at bedside. However, lung EIT is still needed to improve current reconstruction methods from time-varying EIT data, which are driven by various dynamic factors including pulmonary activities, cardiac activities, and diaphragm movement.

OBJECTIVES This paper proposes a principal component analysis (PCA)-based EIT technique, which aims to provide characteristic features for diagnosis of the lung conditions. We use PCA on the time series of EIT data to extract different features of the lung conditions with separating the pulmonary and cardiac signals.

METHODS Construct two different covariance matrices from time-difference EIT data matrix with its row having location information and its column having time information. The eigenvector matrix for the row covariance matrix contains the information of position of current injection and voltage measurement; its first column is the direction of the maximum variance of measurements in position which helps to characterize the lung collapse location. The eigenvector matrix for the column covariance matrix contains the information of time change of the lungs; its first column is the direction of the maximum variance of measurements in time which helps to separate the lung ventilation signal from the others. With the transformed data under the eigenvectors basis, reconstruction of the lung ventilation and lung collapse localization can be done.

RESULTS The simulation with different cases show that the proposed methods achieve more accurate reconstruction for lung conditions as shown in the following figures.

CONCLUSION The proposed PCA-based EIT technique allows to localize lung collapse and the pattern of ventilation.

KEYWORDS Electrical impedance tomography (EIT), lung collapse, lung condition features, principal components analysis (PCA)

IMAGE

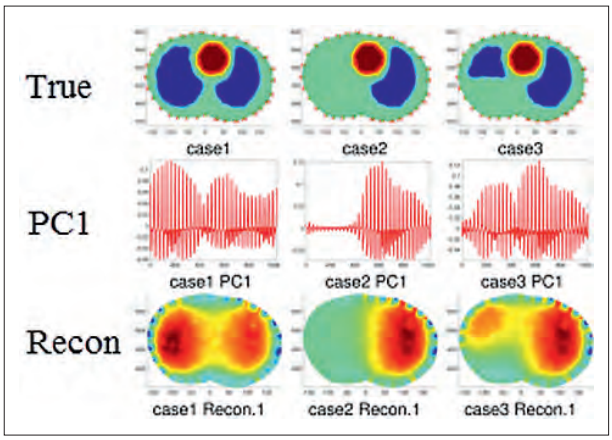

Abstract Id: 265
Topic: *Electrical impedance tomography*

FABRICATION OF PRESSURE DISTRIBUTION SENSOR FOR EIT IMAGING

Tong In Oh*[1], Hun Wi[1], You Jeong Jeong[1], Kap Jin Kim[2], Eung Je Woo[1]

[1]Department of Biomedical Engineering, [2]Department of Advanced Materials Engineering for Information & Electronics, Kyung Hee University, Seoul, Republic of Korea

INTRODUCTION Fabric based pressure distribution sensor is useful in wearable healthcare monitoring devices and tactile sensing interface. The pressure measurement method using conductive fabrics and electrical impedance imaging technique has a high potential to present pressure distribution with cost-effective way [1]. However, this method has intrinsic difficulties due to non-linearity and less sensitivity [2].

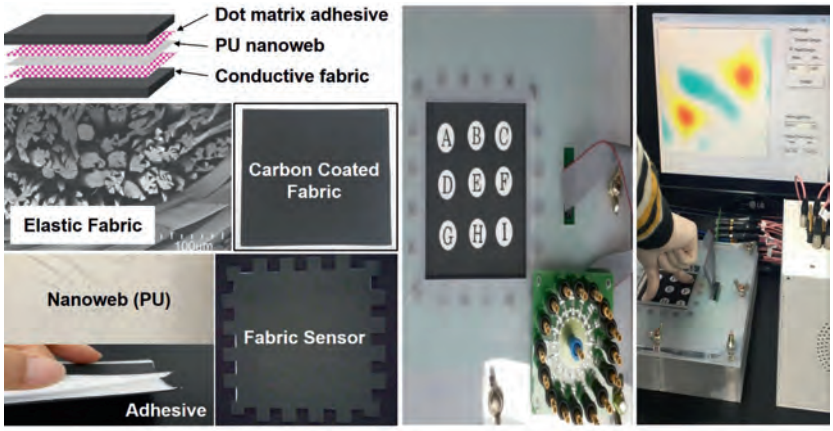

OBJECTIVE We proposed the multi-layered structure of fabric and polyurethane(PU) nanoweb to improve the sensitivity of compressive pressure. In order to maintain the stable characteristic of fabric sensor, it requires optimized materials and well-developed fabrication method with them. In this paper, we introduce the fabrication method and materials for piezo-impedance based pressure distribution sensor and pilot imaging results.

METHOD We prepared highly elastic fabric material made by Nylon and Polyester. It was coated by nano size conductive carbon with urethane binder. The surface resistance (4.47 kOhm was not low because conductive fabric was used for impedance imaging for pressure distribution sensing. If it was too low, we could not obtain the good spatial resolution. PU nanoweb has highly porous structure to provide the piezo-capacitive effect. Each materials must be well attached each other using non-conductive adhesive for stable characteristic. Also, it pulls the next part when they tightly attached. We selected the hot melt type dot matrix adhesive using copolyamide.

RESULTS We measured the relative impedance changes due to compressive force of 0.5, 1, 2, 5, 10, 15 and 20 kgf. The hysteresis errors for sensor with adhesive and without adhesive were 28.29% and 80.70%, respectively. We applied impedance imaging technique of KHU mark2.5 EIT system [3]. We could reconstruct the pressure distribution using piezo-impedance based fabric sensor.

CONCLUSION We proposed the multi-layered structure of conductive fabric and PU nanoweb to improve the sensitivity of compressive pressure. We prepared carbon black coated highly elastic fabric and hot melt type dot matrix adhesive. The assembled piezo-impedance based pressure distribution sensor can show the impedance images for pressure sensing.

REFERENCES

1. F. Carpi et al., Information Technology in Biomedicine, IEEE Trans. on, vol. 9, no. 3, pp. 295–318, 2005.
2. T.K. Bera et al., Sensors, vol. 14, no. 6, pp. 9738–9754, 2014.
3. H. Wi et al., IEEE Trans. on BioCAS., vol. 8, pp. 119–128, 2014.

Abstract Id: 267
Topic: *Electrical impedance tomography*

LIVER STIFFNESS MEASUREMENT BY MR-BASED CONDUCTIVITY IMAGING

Hun Wi*[1], Woo Chul Jeong[1], Saurab Zk Sajib[1],
Hyung Joong Kim[1], Oh In Kwon[2], Eung Je Woo[1]

[1]Department of Biomedical Engineering , Kyung Hee University,
[2]Department of Mathematics, Konkuk University, Seoul, Republic of Korea

INTRODUCTION Liver tissues consist of relatively single cells and the amount of concentration and mobility of its ions show almost similar pattern [1]. This indicates the liver tissues show uniform distribution of electromagnetic tissue properties. MREIT can provide electrical conductivity information of suspicious tissue using a current-injection MRI method [2]. The measurement of liver stiffness using MREIT conductivity imaging may provide direct, immediate, and high sensitive information based on the changes of the concentration and mobility of ions around the cells.

OBJECTIVE The purpose of this study is to show the clinical feasibility of electrical conductivity-based liver stiffness measurement which is related to the tissue degeneration from the animal liver cirrhosis models.

METHODS Liver cirrhosis was induced in healthy rats by an intraperitoneal injection of dimethylnitrosamine (DMN) in dose of 1 ml per 100g weight [3]. After the induction, four electrodes were attached on the abdomen and the rat was placed inside the MRI bore for the MREIT imaging experiment. Using a current source, we injected a current of amplitude 3 mA and a pulse width of 81 ms. A multi-echo ICNE pulse sequence was used to obtain the magnetic flux density (B_z) data. After the imaging experiment, we sacrificed the rats and obtained the liver tissue samples for the immunohistochemical examination to prove our model. Figure(a) shows the experimental setup for MREIT conductivity imaging in liver cirrhosis model.

RESULTS Figure(b) and(c) show the MR magnitude and reconstructed conductivity images of rat liver, respectively, before and after the induction of liver cirrhosis. Compared with the conventional MR image, the present MREIT conductivity images show variation of conductivity contrast pattern corresponding to the degree of malignancy of liver cirrhosis.

CONCLUSION To investigate any change of electrical conductivity due to liver cirrhosis, rat livers having a regional cirrhosis were scanned along with separate scans of rat livers having no disease. Conductivity images shown in this study indicated that time-course variations of conductivity contrast between normal and cirrhotic regions are distinguishable in a different way compared with conventional MR image techniques.

IMAGE

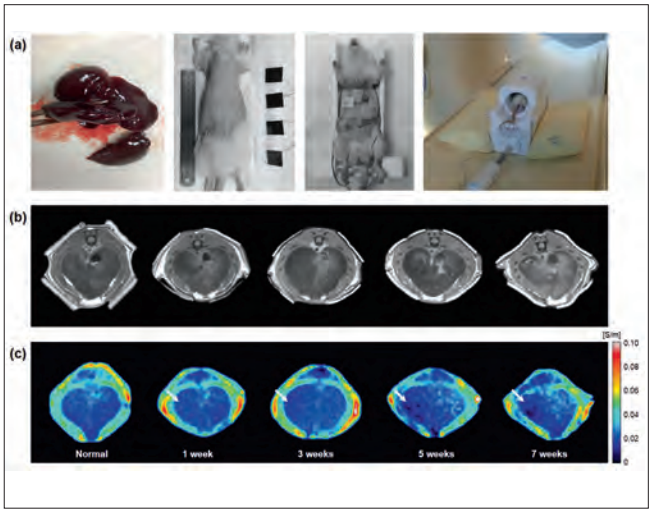

REFERENCES

1. Chauhan et al., Int. J Hyperthermia, vol. 29, pp. 643–652, 2013.
2. Woo et al., Physiol. Meas., vol. 29, pp. R1-R26, 2008.
3. George et al., Toxicology, vol. 156, pp. 129-138, 2001.

Abstract Id: 268
Topic: *Electrical impedance tomography*

MULTISPECTRAL EIT: A MANIFOLD APPROACH

Stephane Bonnet*[1], Alexandre Fouchard[1], Olivier David[2]

[1]LETI/DTBS, CEA LETI, Univ. Grenoble Alpes, Minatec, Campus,
[2]Univ. Joseph Fourier, Grenoble Institue of Neuroscience, Grenoble, France

INTRODUCTION MFEIT using spectral constraints has been introduced recently by Holder and collaborators in [1]. It makes use of material basis decomposition where the conductivity at a given element is a linear combination of known tissue conductivities. This approach is well suited for the case of static imaging where the source of contrast lies entirely in the electrical difference between tissues.

OBJECTIVES The proposed article proposes to perform minimization over the oblique manifold to deal with the constraint that proportions sum to one for each finite element. A fraction volume approach is demonstrated with explicit Euclidean gradient and minimization over the oblique manifold. we reconstruct the proportion distribution map for each supposed material. Results are shown with encouraging results on simulated data.

METHODS The conductivity in each finite element is a linear combination of several known tissue conductivities. By using a change of variable , it is possible to consider the oblique manifold . The optimization is carried out over the manifold using Manopt toolbox [2]. The Euclidean gradient is computed using the chain rule. As in [1], a Markov Random field (MRF) regularization term is added. This term can be efficiently computed using the Laplacian matrix of the graph.

RESULTS A medium with two components – background and conductive inclusion – was considered, and their spectra were assumed known. Synthetic multispectral data was predicted by FEM. Reconstructions were performed on a 14 equally-spaced electrode 2D model (3,527 nodes, 6,713 elements, different from the forward mesh). The estimated proportions were deduced using FVE [3]. Compared with a one frequency implementation, the quality of the reconstruction improved, featuring very few artefacts and low ringing effects.

CONCLUSION The proposed MFEIT framework is efficient to reconstruct EIT images by using spectral constraints. Minimization over oblique manifold allows ensuring valid proportion of materials at each finite element.

REFERENCES

1. Malone E, dos Santos G S, Holder D, Arridge S, *IEEE Med. Imaging,* **33** (2): 340, 2014.
2. Absil P-A, Mahony R, Sepulchre R, Optimization algorithms on maxtrix manifolds, Princeton University Press, 2008.
3. Fouchard A, Bonnet S, Hervé L, David O, *Journal of Physics: Conf Series*, **542** (1) 2014.

Abstract Id: 269
Topic: *Electrical impedance tomography*

IMAGE FUSION OF CT/EIT USING 3D DISCRETE COSINE TRANSFORM

Benjamin Schullcke[*1], Bo Gong[1], Sabine Krueger-Ziolek[1], Knut Moeller[1]

[1]Institute of Technical Medicine, Furtwangen University, VS-Schwenningen, Germany

INTRODUCTION Compared to X-ray computed tomography (CT), Electrical Impedance Tomography (EIT) lacks of spatial resolution, but is able to track fast processes in the lung and therefore identify functional abnormalities in obstructive lung diseases [1, 2]. We propose an approach that utilizes morphological information extracted from CT to reconstruct 3D images of lung ventilation, which can be regarded as patient-specific Electrical Impedance Tomography.

OBJECTIVES To obtain a comprehensive insight into the pulmonary pathophysiology it is required to combine functional and structural data, as it is already done in combined imaging modalities, such as e.g. PET-CT. The proposed EIT reconstruction approach is based on a three-dimensional Discrete Cosine Transform (3D-DCT), with the objective to enable image fusion of morphologic (CT) and functional (EIT) images.

METHODS Voltage changes caused by ventilation inhomogeneities of the lungs were simulated on a realistic virtual phantom, with 2 belts and 32 electrodes. The dimensionality of the reconstruction problem was reduced utilizing 3D-DCT. A one-step Gauss-Newton solver was used to reconstruct DCT coefficients from which three dimensional images of lung ventilation were generated.

RESULTS Blurring of reconstructed images into regions not belonging to the lungs is prevented. Images of lung ventilation reconstructed with the 3D-DCT approach can easily be superimposed with morphological data. Due to the decrease in dimensionality of the model formulation the computational costs are reduced.

CONCLUSION Merged CT-EIT data might be used by pulmonologists or radiologist to correlate morphological changes in the lungs with ventilation distribution especially whenever CT is available anyway.

IMAGE

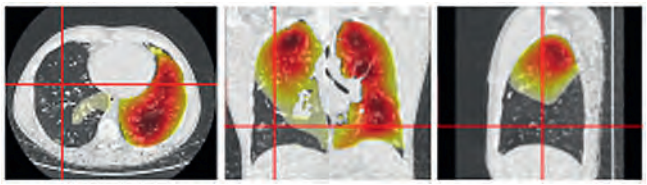

REFERENCES

1. Z. Zhao, et al., "Regional airway obstruction in cystic fibrosis determined by electrical impedance tomography in comparison with high resolution CT," Physiol Meas, vol. 34, pp. N107–14, Nov 2013.
2. B. Vogt, et al., "Spatial and temporal heterogeneity of regional lung ventilation determined by electrical impedance tomography during pulmonary function testing," Journal of Applied Physiology, vol. 113, pp. 1154–1161, 2012.

Abstract Id: 270
Topic: *Electrical impedance tomography*

EIT DIAGNOSIS OF PRE- AND MICROINVASIVE CERVICAL CANCER

Olga Trokhanova*[1], Yulia Chijova[1], Mikhail Hitrov[1],
Timur Tuykin[2], Alexander Korjenevsky[2]

[1]Yaroslavl State Medical University, Yaroslavl, [2]Kotel'nikov Institute of
Radio Engineering and Electronics of the RAS, Moscow, Russian Federation

INTRODUCTION Cervical cancer ranks second or third place in terms of incidence. Cervical cancer is infrequently diagnosed on microinvasive stage by the standard methods of investigation. A high percentage of advanced forms of cancer and unsatisfactory treatment results determine the need for new in-depth methods of diagnostics.

OBJECTIVES to reveal possibilities of the method of electrical impedance tomography in the diagnosis of preinvasive (0 stage) and microinvasive (IA stage) cervical cancer.

METHODS A comprehensive examination of the cervix has been carried out in 90 women aged 18 to 60 years (63 women without cervical pathology, 27 women with cervical cancer). Methods of diagnosis have included: clinical and anamnestic, pelvic examination, direct microscopic and bacteriological research, oncocitology, molecular-biological method, immunocytochemical determination of tumor marker r16ink4a, extended colposcopy, cervical biopsy, cervical electrical impedance tomography. The EIT was carried out using dual-frequency measuring system with 48 electrodes arranged in planar circular array and 3D backprojection image reconstruction [1].

RESULTS The features of electrical conductivity in norm and cervical cancer have been revealed in the scanning depth of 2, 5 and 8 mm, as well as in the area of transformation. A comparative analysis between the conductivity at scanning level 1 (2 mm) has been carried out, which showed statistically significant differences in the absence of pathology and cancer of the cervix in stage 0 (carcinoma in situ) and stage IA (microinvasive cancer) in all age groups. The sensitivity of the method of electrical impedance tomography in the diagnosis of preinvasive and microinvasive cervical cancer is 93%.

CONCLUSION The differences in conductivity between norm and early forms of cervical cancer revealed during the research can be used as reliable criteria for the diagnostics of the cervix using the method of electrical impedance tomography. Electrical impedance tomography is a good addition to the traditionally used methods of diagnosis of cervical diseases. But despite the reliability and detection of minimal deviations in the conductivity with the primary forms of cancer, it is necessary to be guided by the results of a comprehensive examination including histological verification of the diagnosis.

REFERENCES

1. Cherepenin V A *et al* 2012 *Physiol. Meas.* **33** 849–862.

Abstract Id: 271
Topic: *Electrical impedance tomography*

OPTIMISING THE INJECTION PROTOCOL FOR FAST NEURAL EIT

Mayo Faulkner*[1], Markus Jehl[1], Kirill Aristovich[1], David Holder[1]

[1]Medical Physics and Biomedical Engineering, UCL, London, United Kingdom

INTRODUCTION EIT can image fast neural activity in the cortex with temporal and spatial resolution of 2ms and 200 μm respectively [1]. There is the potential for it to concurrently image activity from deep structures, which would allow the propagation of activity to be tracked throughout the brain. For this to be realised, the EIT measurement protocol must concentrate current into deep structures.

OBJECTIVES The objective of this work was to develop a method to optimise the current injection protocol based on a region of interest (ROI) in the brain. The optimal protocol was defined as that which concentrates as much current in the ROI, while acquiring the maximum number of independent measurements.

METHODS A 3D atlas of the rat brain was created using a method based on that described in [2]. Areas of interest were highlighted in slices of a rat atlas [3] (fig 1a). The slices were stacked together into a 3D volume and highlighted areas segmented (fig 1b). A 2 million element mesh of the rat brain was overlaid onto this atlas and the coordinates of the ROI within the mesh determined (fig 1c). Electrodes, in positions identical to those used in realistic experiments, were then placed on the surface of the mesh (fig 1d). The current density in the brain was evaluated for every possible injection pair. A maximum spanning tree, weighted by the total current density in the ROI, was then applied to find the optimal injection protocol.

RESULTS The average current density per injection concentrated in the ROI using the optimal protocol was 0.39 A/m^2. This compares with a value of 0.19 A/ m^2 that was used in previous experiments attempting to image deep activity.

CONCLUSION A method has been developed to optimise the current injection protocol based on a ROI. This method is flexible allowing the protocol to be tailored to investigating different areas of the brain. Experiments are currently being undertaken using this optimised protocol to attempt to image fast neural activity in the thalamus of anesthetised rats during forepaw and whisker stimulation.

IMAGE

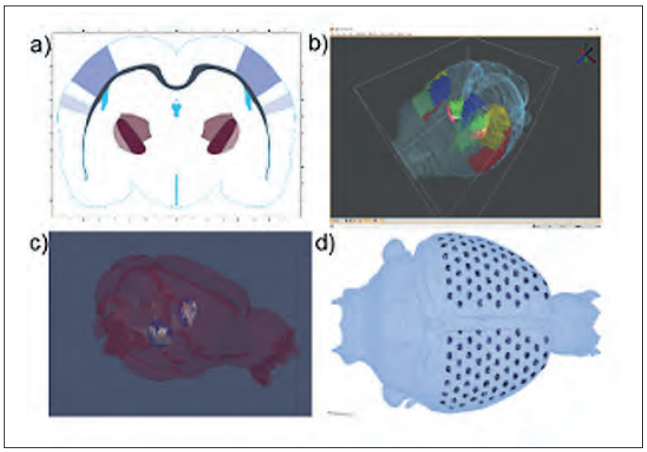

***Figure 1a**) Highlighted structures in coronal slice of rat brain **b)** 3D segmentation of structures in rat brain **c)** FEM mesh with ROI overlaid **d)** FEM mesh with electrodes on surface.*

REFERENCES

1. Aristovich, K. Y et al. *NeuroImage*, *124* (2016), 204–213.
2. Hjornevik T et al. *Frontiers in Neuroinformatics*. 2007;1:4.
3. Paxinos G and Watson, C. (2014). The Rat Brain in Stereotaxic Coordinates, 7th Edition, Elsevier Academic Press.

Abstract Id: 272
Topic: *Electrical impedance tomography*

DRIFT – THE CHALLENGE IN BRAIN MONITORING WITH TD-EIT

Nir Goren*[1], James Avery[1], Kirill Aristovich[1], Markus Jehl[1], David Holder[1]

[1]Medical Physics & Bio-medical Engineering, University College London, London, United Kingdom

INTRODUCTION After brain injury, early detection of intracranial injury such as Intracerebral haemorrhage (ICH) could benefit stroke and TBI patients. In EIT, noise in recorded boundary voltages (BV) over time, including drift caused by contact impedance (CI) changes, can degrade the resulting images (Boone & Holder, 1996). In our recent feasibility study, the drift in baseline BV was 4±2.9% (mean ±1SD) over 3.5 hours while the simulated expected signal for ICH was 2–8% depending on size and location. The detection of secondary ICH might therefore be possible in spite of boundary voltage drift.

OBJECTIVES To describe drift characteristics, and investigate the underlying causes in order to compensate for these factors and enable smaller and slower changes to be detected.

METHODS Continuous EIT recordings over 6 hours, at 2KHz were taken in 6 healthy subjects, with Easycap 16 EEG scalp electrodes headnet. BV were corrected with a reciprocity drift eliminating (RDE) protocol which used redundant reciprocal measurements to compute and reduce CI related drift. Equivalent recordings were made on a resistor phantom to measure the inherent drift in the system. The spatial distribution of the drift across the scalp and correlation to baseline BV amplitude were analysed. The contribution of CI changes (using RDE) and electrode movement (EM) (Jehl et al, 2015) to the overall drift were calculated.

RESULTS Across all subjects, drift was between 2.6±6.6% to 6±23.1% (mean ±1SD) across channels, of the standing BV over 6 hours. Drift was linear over time and higher in the frontal (~7%) than the rear (~3%) parts of the scalp. System drift as measured on a resistor phantom was 0.8±1%. ΔCI and movement related drifts were ~0.5 and ~ 0.2% respectively and so much smaller than the BV drift.

CONCLUSIONS Drift values were consistent with our former findings. They did not appear to be caused by instrumentation, ΔCI or by electrode movement and most probably reflected actual impedance changes in the scalp or in the gel between the electrodes and scalp. Work is in progress to collect additional data to isolate the cause of drift, to determine how it can be corrected, and to record pilot clinical data in stroke patients.

IMAGE

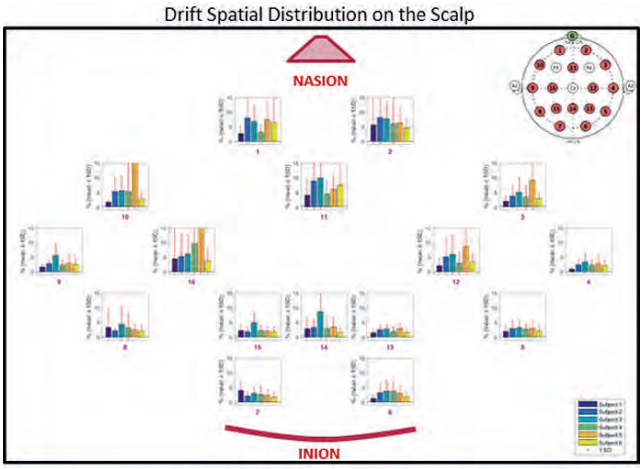

Spatial distribution of drift in EIT measurement on the human scalp.
Each bar graph represents drift (% of the standing BV, mean ±1SD) of 6 healthy subjects at a specific electrode location. Electrodes montage is illustrated also on the upper right corner.

Abstract Id: 273
Topic: *Electrical impedance tomography*

FEASIBILITY OF PARALLEL EIT SIMULTANEOUS TO EEG IN NEONATES

James Avery*[1], Thomas Dowrick[1], Markus Jehl[1], Kirill Aristovich[1], David Holder[1]

[1]Department of Medical Physics and Biomedical Engineering, UCL, London, United Kingdom

INTRODUCTION Simultaneous measurement of EIT with conventional EEG recordings has been proposed as a method for improvement of epileptic foci localisation[1]. Recent work has demonstrated the feasibility of imaging with conventional serial-inject EIT measurements in a realistic tank. However, EIT switching artefacts prevent correlation with EEG, and limit its clinical potential. Frequency multiplexed EIT (FM-EIT), wherein current is injected continuously on a subset of electrodes at different frequencies, has been proposed as a solution, allowing simultaneous uncorrupted EEG recordings. However, this imposes restrictions on the EIT measurement paradigm, in reduced current amplitude and fewer injection pairs. The extent to which this is detrimental to image quality is not yet understood.

OBJECTIVES To assess the feasibility of localisation of epileptic foci with FM-EIT with a reduced number of injections in a realistic neonatal head tank.

METHODS Data were collected in a neonatal head tank with a skull of realistic conductivity. Current was injected continuously between four pairs of electrodes, with 60 μA amplitude 500 Hz spacing. Voltages were recorded on all 32 electrodes in parallel. Injection pairs were chosen to align with the fontanelles. The signal at each carrier frequency was demodulated separately with a temporal resolution of 100 ms. Images of each time point were reconstructed in a 220,000 element hexahedral mesh of 1.5 mm element size using cross validated zeroth-order Tikhonov regularisation with noise based correction[2]. Images were collected during the insertion of a 18 mm plastic perturbation, and a sponge of 10% contrast into an area approximating the frontal lobe.

RESULTS The plastic perturbation (fig 1a) was reconstructed with similar localisation accuracy to conventional serial injections <2.5 %, however; the shape and noise error doubled. The reconstruction of the sponge perturbation (fig 1d) had a 5.2% localisation error, albeit with significant artefacts compared to simulation (fig1 b), with 5% shape error and 10% noise error values.

CONCLUSION Results suggest that FM-EIT may have sufficient resolution to enable localisation of superficial seizures. However, the reduced SNR necessitates improvements of the choice in injection pairs and signal processing. Work is ongoing to optimise the image reconstruction for this specific application.

IMAGE

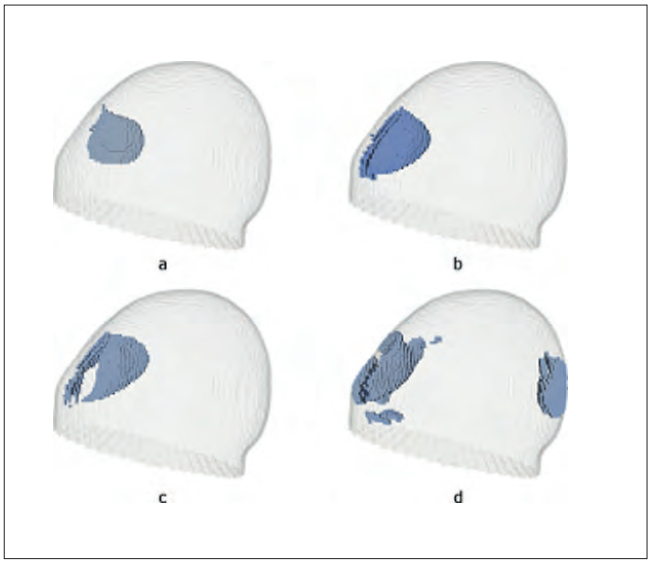

REFERENCES

1. Fabrizi L, et al (2006) *Phys Meas*, 27(5), S163–S174.
2. Aristovich K, et al (2014) *Phys Meas*, 35(6), S1095–S109.

Abstract Id: 274
Topic: *Electrical impedance tomography*

A METHOD FOR IMAGING EPILEPSY WITH EIT AND DEPTH ELECTRODES

Anna Witkowska-Wrobel[*1], Kirill Aristovich[1], James Avery[1], David Holder[1]

[1]Department of Medical Physics and Biomedical Engineering, University College London, London, United Kingdom

INTRODUCTION EIT can image fast neural activity in the rat somatosensory cortex with an accuracy of <200 µm and 2ms with an array of 30 epicortical electrodes and 50 µA current at 1.7 kHz [1]. However, sensitivity is reduced for deeper structures. Currently, depth and subdural surface electrodes are used for presurgical screening in severe epilepsy patients [2] and could be used to perform fast neural EIT for improved clinical imaging of epilepsy.

OBJECTIVES A pilot study was planned but, for ethical reasons, had to use available depth electrodes implanted for clinical purposes. The aim of this study was to evaluate our fast neural EIT method with such a novel electrode arrangement in computer simulation.

METHODS A 6.5mln tetrahedral elements mesh of a human head was generated from segmented tissue layers from one patient using preimplantation MRI and post-implantation CT scans [3]. 7 depth electrodes with 48 recording contacts (1.1 x 2.4mm each) were implanted in mesial temporal, orbitofrontal and cingulate regions and modelled. Tissue conductivities and electrode locations were defined from the imaging data. The accuracy of reconstruction was evaluated by placing a sphere 5 mm in diameter and local conductivity increase of 10% were in 957 locations throughout the head. A current injection protocol was chosen to maximize the distance between injecting contacts with 47 injections of 50 µA current and 2 162 individual measurements for each perturbation. 10 000 hexahedral elements mesh was used for inverse reconstruction.

RESULTS AND CONCLUSION Using the current reconstruction technique [4], 60% of locations were identified with accuracy <5mm, however 40 % of perturbations were not reconstructed correctly (error > 10mm). This may be attributed to the limited coverage of the brain overall by depth electrodes placed in restricted regions of clinical interest. Accuracy was high for reconstruction within the volume enclosed by the depth electrodes. For example (Fig. 1), a single perturbation in the cingulate gyrus was reconstructed with 0.4mm centre-to-centre error, and 70% distortion (FWHM shape error).

Work in progress is to improve accuracy by the addition of subdural electrode grids and scalp electrodes and to cross-correlate with simultaneous EEG inverse solutions.

IMAGE

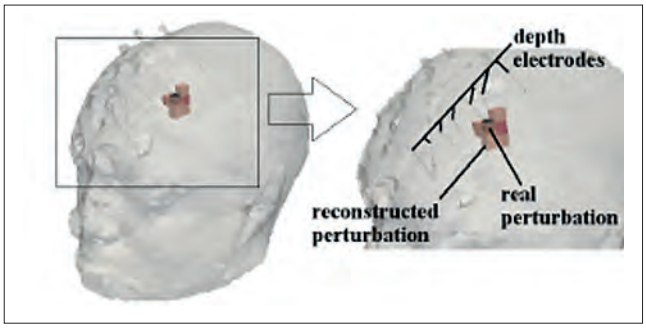

REFERENCES

1. Aristovich KY, et al. Neuroimage 2016; 124(Pt A): 204–213.
2. Wellmer J, et al. Epilepsia 2012; 53(8): 1322–1332.
3. Jehl M, et al. Phys.Meas. 2016; in press.
4. Aristovich KY, et al. Phys. Meas. 2014; 35(6): 1095–1109.

Abstract Id: 275
Topic: *Electrical impedance tomography*

MULTI-MODAL HOME SLEEP APNEA MONITOR USING EIT

Guek Young Jang*[1], Min Hyung Lee[1], Hun Wi[1], Tong In Oh[1], Eung Je Woo[1]

[1]Department of Biomedical Engineering, Kyung Hee University, Seoul, Republic of Korea

INTRODUCTION There is a growing prevalence of obstructive sleep apnea (OSA) among the middle-aged or aged men and women. Recent studies have shown the high coincidence of OSA with cardiovascular diseases [1]. Though the polysomnography is a current gold standard to for its diagnosis, there exist unmet clinical needs for a portable sleep apnea monitor for home use. The portable monitor provides long-term (8 hours, for example) direct quantification of different breathing stages using chest EIT as well as ECG, SpO2, body position and snoring sound.

OBJECTIVE We developed a prototype of a multi-modal home apnea monitoring system and conducted experimental studies for its performance analysis. The main goal was to validate the feasibility and significance of chest EIT as a direct image-based method for breathing stage classification including OSA and different levels of insufficient breathing.

METHODS We designed the multi-modal home sleep apnea monitor as a long-term real-time data logger for chest EIT, ECG, SpO2, body position and snoring sound. The system includes a compact data recorder connected to a chest sensor belt for EIT, ECG, body position and snoring sound. For SpO2 signals, a conventional finger sensor should be also connected to the data recorder. We collected data during 8-hour sleeps and analyzed them using a custom-developed sleep apnea analysis software.

RESULTS We could reliably collect EIT, ECG, SpO2, body position and snoring sound data using the developed battery-power compact device and sensor belt. Functional EIT image analysis results clearly distinguished different breathing stages including OSA. Integrated time-series analyses combining all acquired signals showed consistent causality among them.

CONCLUSION The developed multi-modal apnea monitor can be used to collect 8-hour data of chest EIT, ECG, SpO2, body position and snoring sound. With the addition of compact chest EIT data logging capability, the home monitoring system is expected to replace the expensive and cumbersome polysomnography at hospital.

REFERENCES

1. Mueller et al., Journal of Sleep Research, vol. 15, pp. 455–462, 2006.
2. Collop et al., J. Clin. Sleep Med., vol. 3(7), pp. 737–747, 2007.
3. H. Wi et al., IEEE Trans. on BioCAS , vol. 8, pp. 119–128, 2014.

Abstract Id: 276
Topic: *Electrical impedance tomography*

COMPARING PARALLEL & SEQUENTIAL EIT IN HEAD TANKS AND NERVE

Thomas Dowrick[*1], James Avery[1], David Holder[1]

[1]Medical Physics, University College London, London, United Kingdom

INTRODUCTION Frequency division multiplexed EIT (FDM-EIT) uses parallel injection at multiple frequencies [1], and can result in increased temporal resolution when compared to single frequency, time division multiplexed EIT. For certain applications, where switching artefacts are undesirable, or where the frequency range of interest is limited, e.g. imaging of neural signals [2], FDM may offer superior performance when compared to sequential measurements.

OBJECTIVES Carry out a side-by-side comparison of parallel and sequential EIT in realistic head tanks and animal models, to answer the following questions: 1) Can parallel EIT produce images of comparable quality to sequential measurements? 2) Are there trade-offs in terms of signal bandwidth/spatial accuracy?

METHODS Tank experiments have been carried out to image static objects in a realistic neonatal head tank, with a saline background. Both parallel (4 injection pairs - 500 Hz, 1000 Hz, 1500 Hz, 2000 Hz) and sequential (2 kHz, 31 injection pairs) measurements were made. A plastic ball, 30 mm in diameter was placed at various locations in the tank. Experiments are ongoing to compare the two techniques in in-vivo experiments, to image inside nerve bundles in rats.

RESULTS Both methods successfully reproduce the location of tank perturbations (Figure 1). More artefacts are visible for the parallel method, due to the smaller number of injection pairs used.

CONCLUSIONS FDM has been shown to offer comparable imaging performance in a realistic head tank. Further work is being undertaken to investigate any trade-offs in performance between signal bandwidth, temporal accuracy and spatial accuracy.

IMAGE

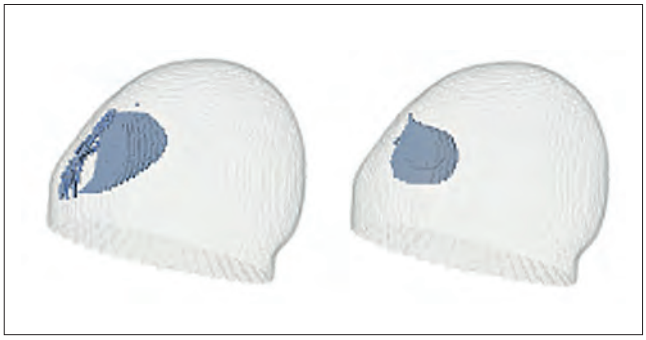

***Figure 1**. Image reconstruction in neonatal head tank using parallel (left) and sequential (right) injections.*

REFERENCES

1. Y. Granot, A. Ivorra, and B. Rubinsky, "Frequency-division multiplexing for electrical impedance tomography in biomedical applications.," *Int. J. Biomed. Imaging*, vol. 2007, p. 54798, Jan. 2007.
2. A. Liston, R. Bayford, and D. Holder, "A cable theory based biophysical model of resistance change in crab peripheral nerve and human cerebral cortex during neuronal depolarisation: implications for electrical impedance tomography of fast neural activity in the brain.," *Med. Biol. Eng. Comput.*, vol. 50, no. 5, pp. 425–37, May 2012.

Abstract Id: 277
Topic: *Electrical impedance tomography*

A NOVAL LOW COST, PORTABLE AND MULTI-FREQUENCY EIT SYSTEM

Gurmeet Singh*[1], Harsahib Singh[2], Sneh Anand[3], Brejesh Lall[4], Vaneet Singh[2]

[1]Electronics and Communication Engineering, Indian Institute Of Technology,
[2]Electronics and Communication Engineering, Guru Tegh Bahadur Institute Of Technology,
[3]Center For Biomedical Engineering, [4]Electrical Engineering, Indian Institute Of Technology, New Delhi, India

This paper describes the methodology of design and development of a multi-frequency, Arduino Uno based 16 SS electrode EIT device. Several iterative and non-iterative algorithms have been implemented to achieve better spatial resolution keeping the SNR around 50dB. The design offers image reconstruction of both the permittivity and conductivity distributions and is low cost and portable.

INTRODUCTION After morphological and structure imaging technologies, EIT is the most potential and promising imaging technique for bioimpedance monitoring. It has wide range applications in medical and industrial fields. EIT provides both functional and structural information, also one can construct spatial of any closed domain from the potential developed at object boundaries by injecting current through an array of surface electrodes. An EIT system mainly consists of two parts: a data acquisition system and image reconstruction software. An EIT system must be tested on practical phantoms that accurately mimic the physiology and anatomy of the tissue before human subjects.

METHOD A variable frequency VCO is developed and its output is fed to a Howland current pump to obtain constant current, which is applied to electrode array surrounding the phantom tank (containing 0.9% NaCl solution), via common ground current injection method in progression. The corresponding voltages are measured from the remaining electrodes. An automatic switching circuit is developed using two 16:1 mux's which acts as digitally controlled switch having low ON impedance and low leakage current. Arduino Uno provides the control signals for the switching operation which is programmed via algorithm written in MATLAB. The signal obtained is sent to Analog input pin of Arduino Uno to transfer serially into PC for storing in MATLAB(1X256 array of data) through which image is reconstructed via interfacing with EDIORS.

RESULTS Different organic and inorganic inhomogeneties of different conductivities like vegetable and nylon are placed in tank and the output voltages are measured, analysed based on their conductivities with the designed system. From the boundary potential database and econstructed image obtained one can clearly observe the difference in conductivity and permittivity of inhomogeneties.

CONCLUSIONS The device is economical and has a huge potential to become a new and successful medical imaging modality for detection of cancer as it can distinguish different biological tissue properties.

IMAGE

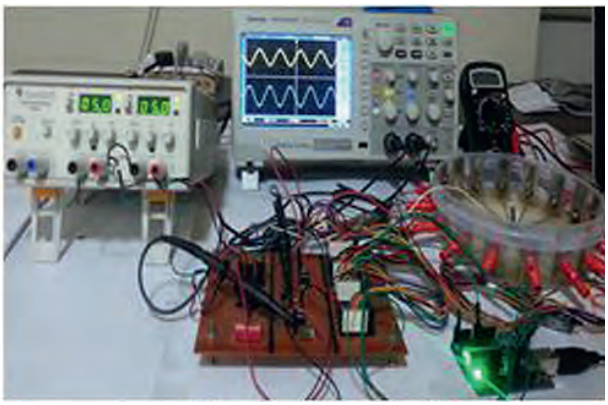

Experimental setup for EIT system.

Abstract Id: 278
Topic: *Electrical impedance tomography*

SPARSE REGULARIZATION BASED ON SPECTRAL GRAPH WAVELETS

Bo Gong[*1], Benjamin Schullcke[1], Sabine Krueger-Ziolek[1], Knut Moeller[1]

[1]Institute of technical Medicine (ITeM), Furtwangen University, VS-Schwenningen, Germany

INTRODUCTION In time-difference EIT, the underlying solution might be (partial) sparse. The EIT reconstruction under sparse regularization can be identified as a solver of the optimization problem:

$$\text{argmin}_s \| \boldsymbol{V} - \boldsymbol{J} \cdot \boldsymbol{s} \|_2^2 + \lambda \| \boldsymbol{R} \cdot \boldsymbol{s} \|_1$$

where $\boldsymbol{s}$ represents the conductivity changes, $\boldsymbol{V}$ denotes the voltage difference, $\boldsymbol{J}$ is the Jacobian matrix, $\lambda>0$ is the regularization parameter and $\boldsymbol{R}$ is the regularization matrix.

OBJECTIVES Instead of standard sparse regularization where $\boldsymbol{R}$ is the identity matrix, we employ a wavelet transform as regularization matrix to introduce local flexibility.

METHODS

1. Spectral graph wavelets

Canonical wavelet transforms are not compatible with triangular meshes with irregular boundary shape. To integrate wavelet techniques into the finite element framework, we view the meshes as undirected graphs and introduce the spectral graph wavelet transform [1] for sparse regularization.

2. Wavelet based sparse regularization

Identifying the mesh as a graph, the inverse problem will be solved on nodes instead of elements. The workflow of the reconstruction is:

1. Calculate the Nodal Jacobian [2]: $\boldsymbol{J}^{\mathrm{N}}$
2. Calculate graph wavelet transform: $\boldsymbol{W}_{\mathrm{g}}$
3. Solve the inverse problem [3]:
   $\text{argmin}_s \| \boldsymbol{V} - \boldsymbol{J}^{\mathrm{N}} \cdot \boldsymbol{s} \|_2^2 + \lambda \| \boldsymbol{W}_{\mathrm{g}} \cdot \mathrm{s} \|_1$

RESULTS The performances of standard and wavelet based sparse regularization were demonstrated on simulation and real data. For brevity, in the figure below, just results of simulated data with respect to different noise levels are shown. Compared to standard sparse regularization (upper row of subfigure (c)), wavelet based regularization obtains smoother images (lower row of subfigure (c)). The same effect is found in clinical reconstructions for functional ventilation and perfusion imaging.

CONCLUSION Wavelets introduce local flexibility which may reduce small turbulences of reconstructed images.

IMAGE

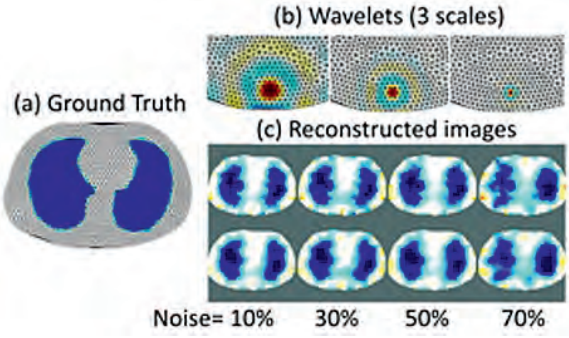

REFERENCES

1. Hammond, D.K., ACHA, 2011. **30**(2): p. 129–150.
2. Graham, B., *et al.,* Int. J. Inform. Syst. Sci., 2006. **2**.
3. S. Osher., *et al.,* COMMUN MATH SCI, 2010. **8**(1): p. 93–111.

Abstract Id: 279
Topic: *Electrical impedance tomography*

DETERMINING HEART REGION IN EIT IMAGES BY LINEAR REGRESSION

Sabine Krueger-Ziolek[*1], Zhanqi Zhao[1], Benjamin Schullcke[1], Bo Gong[1], Knut Moeller[1]

[1]Institute of Technical Medicine, Furtwangen University, Villingen-Schwenningen, Germany

INTRODUCTION EIT has the potential to measure ventilation and perfusion related impedance changes in the lung. During pulmonary perfusion analysis, the influence of impedance changes caused by the heart is often reduced by choosing regions of interest (ROI) excluding the ventricular regions. Frerichs et al. [1] proposed a procedure involving frequency filtering and a linear regression fit to define ventilated and perfused lung regions as well as the ventricular region. We systematically investigated the influence of the size of the perfused lung region used for the linear regression fit on the size of the identified ventricular region.

OBJECTIVES To analyze the impact of threshold values (size of perfused lung region) on the size of the ventricular region within functional EIT images obtained by linear regression.

METHODS A slightly modified version of the method of Frerichs et al. [1] was applied to EIT measurements in the 5th intercostal space of 5 healthy spontaneously breathing subjects. A bandpass filter was used to separate ventilation from cardiac/perfusion signals. Pixels belonging to the lung were identified by a linear regression fit with this ventilation signal. Lung pixels with values larger than a threshold (from 1 to 100 %) of the maximum value found in the EIT image were utilized to extract the cardiac/perfusion signal used for the determination of the ventricular region (quantity of pixels) by linear regression. Pixel values less than 20 % of the minimum value of the functional image were included to the ventricular region.

RESULTS In all subjects the size of the ventricular region (number of pixels) depended on the size of the perfused lung region used for the linear regression fit (Figure). An increase of the number of pixels as a function of a decrease of the size of the perfused lung region was obtained. Inter-subject variability of the results is displayed as error-bars.

CONCLUSION Identification of the ventricular region relies on the size of the perfused lung region used in the linear regression fit.

IMAGE

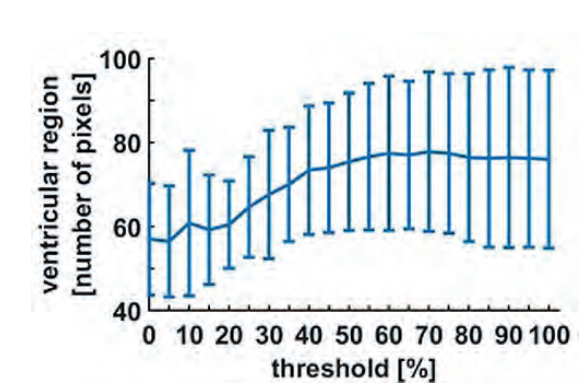

REFERENCES

1. I. Frerichs, S. Pulletz, G. Elke, F. Reifferscheid, D. Schadler, J. Scholz, and N. Weiler, "Assessment of changes in distribution of lung perfusion by electrical impedance tomography," Respiration, vol. 77 (3), pp. 282–91, 2009.

Abstract Id: 280
Topic: *Electrical impedance tomography*

ROTATIONAL EIT SETUP OPTIMIZATION

Mari Lehti-Polojärvi[*1], Olli Koskela[1], Akseli Leino[1], Edite Figueiras[2], Jari Hyttinen[1]

[1]Tampere University of Technology, BioMediTech, Tampere, Finland,
[2]International Iberian Nanotechnology Laboratory, Braga, Portugal

INTRODUCTION We propose to build a new rotational electrical impedance tomography (EIT) setup to be used for cell culture monitoring.[1,2] In this setup, the sample is rotated and measurements are done using fixed electrodes on each side of the sample.

OBJECTIVES The rotation of the sample allows us to use small amount of electrodes to achieve EIT. The aim of this study is to develop and demonstrate the use of different current stimulation and voltage measurement patterns using computational simulations.

METHODS We simulate an eight electrode system; four on each side of the sample (1-4, 5-8), as is shown in Fig.1 (a). Three different methods are designed based on sensitivity field simulations[2].

Method 1: current is injected with opposing electrodes 2-6 and voltage measured using three possible opposites, and also pattern 1-3:2-4 is used.

Method 2: current is injected with opposing electrodes 2–6 and voltage measured using nine possible opposites, and also patterns 1-3:2-4 and 1-4:2-3 are used.

Method 3: current is injected with opposing electrodes and, additional to Method 2, all three possible pairings on both sides are measured, also patterns 1-3:2-4, 1-4:2-3 and 2-1:3-4 are used. 32 rotational locations are used in the finite element method simulation for all the electrode arrangements.

Images are reconstructed in EIDORS with a PDIPM TV solver using Total Variation prior[3]. Gaussian noise was added to the simulated voltages. Model consists of three different conductivity regions: outer ring = 0.2, background = 0.8 and clusters = 0.01. Clusters are the regions of interest.

RESULTS Schematic of the rotational EIT setup and the inhomogeneous model used in the reconstructions is shown in Fig. 1 (a). Resulting images for Methods 1–3 are shown in Fig. 1 (b). High conductivity areas are filtered from reconstructed images for better visualization in Fig. 1 (c).

Measurements in Method 1 are not enough to produce a proper image of the model. Using Method 2, regions of interest become visible, and using Method 3, image quality enhances slightly.

CONCLUSIONS Simulations show that it is possible to obtain rotational EIT images with very limited electrode positioning. However, several different stimulus and measurement patterns are required.

IMAGE

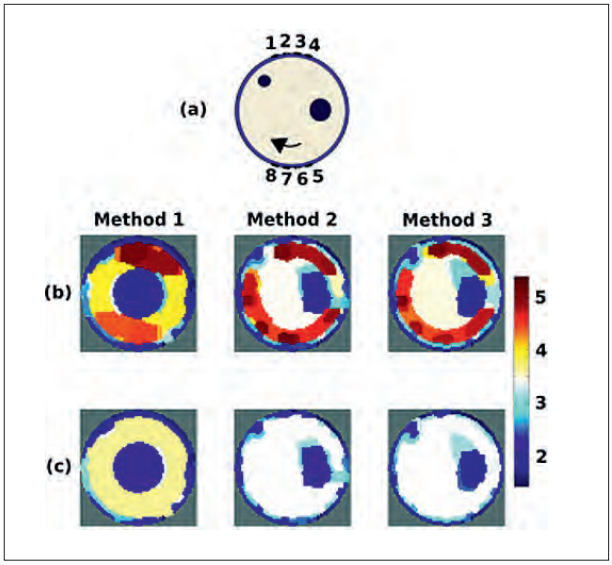

REFERENCES

1. Appel A A. et al. Biomaterials 34: 6615–30, 2013.
2. Lehti-Polojärvi M. MSc thesis, Tampere University of Technology, 2014.
3. Borsic A. et al. The University of Manchester. 2007.

Abstract Id: 281
Topic: *Electrical impedance tomography*

CONTINUOUS REGIONAL ANALYSIS DEVICE FOR NEONATE LUNG (CRADL)

Richard Bayford*[1], Andrew Tizzard[1], Inéz Frerichs[2], Norbert Weiler[2], Tobias Becher[2], Christina Karaoli[3], Christofides Christofides[4], Charalambos Yiannakkaras[4], Peter Rimensberger[5], Sven Nordebo[6], Stephan Böhm[7], Anton van Kaam[8], Bruce Fifield[9], Christopher Knox[10], Lotte Steuten[11], Gimon de Graaf[11], Rebecca Yerworth[12], Micheal Butterworth[1], Andreas Demosthenous[12]

[1]Middlesex University, London, United Kingdom, [2]Universitätsklinikum Schleswig-Holstein, Kiel, Germany, [3]Archbishop Makarios III , [4]Biomedical research Foundation, Nicosia, Cyprus, [5]HCUGE, University of Genève, Switzerland, [6] Linnaeus University, Kalmar, Sweden, [7]Swisstom, Landquart, Switzerland, [8]CAU-UKSH, Amsterdam, Netherlands, [9]Studiofifield.com, [10]Studiofifield.com, Milano, Italy, [11]PANAXEA b.v., Antwerpen, Netherlands, [12]UCL, London, United Kingdom

INTRODUCTION Each year 15 million babies are born prematurely and many suffer from respiratory failure due to immaturity of the lung and lack of control of breathing. Heterogeneity of lung aeration, resulting in areas of lung over inflation and lung collapse, plays a crucial part in the risk of mortality and morbidity due to respiratory failure. This distribution of lung aeration cannot be detected by conventional bedside monitoring tools and imaging methods. Thus, an imaging technique for continuous non-invasive bedside monitoring of infants lung function is urgently needed. In order to address this, a new project known as CRADL has been estabished which will use EIT technology to monitoring interventions in the paediatric population by providing quantative information on regional lung aeration and ventilation to guide the optimization of respiratory therapy by applying EIT-based imaging system for *in-vivo* monitoring of neonatal and paediatric lung function in ICUs.

METHOD The purpose of this research project is to provide quantative information on regional lung aeration and ventilation to guide the optimization of respiratory therapy by applying an EIT-based imaging system for *in-vivo* monitoring of neonatal and paediatric lung function in ICUs. The system will provide a non-invasive measure of lung homogeneity and lung function, suitable for use in small infants, whether breathing spontaneously or requiring assisted ventilation, and also older infants and children with respiratory failure. Furthermore, the results of this project can also translate to adults with respiratory failure, because the basic concepts are similar in the paediatric and adult population.

RESULTS The project started in January 2016 funded by the EU and Swiss government to the value of 5.5 MEuros, consisiting of 11 parteners. It represents a milestone in the development of EIT for clinical use; initial results on the projects progress will be presented during the conference. Figure 1 illustrates the overall concept of the project.

ACKNOWLEDGEMENTS This project has received funding from the European Union's Horizon 2020 research and innovation programme under grant agreement No 668259. This reflects only the author's views and that the Commission is not responsible for any use that may be made of the information it contains. (www.cradlproject.org)

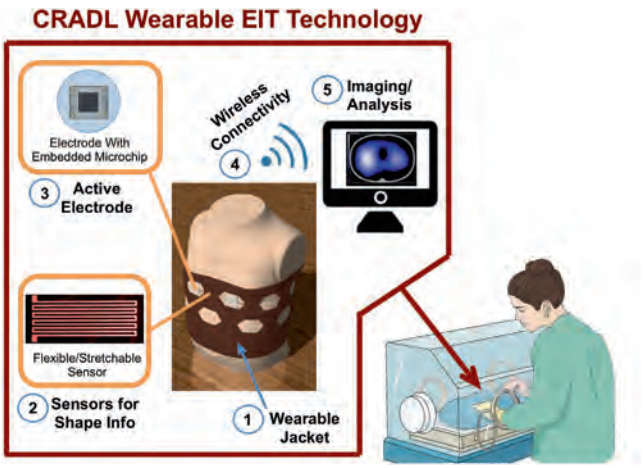

Abstract Id: 282
Topic: *Electrical impedance tomography*

INFLUENCE OF BODY MOVEMENT IN EIT BLADDER VOLUME ESTIMATION

Carlos Castelar*[1], Niklas Schmidt[1], Thomas Schlebusch[1], Dorothea Leonhäuser[2], Ferdinand Bergamo[3], Catherine Disselhorst-Klug[3], Steffen Leonhardt[1], Marian Walter[1]

[1]Philips Chair for Medical Information Technology, RWTH Aachen University, [2]Department of Urology, RWTH Aachen University Hospital, [3]Dept. of Rehabilitation and Prevention Engineering, Institute of Applied Medical Engineering, RWTH Aachen University, Aachen, Germany

INTRODUCTION Paraplegics suffer from an impaired bladder volume sensation and empty their bladders by self-catheterization under fixed time schemes. A demand-driven approach aided by a continuous non-invasive bladder volume estimation technique would be preferred. Electrical impedance tomography has been proposed as an alternative [1]. However, strong movement artifacts have been observed.

OBJECTIVES Analyze whether a correlation exists between lower abdomen EIT measurements and electrode displacement by performing simultaneous EIT and motion capture measurements on a male subject.

METHODS EIT measurements were conducted on a male subject with a Goe MF II device (Abimek, Friedland, Germany) and a 1 x 16 electrode ring arrangement of standard ECG electrodes (3M, Minnesota, United States) placed at the level of the symphysis. A 5 mA current at 50 kHz was injected in an adjacent pattern. Simultaneously, a Vicon motion capturing system (Vicon, Oxford, Great Britain) was used to record the space coordinates of all EIT electrodes. 20 pre-defined movement patterns were performed by the subject while sitting, standing, and on the supine position. Since liquid ingestion was interrupted and the measurements were done during a short time span, the influence of own diuresis is considered negligible.

RESULTS The graph shows the result for EIT voltage index 11 while the subject bent his right knee three consecutive times on the supine position. The solid curve is the normalized raw voltage data measured between electrodes 13 and 14, located on the right hip. The z-component of the hip angle trajectory is depicted as a dashed line. There is a strong correlation between both curves ($r > 0.95$). Similar results are obtained for the influence of electrode pair displacement and single electrode pair voltages (e.g. voltage indexes 13, 23, 159).

CONCLUSION Electrode displacement has a strong influence on EIT measurements of the lower abdomen. The fact that the curves follow the same pattern but do not match exactly hints to a probable additional influence of internal organ and muscle shift due to different body postures and movements, which affect the reproducibility of the impedance cystovolumetry method. Therefore a standardized position and minimal movement of the subject is recommended. Methods to movement artifact compensation will be addressed in future work.

IMAGE

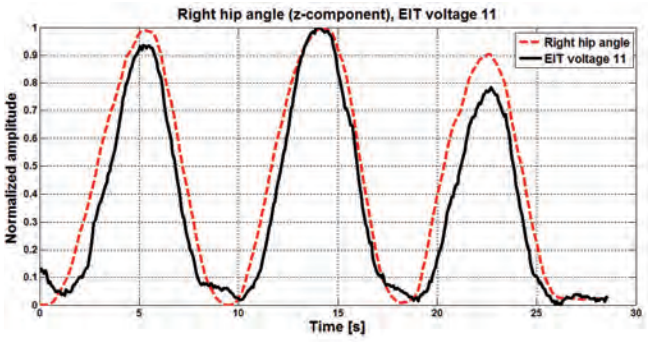

REFERENCES

1. Schlebusch T, et al. *Pysiol. Meas*. 35:1813–1823, 2014.

Abstract Id: 283
Topic: *Electrical impedance tomography*

CONSTRUCTION OF A ROBUST BEAGLE MODEL FOR EIT APPLICATIONS

Andreas Waldmann[*1], Carolina Meira[2],
Stephan Böhm[1], Matthias Dennler[2], Martina Mosing[2]

[1]Swisstom AG, Landquart, [2]Vetsuisse Faculty, University of Zurich, Zurich, Switzerland

INTRODUCTION Finite element (FE) models are used to reconstruct electrical impedance tomography (EIT) images from surface voltage measurements. The main objective of this abstract was to calculate an averaged FE model using helical CT scans.

METHODS The anatomical landmark-based "best belt position" was determined according to the equation: sternum-length in cm x 0.17 = cm cranial to xyphoid [1] and an EIT belt without metal electrodes placed around the thorax of 9 healthy anaesthetised supine (dorsal recumbency) beagles (12.9+/-1.7 kg, 2.8+/-0.2 yrs). Inspiratory apnoea CT images were acquired of the whole thorax. The CT slice from the intervertebral space (IVS) where the belt was identified was exported as DICOM file. Thereafter heart, lungs and thorax contours were segmented by ITK-SNAP [2] and exported as vtk-files. Matlab was used to align, to calculate an average contour from all dogs and to generate the corresponding average FE model.

RESULTS AND CONCLUSION It was easy to find the landmark. However, based on the CT scout view the belt was too caudal in three dogs due to the relocatable skin. CT scans were redone after correcting the belt position. The belt was identified in the CT images in all dogs over the 6th intercostal space and at the level of the 6th (n=5) and 7th (n=4) sternebrae. Contours of thorax shape were similar in all animals. The left lung shape varied in the ventral non-dependent parts, while the right lung shape varied in the medio-ventral parts. As could be expected the heart contours differed substantially between individuals. Further studies and calculations are necessary to validate the contours in other breeds and to characterize the differences between an averaged and an intra-individual model.

This study gained governmental approval from the Canton Zürich, Switzerland (Nr. 185/2012).

IMAGE

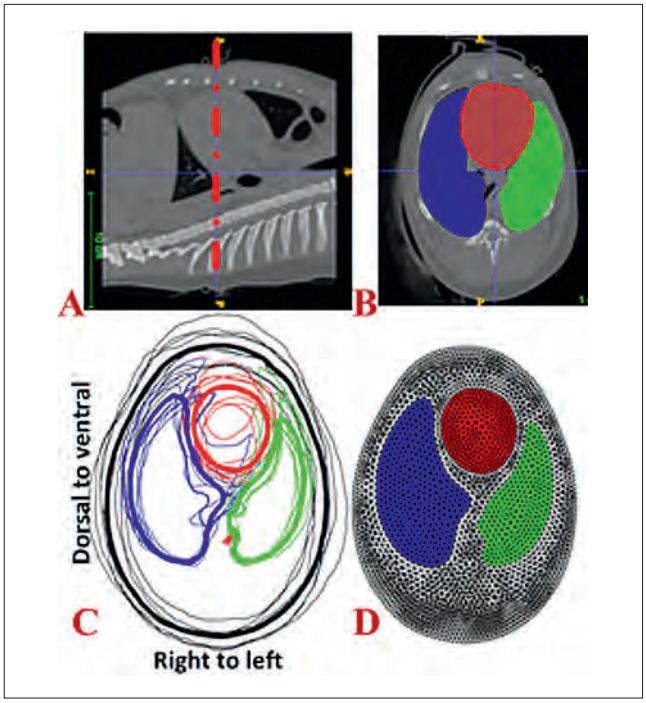

REFERENCES

1. Rocchi A, Hagen R, Rohrer Bley C, Auer U and Mosing M "Comparison of three positions for the thoracic electric impedance tomography (EIT) belt in dogs", Vet Anaesth Analg, 41, A47.
2. P. A. Yushkevich, J. Piven, H. C. Hazlett, R. G. Smith, S. Ho, J. C. Gee, and G. Gerig, "User-guided 3D active contour segmentation of anatomical structures: Significantly improved efficiency and reliability," *Neuroimage*, vol. 31, no. 3, pp. 1116–1128, 2006.

Abstract Id: 285
Topic: *Electrical impedance tomography*

EIT -BASED SENSING SKIN FOR DETECTION OF DAMAGE IN CONCRETE

Aku Seppänen[*1], Milad Hallaji[2], Mohammad Pour-Ghaz[2]

[1]Department of Applied Physics, University of Eastern Finland, Kuopio, Finland, [2]Department of Civil, Construction, and Environmental Engineering, North Carolina State University, Raleigh, NC, United States

INTRODUCTION In reinforced concrete, cracking and ingress of corrosive ions are of concern, because they can induce a deformation and decrease the serviceability of structures. Rapid detection of cracking and harmful ions is thus important, particularly in critical structures, such as nuclear waste storages and containment facilities.

OBJECTIVES We study whether an electrical impedance tomography (EIT) – based 2D surface sensor, or sensing skin, could detect and localize cracks and corrosive elements in concrete, and to distinguish between them.

METHODS In the developed sensing skin, a thin layer of electrically conductive paint is applied on the surface of the concrete substrate. When the substrate cracks, the paint layer ruptures, and the local decrease in conductivity of the paint is detected with EIT (Hallaji et al 2014). Further, to detect simultaneously cracks and corrosive elements, we propose a sensing skin consisting of two paint layers: one layer is sensitive to both corrosive ions and cracking, and another layer is sensitive to cracking only.

We test the sensing skins experimentally on reinforced concrete beams. In the EIT image reconstruction, we utilize application-specific models and computational methods, including a total variation (TV) prior model for the damage and an approximate correction of the modeling errors caused by the inhomogeneity of the painted sensing skin.

RESULTS The EIT-based sensing skins are able to detect cracks on concrete surfaces (see Figure 1 for an example). The developed application-specific reconstruction methods lead to EIT reconstructions with surprisingly high resolution. Moreover, the multi-layer sensing skins are able to detect and distinguish between cracks and chlorides.

CONCLUSION The results demonstrate that multi-layer sensing skins can be used for simultaneously detecting cracks and aggressive agents, such as chlorides. The proposed sensing system could potentially be used for monitoring the health and deterioration risk of critical infrastructure.

IMAGE

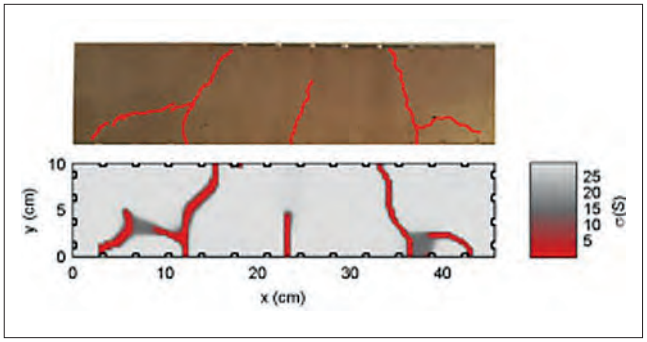

REFERENCES

1. M. Hallaji, A. Seppänen, M. Pour-Ghaz: "Electrical impedance tomography-based sensing skin for quantitative imaging of damage in concrete", *Smart Materials and Structures*, **23:** 085001, 2014.

Abstract Id: 286
Topic: *Electrical impedance tomography*

MEASURING STROKE VOLUME WITH ELECTRICAL IMPEDANCE TOMOGRAPHY

Saaid Arshad[*1,2], Ethan Murphy[1,2], Ryan Halter[1,2]

[1]Thayer School of Engineering, Dartmouth College, [2]Center for Imaging Medicine at Dartmouth, Dartmouth-Hitchcock Medical Center, Hanover, United States

INTRODUCTION Current methods of measuring cardiac output (CO) are invasive and cumbersome or do not provide the sensitivity or specificity required to yield reliable information for clinicians to deliver proactive healthcare. A CO monitoring device is in development that uses a custom smartphone application, wearable electrical impedance tomography (EIT) system, and synchronous ECG and respiratory-gated triggering. A smartphone application has been developed[1] and a simulation study has demonstrated the sensitivity of the surrogate measure of stroke volume (SV), where CO = SV*(heart rate)^2.

OBJECTIVES The objective of this work was to explore the sensitivity of this device with respect to the clinically desired changes in SV through a human study.

METHODS EIT data was collected using a 32-channel SwissTom Pioneer Set with electrodes positioned on the thorax two inches above the nipple plane (T4). Heart-rate data was collected using a pulse oximeter. 3D reconstructions are computed with a standard Gauss-Newton EIT algorithm using the dual-mesh method. The measure of SV is defined as a scaled version of the change in EIT-based heart area between systole and diastole.

RESULTS The left figure below shows a sample heart reconstruction from a single patient. It represents the heart volume differential between end-diastole and end-systole (i.e. measure of SV). The right figure plots the normalized areas of the high conductivity areas shown in the left figure over 20 seconds along with the pulse-ox derived true heart rate. The average pulse-ox heart-rate was 1.47 +/-0.18 beats per second (bps) and our EIT derived heart rate was 1.50 +/-0.36 bps. A normalized average SV of 0.82 +/- 0.07 was calculated.

CONCLUSIONS A metric for extracting a measure of SV appears to be feasible. Future work includes refining the area metric to better approximate SV, validating through a phantom study, and recording in vivo data in tandem with gold-standard SV sensing technologies.

IMAGE

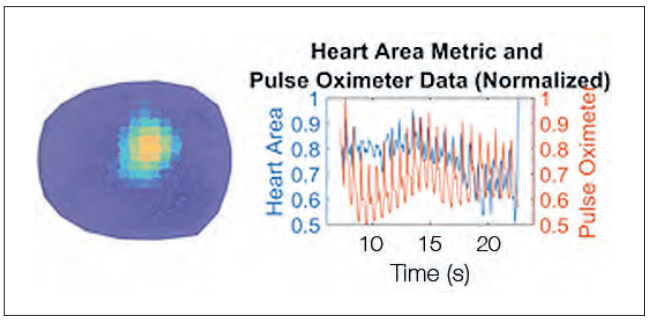

REFERENCES

1. Arshad et al. Towards a Smart Phone-Based Cardiac Monitoring Device using Electrical Impedance Tomography. *IEEE Biomedical Circuits and Systems Conference (BIOCAS),*. October, 2015
2. Arshad et al. Respiratory-gated electrical impedance tomography: a potential technique for quantifying stroke volume. *SPIE Medical Imaging,* February 2016.

Abstract Id: 287
Topic: *Electrical impedance tomography*

CONTRIBUTION OF FINITE ELEMENT MODEL OF ANIMALS TO DATA BASE

Andreas Waldmann*[1], Carolina Meira[2], Ulrike Auer[3], Stefan Böhme[4], Christina Braun[3], Stephan Böhm[1], Martina Mosing[2]

[1]Swisstom AG, Landquart, [2]Vetsuisse Faculty, University of Zurich, Zurich, Switzerland, [3]Anaesthesiology & Intensive Care, University of Veterinary Medicine Vienna, [4]Department of Anesthesia, Pain Management and General Intensive Care Medicine, Medical University of Vienna, Vienna, Austria

INTRODUCTION Finite element (FE) models are used to reconstruct electrical impedance tomography (EIT) images from boundary voltage measurements. Usually, these models are created by segmenting computer tomography (CT) scans of individual subjects and by building respective FE models from these segments. While for humans several pre-complied modes have become publicly available, animal models are obtainable only for those species (sheep and pig) frequently used as experimental models in human medicine.

OBJECTIVES The objective of this study was to create FE models for veterinary use of four different species, to integrate them into ibex [1] and to contribute them to EIDORS [2].

METHODS CT scans from 8 individuals per species were evaluated. One CT image corresponding with the electrode plane in beagles (6th intercostal space [ICS]), calves (6th ICS), pigs (5–6th ICS) and in ponies (7–8th ICS) were manually segmented. In order to increase the robustness of these models the 8 segmented scans were averaged to obtain a mean model per species. Lungs, heart and thorax were segmented in the electrode plane and mean contours were calculated. The corresponding FE model was created by extruding the models along the animals' caudal to cranial axis. 32 electrodes were then placed equidistantly onto the models.

RESULTS The models for the first four species are illustrated in Fig. 1 with obvious anatomic differences between them. These finite element models will be made publically available on EIDORS. In addition, the models were converted into a reconstruction matrix and integrated in ibeX. This way, recorded animal EIT data can easily be reconstructed and analysed.

CONCLUSION The importance of accurate boundary shapes for EIT was emphasized by Grychtol et al. [3]. We believe that the models developed in this project will facilitate and improve the image reconstruction of these four species.

IMAGE

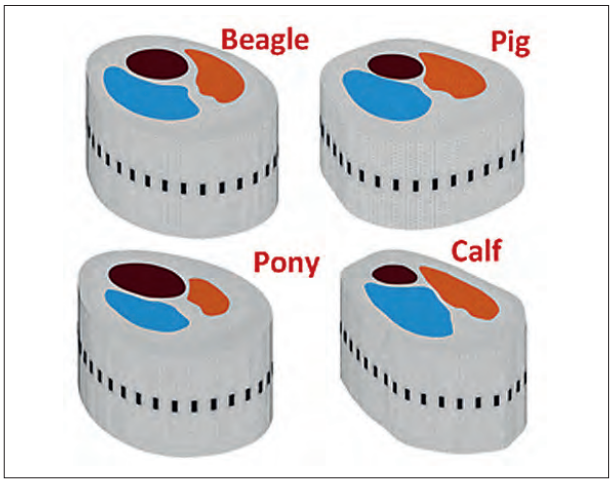

REFERENCES

1. P. Róka et al. Software tool for analysing ventilation EIT data, 16th Conf. Biomedical Applications of Electrical Impedance Tomography, Neuchâtel, CH, 2015.
2. A. Adler and W. R. B. Lionheart, "Uses and abuses of EIDORS: an extensible software base for EIT," *Physiol. Meas.*, vol. 27, no. 5, p. S25, 2006.
3. B. Grychtol, W. R. B. Lionheart, M. Bodenstein, G. K. Wolf, and A. Adler, "Impact of model shape mismatch on reconstruction quality in electrical impedance tomography.," *IEEE Trans. Med. Imaging*, vol. 31, no. 9, pp. 1754–60, Sep. 2012.

Abstract Id: 288
Topic: *Electrical impedance tomography*

WEIGHTING FUNCTIONS FOR IMAGE-BASED VALIDATION OF EIT

Birgit Stender*[1], Julian Maier[2]

[1]Drägerwerk AG & Co KGaA, Lübeck, [2]University of Stuttgart, Stuttgart, Germany

INTRODUCTION Electrical impedance tomography (EIT) is a non-invasive functional imaging modality, which has the capability to monitor changes in both regional distribution of ventilation and lung perfusion at the bedside [1]. Still, there is a need for more profound clinical validation based on functional imaging modalities. In previously published validation approaches EIT images have been compared with a single axial slice of a reference modality [2,3]. Although the reconstructed images of clinically approved EIT devices are two-dimensional such an approach does not reflect the inherently three-dimensional imaging properties corresponding to the current density distributions in EIT.

OBJECTIVES The goal of this work is to compute the amplitude response of EIT towards localized conductivity changes in realistic thoracic conductivity distributions.

METHODS Finite element simulations were conducted using three-dimensional forward models created based on porcine computed tomography scans. These images were recorded in ten animals during expiratory hold phases at a positive end-expiratory pressure of 5 mbar. EIT signals were recorded simultaneously. The conductivity mapping and the process of forward model creation was described previously [4]. In addition the conductivity distribution of the lung parenchyma was assumed to be linearly dependent on the Hounsfield units. The conductivity distribution of this reference model was then locally changed by 3% and the corresponding amplitude response in EIT difference images determined as described by Yasin et al. [5]. The position of the disturbance was successively changed in order to sample the lung region equidistantly.

RESULTS A resulting three-dimensional distribution of the amplitude response is displayed in Figure 1. The distributions computed for different animals were similar. Up to a distance of approximately 10cm the relative response with respect to the electrode plane exceeded 20%.

CONCLUSION The distributions of the amplitude response potentially represent an appropriate weighting function for three-dimensional functional reference images in EIT validation studies.

IMAGE

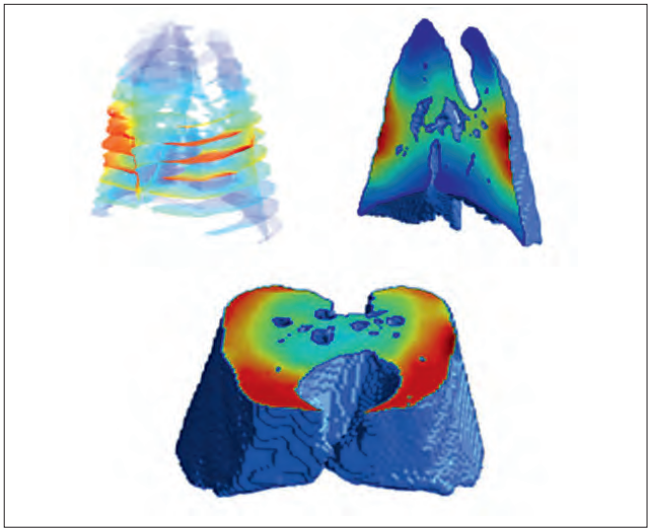

REFERENCES

1. Adler A, Amato MBP, Arnold JH, et al. *Physiol Meas* **33**(5): 679–94, 2012.
2. Elke G, Fuld MK, Halaweish AF, et al. *Physiol Meas* **34**(10): 1303–18, 2013.
3. Borges JB, Suarez-Sipmann F, Bohm SH, et al. *J Appl Physiol* **112**(1): 225–236, 2012.
4. Dinkelbach J, Stender B. *Proceedings EIT 2015* p109.
5. Yasin M, Böhm S, et al. *Physiol Meas* **32**(7): 851–65, 2011.

Abstract Id: 289
Topic: *Electrical impedance tomography*

MULTISHOT SE-EPI SEQUENCES FOR FUNCTIONAL MREIT

Munish Chauhan[1], Neeta Ashok Kumar[1], Vikram Kodibagkar[1], Rosalind Sadleir[*1]

[1]School of Biological and Health Systems Engineering, Arizona State University, Tempe, United States

INTRODUCTION Recently, one of the many challenging problems in Magnetic Resonance Electrical Impedance Tomography (MREIT) has been to implement a new imaging technique with a very short acquisition time for the imaging of neural activities of brain related to the conductivity change. In some cases multishot EPI sequences are preferred over single-shot methods because they involve less artifact. While SE techniques are less sensitive to the BOLD response used in fMRI, they are potentially very useful in functional MREIT (fMREIT). We therefore used Spin Echo based multiple shot (16, 8, 4, and 2) Echo Planar Imaging (SE-EPI) sequences to calculate magnetic flux density (Bz) and made a comparison with conventional spin echo (SE) sequences.

OBJECTIVES Earlier studies have demonstrated the feasibility of SE-EPI pulse sequence for data acquisition in MREIT [1]. The objective of this study is to evaluate the performance of data acquired using multiple shot EPI for fMREIT.

METHODS An octagonal-shaped imaging phantom 5cm of arm length and 42 mm of height was filled with 0.4S m^{-1} conductivity agarose solution including a cylindrical object of a conductivity of 1.5S m^{-1} at the center. We acquired data using Bruker Biospec 7-Tesla MRI with Current injection of ±10mA through opposite pair of electrodes. SE-EPI Scan parameters were: FOV= 80x80 mm^2, matrix size= 64x64, TR/TE= 1000/24 ms, Slice thickness=4mm, Average=1, current injection time TC1/TC2=10/0ms and EPI segments (shots)= 16, 8, 4, and 2. Additionally, for the purpose of comparison, we acquired conventional SE data with the same imaging parameters. Prior to the calculation of Bz distribution, EPI data was phase corrected.

RESULTS Figure 1 shows (a) phantom setup and direction of MREIT current injection, (b) MR magnitude and Bz images, and (c) comparison of Bz in spin echo and multiple shots SE-EPI sequences.

CONCLUSION We demonstrated the comparison of magnetic flux density between SE and multiple shots SE-EPI sequences. In future, we will reconstruct current density and conductivity distributions in all shots of EPI, along with investigations in phantoms of greater complexity and *in-vivo* studies.

Table 1. *Noise in measured Bz.*

Scan	sd(Bz) [nT]
Spin Echo	0.89
16 SSE-EPI	2.54
8 SSE-EPI	3.38
4 SSE-EPI	3.93
2 SSE-EPI	14.23

IMAGE

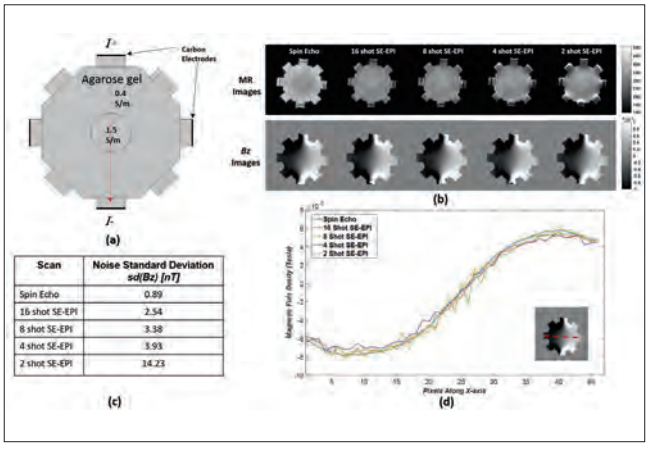

REFERENCES

1. M.J. Hamamura, L.T. Muftuler, "Fast imaging for magnetic resonance electrical impedance tomography", Magn Reson Imaging. 2008 vol. 26, no. 6, pp. 739–45, 2008.

Abstract Id: 290
Topic: *Electrical impedance tomography*

LUNG VENTILATION CHANGES DURING PERCUTANEOUS TRACHEOSTOMY

Lars Eichler[*1], Jakob Müller[1], Christian Zöllner[1], Inez Frerichs[2], Stefan Kluge[3]

[1]Department of Anaesthesiology, University Medical Center Eppendorf, Hamburg,
[2]Department of Anaesthesiology, University Medical Center Schleswig Holstein Campus Kiel, Kiel,
[3]Department of Intensive Care Medicine, University Medical Center Eppendorf, Hamburg, Germany

INTRODUCTION Percutaneous dilatational tracheostomy (PDT) guided by bronchoscopy is a routine bedside intervention in critically ill patients demanding long-term ventilatory support. However, application of high oxygen concentration, repetitive suction maneuvers and hypoventilation during the course of the procedure often lead to impaired respiratory function immediately thereafter.

OBJECTIVES Potential changes of global and regional ventilation during percutaneous tracheostomy were examined by thoracic EIT.

METHODS 29 consecutive patients receiving PDT were monitored with a 16-electrode EIT monitor (PulmoVista 500, Dräger, Lübeck, Germany) at 4 defined time points: a) after final positioning for surgery b) after application of neuromuscular blocking agent c) after insertion of tracheal canulla and d) after a final standardized recruitment maneuver. 2-minute EIT measurements were performed at 30 Hz at a midthoracic level and recorded images were analyzed for regional impedance changes in dorso-ventral direction and between right and left hemithoraces.

RESULTS While initiation of neuromuscular blockade had little to no effect on dorso-ventral ventilation distribution, the PDT itself lead to significant decreases in aeration of dorsal lung parts. This effect could be reversed by a standardized recruitment maneuver following surgery. Ventral aeration was further increased by recruitment.

CONCLUSION PDT results in dorso-ventral redistribution of lung aeration. Dorsally located impairment in ventilation may be reversed by a recruitment maneuver at the end of the procedure.

IMAGE

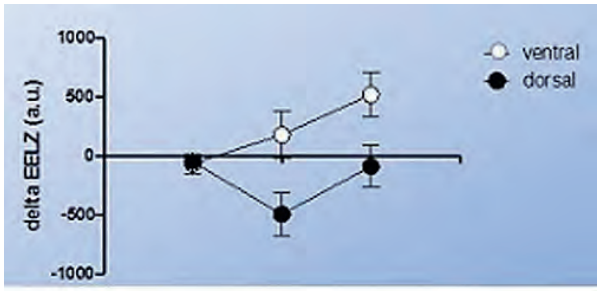

Fig.1:
Changes in EELZ (Mean and SEM) compared to baseline measurement a.) after neuromuscular blockade, b.) after tracheostomy and c.) after a subsequent recruitment maneuver.

Abstract Id: 291
Topic: *Electrical impedance tomography*

HIGH SPEED EIT DATA ACQUISITION SYSTEM

Bryan Loyola[*1], Michael Empey[2], Steven Brown[2],
Randy Kellen Madsen[1], Steven Paradise[1], Neal Patwari[2]

[1]Sandia National Laboratories, Livermore, CA, [2]Electrical and Computer Engineering,
University of Utah, Salt Lake City, UT, United States

INTRODUCTION As the use of electrical impedance tomography (EIT) expands to more applications, it has become evident that the ability to acquire fast EIT measurements is highly desirable. Specifically, we are interested in performing EIT measurements at a collection rate that can resolve the change in the strain field of a metal or composite specimen under quasi-static loading. Similarly, these time scales would also include that of a human breathing or other dynamic human functions.

OBJECTIVES We aim to develop a system that performs EIT measurements at a rate of 100 Hz with each measurement consisting of 960 voltage measurements. Furthermore, we aim to make this data acquisition system compact, light-weight, and expandable.

METHODS We have developed several approaches for integrating current injection and voltage measurements in the pursuit of the high speed EIT data acquisition. Each of these units can connect up to 32 electrodes, has a fully configurable current injection and voltage measurement scheme, and can fit in the palm of your hand.

RESULTS Currently, we are able to obtain a single EIT measurement consisting of 960 voltage measurements in 1.7 s, In addition, we have implemented an architecture that can link up to 256 DAQs.

CONCLUSION In this presentation, we will present the progression of the development of these data acquisition units, concluding with our current design which is calculated to deliver on our goal of EIT measurements collected at a rate of 100 Hz. Furthermore, we will give some examples of how we will be using this data acquisition unit for measurements pertaining to structural health monitoring.

Sandia National Laboratories is a multi-program laboratory managed and operated by Sandia Corporation, a wholly owned subsidiary of Lockheed Martin Corporation, for the U.S. Department of Energy's National Nuclear Security Administration under contract DE-AC04-94AL85000.

Abstract Id: 292
Topic: *Electrical impedance tomography*

COMPARISON OF ELECTRICAL AND MOLECULAR TRANSPORT PROPERTIES

Neeta Ashok Kumar*[1], Munish Chauhan[1], Rosalind Sadleir[1]

[1]School of Biological and Health Systems Engineering, Arizona State University, Tempe, United States

INTRODUCTION Both electrical and molecular transport phenomena in living tissues can exhibit anisotropy, with the best known examples being in the white matter of the brain and skeletal and cardiac muscle. A linear relationship between the two transport modes in terms of electrical conductivity and water diffusion has been observed[1]. In this study, Magnetic Resonance Electrical Impedance Tomography (MREIT) was used for conductivity imaging and Diffusion-Tensor MRI (DT-MRI) to measure the diffusivity of water in anisotropic phantoms.

OBJECTIVES The objective of this study was to compare the directional derivatives (gradient and laplacian) of conductivity and diffusion tensors.

METHODS Alternate gel layers of low and high conductivity were housed in an octagonal sample chamber[2]. Bruker Biospec 7T MRI was used for MREIT and DT-MRI acquisitions in 1, 25 (Fig. a) and 31 layered anisotropic phantoms.
MREIT: A spin-echo based MREIT (SE-MREIT) sequence was used with ±10 mA orthogonal current injection pairs after 90 and 180 degree pulses respectively. SE-MREIT scan parameters were FOV: 256 x 256 mm^2, Matrix size = 64 x 64, Repetition/Echo time = 1000/25 ms, Slice thickness = 4 mm, Averages = 2.
DT-MRI: Spin-echo (DT-MRI) parameters were FOV: 336 x 336 mm^2, Matrix size = 32 x 32, Repetition/Echo time = 2094.305/210 ms, Slice thickness = 10.5 mm, Averages = 1, b-value = 1000/500 s mm^{-2}, Diffusion weighting gradient directions = 6.

RESULTS MREIT scans were processed to reconstruct the Magnetic Flux Density (B_z) distribution and spatial derivatives of conductivity. Fig. b shows the B_z profile in the insulated anisotropic phantom (25 layers) had a greater slope compared to the other two conductive phantoms (1 and 31 layers). DT-MRI scans were processed to calculate the diffusion tensor (D).

CONCLUSION Similarities and differences between conductivity and diffusion associated with variation in anisotropy were demonstrated. The influence of boundary conditions imposed by the geometry of gel layers at a micro-scale on conductivity and diffusivity properties of TX-151 gel phantoms was also observed.

IMAGE

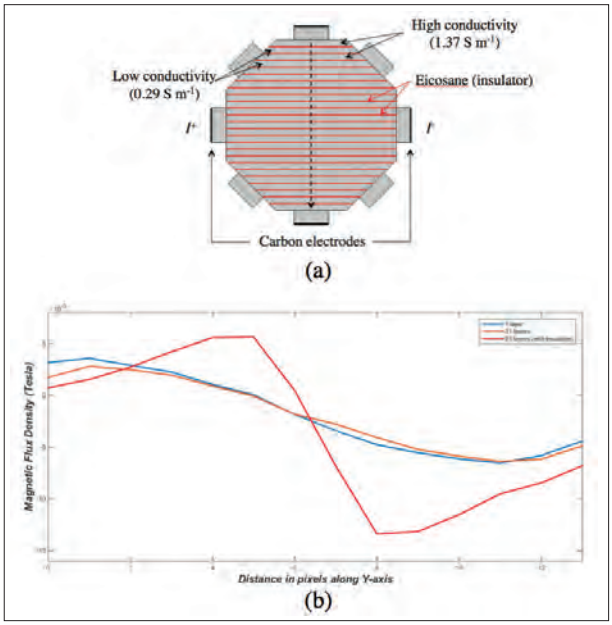

REFERENCES

1. D.S. Tuch, et al., "Conductivity tensor mapping of the human brain using diffusion tensor MRI," Proceedings of the National Academy of Sciences, vol. 98, no. 20, pp. 11697–11701, 2001.
2. R. J. Sadleir, et al., "A Controllably Anisotropic Conductivity or Diffusion Phantom Constructed from Isotropic Layers," Annals of Biomedical Engineering, pp. 2522–2531, 2009.

Abstract Id: 293
Topic: *Electrical impedance tomography*

INTRAOPERATIVE PROSTATE IMAGING WITH ENDOSCOPIC EIT

Andreas Tzavelis*[1], Aditya Mahara[1], Ryan Halter[1]

[1]Thayer School of Engineering, Dartmouth College, Hanover, United States

INTRODUCTION Electrical Impedance Spectroscopy (EIS) provides sufficient contrast for distinguishing between malignant and benign prostate tissue [1]. Intraoperatively imaging these properties using endoscopic Electrical Impedance Tomography (EIT) has the potential to provide surgeons with real-time assessment of surgical margin status during Robot-Assisted Laparoscopic Prostatectomy (RALP) procedures.

OBJECTIVE The objective of this study is to evaluate in vivo EIT measurements of the prostate and surrounding tissues recorded during RALP.

METHODS An FPGA-based voltage-current dual drive EIT system [2] coupled to a 21 electrode endoscopic EIT probe [3] (Fig.1a) is used for data acquisition. During a RALP procedure, the probe is introduced to the surgical space through an auxiliary laparoscopic port (Fig.1b); data is acquired at four angles (12, 3, 6, and 9 o'clock) and 5 frequencies (20 kHz, 40 kHz, 80 kHz, 400 kHz, 800 kHz) around each anatomic location scanned: prostatic apex, prostatic base, urethral opening, and bladder neck.

RESULTS The endoscopic EIT probe was successfully deployed during RALP procedures at our institution. Data acquisition took approximately 10 minutes to introduce the probe into the surgical field and to record impedance spectra from 16 locations (4 angles at 4 locations). Initial findings suggest that impedances decrease with increasing frequency for all in vivo tissue sites probed (Fig. 1c) which is consistent with ex vivo findings [1]. Impedances vary for the different anatomic sites; these differences need further exploration, but may arise from tissue differences, blood pooling, or presence of char at the surgical site.

CONCLUSION This represents the first time that in-vivo impedances have been recorded from a surgical site during a RALP procedure. Impedances followed the expected spectral trends. Additional data and further evaluation is necessary in the in vivo setting to assess the efficacy of this approach for characterizing surgical margin pathology.

IMAGE

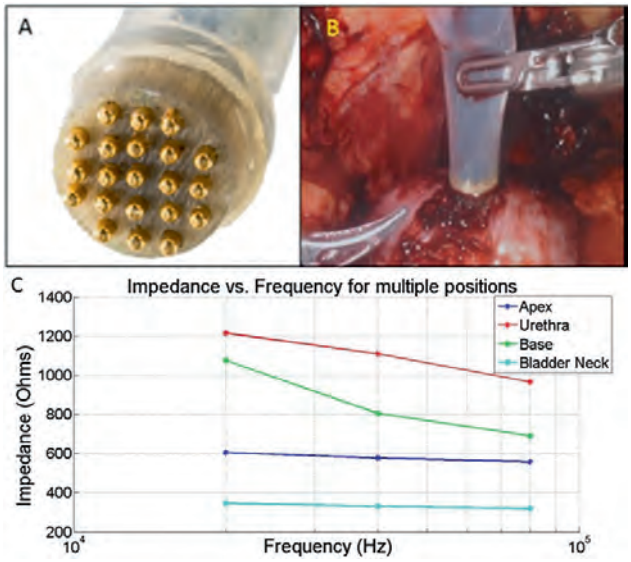

Fig. 1. *A. Cross-sectional view of the 21 electrode probe, B. In vivo data acquisition at the apex during a RALP procedure, C. In vivo impedance spectra of different anatomic sites.*

REFERENCES

1. Halter et al, *Journal of Urology*, 2009.
2. Khan et al, *IEEE TMI*, 2015.
3. Mahara et al, *IEEE TMI*, 2015

Abstract Id: 294
Topic: *Electrical impedance tomography*

EIT MONITORING OF THE LIQUID-VENTILATED LUNG

Andy Adler*[1], Etienne Fortin-Pellerin[2], Mathieu Nadeau[2], Jonathan Vandamme[2], Julien Mousseau[2], Philippe Micheau[2], Michaël Sage[2], Jean-Paul Praud[2]

[1]Carleton University, Ottawa, [2]Université de Sherbrooke, Sherbrooke, Canada

INTRODUCTION Total liquid ventilation uses liquid perflubron instead of air for gas exchange. It has several possible applications, especially for the immature lungs of extremely premature neonates, and in the damaged lungs of ARDS patients. Perflubron is dense ($\varrho \approx 2$) and helps open dependent lung regions which can be collapsed (atelectatic) with traditional positive-pressure ventilation. One challenge is the liquid induction phase, during which a mixture of air and fluid is in the lung. We are hopeful EIT can help improve liquid ventilation strategies. One previous report [1] did not address the induction phase.

OBJECTIVE investigate whether EIT can help clarify the distribution of ventilation during the liquid-ventilation induction phase.

METHODS One healthy lamb (male, age 3 days, 4.2 kgs) was anesthetized and ventilated in a supine position using pressure control ventilation (PIP 14 cmH_2O, PEEP 4 cm H_2O). Sixteen EIT electrodes were attached in a tranverse plane and images acquired at 4.7 frames/s using the Sigmatome II EIT device. During the experimental phase of interest, the ventilator was disconnected and perflubron was introduced and liquid ventilation commenced.

RESULTS Images were reconstructed using a GN algorithm with electrode movement compensation. The figure shows the global EIT image (arbitrary units, non-conductive changes are positive) vs. time (seconds). At four instants (vertical lines) the EIT image is shown. Phases of A) air ventilation, D) disconnection, L) liquid ventilation are seen. Images show a movement of the ventilated region in the dependent direction. From L2 and L3 show a stable ventilated region in the dependent lungs. L1 appears to show both air and liquid in the lungs.

DISCUSSION EIT images appear to show useful information about the physiological changes during the induction of liquid ventilation. As understood, the perflubron ventilation occurs primarily in the dependent lobes of the lung, while gas ventilation occurs more ventrally. We see an initial phase where both air and fluid are seen in the lungs. In further monitoring over the next 30 minutes (not shown) there is a redistribution of ventilation to achieve a more uniform pattern. These results suggest EIT can help understand the physiological changes during liquid ventilation.

IMAGE

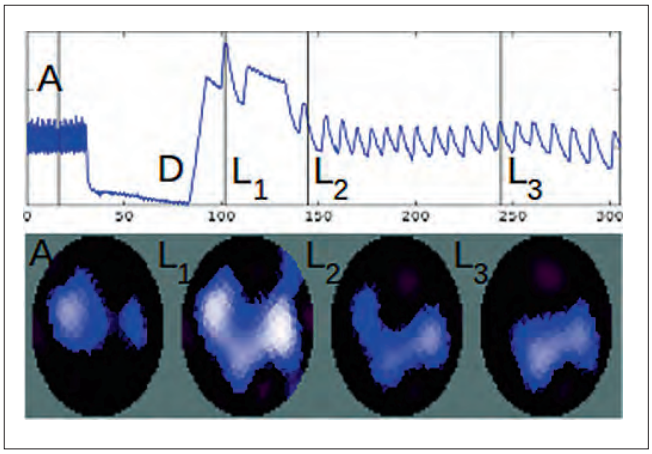

REFERENCES

1. GK Wolf, B Grychtol, TK Boyd, D Zurakowski, JH Arnold, "Regional overdistension identified with electrical impedance tomography in the perflubron-treated lung", 31:S85–S95, 2010.

Abstract Id: 297
Topic: *Electrical impedance tomography*

IDENTIFICATION OF STABLE BREATHING PERIODS IN EIT RECORDINGS

Barbara Vogt[*1,2], Kostas Haris[2,3], Ioanna Chouvarda[3], Tobias Becher[1], Norbert Weiler[1], Nikolaos Maglaveras[3], Inez Frerichs[1]

[1]Department of Anaesthesiology and Intensive Care Medicine, University Medical Centre Schleswig-Holstein, Campus Kiel, Kiel, Germany, [2]Both authors contributed equally to this work, [3]Laboratory of Medical Informatics, Medical School, Aristotle University of Thessaloniki, Thessaloniki, Greece

INTRODUCTION In a clinical setting, EIT has been used mainly in mechanically ventilated patients so far. These patients typically do not move and their breathing pattern is stable. Development of wearable EIT systems will create the possibility of monitoring regional lung ventilation in other patient groups as, even outside the hospital. These patients will breathe spontaneously, thus, their breathing pattern will not be stable. Effects like body movement, speech, cough, sigh, exercise, change/loss in electrode contact will impact the recordings.

OBJECTIVES The aim of our study was to determine whether stable tidal breathing periods suitable for the assessment of regional lung function can automatically be identified in EIT waveforms acquired during spontaneous breathing.

METHODS The study took place within the framework of the European Union project WELCOME (Grant No. 611223) aiming to develop an integrated care approach for continuous monitoring, early diagnosis and detection of worsening events and treatment of patients suffering from chronic obstructive pulmonary disease with comorbidities. We analysed twelve ten-minute EIT recordings obtained in healthy adult subjects. The data were recorded with the Goe-MF II EIT system (CareFusion, Höchberg, Germany) at 33 images/s. The examined subjects were instructed to perform different ventilation and non-ventilation manoeuvres during the data acquisition. These included: deep breaths, coughing, talking, laughing, change in posture, eating. Raw EIT images were reconstructed using the GREIT algorithm. The identification of stable tidal breathing periods was based on the breath-by-breath analysis of the amplitude of ventilation-related signal variation and the duration of respiratory cycle.

RESULTS We tested different threshold values of breath-by-breath variation in both inspiration-to-expiration EIT signal differences and respiratory cycle durations (5%, 10%, 20% and 30%). The threshold of 20% variation performed best in identifying stable tidal breathing periods.

CONCLUSION Our study findings imply that automated selection of undisturbed, stable tidal breathing periods is feasible when spontaneously breathing subjects are monitored by EIT. Such stable phases of EIT data can be used to generate various measures characterizing regional lung function over time. Time-dependent changes in these measures might be applied to identify lung disease deterioration or to assess the therapy effects.

Abstract Id: 299
Topic: *Electrical impedance tomography*

DEPTH ELECTRODE FOR NEURAL ELECTRICAL IMPEDANCE TOMOGRAPHY

Hargsoon Yoon*[1], Min Kim[1], Darryl Scott[1]

[1]Engineering, Norfolk State University, Norfolk, United States

INTRODUCTION Real time imaging of fast electrical activity in the nervous system is a major current goal in neuroscience. Electrical Impedance Tomography (EIT) enables tomographic imaging of impedance changes related to fast neuronal activity. For neural activity imaging, EIT has been implemented with surface electrodes placed on the skull or directly on the surface of the cerebral cortex.

OBJECTIVES The aim of this research is to perform EIT in the deep brain using depth electrode arrays. This presentation will provide novel and informative data for anatomic location of neural activity and allow visualization of neural networks in deep brain.

METHODS AND RESULTS As part of an effort to develop deep electrode array, we applied nanotechnology on electrodes to enhance electrochemical impedance characteristics. In this research, various designs of depth probes were investigated to minimize damage to the brain tissue and overcome size constraints in the brain (Fig. 1). For nano-electrode fabrication, we applied electrodeposited iridium oxide film neural probes. Iridium oxide showed high charge density and high charge injection rate which are ideal for EIT application. To enhance mechanical adhesion of the nanostructure film, we developed a new fabrication process that amplifies the nucleation of iridium oxide at the initial stage of deposition process (Fig. 1). Measured results were analyzed using electrical impedance spectroscopy and compared with theoretical models.

CONCLUSION This work demonstrates the design and development of depth probe and functional advantages of nanotechnology in EIT for fast neural activity imaging in deep brain. Future work is required to apply nano-depth probes for in-vitro and in-vivo studies and characterize their functionality in the rat brain model. This work is supported by the NSF-RISE Grant (HRD 1345215).

IMAGE

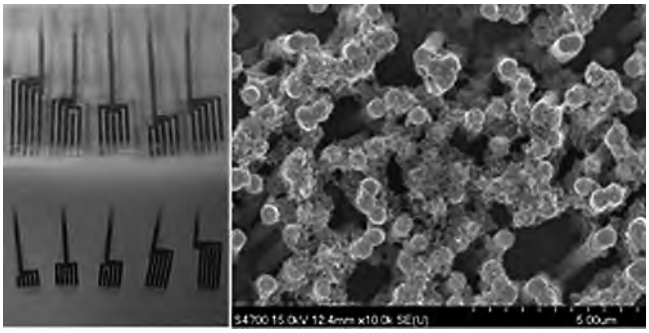

Figure 1. *EIT Depth Electrodes (left) and IrO_X on Au nanowires fabricated by amplifying nucleation process (right).*

Abstract Id: 300
Topic: *Electrical impedance tomography*

WIRELESS POWER TRANSFER FOR AN IMPLANTABLE EIT SYSTEM

Kyo Song[*1], John Day[1], Min Kim[1], Hargsoon Yoon[1]

[1]Engineering, Norfolk State University, Norfolk, United States

INTRODUCTION A wireless power transfer module has been investigated for powering implanted Electrical Impedance Tomography devices using magnetic resonance coupling. With a power transmission coil set located on the body surface and a receiving unit inside the body, an Electrical Impedance Tomography system can be powered to image the body without wired power delivery through the skin. This research presents an experimental set-up and measurement results from magnetic resonance coupling devices.

OBJECTIVES For operation in the body, a wireless power transfer module is developed to deliver power to an EIT electronic system containing a microcontroller, a current source, a multiplexer, a wireless communication module and a power management module with a rechargeable battery (Fig. 1).

METHODS AND RESULTS In this research, we investigated wireless power transfer module designs using magnetic resonance coupling and measured wireless power transfer efficiency in various conditions of receiving electronics and coils. This research demonstrated that the wireless power transfer module can supply at least 150 mW at any place on the plane of the source coil, which would suffice the power budget for a miniaturized EIT data acquisition and wireless communication electronics. With the use of a rechargeable battery, measured power transfer capacity can also cover more complex systems.

CONCLUSIONS In this research, we demonstrated a wireless power transfer module for an implantable electrical impedance tomography system. Various design parameters concerning geometrical location of coils and load impedance were also analyzed to optimize power transfer efficiency to an implantable EIT electronics system with adaptive power management function.

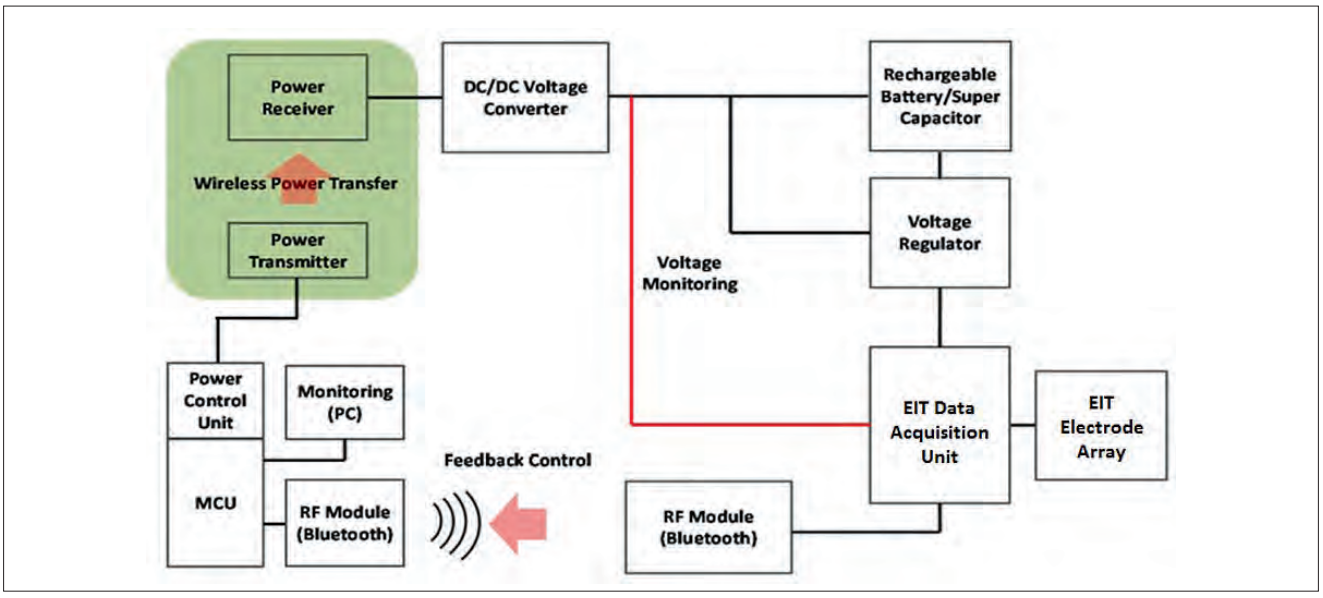

Figure 1. *Conceptual diagram of an adaptive wireless power transfer system.*

Abstract Id: 301
Topic: *Biosensors*

IMPEDANCE & EXTRACELLULAR FIELD POTENTIAL OF CARDIOMYOCYTES

Krisztina Juhasz[1,2], Sonja Stölzle-Feix[1], Corina Bot [3], Nadine Becker[1], Ulrich Thomas[1], Leo Doerr[1], Matthias Beckler[1], Michael George[1], Andrea Brüggemann[1], Niels Fertig[1]

[1] Nanion Technologies, Munich, Germany, [2] Technical University of Munich, Munich (Germany), [3] Nanion Technologies Inc., Livingston, NJ, 07039 (USA)

INTRODUCTION Drug induced arrhythmia is one of the most common causes of drug development failure. Human induced pluripotent stem cell-derived cardiomyocytes (iPSCMs) have a great potential for cardiovascular research and predictive in-vitro cardiac safety screening when it comes to early detection of arrhythmic compounds.

METHODS The CardioExcyte 96 system provides a non-invasive, label-free, high temporal resolution approach for safety screening on iPSCMs (1). It is a hybrid screening instrument that combines impedance with MEA-like extracellular field potential (EFP) recordings (2,3). It can be either used in an incubator or directly on a lab bench. The system is capable of electrically pacing the cells, allowing screening of cells which beat with individual frequencies and investigations of frequency dependent compound inhibition.

RESULTS Changes in the impedance signal indicate effects on cell contractility and shape whereas the field potential parameters provide information about the electrophysiological activity of the beating network of cells. In accordance with the Comprehensive In Vitro Proarrhythmia Assay (CiPA) guidelines, standard reference compounds were tested on iPS-derived cardiomyocytes.

DISCUSSION & CONCLUSION Combined impedance and EFP measurements using a commercially available platform can be made reliably from a number of different hiPSC-CMs including Cor.4U (Axiogenesis AG), iCell Cardiomyocytes2 (Cellular Dynamics International), Pluricytes (Pluriomics) and Cellartis® hiPS-CM (Takara Bio Europe AB). These cells are becoming increasingly important for cardiac safety testing. The CardioExcyte 96 is, so far, the only platform on the market capable of recording impedance and EFP measurements from same cell. This provides a unique opportunity to detect changes in both contractility and ion channel function at a high throughput which may prove crucial for cardiac safety screening particularly in the light of the new CiPA guidelines.

REFERENCES

1. Doerr, L., Thomas, U., Guinot, D. R., Bot, C. T., Stoelzle-Feix, S., Beckler, M., George, M., Fertig, N., J. Lab. Autom., 20(2), 175–188. (2015).
2. Giaever, I., & Keese, C. R., Proc. Natl. Acad. Sci. U. S. A., 88(17), 7896–900. (1991).
3. Clements, M., & Thomas, N., Toxicol. Sci., 140(2), 445–61. (2014).

Compound		Impedance				EFP				Effect
		Amp	Rate	PW50	BRRI	Amp	Rate	FPD	BRRI	
Dofetilide	10 nM									hERG blocker
Cisapride	1 µM									hERG blocker
E-4031	30 nM									hERG blocker
Sotalol	1 µM									hERG blocker
Astemizole	1 nM									hERG blocker
Quinidine	1 µM									mixed blocker
Terfenadine	1 µM									hERG, Na_V blocker
Isoproterenol	1 µM									β-adrenergic agonist
Nifedipine	300 nM									Ca_V blocker
BAYK8644	1 nM									Ca_V activator

decrease
increase

Table 1: Changes of cardiomyocytes (Cor.4U) beating pattern measured by impedance and EFP.

AUTHOR INDEX (Name / Abstract ID)

A

Abbas, Samer 125
Abie, Sisay Mebre 202
Abramov, Alexander 184
Acciaro, Marco 176
Adamkiewicz, Przemysław 257
Adler, Andy 237, 294, 215, 236, 242
Albuquerque, Thiago 118
Amorós-Figueras, Gerard 158
Anand, Sneh 277
Annala, Kari 129
Annus, Paul 173, 201, 138, 172
Antony, Alice 151
Aristovich, Kirill 273, 271, 235, 274, 272, 244
Armitage, David W 134
Arnold, David 145
Arshad, Saaid 286
Ashok Kumar, Neeta 292, 289
Auer, Ulrike 287
Avery, James 273, 276, 235, 274, 272
Azan, Antoine 139

B

Bach, Thomas 226
Balleza Ordaz, Marco 169
Barthel, Andreas 183, 149, 150
Barthod, Christine 197
Battacone, Gianni 176
Bayford, Richard 281, 262, 251
Becher, Tobias 281, 233, 297
Becker, Nadine 301
Beckler, Matthias 301
Ben Salah, Ihsen 148
Ben Salah, Ridha 187, 148
Bergamo, Ferdinand 282
Bergli, Joakim 202
Bergmans, Dennis 227
Bertemes Filho, Pedro 170
Bertemes-Filho, Pedro 118, 189, 208
Beskok, Ali 168
Blochet, Camille 235
Bogdanik, Laurent 145
Böhm, Stephan 283, 281, 287
Böhm, Stephan H. 241
Böhme, Stefan 287, 243
Bonnet, Stephane 268
Borreguero, Samuel 159
Bot, Corina 301
Boyle, Alistair 215
Braeken, Dries 198
Bragos, Ramon 141, 139, 158
Brajkovič, Robert 189, 170
Brandt, Thorsten 175
Brandusecu, Alin 238
Braun, Christina 287
Braun, Fabian 181, 242
Broeze, Kirsten 136, 135
Brown, Brian 260
Brown, Steven 291
Brüggemann, Andrea 301
Buchholz, Valerie 233
Buendia, Ruben 109, 199
Butterworth, Micheal 281

C

Cahill, Brian P. 183
Callegaro, Luca 223
Cambiaghi, Barbara 220
Campos-Pareja, Ana Maria 159
Can, Osman Melih 192
Candefjord, Stefan 199
Caragounis, Eva-Corina 199
Carbonaro, Nicola 256
Cárdenas-Villamizar, Vladimir 119
Castano, Pablo 214
Castelar, Carlos 282
Castillo, Diego M 141
Cerri, Graziano 117, 116
Chabchoub, Souhir 187
Chang, Mei - Yun 229
Chatwin, Chris 226
Chauhan, Munish 249, 292, 289
Chernyshenko, Alexey 143
Chijova, Yulia 270
Chilcott, Terry 151, 111
Chouvarda, Ioanna 297
Christofides, Christofides 281
Chung, Chi Ryang 259
Cinca, Juan 158
Clarion, Antoine 112
Colina-Gallo, Evelyn 119
Coll, Nuria 141

Concu, Alberto 176
Concu, Daniele 176
Connolly, Patricia 188
Corzo, Alejandro 160
Cosoli, Gloria 117, 116
Crabb, Michael 228, 258
CUI, Ruihang 182
Cultrera, Alessandro 223
Czaplik, Michael 252

D

Danilov, Alexander 143
Darras, Basil 126
Dassonville, Yohan 197
David, Olivier 268
Davidson, John L 134
Day, John 300
De Cannière, Hélène 147
de Graaf, Gimon 281
De Weert, Ami 198
Demosthenous, Andreas 281, 262, 251
Demuth, Caspar 150
Dennler, Matthias 283
Derbel, Nabil 203
Disselhorst-Klug, Catherine 282
Dittmar, Joerg 220
Doerr, Leo 301
Dittmar, Jörg 255
Donega, Matteo 235
Dong, Xiuzhen 263
Dowrick, Thomas 276, 273
Dussan, Carmen 122
Dussán-Luber, Carmen 119

E

Ehlers, Kathinka 224
Eichler, Lars 290
Elvebakk, Ole 130
Empey, Michael 291
Eng, Stephanie 237
Ermishkin, Vladimir 184
Eryukova, Tatiana 156
Essex, Tim 109

F

FAN, Shaoran 182
Faulkner, Mayo 271, 261
Fernandez-Corazza, Mariano 239
Fertig, Niels 301
Fifield, Bruce 281
Figueiras, Edite 280
Flattum, Morten 179
Fois, Andrea 176
Fortin-Pellerin, Etienne 294
Fouchard, Alexandre 268
Frangež, Robert 170
Frerichs, Inéz 281, 224, 233, 290, 297
Fu, Feng 263

G

Galperin, Yuri 202
García Pérez, Marysol 169
Garcia-Sanchez, Tomas 139
García-Sánchez, Tomás 158
Gaspar, Melisa 108
Gastrock, Gunter 183
Gavrilov, Vasyliy 140
George, Michael 301
Gheorghiu, Eugen 137
Goikoetxea, Erkuden 198
Golev, Victor 167
Gong, Bo 278, 279, 269
Gonzalez, Carlos 122
González, César A. 160
González, José A. 160
Gonzalez, Clara 214
Gonzalez-Correa, Clara Helena 204
González-Correa, Carlos Augusto 119
González-González, David Ricardo 204
Goren, Nir 272
Grambone, Martin 237
Granhed, Hans 199
Grässler, Michael F. 241
Green, Peter 228, 258
Grieten, Lars 147
Grimnes, Sverrre 171
Grounauer, Pierre-Alain 112

Guermazi, Mahdi 203
Guerrero, Carla I. 160
Guo, Chuan 111
Gutierrez-Carretero, Encarnación 159

H

Hahn, Guenter 220
Hahn, Günter 255
Hallaji, Milad 285
Halonen, Sanna 129
Halter, Ryan 222, 253, 286, 293, 196
Hamilton, Sarah 248
Hannan, Sana 261
Haris, Kostas 297
Hauptmann, Andreas 231
Heines, Serge 227
Hennig, Victoria 224
Hentze, Benjamin 225
Hifumi, So 260
Hitrov, Mikhail 270
Hochhausen, Nadine 252
Høgetveit, Jan Olav 179, 130, 157
Holder, David 276, 273, 271, 261, 235, 274, 272, 244
Holland, Ian 188
Holthusen, Johannes 175
Huerta Franco, María Raquel 169
Hyttinen, Jari 280

I

Indahlastari, Aprinda 249
Iyer, Shama R 165

J

Jahnke, Heinz-Georg 131
Jang, Guek Young 275, 259
Jehl, Markus 271, 273, 272
Jeong, Woo Chul 267
Jeong, You Jeong 265
JIAO, Meiling 182
Jivet, Ioan 238
Joel, Varonier 150
Jorge, Esther 158
Juhasz, Krisztina 301
Just, Anita 255, 220

K

Kabanova, Irina 186
Kalvøy, Håvard 179, 130, 177
Kampusch, Stefan 241, 243
Kaniusas, Eugenijus 241, 243
Kanoun, Olfa 203
Kapelko, Valeri 184
Karaoli, Christina 281
Kari, Juho 129
Khan, Shadab 196
Kheimets, Gregory 184
Kim, Hyung Joong 267
Kim, Kap Jin 265
Kim, Min 299, 300
Kirpatovsky, Vladimir 186
Kluge, Stefan 290
Klukas, Ralf 149
Knox, Christopher 281
Köbli, Viktória 142
Koch, Juri 167
Kodibagkar, Vikram 289
Kolesnikov, Vladimir 162, 156
Korhonen, Anna 206
Korjenevsky, Alexander 270
Korostylev, Konstantin 156
Koskela, Olli 280
Kotanko, Peter 125
Kraft, Kadri 138
Krivoshei, Andrei 172
Krizaj, Dejan 170
Križaj, Dejan 189
Kronström, Kai 129
Krueger-Ziolek, Sabine 279, 278, 269
Kumagai, Hiroshi 260
Kunze-Szikszay, Nils 220
Kusuhara, Toshimasa 185, 124
Kwon, Hyeuknam 240
Kwon, Oh In 267

L

Lakomkin, Vladimir 184
Lall, Brejesh 277
Lamp, Jürgen 172
Land, Raul 178, 201, 138

Langlois, Peter 262
Lee, Kyounghun 221
Lee, Min Hyung 275
Lee, Seulki 166, 147
Lee, Seungri 240
Lehti-Polojärvi, Mari 280
Lehto, Tarja 206
Leino, Akseli 280
Lemay, Mathieu 181, 242
Leonhardt, Steffen 282, 252, 225
Leonhäuser, Dorothea 282
Leray, Isabelle 139
Leslie, Greg 151
Levin, Nathan 125
Li, Gen 210
Li, Jia 145, 165
Li, Yingjia 183
Lionheart, William 245, 228, 258, 236
Liu, Benyuan 263
López-Marín, Antonio 159
López-Salazar, Ana Milena 204
Louarroudi, Ebrahim 105
Lovering, Richard M 165
Loyola, Bryan 291
Lozano, Lucila M. 160
Lu, Mingyang 194
Luepschen, Henning 225
Lukoshkova, Elena 184
Lutz, Cathleen 145

M

Madsen, Randy Kellen 291
Maglaveras, Nikolaos 297
Mahara, Aditya 222, 253, 293, 196
Mahdavi, Hadiseh 110, 121
Maier, Julian 288
Manca, Carla 176
Mansoorifar, Amin 168
Mansouri, Sofienne 187
Marsh, Liam A 134
Märtens, Olev 178
Martínez, Honorina 160
Martinsen, Ørjan G 136, 130, 135
Martinsen, Ørjan G. 157, 177
Martinsen, Ørjan G. 171, 133, 179, 202
Marulanda, Felipe 214
Mauri, Tomaso 220
McCann, Hugh 258
McCormick, Christopher 188
Meena, Ramesh Kumar 114
Meijer, Jan 128
Meijer, Jan H 136, 135
Meijer, Jan H. 108
Meinel, Timo 233
Meira, Carolina 283, 287
Melchor, Angel 121
MENG, Yu 182
Micheau, Philippe 294
Min, Mart 178, 173, 201, 174, 172
Mir, Lluis M. 139
Miranda, David 122
Miranda-Mercado, David Alejandro 119
Moeller, Knut 278, 279, 269
Moerer, Onnen 220
Möller, Knut 230, 229
Moreno, Marie-Valerie 112
Moreno, Marie-Valérie 197
Mosing, Martina 283, 287
Mousseau, Julien 294
Muders, Thomas 225
Mudraya, Irina 186
Mulett, Edelberto 122
Müller, Jakob 290
Muñoz-Fernández, Ana Maria 141
Murphy, Ethan 222, 253, 286, 196

N

Nacke, Thomas 183, 149, 150
Nadeau, Mathieu 294
Nakamura, Takao 185, 124
Nebuya, Satoru 260
Nefti-Meziani, Samia 256
Nesterov, Andrey 186
Nikolaev, Dmitriy 140
Nikolaev, Dmitry 162, 156
Nishimoto, Sarah 241
Nobu, Karippai 183
Nordebo, Sven 281
Noveletto, Fabricio 189

O

Obeedallah, Hadeel 151
Objartel, Mart 138

Odland, Hans Henrik 179
Oh, Tong In 275, 259, 265
Ojarand, Jaan 174
Ollmar, Stig 191
Ordoñez, Antonio 159
Orschulik, Jakob 252
Örtenwall, Per 199
Ortíz, Juan L. 160
Osorio, Mauricio 122
O'Toole, Michael D 134
Ouni, Kaïs 148
Ouypornkochagorn, Taweechai 258

P

Pabst, Oliver 171, 133
Pahuja, Sarwan Kumar 114
Pajares, Virginia 141
Palko, Tadeusz 219
Panayi, George 167, 164
Paradise, Steven 291
Parry, Monica 108, 128
Passard, Michelle 197
Patterson, Robert P 155
Patwari, Neal 291
Patz, Ralf 167, 164, 175
Peczalski, Kazimierz 219
Pettersen, Fred-Johan 179
Pevzner, Alexander 184
Peyton, Anthony 194
Peyton, Anthony J 134
Plank, Lindsay 127
Pliquett, Uwe 132
Podtaev, Sergey 140
Poggendorf, Iris 150
Poppitt, Sally 127
Pour-Ghaz, Mohammad 285
Praud, Jean-Paul 294
Proença, Martin 181, 242
Prosch, Helmut 243
Pulina, Giuseppe 176
Putensen, Christian 225

Q

Qin, Mingxin 209, 210, 213
Quintel, Michael 255
Qureshi, Tabassum 226

R

Reidla, Marko 173
Repo, Tapani 206
Reuter, Daniel 241
Revenko, Sergey 186
Rimensberger, Peter 281
Rimoldi, Stefano 242
Rist, Marek 173, 174
Riu, Pere J 141
Robitzki, Andrea 131
Rodriguez, Saul 191
Rogoza, Anatoly 184
Rosell Ferrer, Javier 110, 121, 159, 158
Rozman, Janez 170
Rubió-Pons, Jordi 159
Rudnev, Sergey 162, 156
Russo, Paola 117, 116
Russo, Stefania 256
Rusu, Ana 191
Rutkove, Seward 145, 165, 105, 126
Ruud, Tom Erik 157
Rymarczyk, Tomasz 257

S

Sabuncu, Ahmet 168
Sadleir, Rosalind 292, 289, 239
Sadleir, Rosalind Jane 249
Sage, Michaël 294
Sajib, Saurab Zk 267
Samartsev, Vladimir 140
Sanchez, Benjamin 165, 105
Sánchez, Benjamín 158
Santacesaria, Matteo 231
Santos, Susana 252
Sauter, Axel R. 177
Scalise, Lorenzo 117, 116
Schädler, Dirk 233
Schlebusch, Thomas 282
Schmidt, Niklas 282
Schullcke, Benjamin 279, 278, 269
Scott, Darryl 299
Seidel, Diana 131
Sengupta, Amit 114
Seo, Jin Keun 264, 221, 240
Seppänen, Aku 285
Shchelykalina, Svetlana 162, 156
Shirai, Kiyoko 185

Sikora, Jan 257
Siltanen, Samuli 231
Silvennoinen, Raimo 206
Şimşek, Fatma Gülden 192
Singh, Gurmeet 277
Singh, Harsahib 277
Singh, Vaneet 277
Sjöqvist, Bengt-Arne 199
Smirnov, Aleksandr 162
Smirnov, Alexander 140
Solà, Josep 181, 242
Soleimani, Manuchehr 226
Song, Kyo 300
Squillace, Gabriel 166, 147
Starodubov, Vladimir 156
Starunova, Olga 162, 156
Steenackers, Hans 198
Stender, Birgit 288
Steuten, Lotte 281
Strand-Amundsen, Runar 157
Strauch, Ulrich 227
Stölzle-Feix, Sonja 301
Suh, Gee Young 259

T

Takács, Anna 142
Tamm, Martti 138
Tan, Yee Mei 134
Tarasova, Olga 184
Tarotin, Ilya 244
Thiran, Jean-Philippe 181, 242
Thuerk, Florian 241
Thürk, Florian 243
Tilly-Mándy, Andrea 142
Tizzard, Andrew 281, 251
Tocco, Filippo 176
Toemboel, Frederic 243
Tognetti, Alessandro 256
Thomas, Ulrich 301
Tomasini, Enrico Primo 116
Tønnessen, Tor Inge 157
Torrego, Alfons 141
Tregidgo, Henry 245
Trepte, Constantin J. 241
Tricarico, Gerardo 117, 116
Trokhanova, Olga 270
Tronstad, Christian 171, 130, 157, 177
Tsiberkin, Kirill 140
Tucker, Don 239
Turovets, Sergei 239
Tuykin, Timur 270
Tzavelis, Andreas 293

U

Ülgen, Yekta 153, 192
Uscanga, María C. 160
Uuetoa, Hasso 172
Uuetoa, Tiina 172

V

van Acht, Victor 166
van der Elzen, Richard 136, 135
van der Stappen, Ruud 128
van Eijnatten, Maureen A 136, 135
van Kaam, Anton 281
van Lien, Rene 108
van Rijssel, Michael J 136, 135
Vandamme, Jonathan 294
Vandecasteele, Marianne 166
Vanderleyden, Jos 198
Vargas Luna, Miguel 169
Verdaasdonk, Rudolf M 136, 135
Vervloet, Marc 128
Vincence, Volney 208
Vinogradova, Olga 184
Vogt, Barbara 297, 224
Voskarides, Sotos 164
Vozary, Eszter 142

W

Waldmann, Andreas 283, 287, 241
Walter, Marian 282, 225
Ward, Leigh 109, 127
Watson, Stuart 164
Weiler, Norbert 281, 233, 297, 224
Weinert, Rodolfo 118
Wi, Hun 267, 275, 259, 265
Wiedemeier, Stefan 183
Wielandner, Alice 243
Witkowska-Wrobel, Anna 274
Wodack, Karin H. 241
Woo, Eung Je 267, 275, 259, 265
Wright, Paul 228, 258
Wu, Yu 262

X

Xia, Junying 263
Xu, Canhua 263

Y

Yamamoto, Yoshitake 185, 124
Yan, Qingguang 209
Yang, Bin 263
Yerworth, Rebecca 281
Yiannakkaras, Charalambos 281
YIN, Wuliang 194
Yip, Wilson 127
Yli-Hankala, Arvi 129
Yoon, Hargsoon 299, 300
Yumak, Mehmet 192
Yurova, Alexandra 143

Z

Zaikou, Yahor 149
Zarafshani, Ali 226
ZHANG, Gang 182
Zhao, Zhanqi 279, 224, 229, 230
Zhou, Liangdong 264
Zhu, Fansan 125
Zhuang, Wei 213
Zöllner, Christian 290
Žužek, Monika 170

NOTES

Main Sponsor

www.sciospec.de

Exhibitors

www.draeger.com

www.swisstom.com

www.eliko.ee

www.iopscience.iop.org

www.zhinst.com

www.scibase.se/en/

Sponsor of the Herman P. Schwan Award

www.impedimed.com/

City Hall Reception Hosts

www.stockholm.se

www.sll.se

Wikitorp, Uppsala 1160054
Tryckeri, Licens 3041 0051